**PALACKY UNIVERSITY IN OLOMOUC**

Faculty of Science

Department of Inorganic Chemistry

**Ph.D. thesis**

# SYNTHESIS AND STUDY OF CYTOKININ DERIVATIVES AND CDK-INHIBITORS DERIVED FROM 6-BENZYLAMINOPURINE AND THEIR COMPLEXES WITH SELECTED TRANSITION METALS

*Syntéza a studium derivátů cytokininů a CDK-inhibitorů odvozených od 6-benzylaminopurinu a jejich komplexů s vybranými přechodnými kovy*

**Author: Mgr. Pavel Štarha**

Study Programme: P1407 Chemistry

Field of Study: 1401V002 Inorganic Chemistry

Supervisor: Prof. RNDr. Zdeněk Trávníček, Ph.D.

Olomouc, 2010

# TABLE OF CONTENTS

# 1. INTRODUCTION

Platinum complexes became extraordinarily interesting, within the field of transition metal coordination compounds, after Barnett Rosenberg's accidental discovery of antineoplastic properties of *cis*-diamminedichloridoplatinum(II) named *cisplatin* in the 1960s [1]. This substance was approved as chemotherapeutic agent in the late 1970s and nowadays it is one of the world-leading drugs in the treatment of cancer [2]. The *cisplatin* success motivated inorganic chemists to synthesize new platinum complexes. Only few of several thousand platinum complexes, namely diammine-1,1´-cyclobutanedicarboxylatoplatinum(II) (*carboplatin*), (*1R,2R*-diaminocyclohexane)oxalatoplatinum(II) (*oxaliplatin*), diammineglycolatoplatinum(II) (*nedaplatin*) and (1,2-diaminomethylcyclobutane)-lactatoplatinum(II) (*lobaplatin*), reached the clinical use similar to *cisplatin*, and thus became the members of so called platinum-based drugs [2–4]. Complexes of other transition metals, including palladium, were gradually prepared and tested for their anticancer activity. A large number of the complexes were determined as significantly, in many cases even more active, against various types of tumours compared with the above-mentioned platinum-based drugs. Nevertheless, none of these non-platinum complexes is currently clinically used in the oncology practice [3].

The preparation of novel highly cytotoxic active both platinum and non-platinum coordination compounds successfully uses a combination of potentially active organic compounds with a suitable transition metal. For example, N6-benzyladenine derivatives represent a group of organic compounds usable for the synthesis of the complexes, because 2-(3-hydroxypropylamino)-N6-benzyl-9-isopropyl-adenine (*bohemine*) [5], 2-(1-ethyl-2-hydroxyethylamino)-N6-benzyl-9-isopropyladenine (*roscovitine*) [6] or 2-(1-ethyl-2-hydroxyethylamino)-N6-(2-hydroxybenzyl)-9-isopropyladenine (*olomoucine II*) [7], the substances derived from N6-benzyladenine, are potent inhibitors of cyclin-dependent kinases (CDK). This effect can be used in the antitumour therapy and *roscovitine*, under the name *Seliciclib*, has successfully entered the IIb phase of clinical testing on patients suffering with non-small cell lung cancer (NSCLC) [8]. Up to now, plenty of transition metal complexes, namely iron(II/III) [9–11], cobalt(II) [12,13], nickel(II) [14,15], copper(II) [9,16–19], zinc(II) [20,21], ruthenium(III) [22], palladium(II) [23–26], platinum(II) [23,25,27–29] and platinum(IV) [30], have been prepared, characterized and tested *in vitro* for their cytotoxic activity against selected human cancer cell lines. Especially, *in vitro* cytotoxic activity of some platinum(II) and palladium(II) complex representatives was determined as significantly higher as compared with both *cisplatin* and *roscovitine*.

The first part of this thesis, called Background, deals with the literature research regarding platinum and palladium and their complexes, focusing on the complexes with significant antitumour activity. An attention is also paid to, generally said, N6-benzyladenine, its variously substituted derivatives and the coordination compounds of different transition metals, where these organic compounds act as N-donor ligands. Accessible internet databases (e.g. www.isiknowledge.com,

www.sciencedirect.com, www.rsc.org, www.acs.org, www.scopus.com and www.ccdc.cam.ac.uk) and available books were used for this research.

The second part (Results and Discussion) describes the synthesis and characterization of twelve palladium(II) (**1**–**12**) and eleven platinum(II) (**13**–**23**) oxalato complexes with variously substituted N6-benzyladenine derivatives as N-donor carrier ligands. The detailed characterization of the obtained complexes was provided by the suitable physical-chemical methods, concretely elemental analysis (C, H, N), IR, Raman and multinuclear ($^{1}$H, $^{13}$C and $^{195}$Pt) and two dimensional ($^{1}$H–$^{1}$H gs-COSY, $^{1}$H–$^{13}$C gs-HMQC, $^{1}$H–$^{13}$C gs-HMBC and $^{1}$H–$^{15}$N gs-HMBC) NMR spectroscopy, ESI+ mass spectrometry, molar conductivity measurement, thermal studies [thermogravimetry (TG) and differential thermal analysis (DTA)] and single crystal X-ray analysis. Further, the results of the *in vitro* cytotoxic activity testing of the prepared complexes against ovarian carcinoma (A2780), ovarian carcinoma *cisplatin* resistant (A2780cis), malignant melanoma (G361), breast adenocarcinoma (MCF7), lung carcinoma (A549), osteosarcoma (HOS) and cervix epitheloid carcinoma (HeLa) human cancer cells and against primary culture of the human hepatocytes are discussed within the Results and Discussion section.

Finally, the main objectives of the thesis can be summarized as follows:

1. detailed literature research related to the studied topic in accessible literature and internet databases;
2. synthesis of palladium(II) and platinum(II) oxalato complexes involving N6-benzyladenine derivatives as N-donor carrier ligands, which is connected with preparation and characterization of the necessary starting compounds, *i.e.* potassium bis(oxalato)palladate dihydrate {$K_2[Pd(ox)_2]\cdot 2H_2O$}, potassium bis(oxalato)platinate dihydrate {$K_2[Pt(ox)_2]\cdot 2H_2O$} and N6-benzyladenine derivatives involving the 2-chloro-N6-benzyl-9-isopropyladenine or 2-(1-ethyl-2-hydroxyethylamino)-N6-benzyl-9-isopropyladenine moiety;
3. characterization of the prepared palladium(II) and platinum(II) oxalato complexes with N6-benzyladenine derivatives using various techniques (elemental analysis, IR, Raman and NMR spectroscopy, ESI+ mass spectrometry, molar conductivity measurement, TG/DTA thermal analysis and single crystal X-ray analysis;
4. evaluation of the *in vitro* cytotoxic activity of the prepared palladium(II) and platinum(II) oxalato complexes against selected human cancer cell lines (A2780, A2780cis, G361, MCF7, A549, HOS, HeLa) and human hepatocytes;
5. evaluation of the structure-activity relationship of the prepared palladium(II) and platinum(II) oxalato complexes.

It has to be stated in this place that the results of the literature research and author's Ph.D. study were, together with co-authors, reported in five scientific papers attached at the end of the thesis as *Appendix I*, *Appendix II*, *Appendix III*, *Appendix IV* and *Appendix V*. That is why only a brief summary of the obtained theoretical and experimental results as well as connections among the results reported in different papers are given in this thesis.

# 2. BACKGROUND

## 2.1. PALLADIUM AND PLATINUM

Palladium {[$_{36}$Kr]: $5s^0\ 4d^{10}$} and platinum {[$_{54}$Xe]: $6s^1\ 4f^{14}\ 5d^9$}, together with nickel called the elements of the nickel group, belong to the Group 10 (3$^{rd}$ column of Transition Group VIII) of the Periodical Table of the Elements [31–33]. Their principal oxidation states are +II and +IV, but 0, +I, +III, +V, +VI and even negative oxidation states occur as well. Both metals form several types of binary compounds, such as oxides (*e.g.* PdO), sulphides (*e.g.* $PtS_2$) and above all halides {*e.g.* $PtF_6$, $[PtF_5]_n$, $PdF_4$, $PtCl_2$}. Both metals are used as catalysts (industrial ammonia oxidation, hydrogenation reactions), platinum is also employed in the field of electrochemistry (Pt electrodes) and for production of chemical apparatus, jewellery and dental prostheses. The literature sources also describe a large number of organopalladium and organoplatinum compounds.

The most common palladium(II) and platinum(II) complexes are those with the coordination number of 4 {*e.g.* $[Pd(CN_4)]^{2-}$, *cis*-$[PtCl_2(NH_3)_2]$}. The square-planar particles can act as complex cations or anions or regular electroneutral complexes. The complexes with the central ion in the oxidation state +II are rarely of the trigonal-bipyramidal or octahedral geometry. The oxidation state +IV is typical especially for platinum complexes, such as $K_2[PtCl_6]$ (octahedral geometry). Several examples of the palladium and platinum complexes with the central atom in some of the other above-mentioned oxidation states can be found for example in ref. [31].

The detailed literature research regarding platinum and palladium oxalato complexes was done, because these complexes represent the main objective of the thesis. Up to now (august 2010), 261 platinum and 87 palladium square-planar complexes involving the bidentate-coordinated oxalate dianion have been reported (SciFinder Scholar, 2004 ed.). 200 platinum and 55 palladium complexes of them involve the $[Pt(ox)N_2]$, and $[Pd(ox)N_2]$ motif, respectively, and 35 platinum and 27 palladium complexes of the mentioned motif contain two monodentate N-donor ligands. Similarly, the Crystallographic Structural Database (CSD ver. 5.31, May 2010 update) [36] reports 54 platinum and 11 palladium square-planar oxalato complexes; 15, and 6 of them are of the $[Pt(ox)N_2]$, and $[Pd(ox)N_2]$ motif, respectively. The examples of these complexes are given in Fig. 1.

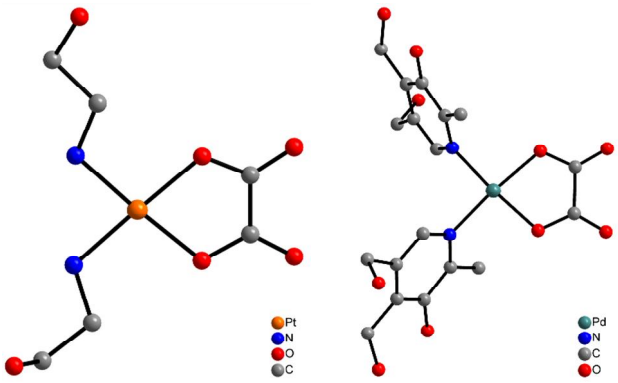


**Fig. 1.** $[Pt(ox)(ae)_2]$ (left; adopted from [34]) and $[Pd(ox)(pn)_2]$ complexes (right; adopted from [35]); ae = aminoethanol and pn = pyridoxine

## 2.2. PALLADIUM(II) AND PLATINUM(II) COMPLEXES WITH ANTICANCER ACTIVITY

Barnett Rosenberg discovered the antineoplastic activity of *cis*-[$PtCl_2(NH_3)_2$] (*cisplatin*; Fig. 2) in the 1960s [1]. This platinum(II) complex is successfully used in oncology since 1978 [2]. However, a lot of platinum complexes, which have been prepared after the discovery of *cisplatin*, have been shown as the substances bearing promising anticancer properties, as well. Some of these compounds, concretely diammine-1,1´-cyclobutanedicarboxylatoplatinum(II) (*carboplatin*), (*1R*,*2R*-diaminocyclohexane)-oxalatoplatinum(II) (*oxaliplatin*), diammineglycolatoplatinum(II) (*nedaplatin*) and (1,2-diamino-methylcyclobutane)lactatoplatinum(II) (*lobaplatin*), are also clinically employed as the platinum-based anticancer drugs (Fig. 2 and Fig. 3) [2–4].

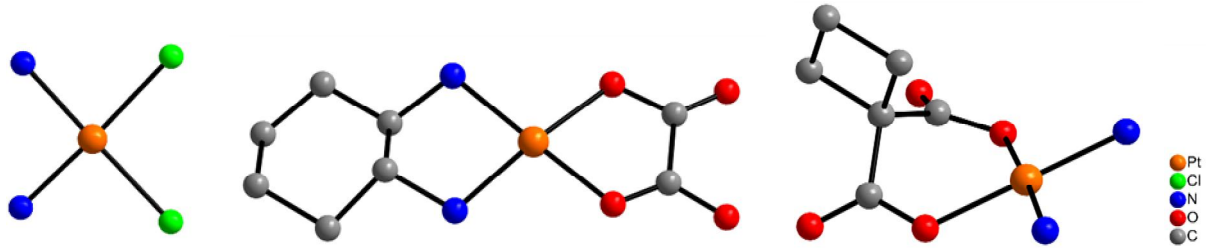


**Fig. 2.** *Cisplatin*, *cis*-diamminedichloridoplatinum(II) complex (left; adopted from [37]), *oxaliplatin*, (*1R*,*2R*-diaminocyclohexane)oxalatoplatinum(II) complex (middle; adopted from [38]) and *carboplatin*, diammine-1,1´-cyclobutanedicarboxylatoplatinum(II) complex (right; adopted from [39])

*Cisplatin* is a chemically quite simple platinum(II) complex that has been known since 1844 (Peyrone´s chloride). Two $NH_3$ ligands represent non-leaving groups while two chloride ions can be replaced by other ligands (leaving groups) [2,3]. It is highly effective against testicular and ovarian cancer, but it has been successfully used for treatment of head, neck, bladder, or non-small lung cancer, osteosarcoma, melanoma etc. However, some kinds of tumours are naturally resistant to the treatment of *cisplatin* and some others develop resistance after initial treatment. The side effects, such as myelosuppression, nephrotoxicity, ototoxicity or neurotoxicity, are also well known in connection with clinical treatment of cancer by *cisplatin*. *Cisplatin* is a quite unreactive molecule and, due to its low water solubility, it has to be administrated intravenously. However, its leaving groups (*i.e.* chloride ions) can be replaced by water molecules in the cell nucleus, where the $Cl^-$ concentration is lower as compared with extracellular fluids. It has been discovered that positively charged mono- or diaqua complexes can bind to DNA. The adducts formed by *cisplatin* in DNA change the secondary structure of DNA, which results in the inhibition of both DNA and RNA synthesis.

Generally, the same tumours as mentioned for *cisplatin* can be treated also by *carboplatin*, *nedaplatin* and *lobaplatin* [2,3,40]. Nevertheless, these platinum-based drugs have been used for the treatment of cancer thanks to their advantages over *cisplatin*, because these substances are significantly less nephrotoxic, ototoxic and neurotoxic as compared with *cisplatin*. On the other hand, these substances are less cytotoxic than *cisplatin*. Both *carboplatin* and *nedaplatin* were found to be cross-resistant with *cisplatin*, which was not clinically observed for *lobaplatin*.

*Oxaliplatin* was developed by Y. Kidani in 1978 [41]. This compound is the most important representative of platinum(II) oxalato complexes, because it belongs among the recently used platinum-based anticancer drugs (approved in 1996) [2,3]. Unlike above-mentioned *carboplatin*, *nedaplatin* and *lobaplatin*, *oxaliplatin* (in combination with 5-fluorouracil and leucovorin) is highly active against colorectal cancer, which is not clinically sensitive to *cisplatin*. Some of undesirable drawbacks, concretely myelosuppression, nephrotoxicity and ototoxicity, do not accompany the clinical treatment by *oxaliplatin*, however, its dose is still limited by neurotoxicity. The fact that *oxaliplatin* is not cross-resistant with *cisplatin* has to be mentioned as well. Similarly to *cisplatin*, the leaving group of *oxaliplatin* (*i.e.* oxalate dianion) has to be substituted by two water molecules (it is facilitated by $HCO_3^-$ and $H_2PO_4^-$ ions) to form diaqua species, which react with the DNA molecule or molecules (mainly with the N7 atom of guanine) giving the d(GpG)Pt, d(ApG)Pt and d(GpNpG)Pt intrastrand adducts or the $d(G)_2Pt$ interstrand one [42]. It was determined that the *oxaliplatin* ability to form DNA adducts is lower as compared with *cisplatin* [43]. Nevertheless, the *oxaliplatin* lesions are more toxic than those of *cisplatin*, because an equal number of DNA adducts is more efficient for *oxaliplatin* compared with *cisplatin*. The difference in cytotoxicity of *oxaliplatin* and other platinum-based drugs is explained by the ability of *oxaliplatin* to fill more of the DNA major groove producing a bulkier and less polar adduct than that of *cisplatin*, which can be a more effective inhibitor of the DNA synthesis.

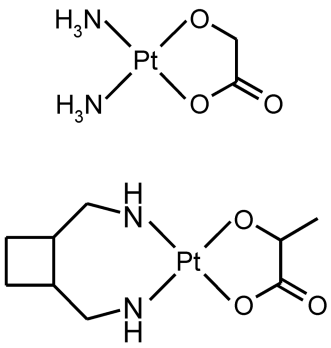


**Fig. 3.** Structural formulas of platinum-based drugs *nedaplatin* (up) and *lobaplatin* (down)

The success of *oxaliplatin* in the field of clinical oncology has been followed by many scientists and a great number of its derivatives has been synthesized and tested for their cytotoxicity against various types of tumours. We can divide *oxaliplatin* derivatives into two basic groups. The first group consists of complexes containing various 1,2-diaminocyclohexane-based (dach) N-donor ligands and a leaving group different from oxalate dianion. On the contrary, the second type of *oxaliplatin* derivatives involves the bidentate oxalate dianion and an N-donor ligand different from dach. The platinum(II) complexes **13**–**23**, presented in this thesis, belong to the latter group.

The elements of platinum and palladium are chemically very similar. That is why palladium complexes were tested for their cytotoxicity among the first non-platinum compounds, not a long time after the discovery of above-described *cisplatin* and its analogues. However, *cis*-$[PdCl_2(NH_3)_2]$ and $[PdCl_2(dach)_2]$, the analogues of the highly cytotoxic platinum(II) complexes, were found to be inactive on a Sarcoma 180 tumour cell line [44]. Generally said, lower efficiency of palladium(II) complexes than the platinum(II) analogues is attributed to about $10^5$ faster substitution of the leaving groups for the water molecules. Despite these early failures, plenty of palladium complexes have been prepared to date and many of these compounds were evaluated as substances with even higher cytotoxic activity against various types of tumours as compared with *cisplatin*, as it is clearly reviewed

by A. Garoufis et al. [3,45]. Nevertheless, up to now none of palladium complexes has successfully entered the clinical trials as a potential palladium-based anticancer drug.

The literature research, regarding platinum(II) oxalato complexes derived from *oxaliplatin* and palladium(II) oxalato complexes, is included in the Introduction section of *Appendix I–III*, together with appropriate citations.

### 2.3. N6-BENZYLADENINE AND ITS DERIVATIVES

N6-benzyladenine (6-benzylaminopurine; Fig. 4) is a representative of the plant growth regulators called cytokinins, which are defined as substances promoting the cell division in the presence of auxins [47]. The cytokinins were discovered in the 1950s, when the effect of various plant extracts on the proliferation of plant cells was observed. F. Skoog and C. Miller, together with their co-workers, reported N6-furfuryladenine (6-furfurylaminopurine; *kinetin*) as the first substance acting as a cytokinin [48]. However, *kinetin* was isolated from herring sperm DNA, and thus the first cytokinin, which occurs naturally in plant tissues, was N6-(2-methylbut-2-en-1-ol)adenine. This compound was named *trans-zeatin* according to maize (*Zea mays* L.), whose endosperm it was isolated from [49].

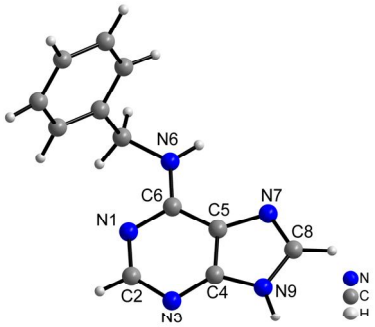


**Fig. 4.** Molecular structure of N6-benzyladenine (adopted from [46]) given with atom numbering scheme of the adenine ring

The structure similarity of *kinetin* and *trans-zeatin* (both belong among N6-substituted adenine derivatives) inspired chemists to prepare a lot of derivatives of these aromatic (*kinetin*) and isoprenoid (*trans-zeatin*) cytokinins. For example, the series of N6-(substituted-benzyl)adenine [51] and N6-(substituted-benzyl)adenosine [52] derivatives were reported. In addition to that, N6-benzyladenine derivatives substituted at the C2 and N9 positions (a benzene ring is mostly substituted as well) were also prepared and their effect on the cell cycle in the animal cells was studied [53].

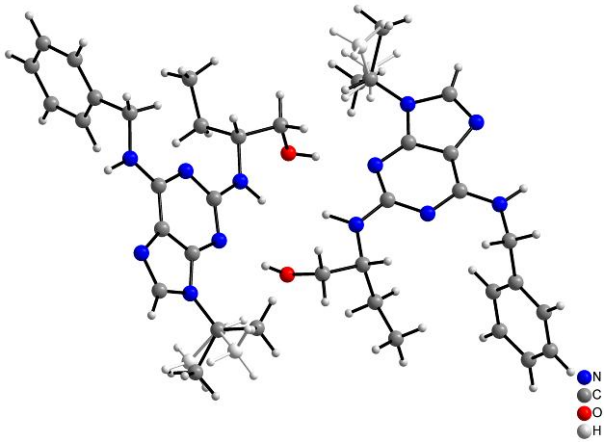


**Fig. 5.** Molecular structure of 2-[(*R*)-(1-ethyl-2-hydroxyethylamino)]-N6-benzyl-9-isopropyladenine (*roscovitine*; adopted from [50])

Generally, the cell cycle is regulated by a system of two types of proteins, namely *cyclins* and *cyclin-dependent kinases* (CDK) [54,55]. Concretely, the enzymatic activity of CDK drives the activity of various proteins, which can in consequence regulate (either start or finish) the cell cycle phases. On the other hand, the *cyclins* do not have enzymatic activity, but they regulate

the activity of *cyclin dependent kinases* by binding to their active site. Over ten CDKs have been found to date and their active site can be inhibited by the substance (generally called *cyclin-dependent kinase inhibitors*) of a various chemical structure, such as for example the mentioned C2,N9-substituted N6-benzyladenine derivatives, which can be used for the reduction of the cell division in various tumours.

The first representative of CDK inhibitors involving the N6-benzyladenine moiety was 2-(2-hydroxyethylamino)-N6-benzyl-9-methyladenine (*olomoucine*) reported in 1994 by J. Veselý and co-workers [53]. This compound inhibits the CDK1 ($IC_{50}$ = 7 μM) and CDK5 ($IC_{50}$ = 3 μM), while the CDK4 and CDK6 are not significantly sensitive to *olomoucine* with the $IC_{50}$ values over 1 mM. In other words, *olomoucine* is a selective inhibitor of CDKs. Nevertheless, even higher efficiency was evaluated for several N6-benzyladenine-based organic compounds, whose structures were derived from that of above-discussed *olomoucine*, such as 2-(1-ethyl-2-hydroxyethylamino)-N6-benzyl-9-isopropyladenine (*roscovitine*; Fig. 5) [6] or 2-(1-ethyl-2-hydroxyethylamino)-N6-(2-hydroxybenzyl)-9-isopropyladenine (*olomoucine II*) [7]. Their $IC_{50}$ values equalled 0.65 μM (for *roscovitine* against CDK2), 0.65 μM (for *roscovitine* against CDK2/cyclinB), 0.45 μM (for *roscovitine* against CDK1/cyclinB) and 0.02 μM (for *olomoucine II* against CDK1/cyclinB). The most promising representative of N6-benzyladenine-based CDK inhibitors, *roscovitine*, has successfully passed *in vivo* and preclinical testing and it is currently tested (named as Seliciclib or CYC202) in the 2b-phase of clinical evaluations on patients with non-small cell lung cancer (NSCLC) [8].

## 2.4. Transition Metal Complexes with N6-benzyladenine Derivatives

The above-mentioned biological activity and the fact that these organic compounds are easily obtainable make N6-benzyladenine derivatives suitable N-donor ligands for coordination compound syntheses. The N6-benzyladenine moiety offers four nitrogen coordination sites within the purine cycle (N1, N3, N7 and acidic N9) and one exocyclic nitrogen atom (N6), as depicted in Fig. 4. It acts as an electroneutral, protonated or deprotonated form within the structure of the complexes. The presence of several tautomeric forms, similarly as described for adenine [56], is presumable for N6-benzyladenine derivatives as well. Some concrete examples will be discussed below within the framework of this work.

Although several works have dealt with transition metal complexes involving an N6-benzyladenine-based N-donor ligand to date {e.g. $[Cu(BaH^+)_2Cl_3]Cl{\cdot}H_2O$ (Fig. 6) [57], $[Cd_2(\mu\text{-}Cl)_4(BaH^+)_2Cl_2]_n$ [58], $[Ru(BaH^+)Cl_4(DMSO)]{\cdot}½H_2O$ [59] or $[Rh_2(\mu\text{-}Ac)_4(Ba)]{\cdot}H_2O$ [60]; Ba stands for an electroneutral form of N6-benzyladenine and $BaH^+$ for its protonated form}, the following text of this section will be concerned with complexes (in order of the atomic number) prepared at our department.

The ionic pair iron(III) complexes of the compositions $(BohH^+)_2[FeCl_5]\cdot xH_2O$ were prepared and tested *in vitro* for their activity against G-361, HOS, K-562 and MCF-7 and on $p34^{cdc2}$ kinase inhibition; $BohH^+$ = a protonated form of *bohemine*, $x = 2$ or 3 [9]. The obtained $IC_{50}$ values of the tested complexes are higher compared to the starting organic compound, *i.e. bohemine*.

The $[FeCl_3(n\text{Ado})]\cdot H_2O$ complexes, where *n*Ado = N6-(2-fluorobenzyl)adenosine, N6-(4-fluorobenzyl)adenosine (*4F*Ado), N6-(2-trifluoromethylbenzyl)adenosine, N6-(3-trifluoromethylbenzyl)adenosine, N6-(4-trifluoromethylbenzyl)adenosine, N6-(4-trifluoromethoxybenzyl)-adenosine (*4OCF*$_3$Ado) and N6-(4-chlorobenzyl)adenosine, were characterized as the mixtures of oxidation states [Fe(III), Fe(II)], spin states (5/2, 4/2, 3/2, 2/2) and geometries (tetrahedral, trigonal bipyramidal) [10]. These substances were tested for their *in vitro* cytotoxic activity by a calcein acetoxymethyl (AM) assay against G-361, HOS, K-562 and MCF-7 human cancer cells, which proved significant cytotoxicity of the $[FeCl_3(4F\text{Ado})]\cdot H_2O$ ($IC_{50}$ = 8, 9, and 16 μM against HOS, K-562, and MCF-7, respectively) and $[FeCl_3(4OCF_3\text{Ado})]\cdot H_2O$ ($IC_{50}$ = 4 μM against MCF-7) complexes.

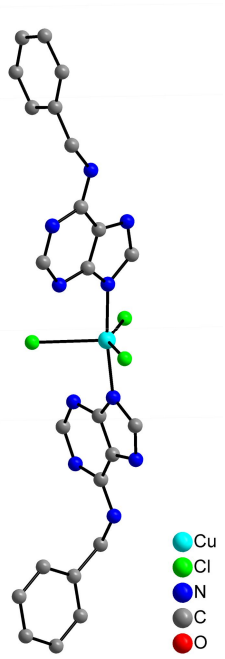


**Fig. 6.** Molecular structure of $[Cu(BaH^+)_2Cl_3]Cl\cdot 2H_2O$ ($BaH^+$ = a protonated form of N6-benzyladenine; adopted from [57]); H-atoms, $Cl^-$ ion and water molecules of crystallization were omitted for clarity

The latest article dealing with iron complexes with N6-benzyadenine derivatives describes mononuclear iron(III) complexes with CDK inhibitors, characterized as $[FeCl_3(Cdki)]\cdot xH_2O$; $x$ = 0–2, Cdki = 2-(3-chloropropylamino)-N6-benzyl-9-isopropyladenine, 2-(1-ethyl-2-hydroxyethylamino)-N6-(2-hydroxy-5-methylbenzyl)-9-isopropyladenine, 2-(1-ethyl-2-hydroxyethylamino)-N6-(3-hydroxybenzyl)-9-isopropyladenine (*3OH*Ros), *roscovitine* (Ros), 2-(2-hydroxyethylamino)-N6-benzyl-9-isopropyladenine (*isopropyl-olomoucine*; *ip*-Olo) and 2-(1-ethyl-2-hydroxyethylamino)-N6-(3,5-dihydroxybenzyl)-9-isopropyladenine [11]. Several of these complexes were determined as highly *in vitro* cytotoxic active against G-361, HOS, K-562 and MCF-7 human cancer cell lines and on CDK2/cyclin E, however, the obtained values were comparable with free organic molecules used as N-donor ligands in this work.

Two papers deal with cobalt(II) complexes involving N6-benzyadenine derivatives in the internal coordination sphere [12,13]. Both of them describe $[CoCl(H_2O)_2(n\text{Ba}^-)]\cdot xH_2O$ ($x$ = 0, 1 or 2) complexes of the tetrahedral geometry with a deprotonated form of N6-(2-hydroxybenzyl)adenine (*2OH*Ba), N6-(2-methoxybenzyl)adenine (*2OMe*Ba), N6-(3-methoxybenzyl)adenine (*3OMe*Ba), N6-(4-methoxybenzyl)adenine (*4OMe*Ba), N6-(2,3-dimethoxybenzyl)adenine (*2,3diOMe*Ba), N6-(3,4-dimethoxybenzyl)adenine (*3,4diOMe*Ba), N6-(3-chlorobenzyl)adenine (*3Cl*Ba), N6-(4-chlorobenzyl)adenine (*4Cl*Ba), N6-(3-fluorobenzyl)adenine (*3F*Ba) and N6-(4-fluorobenzyl)adenine (*4F*Ba). These complexes were found to be very cytotoxic against HOS cells. The obtained $IC_{50}$ values

evaluating their *in vitro* cytotoxicity ranged from 7 μM to 37 μM. The other human cancer cell lines used for testing (G-361, K-562 and MCF-7) were less sensitive.

Seven tetrahedral nickel(II) complexes of the general composition $[Ni(X)(H_2O)_2(nBa^-)]\cdot x$Solv were synthesized and characterized [X stands for $Cl^-$ or $NO_3^-$; $x$ = 0 or 1; Solv = $H_2O$ or EtOH; $nBa^-$ symbolizes a deprotonated form of *3Cl*Ba, *4Cl*Ba, *4F*Ba and N6-(2-chlorobenzyl)adenine (*2Cl*Ba)] [14,15]. Again, these substances underwent the *in vitro* testing evaluating their cytotoxic activity against G-361, HOS, K-562 and MCF-7 human cancer cells, however, the obtained results were not promising for the further studies of nickel(II) complexes with analogues of N6-benzyladenine.

A large scale of copper(II) complexes with N6-(substituted-benzyl)adenine derivatives [concretely, *2OMe*Ba, *3OMe*Ba, *4OMe*Ba, *2,3diOMe*Ba, *3,4diOMe*Ba, *2Cl*Ba, *3Cl*Ba, *4Cl*Ba, *3F*Ba, *4F*Ba and N6-(2-fluorobenzyl)adenine (*2F*Ba)] has been prepared at our department to date [9,16–19]. The structure of the obtained compounds $[Cu_2(\mu\text{-}nBa)_4(X)_2](X)_2\cdot x$Solv (X = $ClO_4^-$ or $Cl^-$; $x$ = 0–4; Solv = $H_2O$, EtOH or MeOH) was, in the case of $[Cu_2(\mu\text{-}4ClBa)_4(ClO_4)_2](ClO_4)_2\cdot 4EtOH\cdot H_2O$, determined by a single crystal X-ray analysis (see Fig. 7). The copper(II) complexes $[Cu_2(\mu\text{-}nBa)_2(\mu\text{-}Cl)_2(L_n)_2Cl_2]$, $[Cu_2(\mu\text{-}Cl)_2(nBa)_2Cl_2]$, $[Cu_2(\mu\text{-}nBa)_2(\mu\text{-}Cl)_2Cl_2]$, $[Cu_2(\mu\text{-}Cl)_2(\mu\text{-}nBa^-)_2(H_2O)_2]$, $[Cu(nBaH^+)_2Cl_3]Cl$ have been also reported together with the crystallographically determined molecular structure of $[Cu(3ClBaH^+)_2Cl_3]Cl\cdot 2H_2O$, whose structure is similar to $[Cu(BaH^+)_2Cl_3]Cl\cdot 2H_2O$ depicted above in Fig. 6; $3ClBaH^+$ = a protonated form of *3Cl*Ba. The mentioned copper(II) complexes were tested for both cytotoxic and antiradical activity. The highest *in vitro* cytotoxic activity was determined for $[Cu_2(\mu\text{-}2ClBa)_2(\mu\text{-}Cl)_2(2ClBa)_2Cl_2]\cdot 2H_2O$ and $[Cu_2(\mu\text{-}Cl)_2(\mu\text{-}2ClBa^-)_2(H_2O)_2]$ and it is equal to 8.2 μM, and 8.5 μM, respectively ($2ClBa^-$ = a deprotonated form of *2Cl*Ba).

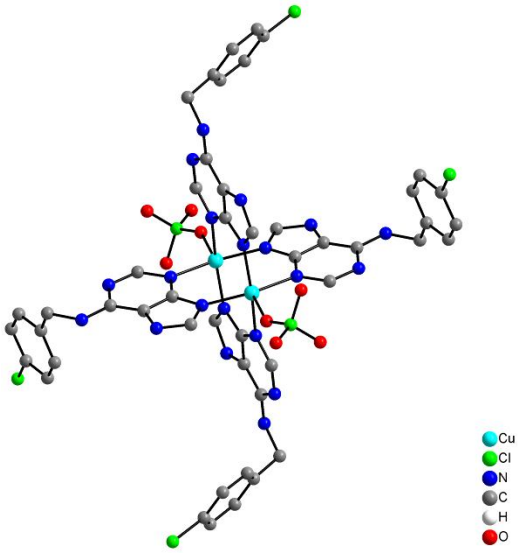


**Fig. 7.** Molecular structure of $[Cu_2(\mu\text{-}4ClBa)_4(ClO_4)_2](ClO_4)_2\cdot 4EtOH\cdot H_2O$ [*4Cl*Ba = N6-(4-chlorobenzyl)adenine; adopted from [19]]; H-atoms, perchlorate ions and solvent molecules of crystallization were omitted for clarity

Some of the $[Cu_2(\mu\text{-}nBa)_4(Cl)_2]Cl_2$ complexes were highly antiradical active (SOD-mimic activity) and their $IC_{50}$ were even lower compared to the native Cu,Zn-superoxide dismutase. Moreover, a significant *in vivo* antiradical activity (tested on alloxan-induced diabetes) was evaluated, because the glycaemia values determined for the mice pre-treated by these complexes were in some cases lower compared to both positive (mice treated only by alloxan) and negative (non-treated mice) controls.

The reactions of $ZnCl_2$ with the N6-benzyladenine derivatives provided three types of complexes, *i.e.* 1D-polymeric $[ZnCl_2(Cdki)]_n$, mononuclear $[ZnCl_3(CdkiH^+)]$ and $[ZnCl_3(nBaH^+)]$ and ionic

($n$BaH$_2^+$)[ZnCl$_4$] [20,21]. Their molecular structures are given in Fig. 8. The complexes involving the CDK inhibitors *bohemine*, *olomoucine* and *isopropyl-olomoucine* were tested for their *in vitro* cytotoxicity against G-361, HOS, K-562 and MCF-7 human cancer cells and for inhibition activity on CDK2/cyclin B. The results indicated significantly higher inhibition activity of CDK2/cyclin B as compared with free CDK inhibitors.

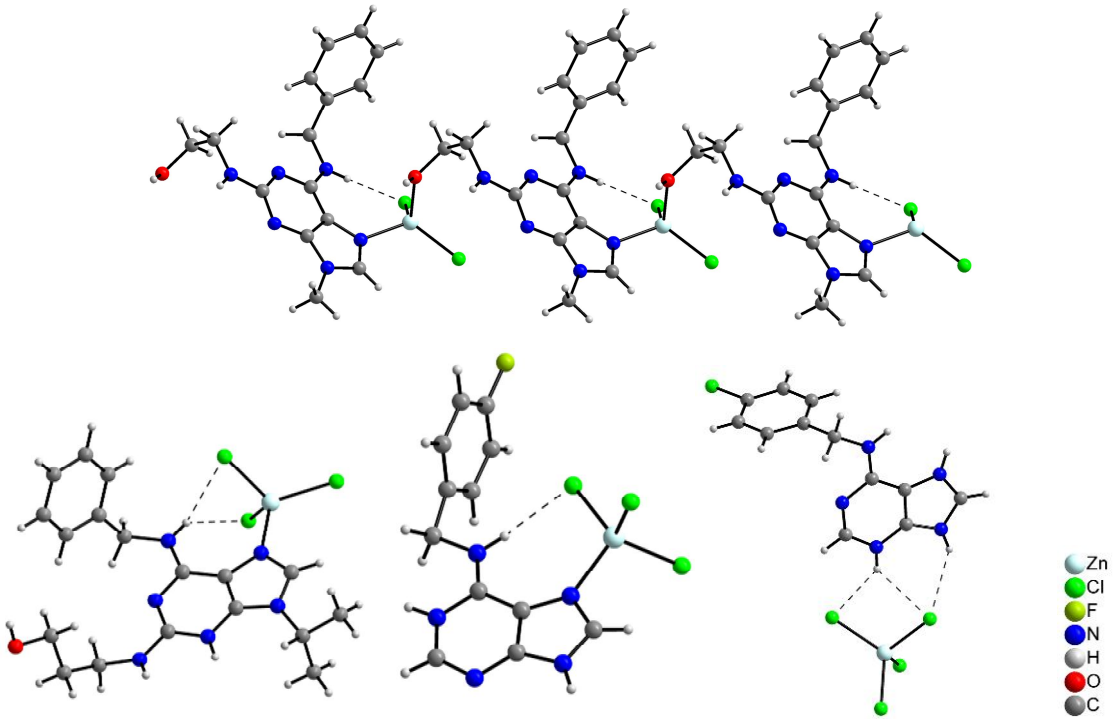


**Fig. 8.** Part of 1D polymeric structure of [ZnCl$_2$(Olo)]$_n$ [Olo = 2-(2-hydroxyethylamino)-N6-benzyl-9-methyladenine (*olomoucin*); adopted from [20]] and the molecular structure of [ZnCl$_3$(BohH$^+$)]·H$_2$O [BohH$^+$ = a protonated form of 2-(3-hydroxypropylamino)-N6-benzyl-9-isopropyladenine (*bohemine*); adopted from [20]], [ZnCl$_3$(*4F*BaH$^+$)]·H$_2$O [*4F*BaH$^+$ = a protonated form of N6-(4-fluorobenzyl)adenine; adopted from [21]] and (*4Cl*BaH$_2^+$)[ZnCl$_4$] [*4Cl*BaH$_2^+$ = a double-protonated form of N6-(4-chlorobenzyl)adenine; adopted from [21]); water molecule of crystallization were omitted for clarity

The ruthenium(III) complexes with the derivatives of the N6-benzyladenine have also been prepared (see Fig. 9) [22].

Finally, the octahedral platinum(IV) complexes of the formula [PtCl$_5$($n$BaH$^+$)] involving a protonated form of the substituted-benzyl derivatives of N6-benzyadenine, *i.e.* *2OMe*Ba, *3OMe*Ba, *4OMe*Ba, *2Cl*Ba, *3Cl*Ba, *4Cl*Ba, *2F*Ba, *3F*Ba, *4F*Ba, *2OH*Ba, N6-(3-hydroxybenzyl)adenine (*3OH*Ba) and N6-(3-hydroxybenzyl)adenine (*4OH*Ba), and [PtCl$_5$(cdkiH$^+$)] with a protonated form of *roscovitine* and *bohemine* have been described [30]. None of these complexes showed significant *in vitro* cytotoxicity. The crystals suitable for a crystallographic study formed in the mother liquors of

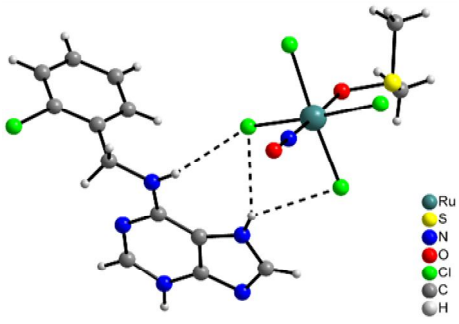


**Fig. 9.** Molecular structure of (*2Cl*BaH$^+$)[RuCl$_4$(NO)(DMSO)]·H$_2$O [*2Cl*BaH$^+$ = a protonated form of N6-(2-chlorobenzyl)adenine adopted from [22]); water molecule of crystallization omitted for clarity

both the [$PtCl_5$(CdkiH$^+$)], however, the structure of these ionic complexes determined by a single crystal X-ray analysis, *i.e.* (Boh$H_2^{2+}$)[$PtCl_6$]·$H_2O$ and (Ros$H_2^{2+}$)$_2$[$PtCl_6$]$Cl_2$·$4H_2O$, differed from the above-mentioned ones (Fig. 10).

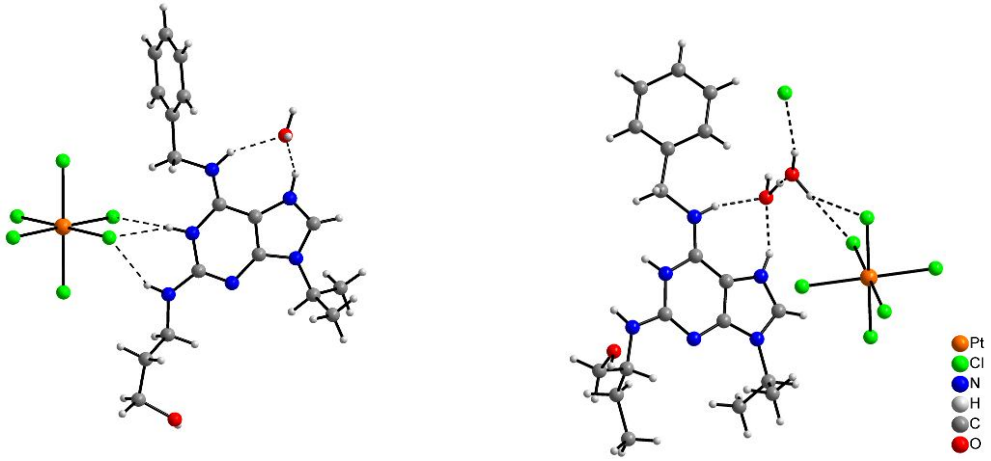


**Fig. 10.** Part of the crystal structure of [Ros$H_2^{2+}$]$_2$[$PtCl_6$]$Cl_2$·$4H_2O$ and molecular structure of [Boh$H_2^{2+}$][$PtCl_6$]·$H_2O$ {Ros$H_2^{2+}$ = a double-protonated form of 2-[(*R*)-(1-ethyl-2-hydroxyethylamino)]-N6-benzyl-9-isopropyladenine (*roscovitine*) and Boh$H_2^{2+}$ = a double-protonated form of 2-(3-hydroxypropylamino)-N6-benzyl-9-isopropyladenine (*bohemine*); adopted from [30]}

## 2.5. PALLADIUM(II) AND PLATINUM(II) COMPLEXES WITH N6-BENZYLADENINE DERIVATIVES

The previously reported palladium(II) and platinum(II) chlorido complexes [23–29] are discussed in more detail, separately from the above-mentioned Fe(II/III), Co(II), Ni(II), Cu(II), Zn(II), Ru(III) and Pt(IV) complexes, because these compounds relate very closely to this thesis, which follows a theme of the platinum(II) and palladium(II) complexes containing N6-benzyladenine-based N-donor carrier ligand.

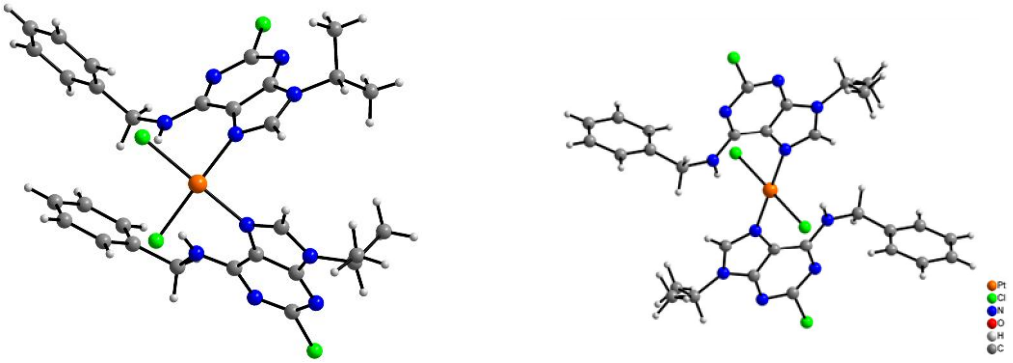

**Fig. 11.** Molecular structures of *cis*-[$PtCl_2(L)_2$] and *trans*-[$PtCl_2(L)_2$] (L = 2-chloro-N6-benzyl-9-isopropyladenine; adopted from [29])

The compositions of the obtained platinum(II) products can be described as *cis*-[$PtCl_2(L_x)_2$] [23,25,27,29], *trans*-[$PtCl_2(L_x)_2$] [28,29], [$PtCl_3(L_xH^+)$] [23], *cis*-[$PtCl_2(L_xH^+)_2$]$Cl_2$ [27] and [$PtCl(L_x^-)(H_2O)_2$] [23]; $L_x$ symbolizes variously substituted derivatives of N6-benzyladenine, $L_xH^+$ its

protonated form and $L_x^-$ its deprotonated form. As for palladium(II) complexes, the *cis*-$[PdCl_2(L_x)_2]$ [26], *trans*-$[PdCl_2(L_x)_2]$ [25,26], $[PdCl_3(L_xH^+)]$ [23,24], *trans*-$[PdCl_2(L_x)(H_2O)]$ [23] and $[PdCl(L_x^-)(H_2O)]$ [23] types of complexes have been prepared (Fig. 11, Fig. 12 and Fig. 13).

The *cis*-$[PtCl_2(L_x)_2]$ complexes, where $L_x$ = Boh, Olo, Ros, *ip*-Olo, 2-chloro-N6-benzyl-9-isopropyladenine (L), 2-chloro-N6-(2-methoxybenzyl)-9-isopropyladenine (*2OMe*L), 2-chloro-N6-(4-methoxybenzyl)-9-isopropyladenine (*4OMe*L), 2-[1-(hydroxymethyl)-2-(methyl)propyl]amino-N6-(3-hydroxybenzyl)-9-isopropyladenine (*3OH*mRos) and *3OH*Ros, were prepared using several strategies differing in the starting platinum(II) compound {$PtCl_2$ or *cis*-$[PtCl_2(DMSO)_2]$}, solvent (EtOH or $CHCl_3$) and reaction time and temperature [23,25,27,29]. The preparation of *trans*-$[PtCl_2(L)_2]$, *trans*-$[PtCl_2(2OMeL)_2]$ and *trans*-$[PtCl_2(4OMeL)_2]$ used appropriate *cis*-isomers, whose recrystallization from the hot DMF provided the named platinum(II) complexes in *trans* arrangement [28,29]. The reactions of the platinum(II) chloride with two molar equivalents of boh, olo, ros or ipolo dissolved in 2M HCl led to the *cis*-$[PtCl_2(L_xH^+)_2]Cl_2$ or $[PtCl_3(L_xH^+)]$ complexes according to reaction time [23,27]. The only platinum(II) complex with a deprotonated form of some N6-benzyladenine derivative was $[PtCl(Boh^-)(H_2O)_2]$ which formed from the mixture (1:1:1) of $PtCl_2$, *bohemine* and $Et_3N$ [23].

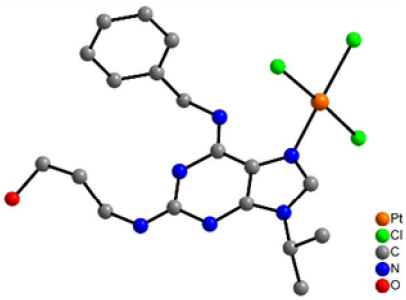


**Fig. 12.** Part of the molecular structure of $[Pt(BohH^+)Cl_3]_5 \cdot 9H_2O$ [$BohH^+$ = a protonated form of 2-(3-hydroxypropylamino)-N6-benzyl-9-isopropyladenine (*bohemine*); adopted from [23]]

The palladium(II) complexes *cis*-$[PdCl_2(L_x)_2]$ were obtained by the reactions (4 days, laboratory temperature) of L, *2OMe*L, *4OMe*L or 2-(chloropropyl)amino-N6-benzyl-9-isopropyladenine dissolved in acetone with $PdCl_2$ suspended in distilled water [26]. The *trans*-$[PdCl_2(L_x)_2]$ complexes with *2OMe*L or 2-chloro-6-(2,3-dimethoxybenzyl)-9-isopropyladenine (*2,3diOMe*L) formed from hot DMF solutions of appropriate *cis*-complexes [26]. However, *trans*-$[PdCl_2(L_x)_2]$ was also synthesized by the reactions of $K_2[PdCl_4]$ or *trans*-$[PdCl_2(DMSO)_2]$ with *3OH*Ros, *3OH*mRos, 2-chloro-6-(3-hydroxybenzyl)-9-isopropyladenine (*3OH*L; Fig. 13) or 2-chloro-6-(2-hydroxy-3-methoxybenzyl)-9-isopropyladenine (*2OH3OMe*L) [25]. The reactions of $PdCl_2$ or $K_2[PdCl_4]$ with variously substituted N6-benzyladenine analogues (Boh, Olo, *2OMe*Ba, *3OMe*Ba, *4OMe*Ba, *2Cl*Ba, *3Cl*Ba, *4Cl*Ba, *2F*Ba, *3F*Ba, *4F*Ba, *2OH*Ba, *3OH*Ba and *4OH*Ba) dissolved in 2M HCl gave the compounds of the general composition $[PdCl_3(L_xH^+)]$ [23,24]. Finally, the reactions of $PdCl_2$ with *bohemine* in ethanol, and ethanol with an

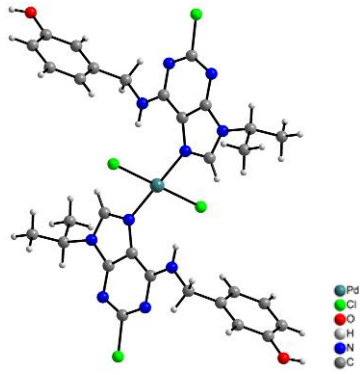


**Fig. 13.** Molecular structure of *trans*-$[Pd(3OHL)_2Cl_2] \cdot 2DMF$ [*3OH*L = 2-chloro-6-(3-hydroxybenzyl)-9-isopropyladenine; adopted from [25]); two DMF molecules of crystallization were omitted for clarity

$Et_3N$ addition, provided *trans*-[$PdCl_2$(Boh)($H_2O$)], and [PdCl(Boh$^-$)($H_2O$)], respectively [23].

The properties of the obtained complexes were studied by various physical-chemical techniques, namely elemental analysis, melting point determination, molar conductivity measurements, ESI+ and MALDI-TOF mass spectrometry, IR and NMR spectroscopy. A single crystal X-ray analysis determined the molecular structure of several types of complexes, *i.e.* *cis*-[$PtCl_2(L_x)_2$] [29], *trans*-[$PtCl_2(L_x)_2$] [28,29], [$PtCl_3(L_xH^+)$] [23] and *trans*-[$PdCl_2(L_x)_2$] [25,26] (see Fig. 11, Fig. 12 and Fig. 13).

Due to the above-mentioned reasons regarding cytotoxic platinum and palladium complexes, both the palladium(II) and especially platinum(II) complexes involving the substituted N6-benzyladenine moiety have been intensively studied due to their possible cytotoxic activity. This research determined most types of the described complexes as significantly *in vitro* cytotoxic against various human cancer cell lines (G-361, HOS, K-562, MCF-7), as compared with *roscovitine* (19.0, 20.0, 50.0 and 15.0 μM) and the commercially used platinum-based anticancer drugs *cisplatin* (2.9, 3.0, 4.7 and 10.9 μM) and *oxaliplatin* (7.1, 6.8, 8.8 and 18.2 μM) [23]. The *in vitro* cytotoxicity of complex [$PtCl_3$(BohH$^+$)]·$H_2O$ was found to be very high against K-562, and MCF-7, with the $IC_{50}$ values equalled to 2.1 μM, and 3.3 μM, respectively [23]. $IC_{50}$ equalled 8.0 μM against K-562 for [PtCl(Boh$^-$)($H_2O$)$_2$]·$H_2O$ which means lower *in vitro* cytotoxic activity as compared with *cisplatin*, but higher than both *roscovitine* and *oxaliplatin* [23]. The same conclusion can be made for [$PdCl_3$(BohH$^+$)]·$H_2O$ ($IC_{50}$ = 18.0 μM), *trans*-[$PdCl_2$(Boh)($H_2O$)] ($IC_{50}$ = 11.0 μM) and [PdCl(Boh$^-$)($H_2O$)]·EtOH ($IC_{50}$ = 13.0 μM) against MCF-7 cells [23]. Another platinum(II) complex with significant *in vitro* cytotoxicity is *cis*-[$PtCl_2$(BohH$^+$)$_2$]$Cl_2$, whose $IC_{50}$ values (2.0 μM, 2.0 μM and 4.0 μM against HOS, K-562, and MCF-7, respectively) were lower even than those of *cisplatin* [27]. The *trans*-[$PdCl_2(L_x)_2$] did not show any significant *in vitro* cytotoxicity, except for *trans*-[$PdCl_2$(*3OH*ros)$_2$]·$H_2O$ and *trans*-[$PdCl_2$(*3OH*mRos)$_2$]·$H_2O$, whose $IC_{50}$ = 3.0 μM (against MCF-7) [25].

The *cisplatin* analogues were found to be the most promising substances in terms of *in vitro* cytotoxicity against several human cancer cell lines. The $IC_{50}$ values obtained against G-361, HOS, K-562 and MCF-7 cancer cell lines for *cis*-[$PtCl_2$(Ros)$_2$] (1.0, 1.0, 1.0 and 2.0 μM) and *cis*-[$PtCl_2$(Boh)$_2$] (3.0, 2.0, 3.0 and 5.0 μM) were in most cases several times higher than *cisplatin* [27]. Because the obtained *in vitro* cytotoxicity was significantly higher than those of *cisplatin*, *oxaliplatin* and *roscovitine*, the attempts to describe the solution behaviour were made. The complexes of this type were studied by means of NMR in the DMF/water mixture in the period of six months [29]. It was proved that N6-benzyladenine-based ligands remain coordinated to the metal centre. On the other hand, no hydrolysis and formation of the [Pt(OH$^-$)$_2(L_x)_2$] or [Pt($H_2O$)$_2(L_x)_2$]$^{2+}$ were detected in the employed mixture by NMR techniques. It should be noted that in case of palladium(II) dichlorido complexes involving N6-benzyladenine derivatives the [Pt(OH$^-$)$_2(L_x)_2$] species formed in the DMF/water mixture, as proved by NMR study [26].

It has to be noted one more time that all of the above-mentioned $IC_{50}$ values were determined by a calcein AM assay, which reduces the comparability with the *in vitro* cytotoxicity results presented below for the complexes **1**–**23**, which were evaluated by an MTT assay.

# 3. RESULTS AND DISCUSSION

The work undertaken by the author of this study was recently published together with co-authors in the papers attached in:

- ***Appendix I:*** P. Štarha, Z. Trávníček, I. Popa: *Synthesis, characterization and in vitro cytotoxicity of the first palladium(II) oxalato complexes involving adenine-based ligands.* J. Inorg. Biochem. *103* (**2009**) 978;
- ***Appendix II:*** P. Štarha, I. Popa, Z. Trávníček: *Palladium(II) oxalato complexes involving N6-(benzyl)-9-isopropyladenine-based N-donor carrier ligands: synthesis, general properties,* $^{1}H$, $^{13}C$ *and* $^{15}N\{^{1}H\}$ *NMR characterization and in vitro cytotoxicity.* Inorg. Chim. Acta *363* (**2010**) 1469;
- ***Appendix III:*** P. Štarha, Z. Trávníček, I. Popa: *Platinum(II) oxalato complexes with adenine-based carrier ligands showing significant in vitro antitumor activity.* J. Inorg. Biochem. *104* (**2010**) 639;
- ***Appendix IV:*** Z. Trávníček, P. Štarha, I. Popa, R. Vrzal, Z. Dvořák: *Potent Roscovitine-based CDK inhibitors acting as N-donor ligands in the platinum(II) oxalato complexes: complex preparations, characterization and in vitro antitumor activity.* Eur. J. Med. Chem. *In press, corrected proof* (**2010**) doi:10.1016/j.ejmech.2010.07.025;
- ***Appendix V:*** R. Vrzal, P. Štarha, Z. Dvořák, Z. Trávníček: *Evaluation of in vitro anticancer activity of platinum(II) and palladium(II) oxalato complexes with adenine derivatives as carrier ligands.* J. Inorg. Biochem. Short Commun. *104* (**2010**) 1130.

That is why this section contains only a brief summary of the obtained results and connections among the results obtained for the analogical platinum(II) or palladium(II) complexes but reported in the different papers.

## 3.1. AUTHOR'S CONTRIBUTION

I would like to declare that my contribution to the presented work covers the following:

- literature and crystallographic research in the accessible sources;
- synthesis of the starting compounds;
- synthesis of the palladium(II) (**1**–**12**) and platinum(II) (**13**–**23**) oxalato complexes;
- preparation of the single crystals suitable for a single crystal X-ray analysis;
- measurement of molar conductivity;
- carrying out the TG/DTA thermal analysis and interpretation of the obtained data;
- interpretation of the IR and Raman spectroscopy and ESI+ mass spectrometry data.

## 3.2. SYNTHESES OF THE PALLADIUM(II) AND PLATINUM(II) COMPLEXES 1–23

### *3.2.1. MATERIALS*

The chemicals and solvents used in this work were purchased from commercial sources, *i.e.* Sigma-Aldrich [potassium oxalate monohydrate (98%), potassium tetrachloropalladate (98%), potassium tetrachloroplatinate (98%), benzylamine (99%), 2,3-dimethoxybenzylamine (99%), 3,5-dimethoxybenzylamine (98%), potassium carbonate (≥99%) and DMF-$d_7$ (99.5 atoms % D)], Acros Organics [2-bromopropane (99%), 2,4-dimethoxybenzylamine (98%), 3,4-dimethoxybenzylamine (97%), 2-methoxybenzylamine (98%), 3-methoxybenzylamine (98%), 4-methoxybenzylamine (98%), 4-methylbenzylamine (98%)], Olchemin [2,6-dichloropurine (> 97%)] and Lach-Ner, s.r.o. [acetone, chloroform, diethyl ether, DMSO, ethanol, ethyl acetate, isopropanol, methanol, DMF]. The mentioned chemicals and solvents were used as received, except for dimethyl sulfoxide, which was dried using magnesium sulphate.

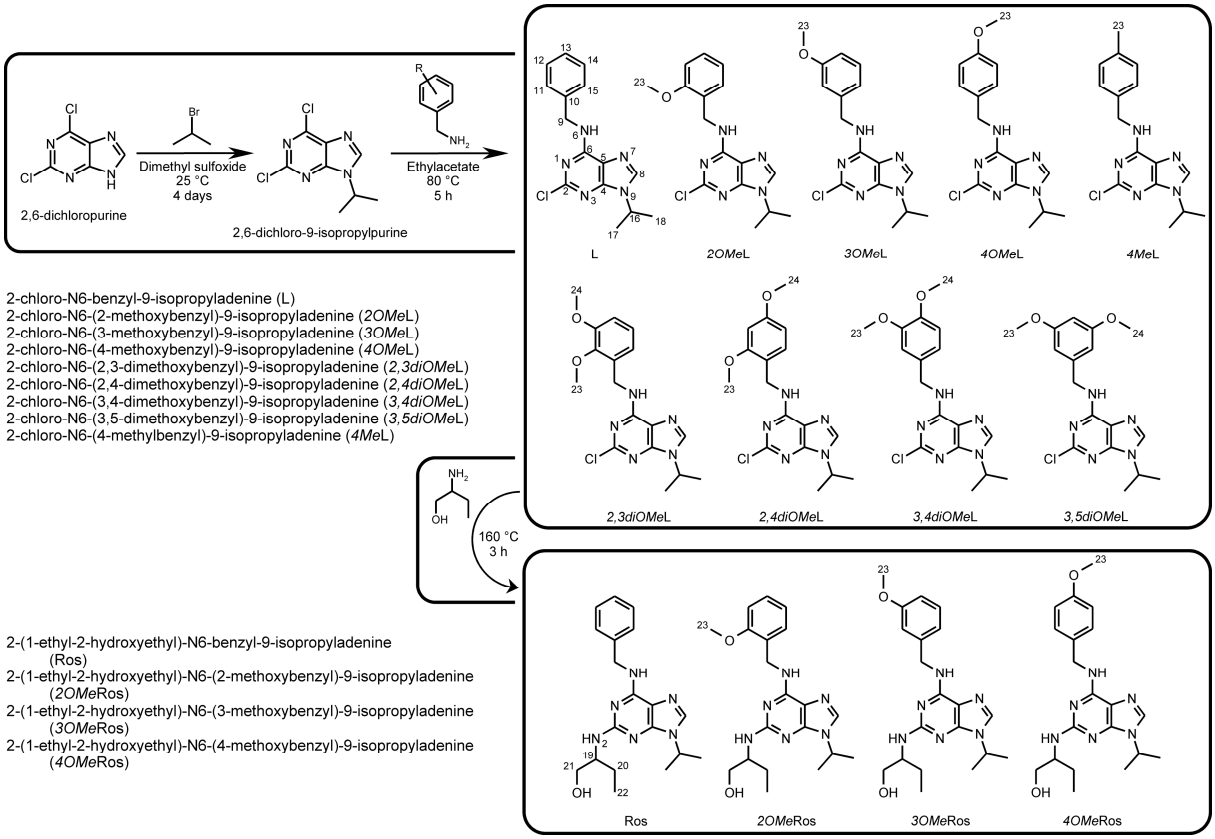


**Scheme 1.** Synthesis of 2-chloro-N6-benzyl-9-isopropyladenine, 2-(1-ethyl-2-hydroxyethyl)-N6-benzyl-9-isopropyladenine and their benzyl-substituted derivatives together with their names and structural formulas

### *3.2.2. STARTING COMPOUNDS*

Nine 2-chloro-N6-benzyl-9-isopropyladenine-based (*n*L) and four 2-(1-ethyl-2-hydroxyethyl)-N6-benzyl-9-isopropyladenine-based (*n*Ros) organic derivatives of the naturally occurring cytokinin N6-benzyladenine have been prepared. The synthesis drew inspiration from several formerly reported literature sources [5–7, 61–64]. An employed procedure is described in *Appendix I*, *Appendix II* and

*Appendix III* and its summarization is depicted in Scheme 1. The products were characterized by elemental analyses, IR, Raman and NMR ($^{1}$H, $^{13}$C, $^{1}$H–$^{1}$H gs-COSY, $^{1}$H–$^{13}$C gs-HMQC, $^{1}$H–$^{13}$C gs-HMBC and $^{1}$H–$^{15}$N gs-HMBC) spectroscopy and the results can be found in the *Appendix I Supplementary Data*, *Appendix II Supplementary Data* and *Appendix III Supplementary Data*. The structural formulas of the obtained organic compounds are given in Scheme 1. The crystals suitable for a single crystal X-ray analysis were obtained for *2,4diOMe*L. The molecular structure is depicted in Fig. 14, while the crystal data and structure refinements are given in Table 1 and the selected bond lengths and angles are summarized in Fig. 14 caption.

**Table 1.** Crystal data and structure refinements for *2,4diOMe*L

| | |
|---|---|
| Empirical formula | $C_{17}H_{20}N_5ClO_2$ |
| Formula weight | 361.83 |
| Temperature (K) | 100(2) |
| Wavelength (Å) | 0.71073 |
| Crystal system, space group | triclinic, P–1 |
| Unit cell dimensions | |
| *a* (Å) | 7.8620(2) |
| *b* (Å) | 9.2015(2) |
| *c* (Å) | 13.3030(3) |
| *α* (°) | 82.447(2) |
| *β* (°) | 74.802(2) |
| *γ* (°) | 66.012(2) |
| *V* (Å$^3$) | 848.16(3) |
| *Z*, $D_{calc}$ (g cm$^{-3}$) | 2, 1.417 |
| Absorption coefficient (mm$^{-1}$) | 0.247 |
| Crystal size (mm) | 0.25 × 0.20 × 0.15 |
| *F* (000) | 380 |
| *θ* range for data collection (°) | $2.86 \le \theta \le 25.00$ |
| Index ranges (*h, k, l*) | $-9 \le h \le 9$ |
| | $-10 \le k \le 8$ |
| | $-15 \le l \le 15$ |
| Reflections collected/unique ($R_{int}$) | 7116/2964 (0.0104) |
| Max. and min. transmission | 0.9638/0.9407 |
| Data/restraints/parameters | 2964/0/230 |
| Goodness–of–fit on $F^2$ | 1.112 |
| Final *R* indices [$I>2\sigma(I)$] | $R_1 = 0.0294$, |
| | $wR_2 = 0.0810$ |
| *R* indices (all data) | $R_1 = 0.0323$, |
| | $wR_2 = 0.0821$ |
| Largest peak and hole (e Å$^{-3}$) | 0.302, –0.221 |

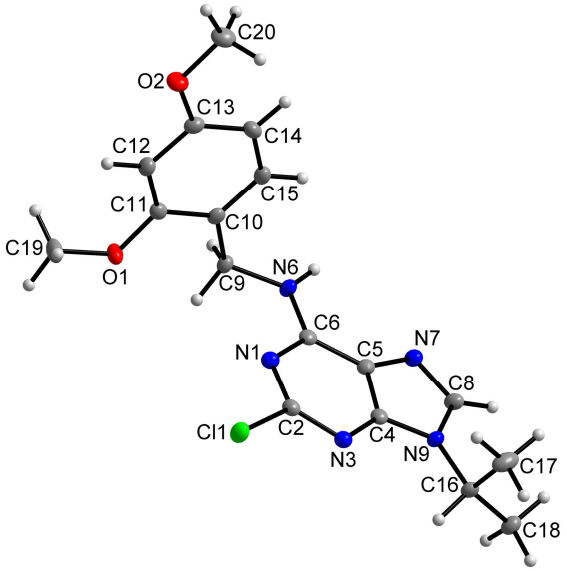


**Fig. 14.** The molecular structure of *2,4diOMe*L; N1−C2 = 1.326(2) Å, N1−C6 = 1.358(2) Å, C2−N3 = 1.313(2) Å, N3−C4 = 1.350(2) Å, C4−C5 = 1.387(2) Å, C4−N9 = 1.365(2) Å, C5−C6 = 1.411(2) Å, C5−N7 = 1.384(2) Å, C6–N6 = 1.335(2) Å, N7−C8 = 1.320(2) Å, C8−N9 = 1.368(2) Å, C2−N1−C6 = 117.18(11)°, N1−C2−N3 = 132.07(12)°, C2−N3−C4 = 109.34(11)°, N3−C4−C5 = 127.05(12)°, N3−C4−N9 = 126.58(12)°, C4−C5−C6 = 116.47(12)°, C4−C5−N7 = 110.21(11)°, C6−C5−N7 = 133.28(12)°, N1−C6−C5 = 117.86(12)°, N1−C6−N6 = 118.05(12)°, N6−C6−C5 = 124.09(12)°, C6−N6−C9 = 121.83(11)°, C5−N7−C8 = 103.91(11)°, N7−C8−N9 = 113.65(12)°, C4−N9−C8 = 105.87(11)°.

*Note:* All of these N6-benzyladenine-based organic compounds were formerly prepared and characterized, so no novelty was obtained in this part of the work. The *n*L and *n*Ros molecules were prepared strictly as starting compounds for the synthesis of below-described palladium(II) and platinum(II) oxalato complexes.

The syntheses of potassium bis(oxalato)palladate dihydrate, $K_2[Pd(ox)_2]\cdot 2H_2O$ [65], and potassium bis(oxalato)platinate dihydrate, $K_2[Pt(ox)_2]\cdot 2H_2O$ [66], were formerly described. The slight modifications applied for their preparation can be found in Appendix I, and Appendix II, respectively.

### 3.2.3. *Synthesis of Palladium(II) and Platinum(II) Oxalato Complexes*

An extensive literature search indicated that both palladium(II) [67] and platinum(II) [41,68] oxalato (or generally carboxylato) complexes have been prepared using a multistep procedure, as follows:

1) *cis*-[$MX_2$(lig)] is prepared (M = Pd or Pt; lig = two monodentate ligands or one bidentate ligand; X = $Cl^-$ or $I^-$);
2) the X ligands are removed with a water solution of a silver(I) salt leading to the mixture of AgX (filtered off) with the water soluble diaqua complex (filtrate);
3) diaqua complex is finally treated by appropriate alkaline oxalate (carboxylate) giving the [M(ox)(lig)] product.

The steps 2 and 3 are sometimes applied during one step using silver(I) carboxylate] [69]. It can be said that this procedure is connected with several drawbacks, such as problems with cis/trans isomerism and water solubility of intermediates, contamination by silver and it is time consuming.

Nevertheless, we believed that a rich experience with preparation of *cis*-[$PdCl_2(L_x)_2$] [26] and *cis*-[$PtCl_2(L_x)_2$] [23,25,27,29] (Section 2.5.) could be utilized for the synthesis of the oxalato complexes. However, several serious problems were faced. At first, the preparation of the pure *cis* form was unsuccessful, although the synthesis proceeded at ca –10 °C, which then prolongs a reaction time up to 14 days. The obtained complexes (a mixture of the *cis* and *trans* isomers with predominance of the *cis* form determined by $^1H$ and $^{13}C$ NMR to be ca 90%) were insoluble in distilled water. Nevertheless, the attempts to provide the reaction of these complexes with silver(I) nitrate in distilled water/acetone mixture were done, but the obtained *cis*-[$Pd(L_x)_2(H_2O)_2$]$^{2+}$ and *cis*-[$Pt(L_x)_2(H_2O)_2$]$^{2+}$ (in case it was prepared) were filtered off together with AgCl.

The described failures made me try a different approach to the preparation of palladium(II) oxalato complexes, which uses $K_2[Pd(ox)_2]\cdot 2H_2O$ as a starting palladium compound (Scheme 2) [70,71]. This complex is easily obtainable and well water soluble. Its reaction with two molar equivalents of N6-benzyadenine derivatives (*n*L and *n*Ros), dissolved in acetone, led to palladium(II)

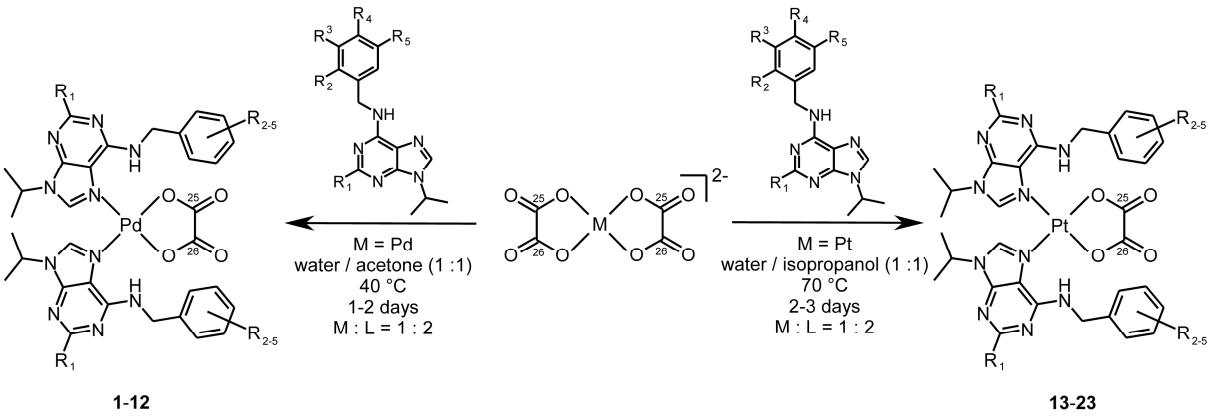


**Scheme 2.** Synthesis of the palladium(II) (**1**–**12**) and platinum(II) (**13**–**23**) oxalato complexes involving N6-benzyl-9-isopropyladenine derivatives (R are specified below in Table 2)

**Table 2.** Characteristics of the prepared palladium(II) and platinum(II) oxalato complexes. The $R_1$–$R_5$ describe substituents depicted in Scheme 2.

| Complex | Coordinated N6-benzyladenine derivative | $R_1$ | $R_2$ | $R_3$ | $R_4$ | $R_5$ | Appendix |
|---|---|---|---|---|---|---|---|
| [Pd(ox)(L)$_2$] (**1**) | 2-chloro-N6-benzyl-9-isopropyladenine | Cl | H | H | H | H | I |
| [Pd(ox)(*2OMe*L)$_2$]·¾H$_2$O (**2**) | 2-chloro-N6-(2-methoxybenzyl)-9-isopropyladenine | Cl | OMe | H | H | H | II, V |
| [Pd(ox)(*3OMe*L)$_2$]·¾H$_2$O (**3**) | 2-chloro-N6-(3-methoxybenzyl)-9-isopropyladenine | Cl | H | OMe | H | H | II |
| [Pd(ox)(*4OMe*L)$_2$] (**4**) | 2-chloro-N6-(4-methoxybenzyl)-9-isopropyladenine | Cl | H | H | OMe | H | I |
| [Pd(ox)(*2,3diOMe*L)$_2$] (**5**) | 2-chloro-N6-(2,3-dimethoxybenzyl)-9-isopropyladenine | Cl | OMe | OMe | H | H | I, V |
| [Pd(ox)(*2,4diOMe*L)$_2$]·2H$_2$O (**6**) | 2-chloro-N6-(2,4-dimethoxybenzyl)-9-isopropyladenine | Cl | OMe | H | OMe | H | I |
| [Pd(ox)(*3,5diOMe*L)$_2$]·3H$_2$O (**7**) | 2-chloro-N6-(3,5-dimethoxybenzyl)-9-isopropyladenine | Cl | H | OMe | H | OMe | II, V |
| [Pd(ox)(*4Me*L)$_2$] (**8**) | 2-chloro-N6-(4-methylbenzyl)-9-isopropyladenine | Cl | H | H | Me | H | I, V |
| [Pd(ox)(Ros)$_2$] (**9**) | 2-(1-ethyl-2-hydroxyethyl)-N6-benzyl-9-isopropyladenine | 2-aminobutan-1-ol | H | H | H | H | II, V |
| [Pd(ox)(*2OMe*Ros)$_2$] (**10**) | 2-(1-ethyl-2-hydroxyethyl)-N6-(2-methoxybenzyl)-9-isopropyladenine | 2-aminobutan-1-ol | OMe | H | H | H | II, V |
| [Pd(ox)(*3OMe*Ros)$_2$]·H$_2$O (**11**) | 2-(1-ethyl-2-hydroxyethyl)-N6-(3-methoxybenzyl)-9-isopropyladenine | 2-aminobutan-1-ol | H | OMe | H | H | II |
| [Pd(ox)(*4OMe*Ros)$_2$] (**12**) | 2-(1-ethyl-2-hydroxyethyl)-N6-(4-methoxybenzyl)-9-isopropyladenine | 2-aminobutan-1-ol | H | H | OMe | H | II, V |
| [Pt(ox)(L)$_2$] (**13**) | 2-chloro-N6-benzyl-9-isopropyladenine | Cl | H | H | H | H | III, V |
| [Pt(ox)(*2OMe*L)$_2$] (**14**) | 2-chloro-N6-(2-methoxybenzyl)-9-isopropyladenine | Cl | OMe | H | H | H | III, V |
| [Pt(ox)(*3OMe*L)$_2$] (**15**) | 2-chloro-N6-(3-methoxybenzyl)-9-isopropyladenine | Cl | H | OMe | H | H | III, V |
| [Pt(ox)(*2,3diOMe*L)$_2$] (**16**) | 2-chloro-N6-(2,3-dimethoxybenzyl)-9-isopropyladenine | Cl | OMe | OMe | H | H | III, V |
| [Pt(ox)(*2,4diOMe*L)$_2$] (**17**) | 2-chloro-N6-(2,4-dimethoxybenzyl)-9-isopropyladenine | Cl | OMe | H | OMe | H | III, V |
| [Pt(ox)(*3,4diOMe*L)$_2$] (**18**) | 2-chloro-N6-(3,4-dimethoxybenzyl)-9-isopropyladenine | Cl | H | OMe | OMe | H | III, V |
| [Pt(ox)(*3,5diOMe*L)$_2$]·4H$_2$O (**19**) | 2-chloro-N6-(3,5-dimethoxybenzyl)-9-isopropyladenine | Cl | H | OMe | H | OMe | III, V |
| [Pd(ox)(Ros)$_2$]·¾H$_2$O (**20**) | 2-(1-ethyl-2-hydroxyethyl)-N6-benzyl-9-isopropyladenine | 2-aminobutan-1-ol | H | H | H | H | IV |
| [Pd(ox)(*2OMe*Ros)$_2$]·H$_2$O (**21**) | 2-(1-ethyl-2-hydroxyethyl)-N6-(2-methoxybenzyl)-9-isopropyladenine | 2-aminobutan-1-ol | H | OMe | H | H | IV |
| [Pd(ox)(*3OMe*Ros)$_2$]·½H$_2$O (**22**) | 2-(1-ethyl-2-hydroxyethyl)-N6-(3-methoxybenzyl)-9-isopropyladenine | 2-aminobutan-1-ol | H | H | OMe | H | IV |
| [Pd(ox)(*4OMe*Ros)$_2$]·¾H$_2$O (**23**) | 2-(1-ethyl-2-hydroxyethyl)-N6-(4-methoxybenzyl)-9-isopropyladenine | 2-aminobutan-1-ol | H | H | H | OMe | IV |

oxalato complexes $[Pd(ox)(nL)_2]\cdot xH_2O$ (**1**–**12**) and $[Pd(ox)(n\text{Ros})_2]\cdot xH_2O$ (**13**–**23**) summarized in Table 2. The syntheses are sufficiently described in Appendix I and II and they are schematically summarized in Scheme 2.

The strategy using bis(oxalato) complex was also employed for the preparation of a series of eleven platinum(II) oxalato complexes, i.e $[Pt(ox)(nL)_2]\cdot xH_2O$ (**13**–**19**) and $[Pt(ox)(n\text{Ros})_2]\cdot xH_2O$ (**20**–**23**) (Table 2), as it is given in Scheme 2. It has to be noted that, to our best knowledge, this was for the first time when the platinum(II) oxalato complexes were prepared using a synthetic strategy employing $K_2[Pt(ox)_2]\cdot 2H_2O$ as a starting platinum(II) compound. For more details see Appendix III and Appendix IV.

Finally, it has to be noted that above-mentioned drawback of the general three-step synthesis of the platinum(II) and palladium(II) carboxylato complexes are eliminated if the appropriate bis(oxalato) complex is employed as a starting compound. The reactions proceed in one step, the products are no longer contaminated by silver and it is not limited by isomerism (in other words, reactions can be carried out at higher temperatures) and solubility of intermediates.

## 3.3. Characterization of Palladium(II) and Platinum(II) Complexes 1–23

### *3.3.1. General Properties*

The following physical-chemical methods were used for the general characterization of the prepared palladium(II) and platinum(II) oxalato complexes **1**–**23** (*Note:* the experimental details of the crucial methods employed for the characterization of the prepared complexes, *i.e.* NMR spectroscopy and single crystal X-ray analysis, can be found in Section 3.3.2. and Section 3.3.3. regarding these two techniques):

- Elemental analysis (C, H, N) was performed on a Flash EA-1112 Elemental Analyzer (Thermo Finnigan) and on a Fisons EA-1108 CHNS-O Elemental Analyzer (Thermo Scientific);
- Conductivity measurements were carried out on a Cond 340i/SET (WTW) in $10^{-3}$ M *N,N′*-dimethylformamide (for **1**–**23**) and acetone (for **1**, **4**–**6** and **8**) solutions at the temperature of 25 °C, and the values of the solvent were subtracted;
- Infrared (IR) spectra were recorded on a Nexus 670 FT-IR (ThermoNicolet) by KBr (400–4000 $cm^{-1}$) and Nujol (150–600 $cm^{-1}$) techniques;
- Raman spectroscopy was performed on an NXR FT-Raman Module (ThermoNicolet) in the 150–3750 $cm^{-1}$ region; the Raman spectrum was not obtained in the case of the complex **2**, which burnt in the light of laser beam;
- Mass spectra of the methanol solutions of the complexes were obtained using LCQ Fleet ion trap mass spectrometer by the ESI+ technique (Thermo Scientific);
- Simultaneous thermogravimetric (TG) and differential thermal (DTA) analyses were carried out using a thermal analyzer Exstar TG/DTA 6200 (Seiko Instruments Inc.). TG/DTA studies were

performed in ceramic pans in dynamic air atmosphere (100 ml $min^{-1}$) from laboratory temperature to 700 °C for platinum(II) complexes **13**–**23** or to the temperature of 900 °C in the case of palladium(II) complexes **1**–**12**. The temperature gradient was 2.5 °C $min^{-1}$.

The percentage content of carbon, hydrogen and nitrogen within the complexes **1**–**23** was determined by an elemental analysis. The obtained results satisfactorily correlated with the theoretical ones with the difference up to 0.5%. Prepared complexes **1**–**23** are well soluble in *N*,*N*′-dimethylformamide, chloroform and acetone, less soluble in ethanol and methanol and only negligibly soluble in water. The solubility of the [Pd(ox)(*n*Ros)$_2$] and [Pt(ox)(*n*Ros)$_2$] complexes is significantly higher as compared with [Pd(ox)(*n*L)$_2$] and [Pt(ox)(*n*L)$_2$] ones. The molar conductivity measurements were carried out in DMF because of excellent solubility of all the prepared complexes in this solvent (measured also in acetone for **1**, **4**–**6** and **8**; see Appendix I for details). The results measured in DMF were similar for [Pd(ox)(*n*L)$_2$] (**1**–**8**), [Pd(ox)(*n*Ros)$_2$] (**9**–**12**), and [Pt(ox)(*n*L)$_2$] (**13**–**19**), since their values equalled 0.1–5.8, 0.3–3.2, and 0.1–2.1 S $cm^2$ $mol^{-1}$, respectively. Although the values between 10.5 S $cm^2$ $mol^{-1}$ and 16.7 S $cm^2$ $mol^{-1}$, obtained for [Pt(ox)(*n*Ros)$_2$] (**20**–**23**), are somewhat higher than those of **1**–**19**, it is still significantly lower than 65.0 S $cm^2$ $mol^{-1}$ separating non-electrolytes and 1:1 electrolytes in DMF [72]. In other words, this method proved the non-electrolytic character of all the **1**–**23** compounds dissolved in DMF.

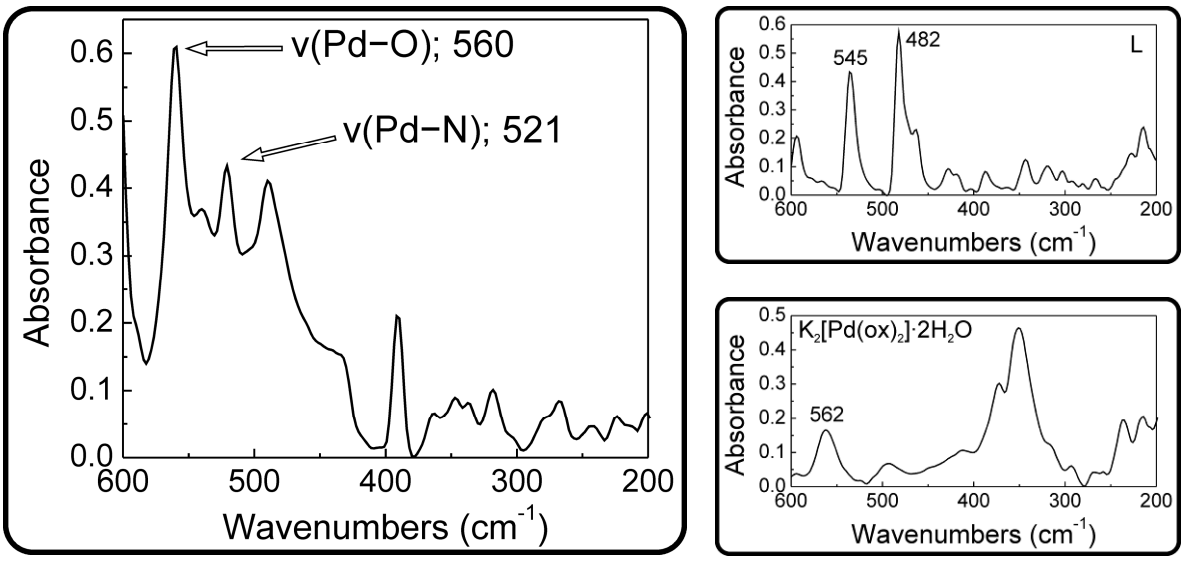


**Fig. 15.** Far-IR spectra (200–600 $cm^{-1}$) of [Pd(ox)(L)$_2$] (**1**), 2-chloro-N6-benzyl-9-isopropyladenine (L) and $K_2[Pd(ox)_2]\cdot 2H_2O$ with assignment of selected vibrations (values in $cm^{-1}$)

IR spectroscopy detected both types of ligands coordinated to the central Pd(II) (for **1**–**12**) and Pt(II) (for **13**–**23**) atoms (Fig. 15 and Fig. 16). The N6-benzyl-9-isopropyladenine derivatives, involved within the structure of **1**–**23**, showed several types of vibrations, *i.e.* $\nu(C{-}H)_{ar}$, $\nu(C{-}H)_{al}$, ν(C=N) and ν(C=C), common for all the complexes (Table 3) [73,74]. However, various compositions of these N-donor ligands brought about some differences, as follows: the $\nu(C{-}O)_{al}$ was found in the IR

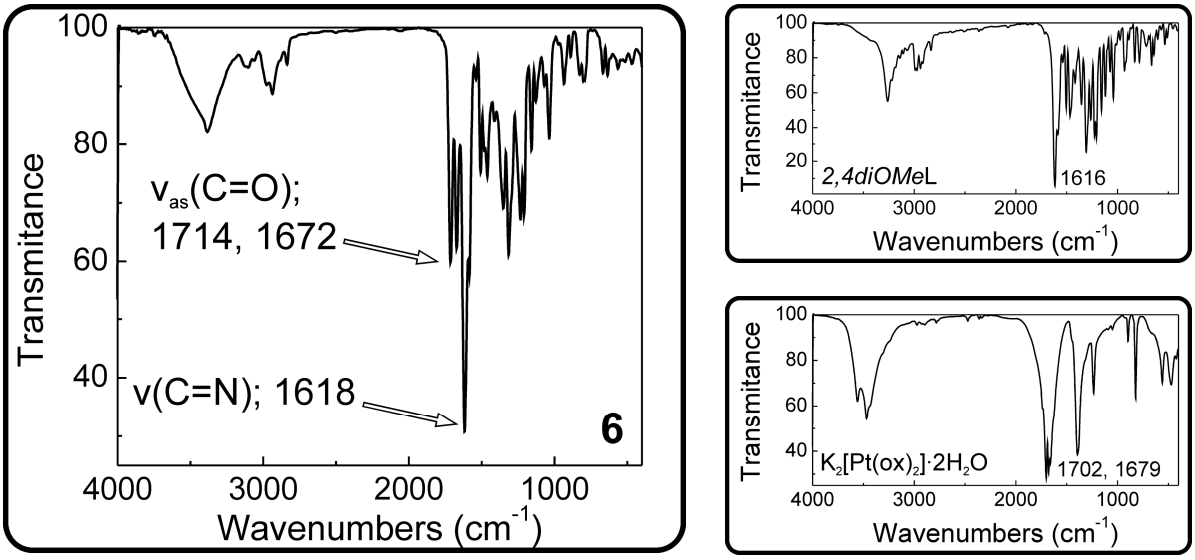


**Fig. 16.** IR spectra (400–4000 $cm^{-1}$) of [Pd(ox)(*2,4diOMe*L)$_2$]·2H$_2$O (**6**), 2-chloro-N6-(2,4-dimethoxybenzyl)-9-isopropyladenine (*2,4diOMe*L) and $K_2$[Pd(ox)$_2$]·2H$_2$O with assignment of selected vibrations (values in $cm^{-1}$)

spectra of **9**–**12** and **20**–**23**, which involve *n*Ros molecules with 2-aminobutan-1-ol in the position 2 of the adenine ring, while the ν(C−Cl) vibration was detected in the IR spectra of the other complexes (**1**–**8** and **13**–**19**) with 2-chloro-N6-benzyl-9-isopropyladenine-based N-donor ligands (Table 3). The ν(C−O)$_{ar}$ vibrations were not observed for the complexes **1**, **8**, **9**, **13** and **20**, which do not have the methoxy substituted benzene ring. The N-donor coordination of the *n*L and *n*Ros molecules to the metal centre was proved by the detection of ν(Pd−N) and ν(Pt−N). The bidentate-coordinated oxalate dianion was proved by the presence of two $\nu_{as}$(C=O) (indirectly proving bidentate-coordination type [75,76]) and one $\nu_s$(C−O) vibration (Table 3) [77]. The deformation of the five-membered chelating ring results in the band with the maximum at *ca*. 470 $cm^{-1}$. The ν(Pd−O) and ν(Pt−O) vibrations were

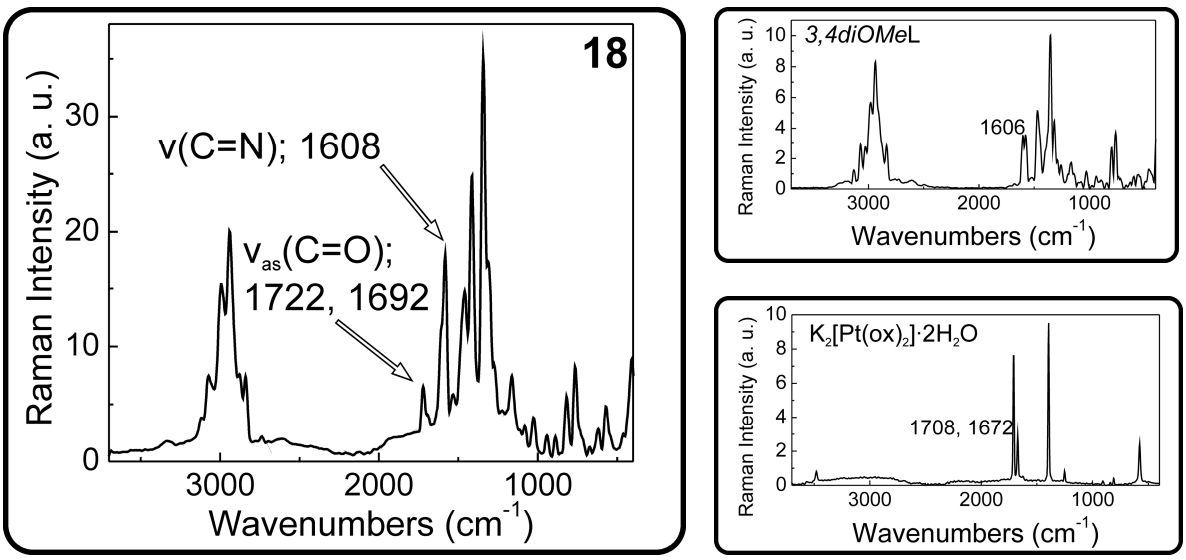


**Fig. 17.** Raman spectra (150–3750 $cm^{-1}$) of [Pt(ox)(*3,4diOMe*L)$_2$] (**18**), 2-chloro-N6-(3,4-dimethoxybenzyl)-9-isopropyladenine (*3,4diOMe*L) and $K_2$[Pt(ox)$_2$]·2H$_2$O with assignment of selected vibrations (values in $cm^{-1}$)

found as well (Table 3). The positions of the maxima of the bands related to the coordinated oxalate dianion correlated well with those detected in the $K_2[Pd(ox)_2]\cdot 2H_2O$ and $K_2[Pt(ox)_2]\cdot 2H_2O$.

Raman spectroscopy (Fig. 17) provided analogical information about the composition of the prepared complexes as compared with the above-discussed IR spectroscopy; the selected results obtained by both spectroscopic methods are given in Table 3 [74,78]. It should be mentioned that several complexes gradually decomposed under laser beam (**2** burnt immediately) which resulted in low quality of spectra and loss of some information.

**Table 3.** Selected results of IR (400–4000 $cm^{-1}$) and Raman (150–3750 $cm^{-1}$) spectroscopy of the complexes **1**–**23** (given as IR/Raman in $cm^{-1}$)

| | ν(M–N)[a,b] | ν(M–O)[a,b] | ν(C–O)$_{al}$ | ν(C–Cl) | ν(C=N) | ν$_{as}$(C=O)$_{ox}$ |
|---|---|---|---|---|---|---|
| **1** | 521s/523w | 560vs/558s | –/– | 1164w/1160m | 1617vs/1606m | 1705s, 1676m/1691w, 1671w |
| **2** | 518s/– | 559vs/– | –/– | 1163m/– | 1622vs/– | 1707vs, 1671s/– |
| **3** | 518m/n.o. | 558vs/559m | –/– | 1165w/1167m | 1618vs/n.o. | 1711m, 1675m/1703m, 1659w |
| **4** | 521vs/523w | 564vs/562s | –/– | 1157w/1157w | 1614vs/1610m | 1709s, 1677m/1695m, 1660w |
| **5** | 516m/515w | 559vs/560m | –/– | 1169w/1170m | 1619vs/1614w | 1709m, 1677m/1695m, 1676w |
| **6** | 517m/526w | 565vs/562m | –/– | 1157m/1159m | 1618vs/1610m | 1714s, 1672s/1706m, 1668w |
| **7** | 521s/521w | 560vs/560m | –/– | 1156s/1166w | 1619vs/n.o. | 1712vs, 1676s/1697m, 1657w |
| **8** | 522vs/526w | 562vs/571m | –/– | 1163w/1157m | 1617vs/1614m | 1716s, 1674m/1702m, 1670w |
| **9** | 524s/n.o. | 559vs/561m | 1058m/n.o. | –/– | 1610vs/1606vs | 1706vs, 1674s/1692m |
| **10** | 527vs/526w | 559vs/560m | 1050w/1049m | –/– | 1609vs/1606vs | 1708m, 1676m/1705w, 1672w |
| **11** | 524s/526w | 557vs/559m | 1047w/n.o. | –/– | 1609vs/1608vs | 1708m, 1676m/1701m, 1669m |
| **12** | 522vs/n.o. | 560vs/561w | 1057m/n.o. | –/– | 1608vs/1609vs | 1707vs, 1675s/1711w, 1672w |
| **13** | 541vs/n.o. | 570vs/569s | –/– | 1164w/1159w | 1618vs/1606m | 1713vs, 1672s/1700m, 1672m |
| **14** | 542vs/n.o. | 565vs/574w | –/– | 1165w/1164w | 1621vs/1602w | 1723s, 1670m/1710w, 1674w |
| **15** | 538s/534w | 572vs/569w | –/– | 1162w/1165w | 1615vs/1606m | 1706s, 1673m/1698m, 1668w |
| **16** | 538m/538w | 574vs/573m | –/– | 1169w/1168m | 1621vs/n.o. | 1722s, 1670m/1710m, 1675m |
| **17** | 540s/537w | 571vs/570m | –/– | 1158m/1160m | 1619vs/1613m | 1720s, 1670m/1709m, 1674w |
| **18** | 543vs/n.o. | 568vs/572w | –/– | 1158m/1165w | 1620vs/1608m | 1724s, 1669m/1722w, 1692w |
| **19** | 540m/n.o. | 568vs/567w | –/– | 1156s/1166w | 1620vs/n.o. | 1712vs, 1677s/1702m, 1666w |
| **20** | 527vs/524w | 566vs/569w | 1058w/1060w | –/– | 1611vs/1609vs | 1718s, 1671m/1710w, 1681w |
| **21** | 526vs/524w | 569vs/570w | 1050m/1049m | –/– | 1611vs/1607vs | 1714s, 1673m/1713m, 1677w |
| **22** | 525vs/529w | 571vs/569w | 1047m/1048w | –/– | 1610vs/1610vs | 1720m, 1691m/1711m, 1677m |
| **23** | 520vs/523w | 571vs/570w | 1058w/1063w | –/– | 1610vs/1611vs | 1711s, 1670m/1711w, 1678w |

[a] M stands for Pd for **1**–**12** and Pt for **13**–**23**
[b] measured in the 150–600 $cm^{-1}$ region
[c] signal intensities are discussed as w = weak, m = middle, s = strong and vs = very strong

TG/DTA thermal analysis proved the complexes **2**, **3**, **6**, **7**, **11** and **19**–**23** as hydrated ones (see Table 2 for details), other products were non-solvated. However, once the mentioned solvated complexes are dehydrated (*in situ*), the course of the thermal decomposition is analogical to those of the anhydrous complexes (see e.g. Fig 5 in *Appendix I*). It proceeded in several partial steps without formation of any thermally stable intermediates up to PdO (for **1**–**12**) and PtO (for **13**–**23**); PtO was stable up to the final temperature, while PdO decomposed to Pd at *ca.* 810 °C. The content of Pd and Pt in the complexes **1**–**23** was indirectly determined using the thermogravimetric method, because the observed total weight losses did not differ significantly from the calculated ones. The information obtained from the DTA curves correlated with the above-mentioned conclusions obtained from the TG curves. The processes of dehydration and thermal decomposition of PdO to Pd were accompanied by

an *endo*-effect, while several *exo*-effects on the DTA curves related to the degradation of the prepared complexes caused by rising temperature.

The results of ESI+ mass spectrometry proved the composition of the complexes **1**–**23**. The determined values of all the observed peaks as well as the observed isotopic distribution representation correlated well with the calculated ones. The molecular peaks, $[M(ox)(nL)_2+H]^+$ and $[M(ox)(nRos)_2+H]^+$, were detected for all the complexes except for **9**–**13**. In several cases the adducts with sodium {$[M(ox)(nL)_2+Na]^+$ and $[M(ox)(nRos)_2+Na]^+$} or potassium {$[M(ox)(nL)_2+K]^+$ and $[M(ox)(nRos)_2+K]^+$} ions were observed as well. The fragmentation of the studied palladium(II) and platinum(II) complexes is depicted in Figure 18, and it can be seen, that it proceeds analogically. The peaks assignable to the fragments of the $[M(ox)(nL)+H]^+$ and $[M(ox)(nRos)+H]^+$ formula were found in most mass spectra. The elimination of the oxalic acid from $[M(ox)(nL)_2+H]^+$, $[M(ox)(nRos)_2+H]^+$, $[M(ox)(nL)+H]^+$, and $[M(ox)(nRos)+H]^+$ provide the $[M(nL^-)_2+H]^+$, $[M(nRos^-)_2+H]^+$, $[M(nL^{2-})+H]^+$, and $[M(nRos^{2-})+H]^+$ fragments, respectively. Finally, the peaks of the appropriate adenine derivatives, *i.e.* $[nL+H]^+$ and $[nRos+H]^+$, were also detected in the mass spectra of the prepared oxalato complexes **1**–**23**.

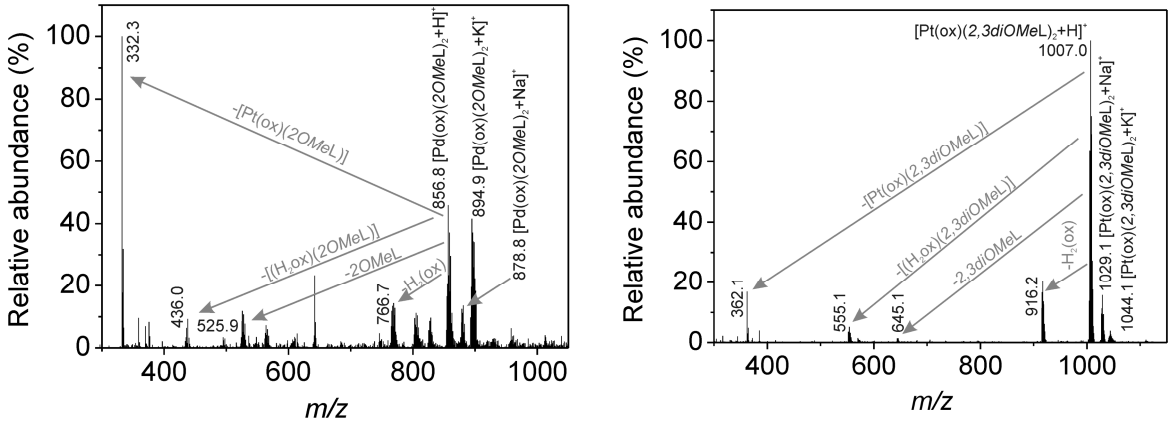


**Fig. 18.** ESI+ mass spectra of the [Pd(ox)(*2OMe*L)$_2$] (**2**; left) and [Pt(ox)(*2,3diOMe*L)$_2$] (**16**) complexes dissolved in methanol.

### *3.3.2. NMR SPECTROSCOPY*

The $^1$H, $^{13}$C and $^{195}$Pt NMR spectra and two dimensional (2D) correlation experiments ($^1$H–$^1$H gs-COSY, $^1$H–$^{13}$C gs-HMQC, $^1$H–$^{13}$C gs-HMBC and $^1$H–$^{15}$N gs-HMBC) of the DMF-$d_7$ solutions of the complexes **2**–**11**, **13**, **14**, **18** and **20**–**23,** and appropriate N6-benzyladenine derivatives, were measured at 300 K on a Varian 400 device at 400.00 MHz ($^1$H), 100.58 MHz ($^{13}$C), 40.53 MHz ($^{15}$N) and 86.00 MHz ($^{195}$Pt); the same NMR experiments of the DMF-$d_7$ solutions of the complexes **1**, **4**–**6** and **8**, **13**, and appropriate N6-benzyladenine derivatives, were measured at 300 K on a Bruker Avance 300 device at 300.00 MHz ($^1$H), 75.43 MHz ($^{13}$C), 30.40 MHz ($^{15}$N) and 64.50 MHz ($^{195}$Pt). $^1$H and $^{13}$C spectra were calibrated against the signals of tetramethylsilane ($Me_4Si$), $^{195}$Pt NMR was adjusted

**Table 4.** Calculated $^1$H NMR coordination shifts ($\Delta\delta = \delta_{complex} - \delta_{ligand}$) for palladium(II) and platinum(II) oxalato complexes **1**–**23**

| | N2H | N6H | C8H | C9H | C11H | C12H | C13H | C14H | C15H | C16H | C17H, C18H | C19H | C20Ha | C20Hb | O20H | C21Ha | C21Hb | C22H | C23H | C24H |
|---|---|---|---|---|---|---|---|---|---|---|---|---|---|---|---|---|---|---|---|---|
| *Palladium(II) complexes* | | | | | | | | | | | | | | | | | | | | |
| **1** | – | 0.57 | 0.49 | 0.06 | 0.05 | –0.02 | 0.03 | –0.02 | 0.05 | 0.04 | –0.05 | – | – | – | – | – | – | – | – | – |
| **2** | – | 0.61 | 0.40 | 0.08 | – | 0.02 | –0.03 | 0.03 | 0.12 | 0.05 | –0.05 | – | – | – | – | – | – | – | 0.04 | – |
| **3** | – | 0.34 | 0.28 | 0.05 | 0.02 | – | 0.00 | –0.03 | 0.07 | 0.01 | –0.06 | – | – | – | – | – | – | – | 0.03 | – |
| **4** | – | 0.52 | 0.44 | 0.01 | 0.00 | –0.08 | – | –0.08 | 0.00 | 0.00 | –0.09 | – | – | – | – | – | – | – | –0.02 | – |
| **5** | – | 0.63 | 0.47 | 0.07 | – | – | 0.00 | 0.00 | 0.00 | 0.06 | –0.05 | – | – | – | – | – | – | – | 0.07 | 0.02 |
| **6** | – | 0.63 | 0.42 | 0.07 | – | 0.02 | – | –0.04 | 0.08 | 0.04 | –0.06 | – | – | – | – | – | – | – | 0.03 | 0.02 |
| **7** | – | 0.52 | 0.47 | 0.07 | 0.07 | – | –0.01 | – | 0.07 | 0.03 | –0.04 | – | – | – | – | – | – | – | 0.03 | 0.03 |
| **8** | – | 0.54 | 0.47 | 0.04 | 0.04 | –0.02 | – | –0.02 | 0.04 | 0.04 | –0.06 | – | – | – | – | – | – | – | 0.03 | – |
| **9** | 0.46 | 0.71 | 0.61 | –0.03 | 0.05 | 0.01 | 0.01 | 0.01 | 0.05 | 0.06 | –0.02 | –0.01 | 0.00 | –0.07 | –0.09 | 0.01 | –0.18 | –0.01 | – | – |
| **10** | 0.49 | 0.95 | 0.54 | 0.02 | – | 0.00 | 0.01 | –0.02 | 0.06 | 0.06 | –0.03 | –0.01 | 0.00 | 0.00 | –0.07 | 0.00 | –0.04 | –0.01 | 0.01 | – |
| **11** | 0.48 | 0.77 | 0.56 | 0.01 | 0.06 | – | 0.00 | –0.02 | 0.06 | 0.07 | –0.04 | –0.02 | –0.02 | –0.03 | 0.06 | 0.00 | –0.03 | 0.01 | 0.03 | – |
| **12** | 0.49 | 0.76 | 0.55 | 0.01 | –0.01 | 0.07 | – | 0.07 | –0.01 | 0.06 | –0.03 | 0.01 | 0.02 | 0.00 | –0.01 | 0.02 | 0.00 | –0.01 | 0.01 | – |
| *Platinum(II) complexes* | | | | | | | | | | | | | | | | | | | | |
| **13** | – | 0.47 | 0.72 | 0.07 | 0.02 | –0.05 | 0.06 | –0.05 | 0.02 | 0.08 | –0.01 | – | – | – | – | – | – | – | – | – |
| **14** | – | 0.55 | 0.65 | 0.07 | – | 0.02 | 0.03 | –0.04 | 0.07 | 0.08 | –0.03 | – | – | – | – | – | – | – | 0.02 | – |
| **15** | – | 0.27 | 0.54 | 0.07 | –0.04 | – | 0.00 | –0.04 | 0.03 | 0.03 | –0.03 | – | – | – | – | – | – | – | 0.02 | – |
| **16** | – | 0.56 | 0.68 | 0.07 | – | – | 0.03 | –0.04 | 0.04 | 0.08 | –0.02 | – | – | – | – | – | – | – | 0.04 | 0.01 |
| **17** | – | 0.58 | 0.60 | 0.07 | – | 0.01 | – | –0.05 | 0.04 | 0.07 | –0.04 | – | – | – | – | – | – | – | 0.02 | 0.02 |
| **18** | – | 0.44 | 0.67 | 0.11 | 0.03 | – | – | –0.03 | 0.04 | 0.09 | –0.03 | – | – | – | – | – | – | – | 0.03 | 0.02 |
| **19** | – | 0.46 | 0.73 | 0.08 | –0.01 | – | –0.02 | – | –0.01 | 0.09 | –0.01 | – | – | – | – | – | – | – | 0.02 | 0.02 |
| **20** | 0.52 | 0.79 | 0.83 | 0.02 | 0.03 | –0.01 | 0.01 | –0.01 | 0.03 | 0.09 | –0.01 | –0.02 | –0.01 | –0.02 | 0.10 | –0.01 | –0.02 | –0.02 | – | – |
| **21** | 0.50 | 1.04 | 0.74 | 0.02 | – | –0.02 | 0.01 | –0.02 | 0.06 | 0.07 | –0.02 | –0.02 | 0.01 | 0.02 | 0.04 | 0.01 | –0.02 | –0.01 | –0.01 | – |
| **22** | 0.52 | 0.79 | 0.92 | 0.02 | 0.00 | – | –0.01 | –0.03 | 0.02 | 0.10 | –0.01 | –0.04 | –0.04 | –0.04 | 0.14 | –0.03 | –0.15 | –0.03 | 0.02 | – |
| **23** | 0.55 | 0.79 | 0.79 | 0.01 | –0.02 | 0.04 | – | 0.04 | –0.02 | 0.07 | –0.01 | –0.01 | 0.13 | 0.10 | –0.03 | 0.00 | –0.02 | –0.02 | 0.01 | – |

**Table 5.** Calculated $^{13}C$ NMR coordination shifts ($\Delta\delta = \delta_{complex} - \delta_{ligand}$) for palladium(II) and platinum(II) oxalato complexes **1**–**23**

| | C2 | C4 | C5 | C6 | C8 | C9 | C10 | C11 | C12 | C13 | C14 | C15 | C16 | C17 | C18 | C19 | C20 | C21 | C22 | C23 | C24 | C25, C26 |
|---|---|---|---|---|---|---|---|---|---|---|---|---|---|---|---|---|---|---|---|---|---|---|
| *Palladium(II) complexes* | | | | | | | | | | | | | | | | | | | | | | |
| **1** | 0.12 | –0.25 | –2.42 | –0.93 | 3.82 | 0.97 | –1.12 | 0.14 | 0.01 | 0.08 | 0.01 | 0.14 | 1.80 | –0.46 | –0.46 | – | – | – | – | – | – | –1.07 |
| **2** | 0.24 | –0.21 | –2.44 | –1.09 | 3.77 | 0.92 | –0.94 | 0.05 | 0.08 | 0.24 | 0.18 | 0.58 | 1.75 | –0.46 | –0.46 | – | – | – | – | 0.16 | – | –1.38 |
| **3** | 0.80 | –0.06 | –1.24 | –1.60 | 3.94 | 0.95 | –0.86 | –0.23 | –0.03 | 0.43 | –0.01 | 0.24 | 1.31 | –0.37 | –0.37 | – | – | – | – | 0.06 | – | –1.23 |
| **4** | –0.02 | –0.26 | –2.46 | –0.84 | 3.84 | 0.97 | –1.16 | 0.24 | –0.02 | 0.03 | –0.02 | 0.24 | 1.79 | –0.50 | –0.50 | – | – | – | – | 0.01 | – | –0.98 |
| **5** | –0.13 | –0.25 | –2.44 | –0.97 | 3.80 | 0.95 | –0.97 | 0.11 | –0.07 | 0.16 | 0.16 | 0.17 | 1.77 | –0.46 | –0.46 | – | – | – | – | 0.08 | 0.03 | –1.28 |
| **6** | 0.11 | –0.24 | –2.43 | –1.00 | 3.84 | 0.84 | –1.56 | 0.06 | 0.07 | 0.13 | 0.15 | 0.44 | 1.71 | –0.45 | –0.45 | – | – | – | – | 0.16 | 0.00 | –1.52 |
| **7** | 0.19 | –0.21 | –2.37 | –0.93 | 3.70 | 1.08 | –1.03 | 0.11 | 0.01 | 0.70 | 0.01 | 0.11 | 1.74 | –0.41 | –0.41 | – | – | – | – | 0.12 | 0.12 | –1.36 |
| **8** | 0.07 | –0.24 | –2.45 | –0.91 | 3.82 | 0.96 | –1.12 | 0.19 | 0.03 | 0.09 | 0.03 | 0.19 | 1.81 | –0.47 | –0.47 | – | – | – | – | 0.09 | – | –1.18 |
| **9** | 0.13 | –0.42 | –3.12 | –2.20 | 3.50 | 0.68 | –1.15 | 0.08 | 0.02 | 0.01 | 0.02 | 0.08 | 1.55 | –0.54 | –0.54 | 0.02 | –0.44 | –0.19 | –0.10 | – | – | –0.75 |
| **10** | 0.21 | –0.28 | –2.97 | –2.22 | 3.53 | 0.67 | –0.97 | 0.07 | 0.04 | 0.36 | 0.17 | 0.16 | 1.52 | –0.51 | –0.51 | 0.12 | –0.39 | –0.13 | –0.03 | 0.12 | – | –1.01 |
| **11** | 0.18 | –0.34 | –3.09 | –2.12 | 3.58 | 0.93 | –1.06 | –0.36 | 0.13 | 0.61 | 0.06 | 0.17 | 1.54 | –0.48 | –0.49 | 0.06 | –0.39 | –0.15 | –0.05 | 0.11 | – | –0.91 |
| **12** | 0.20 | –0.30 | –3.08 | –2.14 | 3.63 | 0.95 | –1.18 | 0.07 | 0.23 | 0.06 | 0.23 | 0.07 | 1.63 | –0.50 | –0.46 | 0.09 | –0.38 | –0.13 | –0.06 | 0.02 | – | –0.85 |
| *Platinum(II) complexes* | | | | | | | | | | | | | | | | | | | | | | |
| **13** | 0.00 | –0.63 | –2.81 | –0.88 | 4.27 | 0.85 | –1.12 | –0.12 | 0.02 | 0.06 | 0.02 | –0.12 | 1.94 | –0.42 | –0.42 | – | – | – | – | – | – | –1.93 |
| **14** | 0.07 | –0.61 | –2.87 | –1.02 | 4.25 | 0.98 | –1.02 | 0.02 | 0.08 | 0.27 | 0.17 | 0.29 | 1.89 | –0.44 | –0.44 | – | – | – | – | 0.14 | – | –2.18 |
| **15** | –0.41 | –0.44 | –1.67 | –0.46 | 4.34 | 0.78 | –0.82 | –0.53 | –0.01 | 0.32 | –0.01 | –0.06 | 1.43 | –0.32 | –0.32 | – | – | – | – | 0.06 | – | –1.95 |
| **16** | 0.51 | –0.66 | –2.87 | –0.93 | 4.26 | 0.92 | –0.95 | –0.26 | –0.69 | 0.05 | 0.16 | –0.38 | 1.84 | –0.43 | –0.43 | – | – | – | – | –0.06 | –0.03 | –2.05 |
| **17** | –0.08 | –0.65 | –2.85 | –0.94 | 4.37 | 0.92 | –1.67 | 0.04 | 0.09 | 0.16 | 0.11 | 0.20 | 1.86 | –0.44 | –0.44 | – | – | – | – | 0.16 | 0.00 | –2.29 |
| **18** | –0.07 | –0.55 | –2.73 | –0.81 | 4.31 | 0.89 | –1.16 | –0.18 | 0.02 | 0.04 | –0.07 | 0.14 | 1.83 | –0.41 | –0.41 | – | – | – | – | –0.01 | 0.11 | –2.06 |
| **19** | 0.04 | –0.61 | –2.85 | –0.89 | 4.07 | 0.86 | –1.00 | –0.29 | –0.01 | 0.52 | –0.01 | –0.29 | 1.86 | –0.40 | –0.40 | – | – | – | – | 0.10 | 0.10 | –1.98 |
| **20** | 0.15 | –0.72 | –3.50 | –2.32 | 3.82 | 0.72 | –1.20 | –0.06 | 0.05 | 0.04 | 0.05 | –0.06 | 1.70 | –0.45 | –0.38 | 0.07 | –0.42 | –0.18 | –0.10 | – | – | –1.57 |
| **21** | 0.20 | –0.80 | –3.52 | –2.42 | 3.86 | 0.73 | –1.12 | 0.09 | 0.05 | 0.30 | 0.18 | 0.28 | 1.76 | –0.46 | –0.46 | 0.11 | –0.40 | –0.15 | –0.03 | 0.13 | – | –1.68 |
| **22** | 0.17 | –0.78 | –3.45 | –2.27 | 3.86 | 0.74 | –1.07 | –0.57 | 0.06 | 0.61 | 0.09 | –0.06 | 1.84 | –0.42 | –0.39 | 0.07 | –0.42 | –0.16 | –0.08 | 0.12 | – | –1.58 |
| **23** | 0.19 | –0.76 | –3.51 | –2.31 | 3.95 | 0.88 | –1.26 | 0.08 | 0.10 | 0.06 | 0.10 | 0.08 | 1.69 | –0.45 | –0.31 | 0.28 | –0.41 | –0.16 | –0.05 | 0.01 | – | –1.64 |

against potassium hexachloroplatinate, $K_2PtCl_6$, in $D_2O$ found at 0 ppm. $^1H–^{15}N$ gs-HMBC experiments were obtained at natural abundance and calibrated against the residual signals of the DMF adjusted to 104.7 ppm. The results (Table 4, Table 5 and Table 6) are discussed as coordination shifts ($\Delta\delta$; ppm), calculated as the difference of the chemical shift of the complex ($\delta_{complex}$; ppm) and the chemical shift of the appropriate N6-benzyl-9-isopropyladenine derivative ($\delta_{ligand}$; ppm).

Formerly, a single crystal X-ray analysis and detail NMR studies proved that N6-benzyl-9-isopropyladenine-based molecules coordinate to the Pd(II) and Pt(II) ions through the N7 atom of the adenine moiety, within the structure of mononuclear palladium(II) and platinum(II) dichlorido complexes [23,25–29]. The oxalato complexes **1**–**23** discussed in this thesis involve the same type of the N-donor ligand, that is why we supposed the same coordination mode, which was unambiguously confirmed by the multinuclear and two dimensional NMR study (described in this section) and a single crystal analysis, which is discussed in the separate section below.

The signals of all the hydrogen atoms detected in free N6-benzyl-9-isopropyladenine analogues were also found in the $^1H$ NMR spectra of the appropriate complexes (Fig. 19 left). The C8H and N6H protons have the highest $\Delta\delta$. It is caused by the electron density redistribution caused by the coordination to the metal centre through the N7 atom. Table 4 summarizes the $^1H$ NMR coordination shifts calculated for all the protons included in the structures of **1**–**23**.

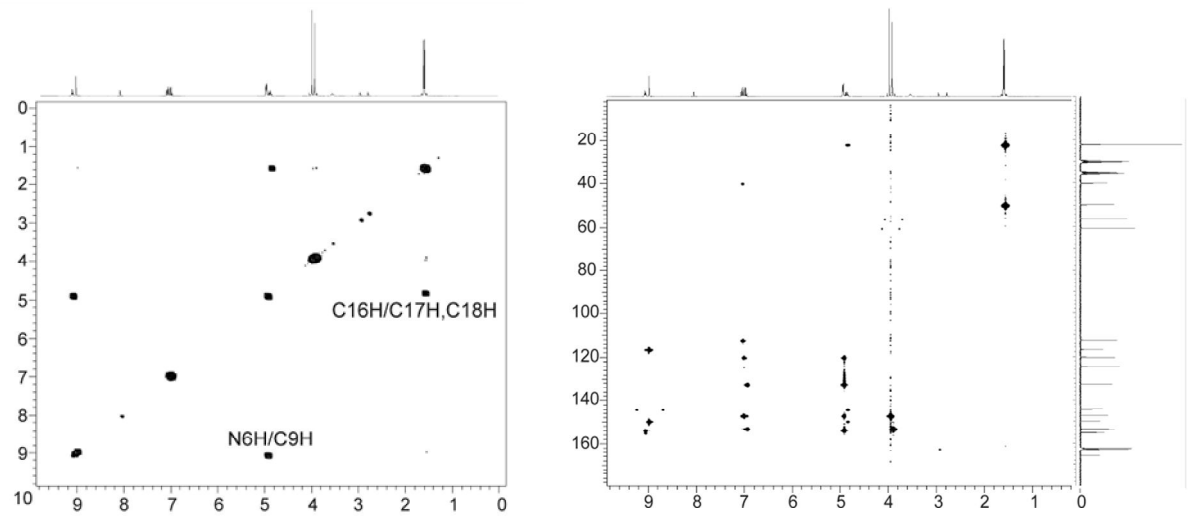


**Fig. 19.** $^1H–^1H$ gs-COSY (left) and $^1H–^{13}C$ gs-HMQC spectra (right) of [Pt(ox)(*2,3diOMe*L)$_2$] (**16**)

The same conclusion can be made also for the $^{13}C$ NMR spectroscopy. Again, the signals of all the carbon atoms of free N6-benzyl-9-isopropyladenine derivatives were observed in the carbon spectra of the complexes, where these organic molecules act as N-donor ligands (Table 5). It should be noted one more time that the signals were assigned by means of $^1H–^{13}C$ gs-HMQC and $^1H–^{13}C$ gs-HMBC experiments (Fig. 19 right). The most shifted signals are those of C8 (downfield) and C5 (upfield) atoms, followed by C6, C9, C10 and C16. These changes of chemical shifts are in cases of C5, C6 and

C8 caused by the coordination of *n*L and *n*Ros molecules to the central atoms. For C9, C10 and C16 it is most likely caused by the different orientation and steric inhibition of the rotation of the benzyl (for C9 and C10) and isopropyl (for C16) groups in consequence of the complex formation. A type of N-donor ligand (*n*L or *n*Ros) involved in the complex structures resulted in different Δδ for some of mentioned carbons. The C8 coordination shifts of **9**–**12** and **20**–**23**, which involve the *n*Ros type of ligands, were determined to be somehow lower as compared with the complexes with *n*L molecules. However, this difference is even more obvious for the C5 and C6 coordination shifts. One more signal was detected at *ca.* 166 ppm in the $^{13}$C NMR spectra of **1**–**23** than for free N6-benzyl-9-isopropyladenine derivatives. This region is typical for the carboxyl group and, moreover, this signal was not detected in the mentioned 2D experiments. This signal unambiguously belongs to the bidentate coordinated oxalate dianion.

**Table 6.** $^{15}$N NMR coordination shifts ($\Delta\delta = \delta_{complex} - \delta_{ligand}$) and $^{195}$Pt NMR chemical shifts for **1**–**23**; n.o. = not observed

| | N1 | N2 | N3 | N6 | N7 | N9 | $^{195}$Pt |
|---|---|---|---|---|---|---|---|
| *Palladium(II) complexes* | | | | | | | |
| **1** | 4.4 | – | 0.1 | 7.1 | –92.4 | 7.1 | – |
| **2** | 2.7 | – | –0.9 | 8.2 | –93.0 | 7.3 | – |
| **3** | 1.5 | – | –5.5 | 1.6 | –98.2 | 1.9 | – |
| **4** | 5.9 | – | 2.0 | 8.3 | –91.2 | 9.0 | – |
| **5** | 4.0 | – | –0.3 | 6.5 | –92.4 | 6.2 | – |
| **6** | 2.5 | – | –1.3 | 7.7 | –94.0 | 6.1 | – |
| **7** | 3.6 | – | –0.9 | 6.5 | –92.7 | 6.4 | – |
| **8** | 4.4 | – | n.o. | 7.3 | –92.8 | 6.9 | – |
| **9** | 2.0 | 2.6 | n.o. | 4.0 | –96.5 | 6.7 | – |
| **10** | –1.3 | –1.3 | | 5.7 | –99.0 | 3.7 | – |
| **11** | –0.3 | 3.6 | n.o. | 8.8 | –94.5 | 7.3 | – |
| **12** | –2.8 | –3.4 | n.o. | 12.6 | –102.6 | 1.5 | – |
| *Platinum(II) complexes* | | | | | | | |
| **13** | 4.9 | – | 0.3 | 5.5 | –111.5 | 6.9 | –1685 |
| **14** | 3.8 | – | –0.8 | 7.9 | –111.6 | 7.0 | –1691 |
| **15** | 6.6 | – | 1.5 | 2.9 | –114.0 | 5.4 | –1689 |
| **16** | 3.9 | – | –1.0 | 5.1 | –111.5 | 5.3 | –1689 |
| **17** | 2.4 | – | –1.7 | 6.8 | –113.1 | 5.7 | –1685 |
| **18** | 3.8 | – | –0.6 | 5.1 | –111.6 | 6.5 | –1688 |
| **19** | 3.7 | – | –1.6 | 3.9 | –112.4 | 5.8 | –1694 |
| **20** | 6.8 | 4.0 | 7.6 | 1.8 | –115.8 | 5.6 | –1676 |
| **21** | –2.0 | –1.4 | 2.1 | 4.1 | –119.1 | 1.3 | –1676 |
| **22** | 4.4 | 3.7 | 10.9 | 6.8 | –114.5 | 6.7 | –1676 |
| **23** | –1.7 | –3.6 | 3.0 | 11.0 | –121.5 | 0.9 | –1676 |

$^{1}$H–$^{15}$N gs-HMBC detected most of the nitrogen atoms involved in the *n*L or *n*Ros ligands coordinated to the Pd(II) and Pt(II) ions in the complexes **1**–**23** (some of the N3 atoms were not

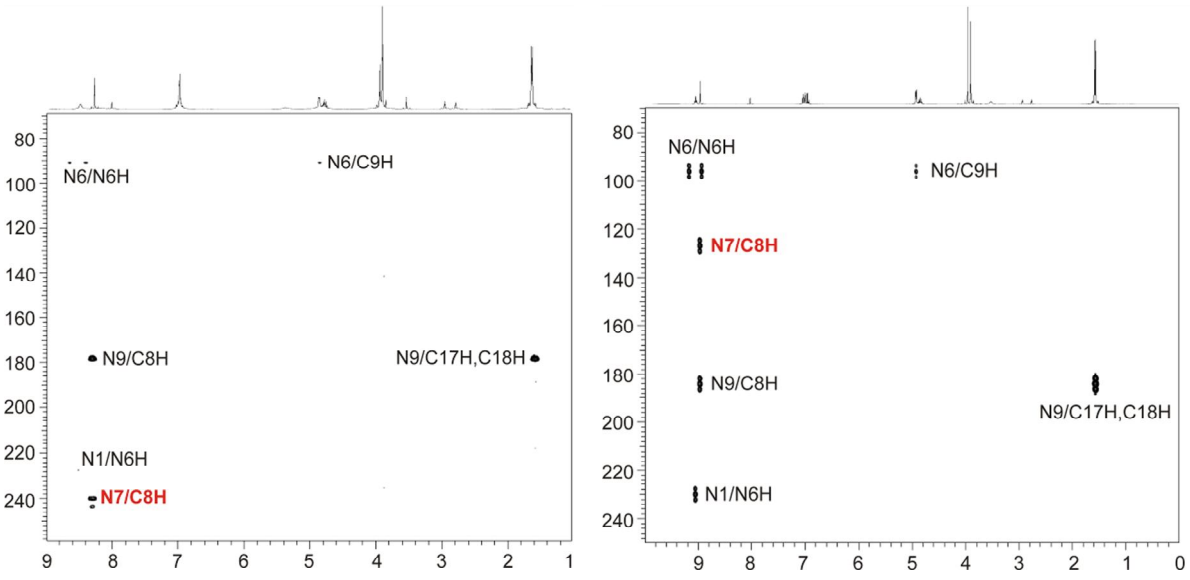


**Fig. 20.** $^{1}$H–$^{15}$N gs-HMBC spectra of 2-chloro-N6-(2,3-dimethoxybenzyl)-9-isopropyladenine (*2,3diOMe*L; left) and [Pt(ox)(*2,3diOMe*L)$_2$] (**16**) (right)

detected). As it is clearly seen from the results given in Table 6 and Fig. 20, Δδ of the N7 atom is several times higher as compared to the other nitrogen atoms, which directly proves the monodentate coordination of the N6-benzyl-9-isopropyladenine derivatives through this atom. The N7 signals of both the palladium(II) and platinum(II) complexes involving *n*Ros ligands are more shifted than the complexes with *n*L ones.

The $^{195}$Pt NMR chemical shifts, observed between –1676 ppm and –1694 ppm, differ between the [Pt(ox)(*n*L)$_2$] and [Pt(ox)(*n*Ros)$_2$] complexes (Table 6).

### *3.3.3. X-RAY CRYSTALLOGRAPHY*

The crystals suitable for a single crystal X-ray analysis were obtained in the cases of the palladium(II) complexes **4** and **8** and platinum(II) complex **17**. The data were collected on an Xcalibur$^{TM}$2 diffractometer (Oxford Diffraction Ltd.) with Sapphire2 CCD detector and with Mo Kα (Monochromator Enhance, Oxford Diffraction Ltd.). Data collection and reduction were performed using CrysAlis RED and CrysAlis CCD software [79]. The same software was used for data correction for an absorption effect by the empirical absorption correction using spherical harmonics,

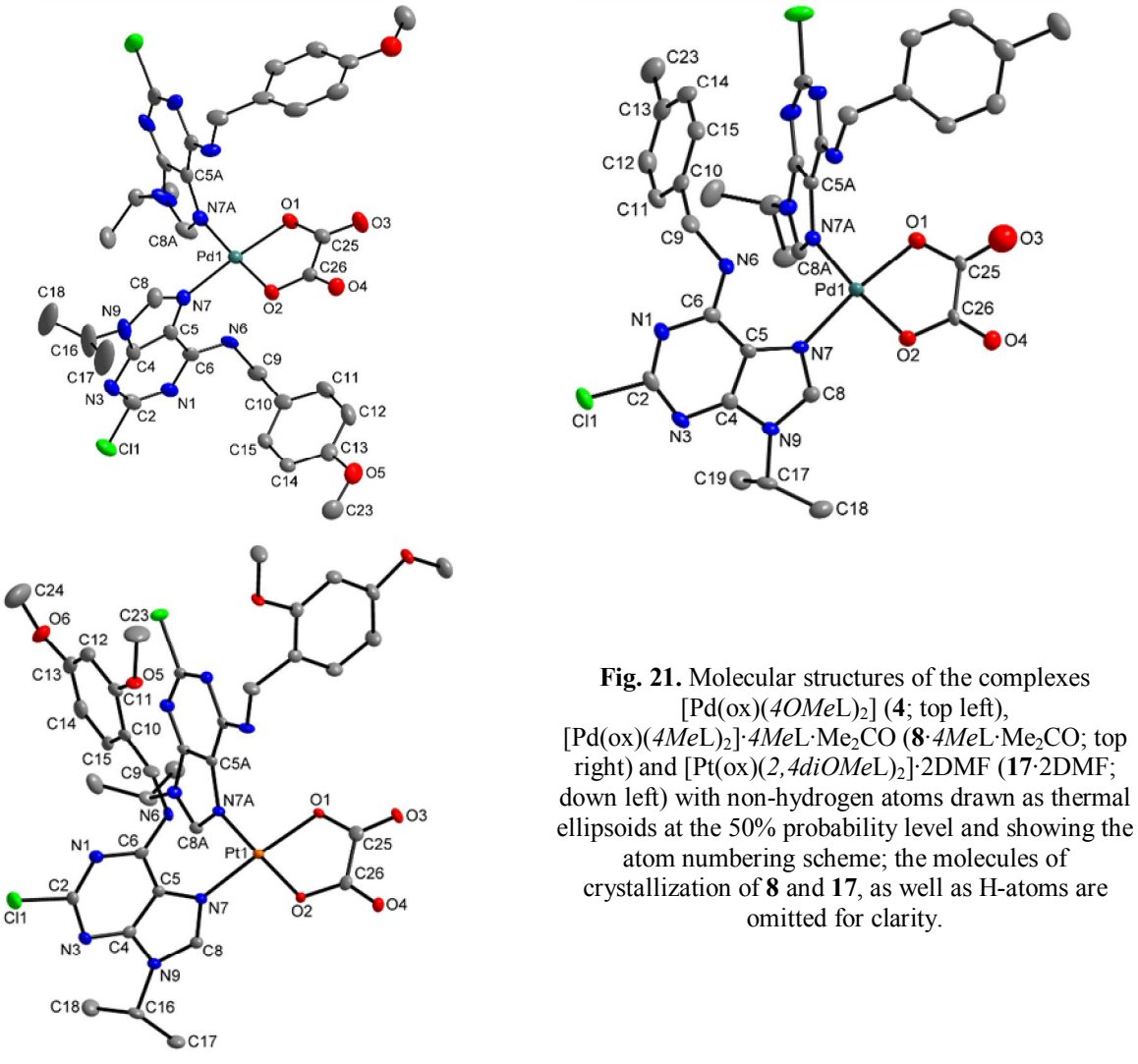


**Fig. 21.** Molecular structures of the complexes [Pd(ox)(*4OMe*L)$_2$] (**4**; top left), [Pd(ox)(*4Me*L)$_2$]·*4Me*L·Me$_2$CO (**8**·*4Me*L·Me$_2$CO; top right) and [Pt(ox)(*2,4diOMe*L)$_2$]·2DMF (**17**·2DMF; down left) with non-hydrogen atoms drawn as thermal ellipsoids at the 50% probability level and showing the atom numbering scheme; the molecules of crystallization of **8** and **17**, as well as H-atoms are omitted for clarity.

implemented in SCALE3 ABSPACK scaling algorithm. The structure was solved by direct methods using SHELXS-97 and refined on $F^2$ using the full-matrix least-squares procedure (SHELXL-97) [80,81]. More details regarding the X-ray crystallography measurement conditions can be found below in the Appendix section. The molecular graphics as well as additional structural calculations were drawn and interpreted using DIAMOND [82].

The crystal data and structure refinements, as well as the figures of the molecular and crystal structures of [Pd(ox)(*4OMe*L)$_2$] (**4**) and [Pd(ox)(*4Me*L)$_2$]·*4Me*L·Me$_2$CO (**8**·*4Me*L·Me$_2$CO) are given in *Appendix I*, while in the case of [Pt(ox)(*2,4diOMe*L)$_2$]·2DMF (**17**·2DMF) it can be found in *Appendix III* and its Supplementary Data.

The complexes **4**, **8** and **17** have the tetra-coordinated central atom and the geometry in its vicinity is distorted square-planar for all these complexes (Fig. 21). An oxalate dianion is bidentate-coordinated through its O1 and O2 atoms. The O3 and O4 atoms are not coordinated to the metal centre and they are more often than the O1 and O2 atoms involved in the network of non-bonding interactions (hydrogen bonds, van der Waals interactions). Both the N6-benzyl-9-isopropyladenine derivatives, involved in the structures of the discussed complexes, were found to be coordinated to the central atoms through the N7 atom of the adenine moiety. An arrangement of the *n*L molecules within the structure of complexes can be described as head-to-head (for **4**) and head-to-tail (for **8** and **17**).

**Table 8.** The selected bond lengths and angles for **4**, **8**·*4Me*L·Me$_2$CO and **17**·2DMF

| | **4** | **8** | **17** | | **4** | **8** | **17** |
|---|---|---|---|---|---|---|---|
| *Bond lengths* | | | | *Bond angles* | | | |
| M1−O1 | 1.992(2) | 1.971(2) | 2.010(2) | O1−M1−O2 | 84.46(9) | 84.20(9) | 83.90(9) |
| M1−O2 | 1.987(2) | 1.983(2) | 1.994(2) | O1−M1−N7 | 174.96(10) | 173.26(10) | 175.93(10) |
| M1−N7 | 2.012(3) | 2.023(3) | 2.001(3) | O1−M1−N7A | 93.09(10) | 89.86(10) | 94.33(10) |
| M1−N7A | 2.024(3) | 2.021(3) | 2.001(3) | O2−M1−N7 | 91.12(10) | 89.38(10) | 92.03(10) |
| O1−C25 | 1.302(4) | 1.332(4) | 1.304(4) | O2−M1−N7A | 177.10(10) | 171.75(10) | 176.98(10) |
| O2−C26 | 1.289(4) | 1.282(4) | 1.303(4) | N7−M1−N7A | 91.39(11) | 96.32(11) | 89.74(11) |
| N7−C5 | 1.394(4) | 1.397(4) | 1.388(4) | M1−O1−C25 | 111.8(2) | 110.6(2) | 112.1(2) |
| N7A−C5A | 1.390(4) | 1.392(4) | 1.397(4) | M1−O2−C26 | 111.8(2) | 111.5(2) | 113.2(2) |
| N7−C8 | 1.327(4) | 1.316(4) | 1.318(4) | M1−N7−C5 | 127.9(2) | 135.8(2) | 128.2(2) |
| N7A−C8A | 1.319(4) | 1.327(4) | 1.327(4) | M1−N7A−C5A | 129.8(2) | 129.9(2) | 132.3(2) |
| | | | | M1−N7−C8 | 126.9(2) | 119.2(2) | 126.2(2) |
| | | | | M1−N7A−C8A | 124.8(2) | 119.6(2) | 121.9(2) |
| | | | | C5−N7−C8 | 105.2(3) | 105.0(3) | 105.6(3) |
| | | | | C5A−N7A−C8A | 105.4(3) | 105.3(3) | 105.5(3) |

The Pd−O bond lengths (Table 8) of the complexes fall to the interval of 1.956–2.068 Å (the mean value is 2.012 Å) determined for ten palladium complexes with the tetra-coordinated central atom in the square-planar geometry and involving the bidentate-coordinated oxalato group {a [Pd(ox)] motif}, which have been up to now deposited in the Cambridge Structural Database (CSD). Five of these complexes have a $PdN_2O_2$ chromophore and their Pd−N bond length mean is equal to 2.006 Å (1.983–2.027 Å interval). In the case of platinum oxalato complexes, 34 compounds with a [Pt(ox)] motif

have been deposited in CSD to date. Their average Pt−O bond length is 2.020 Å (1.947–2.080 Å). Fifteen of these complexes have a $PtN_2O_2$ donor set and their Pt−N bond lengths were determined to be between 1.904 and 2.060 Å (mean value of 2.015 Å).

The molecular structure of 2-chloro-N6-(2,4-dimethoxybenzyl)-9-isopropyladenine (*2,4diOMe*L) was determined by a single crystal X-ray analysis (see Section 3.2.2). This organic compound acts as an N-donor ligand within the structure of the complex **17**, whose structure was also crystallographically determined. It allows us to compare bond lengths and angles of the free *2,4diOMe*L molecule and the coordinated one. The most significant change was due to coordination through the N7 atom found for the C5−N7−C8 angle.

### 3.4. IN VITRO CYTOTOXICITY TESTING

*In vitro* cytotoxic activities of the selected complexes were determined against the human ovarian carcinoma cells (A2780), human ovarian carcinoma *cisplatin* resistant cells (A2780cis), human malignant melanoma (G361), human breast adenocarcinoma (MCF7), human lung carcinoma (A549), human osteosarcoma (HOS) and human cervix epitheloid carcinoma (HeLa) cancer cell lines and against the primary cultures of human hepatocytes obtained from an adult multidonor patient (LH32) by an MTT assay [MTT = 3-(4,5-dimethylthiazol-2-yl)-2,5-diphenyltetrazolium bromide]. The $IC_{50}$ values of the tested complexes were compared with those of commercially used platinum-based drugs *cisplatin*, *carboplatin* and *oxaliplatin* (Table 9, Fig. 22). All the tested complexes were dissolved in DMF instead of DMSO, which is usually used during *in vitro* cytotoxicity testing. DMSO was not used because it easily coordinates the Pd(II) and Pt(II) atoms and thus replaces the ligands in the tested complexes.

The evaluation of the *in vitro* cytotoxic activity was in many cases limited by low solubility of the tested complexes in the mixture of DMF and the cell culture medium with the final DMF concentrations of 0.1%. However, several $IC_{50}$ values are very promising for the future study of these complexes. For example, the complexes **15** and **17** showed significant *in vitro* cytotoxicity against both A2780 and its *cisplatin*-resistant analogue A2780cis, which is several times higher as compared with *cisplatin*. The most promising results within the palladium(II) oxalato complexes, which could be mentioned here, were those of **8** (against HeLa cancer cells) **9** (against MCF7) and **12** (against A2780 cancer cell line), whose $IC_{50}$ values were again significantly lower as compared with platinum-based drug *cisplatin*. The obtained results are graphically depicted in Fig. 22 and summarized in Table 9, while the detail discussion of the *in vitro* cytotoxicity of the prepared compounds can be found in *Appendix IV* and *Appendix V*.

The selected representatives were tested for their *in vitro* toxicity against primary human hepatocytes and they can be considered as safe for the human organism since they did not affect the mentioned hepatocytes in the tested concentration range.

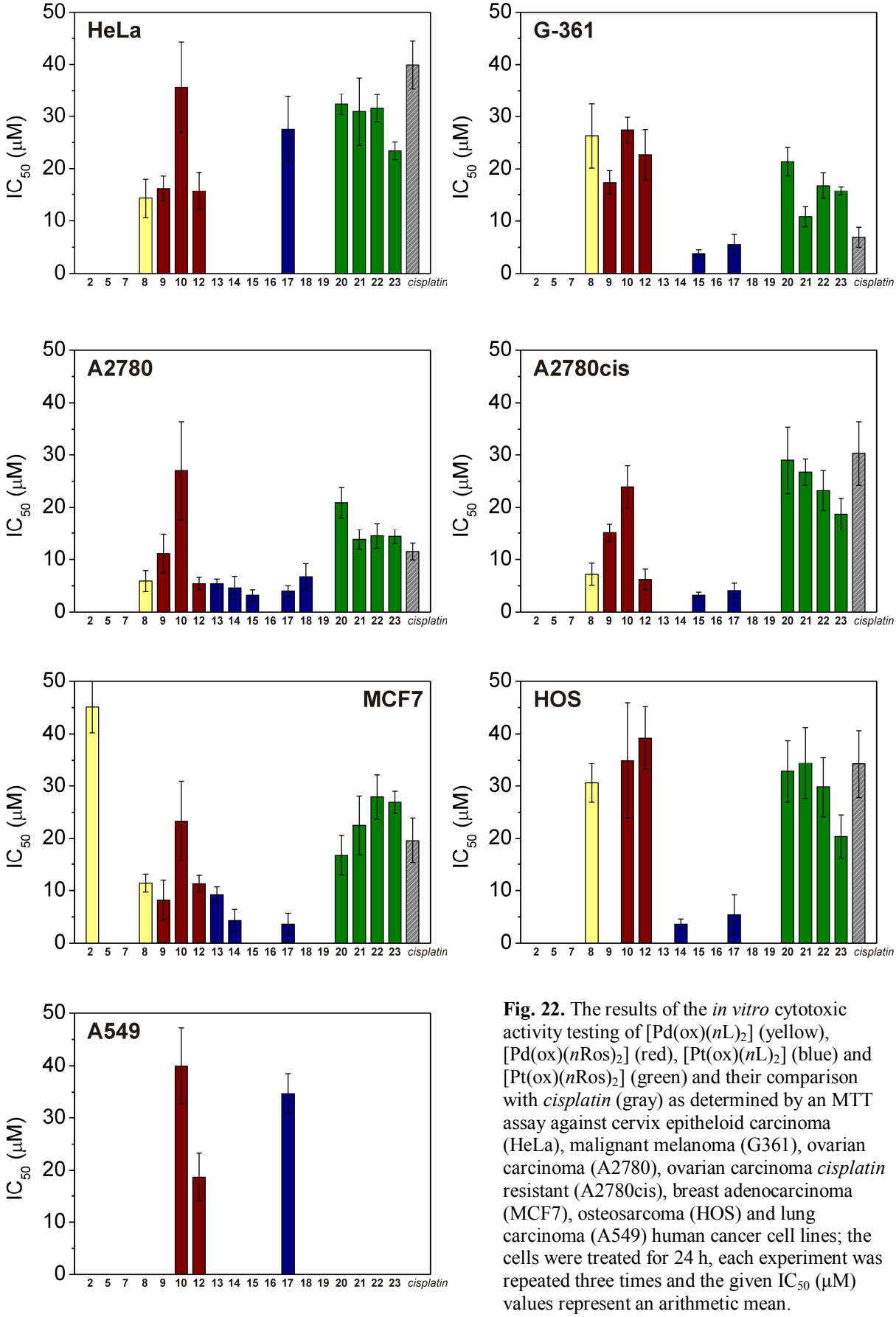


**Fig. 22.** The results of the *in vitro* cytotoxic activity testing of [Pd(ox)(*n*L)$_2$] (yellow), [Pd(ox)(*n*Ros)$_2$] (red), [Pt(ox)(*n*L)$_2$] (blue) and [Pt(ox)(*n*Ros)$_2$] (green) and their comparison with *cisplatin* (gray) as determined by an MTT assay against cervix epitheloid carcinoma (HeLa), malignant melanoma (G361), ovarian carcinoma (A2780), ovarian carcinoma *cisplatin* resistant (A2780cis), breast adenocarcinoma (MCF7), osteosarcoma (HOS) and lung carcinoma (A549) human cancer cell lines; the cells were treated for 24 h, each experiment was repeated three times and the given IC$_{50}$ (μM) values represent an arithmetic mean.

**Table 9.** $IC_{50}$ values (μM) evaluated for the selected palladium(II) and platinum(II) complexes as well as for platinum-based drugs *cisplatin*, *carboplatin* and *oxaliplatin* on different human cancer cell lines and primary culture of human hepatocytes (LH32)

| Complex | A549 | HeLa | G-361 | A2780 | A2780cis | HOS | MCF7 | LH32 |
|---|---|---|---|---|---|---|---|---|
| [Pd(ox)(L)$_2$] (**1**) | – | – | – | – | – | – | >25.0[a] | – |
| [Pd(ox)(*2OMe*L)$_2$]·¾H$_2$O (**2**) | >50.0 | >50.0 | >50.0 | >50.0 | >50.0 | >50.0 | 45.1±4.9 | >50.0 |
| [Pd(ox)(*3OMe*L)$_2$]·¾H$_2$O (**3**) | – | – | – | – | – | – | – | – |
| [Pd(ox)(*4OMe*L)$_2$] (**4**) | – | – | – | – | – | – | >12.5[a] | – |
| [Pd(ox)(*2,3diOMe*L)$_2$] (**5**) | >1.0 | >1.0 | >1.0 | >1.0 | >1.0 | >1.0 | >1.0 (6.2[a]) | – |
| [Pd(ox)(*2,4diOMe*L)$_2$]·2H$_2$O (**6**) | – | – | – | – | – | – | >12.5[a] | – |
| [Pd(ox)(*3,5diOMe*L)$_2$]·3H$_2$O (**7**) | >5.0 | >5.0 | >5.0 | >5.0 | >5.0 | >5.0 | >5.0 | – |
| [Pd(ox)(*4Me*L)$_2$] (**8**) | >50.0 | 14.3±3.7 | 26.3±6.1 | 5.9±2.0 | 7.2±2.1 | 30.6±3.7 | 11.4±1.7 (6.8[a]) | >50.0 |
| [Pd(ox)(Ros)$_2$] (**9**) | >25.0 | 16.2±2.4 | 17.4±2.3 | 11.1±3.7 | 15.1±1.7 | >25.0 | 8.2±3.8 | >25.0 |
| [Pd(ox)(*2OMe*Ros)$_2$] (**10**) | 39.9±7.3 | 35.6±8.7 | 27.4±2.4 | 27.0±9.4 | 23.9±4.0 | 34.9±11.0 | 23.3±7.6 | >50.0 |
| [Pd(ox)(*3OMe*Ros)$_2$]·H$_2$O (**11**) | – | – | – | – | – | – | – | – |
| [Pd(ox)(*4OMe*Ros)$_2$] (**12**) | 18.7±4.6 | 15.7±3.6 | 22.7±4.8 | 5.4±1.2 | 6.2±2.0 | 39.2±6.0 | 11.3±1.6 | >50.0 |
| [Pt(ox)(L)$_2$] (**13**) | >10.0 | >10.0 | >10.0 | 5.4±0.9 | >10.0 | >10.0 | 9.2±1.5 | – |
| [Pt(ox)(*2OMe*L)$_2$] (**14**) | >50.0 | >50.0 | >50.0 | 4.6±2.2 | >50.0 | 3.6±1.0 | 4.3±2.1 | >50.0 |
| [Pt(ox)(*3OMe*L)$_2$] (**15**) | >5.0 | >5.0 | 3.8±0.7 | 3.2±1.0 | 3.2±0.6 | >5.0 | >5.0 | >5.0 |
| [Pt(ox)(*2,3diOMe*L)$_2$] (**16**) | >1.0 | >1.0 | >1.0 | >1.0 | >1.0 | >1.0 | >1.0 | – |
| [Pt(ox)(*2,4diOMe*L)$_2$] (**17**) | 34.7±3.8 | 27.5±6.3 | 5.5±2.0 | 4.0±1.0 | 4.1±1.4 | 5.4±3.8 | 3.6±2.1 | >50.0 |
| [Pt(ox)(*3,4diOMe*L)$_2$] (**18**) | >10.0 | >10.0 | >10.0 | 6.7±2.5 | >10.0 | >10.0 | >10.0 | – |
| [Pt(ox)(*3,5diOMe*L)$_2$]·4H$_2$O (**19**) | >1.0 | >1.0 | >1.0 | >1.0 | >1.0 | >1.0 | >1.0 | – |
| [Pt(ox)(Ros)$_2$]·¾H$_2$O (**20**) | >50.0 | 32.3±2.0 | 21.4±2.7 | 20.9±2.9 | 29.0±6.4 | 32.8±5.9 | 16.8±3.8 | >50.0 |
| [Pt(ox)(*2OMe*Ros)$_2$]·H$_2$O (**21**) | >50.0 | 30.9±6.5 | 10.8±1.9 | 13.8±1.9 | 26.7±2.5 | 34.4±6.8 | 22.5±5.6 | – |
| [Pt(ox)(*3OMe*Ros)$_2$]·½H$_2$O (**22**) | >50.0 | 31.5±2.6 | 16.8±2.5 | 14.5±2.4 | 23.2±3.8 | 29.8±5.7 | 27.9±4.2 | – |
| [Pt(ox)(*4OMe*Ros)$_2$]·¾H$_2$O (**23**) | >50.0 | 23.4±1.7 | 15.8±0.8 | 14.4±1.4 | 18.7±3.0 | 20.4±4.1 | 26.9±2.1 | – |
| *cisplatin* | >50.0 | 39.9±4.6 | 6.9±1.9 | 11.5±1.6 | 30.3±6.1 | 34.2±6.4 | 19.6±4.3 | >50.0 |
| *oxaliplatin* | >50.0 | >50.0 | >50.0 | >50.0 | >50.0 | >50.0 | >50.0 | >50.0 |
| *carboplatin* | >1.0 | >1.0 | >1.0 | >1.0 | >1.0 | >1.0 | >1.0 | – |

[a] the complexes **1**, **4**–**6** and **8** tested also by an AM assay against MCF7 (results in table) and chronic myelogenous leukaemia (K562; $IC_{50}$ = 16.2 μM for **5**, > 12.5 μM for **2** and **4** and >25.0 μM for **1** and **3**

It has been mentioned (Section 2.2.) that the action of *cisplatin* and *oxaliplatin* is conditioned by a substitution of the leaving groups (chloride ions, oxalate dianion) by water or $OH^-$ [42]. Moreover, any other type of platinum-based drugs action has not been observed to date. That is why the formation of diaqua- or dihydroxy-complexes and their subsequent interaction with nuclear DNA is anticipated for the complexes **1**–**23**, as well. However, the mentioned types of palladium(II) and platinum(II) complexes were not observed by NMR spectroscopy in the DMF/water mixture. In more detail, the selected complexes were dissolved in DMF and then water was poured until the studied compounds began to precipitate (a DMF/water ratio was different for each individual complex depending on the solubility of these substances; generally, it can be said as ~10:1, v/v). The $^1$H NMR was carried out right after the preparation of the mixtures and than after the period of one week, two weeks, one months and two months. All the signals of the coordinated N6-benzyladenine derivatives were detected in the same regions as in case of proton spectra of the complexes dissolved in DMF. No other signals belonging to coordinated water molecule or $OH^-$ ion were detected in the $^1$H NMR spectra of the prepared complexes dissolved in the DMF/water mixture, which is most likely caused by a low content of water in the studied mixture. In other words, we did not detect the products of hydrolysis of the studied complexes, whose concentration was under the detection limit of NMR spectrometer.

# 4. CONCLUSIONS

The presented thesis set five objectives, as it is mentioned above in the Introduction. Their fulfilment can be one after another discussed as follows:

1. An extensive literature research regarding N6-benzyladenine, its derivatives and complexes involving these organic molecules, as well as platinum and palladium complexes, with the concentration on the cytotoxic active complexes and carboxylato-complexes (especially oxalato) of both the transition metals, was performed in accessible literature and internet databases. The most relevant results were reported by the author and co-authors within the framework of the Introduction section of the *Appendix I–Appendix III*. That is why only a brief summary of the research of these fields is given in this thesis.

2. Potassium bis(oxalato)palladate dihydrate, potassium bis(oxalato)platinate dihydrate and thirteen N6-benzyladenine derivatives, *i.e.*

   2-chloro-N6-benzyl-9-isopropyladenine (L)
   2-chloro-N6-(2-methoxybenzyl)-9-isopropyladenine (*2OMe*L)
   2-chloro-N6-(3-methoxybenzyl)-9-isopro-pyladenine (*3OMe*L)
   2-chloro-N6-(4-methoxybenzyl)-9-isopropyladenine (*4OMe*L)
   2-chloro-N6-(2,3-dimethoxybenzyl)-9-isopropyladenine (*2,3diOMe*L)
   2-chloro-N6-(2,4-dimethoxybenzyl)-9-isopropyladenine (*2,4diOMe*L)
   2-chloro-N6-(3,4-dimethoxybenzyl)-9-isopropyladenine (*3,4diOMe*L)
   2-chloro-N6-(3,5-dimethoxybenzyl)-9-isopropyladenine (*3,5diOMe*L)
   2-chloro-N6-(4-methylbenzyl)-9-isopropyladenine (*4Me*L)
   2-(1-ethyl-2-hydroxyethyl)-N6-benzyl-9-isopropyladenin (Ros)
   2-(1-ethyl-2-hydroxyethyl)-N6-(2-methoxybenzyl)-9-isopropyladenin (*2OMe*Ros)
   2-(1-ethyl-2-hydroxyethyl)-N6-(3-methoxybenzyl)-9-isopropyladenin (*3OMe*Ros)
   2-(1-ethyl-2-hydroxyethyl)-N6-(4-methoxybenzyl)-9-isopropyladenin (*4OMe*Ros)

   were prepared and characterized by elemental analysis and IR, Raman and NMR spectroscopy. Ros, *2OMe*Ros, *3OMe*Ros and *4OMe*Ros belong to the group of potent cyclin-dependent kinase inhibitors. The molecular structure of *2,4diOMe*L was determined by a single crystal X-ray analysis. All of these compounds were previously reported in the literature, they were prepared as starting compounds of the syntheses of the palladium(II) and platinum(II) oxalato complexes (see below).

   The crucial part of the thesis comprises the synthesis and characterization of the palladium(II) (**1**–**12**) and platinum(II) (**13**–**23**) oxalato complexes involving N6-benzyladenine derivatives acting

as N-donor carrier ligands. The synthetic strategies employed $K_2[Pd(ox)_2]\cdot 2H_2O$ and $K_2[Pt(ox)_2]\cdot 2H_2O$ as starting palladium and platinum compounds. Fifteen complexes - eight palladium(II) and seven platinum(II) - with 2-chloro-N6-benzyl-9-isopropyladenine-based ligands (*n*L), *i.e.*

$[Pd(ox)(L)_2]$ (**1**)
$[Pd(ox)(2OMeL)_2]\cdot \frac{3}{4}H_2O$ (**2**)
$[Pd(ox)(3OMeL)_2]\cdot \frac{3}{4}H_2O$ (**3**)
$[Pd(ox)(4OMeL)_2]$ (**4**)
$[Pd(ox)(2,3diOMeL)_2]$ (**5**)
$[Pd(ox)(2,4diOMeL)_2]\cdot 2H_2O$ (**6**)
$[Pd(ox)(3,5diOMeL)_2]\cdot 3H_2O$ (**7**)
$[Pd(ox)(4MeL)_2]$ (**8**)
$[Pt(ox)(L)_2]$ (**13**)
$[Pt(ox)(2OMeL)_2]$ (**14**)
$[Pt(ox)(3OMeL)_2]$ (**15**)
$[Pt(ox)(2,3diOMeL)_2]$ (**16**)
$[Pt(ox)(2,4diOMeL)_2]$ (**17**)
$[Pt(ox)(3,4diOMeL)_2]$ (**18**)
$[Pt(ox)(3,5diOMeL)_2]\cdot 4H_2O$ (**19**)

were prepared. Moreover, eight complexes - four palladium(II) and four platinum(II) - involving purine-based CDK inhibitors (*n*Ros), namely

$[Pd(ox)(Ros)_2]$ (**9**)
$[Pd(ox)(2OMeRos)_2]$ (**10**)
$[Pd(ox)(3OMeRos)_2]\cdot H_2O$ (**11**)
$[Pd(ox)(4OMeRos)_2]$ (**12**)
$[Pt(ox)(Ros)_2]\cdot \frac{3}{4}H_2O$ (**20**)
$[Pt(ox)(2OMeRos)_2]\cdot H_2O$ (**21**)
$[Pt(ox)(3OMeRos)_2]\cdot \frac{1}{2}H_2O$ (**22**)
$[Pt(ox)(4OMeRos)_2]\cdot \frac{3}{4}H_2O$ (**23**)

were synthesized. It should be pointed out, that the synthesis of the platinum(II) oxalato complexes using $K_2[Pt(ox)_2]\cdot 2H_2O$ as starting platinum compound has not been reported in the accessible literature to date, in other words it was used for the first time for the preparation of platinum(II) oxalato complexes **13**–**23**.

3. The prepared palladium(II) and platinum(II) oxalato complexes with N6-benzyladenine derivatives were characterized using various techniques, namely elemental analysis (C, H, N), molar conductivity measurement, simultaneous TG/DTA thermal analysis, IR, Raman and multinuclear ($^1$H, $^{13}$C and $^{195}$Pt) and two dimensional ($^1$H–$^1$H gs-COSY, $^1$H–$^{13}$C gs-HMQC, $^1$H–$^{13}$C gs-HMBC and $^1$H–$^{15}$N gs-HMBC) NMR spectroscopy and ESI+ mass spectrometry. The molecular and crystal structures of the complexes $[Pd(ox)(4OMeL)_2]$ (**4**), $[Pd(ox)(4MeL)_2]\cdot 4MeL\cdot Me_2CO$ (**8**·*4Me*L·$Me_2CO$) and $[Pt(ox)(2,4diOMeL)_2]\cdot 2DMF$ (**17**·2DMF) were determined by a single crystal X-ray analysis. The compounds **1**–**23** are electroneutral mononuclear complexes with the tetra-coordinated central atom, whose vicinity has the distorted square-planar geometry. An oxalate dianion is bidentate-coordinated while both N6-benzyladenine derivatives are coordinated to the metal centre through their N7 atoms of the adenine moieties.

4. The *in vitro* cytotoxic activity of the selected palladium(II) and platinum(II) oxalato complexes against ovarian carcinoma (A2780), ovarian carcinoma *cisplatin* resistant (A2780cis), malignant melanoma (G361), breast adenocarcinoma (MCF7), lung carcinoma (A549), osteosarcoma (HOS) and cervix epitheloid carcinoma (HeLa) human cancer cell lines was tested by an MTT assay. The platinum-based drugs *cisplatin*, *carboplatin* and *oxaliplatin* were employed as positive controls and the results obtained for the prepared oxalato complexes were compared with those of these commercially used substances. The complexes **15** and **17** showed significant *in vitro* cytotoxicity against both A2780 and A2780cis cell lines with the $IC_{50}$ values equalled 3.2±1.0 μM and 3.2±0.6 μM (**15**) and 4.0±1.0 μM and 4.1±1.4 μM (**17**). These results reveal significantly higher *in vitro* cytotoxicity than that of *cisplatin* with $IC_{50}$ equalling 11.5±1.6 μM (against A2780) and 30.3±6.1 μM (against A2780cis). The most promising results within the palladium(II) oxalato complexes were determined for **8** ($IC_{50}$ = 14.3±3.7 μM against HeLa; $IC_{50}$ = 39.9±4.6 μM for *cisplatin*), **9** ($IC_{50}$ = 8.2±3.8 μM against MCF7; $IC_{50}$ = 19.6±4.3 μM for *cisplatin*) and **12** ($IC_{50}$ = 5.4±1.2 μM against A2780). The testing of the *in vitro* cytotoxicity of the selected representatives against primary cultures of human hepatocytes showed that these coordination compounds are not hepatotoxic in the tested concentration range, which means that these complexes can be considered as safe for the human organism.

   The $^1$H NMR spectroscopy of the selected compounds dissolved in the DMF/water mixture (~10:1, v/v) was performed to prove the formation of diaqua- or dihydroxy-complexes, which are known as particles interacting with DNA. We detected all the signals of the appropriate N6-benzyladenine derivatives coordinated to the metal centre as in case of $^1$H spectra of the complexes dissolved in DMF, however, the signals of coordinated water molecule or $OH^-$ ion were not found in the proton spectra of the studied complexes dissolved in the DMF/water mixture, probably due to low content of water in the DMF/water mixture resulting in low concentration of the hydrolysis products.

5. The structure-activity relationship of the complexes tested for their *in vitro* cytotoxic activity was studied as well. It can be stated that both the palladium(II) and platinum(II) complexes involving *roscovitine* or its benzyl-substituted derivatives (*n*Ros) were better soluble than the complexes with 2-chloro-N6-benzyl-9-isopropyladenine analogues (*n*L), which is crucial for the cytotoxic activity itself. On the other hand, the lowest $IC_{50}$ values (*i.e.* the highest *in vitro* cytotoxicity) were found for the complexes with *n*L type of N-donor ligands. We did not find any relationship between the benzyl group substitution and *in vitro* cytotoxicity.

Fulfilment of the thesis theme provided twelve palladium(II) and eleven platinum(II) oxalato complexes with N6-benzyladenine-based N-donor ligands, which brings several new findings in the field of the cytotoxic active transition metal complexes. The platinum(II) complexes **13**–**23**, which

were prepared by a novel synthetic strategy employing potassium bis(oxalato)platinate dihydrate as a starting platinum compound, represent the novel *oxaliplatin* derivatives involving a different N-donor carrier ligand than the mentioned commercially applied platinum-based anticancer drug. The central atom substitution (palladium instead of platinum) within the structure of the mentioned compounds led to the palladium(II) complexes **1**–**12**. The representatives of both the palladium(II) and platinum(II) compounds exceed the *in vitro* cytotoxic activity of *cisplatin* and *oxaliplatin* against several human cancer cell lines, which is an essential part of new transition metal-based drug development, and it can be stated as the most important result of this thesis contributive for the field of bioinorganic chemistry.

***Outlook:*** Owing to the appreciable medicinal potential of several substances reported in this Ph.D. thesis, the selected representatives will be tested for their capability to activate aryl hydrocarbon (AhR) and pregnane X (PXR) xenoreceptors, which induce the gene expression of cytochrome P450 in the primary cultures of human hepatocytes model of the pharmacokinetic drug interactions [83,84]. Further, the complexes will be tested for their interactions with DNA and solution behaviour of the prepared substances will be studied in detail to better understand the mechanism of cytotoxic action of these complexes. Last but not least, the knowledge and skills gained over a period of author`s Ph.D. study will be used for further work at the Department of Inorganic Chemistry, Faculty of Science, Palacky University, for preparation of another especially platinum and palladium complexes with potential biological activity.

# 5. ACKNOWLEDGEMENT

I would like to thank my parents, brother, sister and the rest of my family and especially my wife from the bottom of my heart for their support and patience during my study. Special thanks have to go to prof. RNDr. Zdeňek Trávníček, Ph.D. for his careful supervision and advice. Finally, it is my pleasure to gratefully acknowledge the financial support of this work, which comes from the Ministry of Education, Youth and Sports of the Czech (a grant no. MSM6198959218).

I would like to gratefully thank my colleagues from the Department of Inorganic Chemistry, Faculty of Science, Palacky University in Olomouc (unless otherwise stated), which participated in this work, namely (in alphabetical order):

- Mgr. Lukáš DVOŘÁK - for carrying out CHN elemental analysis;
- Prof. Zdeněk DVOŘÁK, Ph.D. (Department of Cell Biology and Genetics, Faculty of Science, Palacky University in Olomouc) - for determination of the *in vitro* cytotoxic activity by an MTT assay against selected human cancer cell lines;
- Mgr. Alena KLANICOVÁ - for performing ESI+ mass spectrometry and her help with interpretation of the results obtained by this method;
- RNDr. Miroslava MATÍKOVÁ-MAĽAROVÁ, Ph.D. - for measurements of infrared and Raman spectra;
- Mgr. Radka NOVOTNÁ - for measurements of infrared and Raman spectra and her help with English;
- Mgr. Igor POPA, CSc. - for carrying out NMR spectroscopy, interpretation of the obtained NMR data and his helpful advice especially in the field of both organic and inorganic syntheses;
- Mrs. Pavla RICHTEROVÁ - for carrying out of CHN elemental analysis;
- Prof. RNDr. Zdeněk TRÁVNÍČEK, Ph.D. - for performing the single crystal X-ray analyses, determination of the molecular and crystal structures and DFT calculations;
- Ing. Radim VRZAL, Ph.D. (Department of Cell Biology and Genetics, Faculty of Science, Palacky University in Olomouc) - for determination of the *in vitro* cytotoxic activity by an MTT assay against selected human cancer cell lines.

# 6. REFERENCES


[1] B. Rosenberg, L. Van Camp and T. Krigas, Nature *205* (**1965**) 698–699.

[2] L.R. Kelland and N.P. Farrell, Platinum-Based Drugs in Cancer Therapy, Humana: Totowa, 2000.

[3] M. Gielen and E.R.T. Tiekink, Metallotherapeutic Drugs and Metal-based Diagnostic Agents, Willey: London, 2005.

[4] L.M. Pasetto, M.R. D´Andrea, A.A. Brandes, E. Rossi and S. Monfardini, Crit. Rev. Oncol. Hemat. *60* (**2006**) 59–75.

[5] L. Havlíček, J. Hanuš, J. Veselý, S. Leclerc, L. Meijer, G. Shaw and M. Strnad, J. Med. Chem. *40* (**1997**) 408–412.

[6] L. Meijer, A. Borgne, O. Mulner, J.P.J Chong, J.J. Blow, N. Inagaki, M. Inagaki, J.G. Delcros and J.P. Moulinoux, Eur. J. Biochem. *243* (**1997**) 527–536.

[7] V. Kryštof, R. Lenobel, L. Havlíček, M. Kuzma and M. Strnad, Bioorg. Med. Chem. Lett. *12* (**2002**) 3283–3286.

[8] C. Benson, S. Kaye, P. Workman, M. Garret, M. Walton and J. de Bono, Br. J. Cancer *92* (**2005**) 7–12.

[9] M. Maloň, Z. Trávníček, M. Maryško, R. Zbořil, M. Mašláň, J. Marek, K. Doležal, J. Rolčík, V. Kryštof and M. Strnad, Inorg. Chim. Acta *323* (**2001**) 119–129.

[10] Z. Trávníček, J. Mikulík, M. Čajan, R. Zbořil and I. Popa, Biooorg. Med. Chem. *16* (**2008**) 8719–8728.

[11] Z. Trávníček, I. Popa, M. Čajan, R. Zbořil, V. Kryštof and J. Mikulík, J. Inorg. Biochem. *104* (**2010**) 405–417.

[12] Z. Trávníček, A. Klanicová, I. Popa and J. Rolčík, J. Inorg. Biochem. *99* (**2005**) 776–786.

[13] A. Klanicová, Z. Trávníček, I. Popa, M. Čajan and K. Doležal, Polyhedron *25* (**2006**) 1421–1432.

[14] Z. Trávníček, M. Maloň, M. Biler, M. Hajduch, P. Brož, K. Doležal, J. Holub, V. Kryštof and M. Strnad, Transition Met. Chem. *25* (**2000**) 265–269.

[15] Z. Trávníček, M. Maloň, I. Popa, K. Doležal and M. Strnad, Transition Met. Chem. *27* (**2002**) 918–923.

[16] Z. Trávníček, M. Maloň, Z. Šindelář, K. Doležal, J. Rolčík, V. Kryštof, M. Strnad and J. Marek, J. Inorg. Biochem. *84* (**2001**) 23–32.

[17] M. Maloň, Z. Trávníček, M. Maryško, J. Marek, K. Doležal, J. Rolník and M. Strnad, Transition Met. Chem. *27* (**2002**) 580–586.

[18] P. Štarha, Z. Trávníček, R. Herchel, I. Popa, P. Suchý and J. Vančo, J. Inorg. Biochem. *103* (**2009**) 432–440.

[19] A. Klanicová, Z. Trávníček, J. Vančo, I. Popa and Z. Šindelář, Polyhedron, *In press, corrected proof* (**2010**) doi:10.1016/j.poly.2010.06.007.

[20] Z. Trávníček, V. Kryštof and M. Šipl, J. Inorg. Biochem. *100* (**2006**) 214–225.

[21] Z. Trávníček and J. Marek, J. Mol. Struct. *933* (**2009**) 148–155.

[22] Z. Trávníček, M. Matiková-Maľarová and K. Štěpánková, Acta Crystallogr. Sect. E-Struct. Rep. Online E64 (**2009**) m545–m546.

[23] Z. Trávníček, M. Maloň, M. Zatloukal, K. Doležal, M. Strnad and J. Marek, J. Inorg. Biochem. *94* (**2003**) 307–316.

[24] Z. Trávníček, M. Šipl and I. Popa, J. Coord. Chem. *58* (**2005**) 1513–1521.

[25] L. Szüčová, Z. Trávníček, M. Zatloukal and I. Popa, Bioorg. Med. Chem. *14* (**2006**) 479–491.

[26] Z. Trávníček, L. Szüčová and I. Popa, J. Inorg. Biochem. *101* (**2007**) 477–492.

[27] M. Maloň, Z. Trávníček, R. Marek and M. Strnad, J. Inorg. Biochem. *99* (**2005**) 2127–2138.

[28] Z. Trávníček, J. Marek and L. Szüčová, Acta Crystallogr. Sect. E-Struct. Rep. Online E62 (**2006**) m1482–m1484.

[29] L. Szüčová, Z. Trávníček, I. Popa and J. Marek, Polyhedron *27* (**2008**) 2710–2720.

[30] Z. Trávníček, I. Popa, M. Čajan, R. Herchel and J. Marek, Polyhedron *26* (**2007**) 5271–5282.

[31] J.A. McCleverty and T.J. Meyer, Comprehensive Inorganic Chemistry II, Elsevier, 2005.

[32] A.F. Holleman and E. Wiberg, Inorganic Chemistry, Academic Press; San Diego, 2001.

[33] F.A. Cotton, G. Wilkinson, C.A. Murillo and M. Bochman, Advanced Inorganic Chemistry, Wiley; New York, 1999.

[34] K. Meelich, M. Galanski, V.B. Arion and B.K. Keppler, Eur. J. Inorg. Chem. (**2006**) 2476–2483.

[35] S. Dey, P. Banerjee, S. Gangopadhyay and P. Vojtíšk, Trans. Met. Chem. *28* (**2003**) 765–771.

[36] F.A. Allen, Acta Crystallogr., Sect. B: Struct. Sci. *58* (**2002**) 380–388.

[37] G. Raudaschl, B. Lippert, J.D. Hoeschele, H.E. Howardlock, C.J.L. Lock and P. Pilon, Inorg. Chim. A.-Bioinor. *106* (**1985**) 141–149.

[38] M.A. Bruck, R. Bau, M. Noji, K. Inagaki and Y. Kidani, Inorg. Chim. A.-Bioinor. *92* (**1984**) 279–284.

[39] S. Neidle, I.M. Ismail and P J. Sadler, J. Inorg. Biochem. *13* (**1980**) 205–212.

[40] J. Welink, E. Boven, J.B. Vermorken, H.E. Gall and W.J.F. van der Vijgh, Clin. Cancer Res. *5* (**1999**) 2349–2358.

[41] Y. Kidani, K. Inagaki, M. Iigo, A. Hoshi and K. Kuretani, J. Med. Chem. *21* (**1978**) 1315–1318.

[42] M.M. Jennerwein, A. Eastman and A. Khokhar, Chem. Biol. Interact. *70* (**1989**) 39–49.

[43] J.M. Woynarowski, S. Faivre, M.C.S. Herzig, B. Arnett, W.G. Chapman, A.V. Trevino, E. Raymond, S.G. Chaney, A. Vaisman, M. Varchenko and P.E. Juniewicz, Mol. Pharmacol. *58* (**2000**) 920–927.

[44] J.L. Butour, S. Wimmer, F. Wimmer and P. Castan, Chem. Biol. Interact. *104* (**1997**) 165–178.

[45] A. Garoufis, S.K. Hadjikakou and N. Hadjiliadis, Coord. Chem. Rev. *253* (**2009**), 1384–1397.

[46] S. Raghunathan, B.K. Sinha, V. Pattabhi and E.J. Gabe, Acta Crystallogr. Sect. C-Cryst. Struct. Commun. *39* (**1983**) 1545–1547.

[47] S. Procházka, I. Macháčková, J. Krekule, J. Šebánek et al., Fyziologie rostlin, 1st edition, Praha: Academia, 1998.

[48] C.O. Miller, F.S. Skoog, M.H. Von Saltza and F.M. Strong, J. Am. Chem. Soc. *77* (**1955**) 1392–1393.

[49] C.O. Miller, P. Natl. Acad. Sci. USA *54* (**1965**) 1052–1058.

[50] S. Wang, S.J. McClue, J.R. Ferguson, J.D. Hull, S. Stokes, S. Parsons, R.Westwood and P.M. Fischer, Tetrahedron: Asymm. *12* (**2001**) 2891–2894.

[51] K. Doležal, I. Popa, V. Kryštof, L. Spíchal, M. Fojtíková, J. Holub, R. Lenobel, T. Schmülling and M. Strnad, Bioorg. Med. Chem. *14* (**2006**) 875–884.

[52] K. Doležal, I. Popa, E. Hauserová, L. Spíchal, K. Chakrabarty, O. Novák, V. Kryštof, J. Voller, J. Holub and M. Strnad, Bioorg. Med. Chem. *15* (**2007**) 3737–3747.

[53] J. Veselý, L. Havlíček, M. Strnad, J.J. Blow, A. Donesla-Deana, L. Pinna, D.S. Letnám, J. Kato, L. Detivaud, S. Leclerc and L. Meijer, Eur. J. Biochem. *224* (**1994**) 771–786.

[54] I.R. Hardcastle, B.T. Holding and R.J. Griffin, Annul. Rev. Pharmacol. Toxicol. *42* (**2002**) 325–348.

[55] B. Alberts, D. Bray, A. Johnson, et al., *Základy buněčné biologie,* New York: Garland Publishing, 1998.

[56] A. McNutt, S. Haq and R. Raval, Surface Science *531* (**2003**) 131–144.

[57] T.P. Balasubramanian, P.T. Muthiah, Ananthasaravanan and S.K. Mazumdar, J. Inorg. Biochem. *63* (**1996**) 175–181.

[58] N. Stanley, P.T. Muthiah, P. Luger, M. Weber and S.J. Geib, Inorg. Chem. Commun. *8* (**2005**) 1056–1059.

[59] J.J. Fiol, A. García-Raso, F.M. Albertí, A. Tasada, M. Barceló-Oliver, A. Terrón, M.J. Prieto, V. Moreno and E. Mílina, Polyhedron *27* (**2008**) 2851–2858.

[60] M.A. Zorduu, G. Manca and S. Mosca, Transition Met. Chem. *16* (**1991**) 301–303.

[61] C.H. Oh, S.C. Lee, K.S. Lee, E.R. Woo, C.Y. Hong, B.S. Yang, D.J. Baek and J.H. Cho, Arch. Pharm. Pharm. Med. Chem. *332* (**1999**) 187–190.

[62] M. Legraverend, O. Ludwig, E. Bisagni, S. Leclerc, L. Meijer, N. Giocanti, R. Sadri and V. Favaudon, Bioorg. Med. Chem. *7* (**1999**) 1281–1293.

[63] J.W. Daly and B. E. Christensen, J. Org. Chem. *21* (**1956**) 177–179.

[64] P. Imbach, H.G. Capraro, P. Furet, H. Mett, T. Meyer and J. Zimmermann, Bioorg. Med. Chem. Lett. *9* (**1999**) 91–96.

[65] K. Torigoe and K. Esumi, Langmuir *9* (**1993**) 1664–1667.

[66] K. Krogmann and P. Dodel, Chem. Ber. Recl. *99* (**1966**) 3402–3408.

[67] A.S. Abu-Surrah, T.A.K. Al-Allaf, M. Klinga and M. Ahlgren, Polyhedron *22* (**2003**) 1529–1534.

[68] M. Galanski, A. Yasemi, S. Slaby, M.A. Jakubec, V.B. Arion, M. Rausch, A.A. Nazarov and B.K. Keppler, Eur. J. Med. Chem. *39* (**2004**) 707–714.

[69] X. Chen, M. Xie, W. Liu, Q. Ye, Y. Yu, S. Hou, W. Gao and Y. Liu, Inorg. Chim. Acta *360* (**2007**) 2851–2856.

[70] S. Dey, P. Banerjee, S. Gangopadhyay and P. Vojtíšek, Transit. Met. Chem. *28* (**2003**) 765–771.

[71] G. Devoto, M. Biddau, M. Massacesi, R. Pinna, G. Ponticelli, L.V. Tatjanenko and I.A. Zakharova, J. Inorg. Biochem. *19* (**1983**) 311–318.

[72] W.J. Geary, Coord. Chem. Rev. *7* (**1971**) 81–122.

[73] C.J. Pouchert, The Aldrich Library of Infrared Spectra, third ed., Aldrich Chemical Co., Milwaukee, 1981.

[74] T.A. Mohamed, I.A. Shabaan, W.M. Zoghaib, J. Husband, R.S. Farag and A.E.-N.M.A. Alajhaz, J. Mol. Struct. *938* (**2009**) 263–276.

[75] O. Castillo, A. Luque and P. Roman, J. Mol. Struct. *570* (**2001**) 181–188.

[76] I. Castro, J. Faus, M. Julve and A. Gleizes, J. Chem Soc., Dalton Trans. (**1991**) 1937–1944.

[77] K. Nakamoto, Infrared and Raman Spectra of Inorganic and Coordination Compounds, 5$^{th}$ edition, Willey-Interscience, New York, 1997.

[78] Z. Dhaouadi, M. Ghomi, J.C. Austin, R.B. Girling, R.E. Hester, P. Mojzes, L. Chinsky, P.Y. Turpin, C. Coulombeau, H. Jobic and J. Tomkinson, J. Phys. Chem. *97* (**1993**) 1074–1084.

[79] CrysAlis RED, CrysAlis CCD, Oxford Diffraction Ltd., Abingdon, England, 2006.

[80] G.M. Sheldrick, SHELXS 97, Acta Cryst. *A46* (**1990**) 467–473.

[81] G.M. Sheldrick, SHELXL 97, Program for Crystal Structure Refinement, University of Göttingen, Göttingen, Germany, 1997.

[82] K. Brandenburg, DIAMOND, Relase 3.1f, Crystal Impact GbR, Bonn, Germany, 2006.

[83] P. Maurel, Delivery Reviews *22* (**1996**) 105–132.

[84] Dvořák, R. Vrzal, P. Štarha, A. Klanicová, Z. Trávníček, Toxicology in Vitro *24* (**2010**) 425–429.

# 7. LIST OF PUBLISHED PAPERS, PATENTS, CONFERENCE CONTRIBUTIONS AND AWARDS

**PAPERS RELATED TO THIS THESIS:**

- P. Štarha, Z. Trávníček, I. Popa: *Synthesis, characterization and in vitro cytotoxicity of the first palladium(II) oxalato complexes involving adenine-based ligands*. J. Inorg. Biochem. *103* (**2009**) 978–988
- P. Štarha, I. Popa, Z. Trávníček: *Palladium(II) oxalato complexes involving N6-(benzyl)-9-isopropyladenine-based N-donor carrier ligands: synthesis, general properties, $^{1}H$, $^{13}C$ and $^{15}N\{^{1}H\}$ NMR characterization and in vitro cytotoxicity*. Inorg. Chim. Acta *363* (**2010**) 1469–1478
- P. Štarha, Z. Trávníček, I. Popa: *Platinum(II) oxalato complexes with adenine-based carrier ligands showing significant in vitro antitumor activity*. J. Inorg. Biochem. *104* (**2010**) 639–647
- Z. Trávníček, P. Štarha, I. Popa, R. Vrzal, Z. Dvořák: *Potent Roscovitine-based CDK inhibitors acting as N-donor ligands in the platinum(II) oxalato complexes: complex preparations, characterization and in vitro antitumor activity*. Eur. J. Med. Chem. *In press, corrected proof* (**2010**) doi:10.1016/j.ejmech.2010.07.025
- R. Vrzal, P. Štarha, Z. Dvořák, Z. Trávníček: *Evaluation of in vitro anticancer activity of platinum(II) and palladium(II) oxalato complexes with adenine derivatives as carrier ligands*. J. Inorg. Biochem. Short Commun. *104* (**2010**) 1130–1132

**OTHER PAPERS:**

- P. Štarha, Z. Trávníček, R. Herchel, I. Popa, P. Suchý, J. Vančo: *Dinuclear copper(II) complexes containing 6-(benzylamino)purines as bridging ligands: Synthesis, characterization, and in vitro and in vivo antioxidant activities*. J. Inorg. Biochem. *103* (**2009**) 432–440
- Z. Dvořák, R. Vrzal, P. Štarha, A. Klanicová, Z. Trávníček: *Effects of dinuclear copper(II) complexes with 6-(benzylamino)purine derivatives on AhR and PXR dependent expression of cytochromes P450 CYP1A2 and CYP3A4 genes in primary cultures of human hepatocytes*. Toxicology in Vitro *24* (**2010**) 425–429
- P. Štarha, R. Novotná, Z. Trávníček: *X-ray structure and properties of a dinuclear palladium(II) complex $[Pd_2(\mu\text{-}L)_4]$ with four adenine-based bridges in a paddle wheel-like arrangement*. Inorg. Chem. Commun. *13* (**2010**) 800–803
- Z. Trávníček, R. Pastorek, P. Štarha, I. Popa, V. Slovák: *Nickel(II) N-benzyl-N-methyldithiocarbamato complexes as precursors for the preparation of graphite oxidation accelerators*. Z. Anorg. Allg. Chem. *636* (**2010**) 1557–1564

- L. Dvořák, I. Popa, P. Štarha, Z. Trávníček: *In Vitro Cytotoxic Active Platinum(II) Complexes Derived from Carboplatin and Involving Purine Derivatives.* Eur. J. Inorg. Chem. *2010* (**2010**) 3441–3448.

**PATENTS:**

- National utility model - P. Štarha, Z. Trávníček, I. Popa: *Oxalato Complexes of Platinum with N6-benzyladenine Derivatives*, CZ 19706 U1 (**2009**).
- National patent submitted as an invention - P. Štarha, Z. Trávníček, I. Popa: *Platinum(II) Oxalato Complexes Involving N6-benzyladenine Derivatives, Preparation and Usage of these Complexes as Drugs in Antitumour Therapy.* PV 2009-257 (**2009**).
- International patent submitted as an invention - P. Štarha, Z. Trávníček, I. Popa: *Oxalato Complexes of Platinum with N6-benzyladenine Derivatives, Method of their Preparation and Application of these Complexes as Drugs in Antitumour Therapy,* PCT/CZ 2009/000135 (**2009**).

**CONFERENCE CONTRIBUTIONS AS PRESENTING AUTHOR:**

- poster: P. Štarha, I. Popa, Z. Trávníček: *Novel Palladium(II)-oxalato Complexes Involving N6-Substituted Derivatives of 2-chloro-9-isopropyladenine*, 38$^{th}$ International Conference of Coordination Chemistry, Jerusalem, Israel (07/2008).
- talk: P. Štarha, I. Popa, Z. Trávníček: *Pd(II) a Pt(II) oxalátokomplexy s 2,6,9-trisubstituovanými deriváty purinu: syntéza a vlastnosti [Pd(II) a Pt(II) Oxalato Complexes with 2,6,9-trisubstituted Purine Derivatives: Synthesis and Properties]*, 60. sjezd asociací českých a slovenských chemických společností (60$^{th}$ Congress of Czech and Slovak Chemical Societies Associations), Olomouc (09/2008).
- poster: P. Štarha, I. Popa, Z. Trávníček: *Platinum(II) and Palladium(II) Oxalato Complexes Involving N6-benzyladenine-based CDK-inhibitors*, 14$^{th}$ International Conference on Biological Inorganic Chemistry, Nagoya, Japan (07/2009).
- poster: P. Štarha, R. Vrzal, Z. Dvořák, Z. Trávníček: *In Vitro Cytotoxic Activity of Palladium(II) Oxalato Complexes with N6-benzyl-9-isopropyladenine-based N-donor Ligands,* 61. sjezd asociací českých a slovenských chemických společností (60$^{th}$ Congress of Czech and Slovak Chemical Societies Associations), Vysoke Tatry, Slovakia (07/2009).
- talk: P. Štarha, L. Dvořák, Z. Dvořák, Z. Trávníček: *Platnaté a palladnaté karboxylato komplexy s vybranými N-donorovými ligandy a jejich in vitro cytotoxicita [Platinum(II) and Palladium(II) Carboxylato Complexes with Selected N-donor Ligands and their In Vitro Cytotoxicity],* Anorganická chémia v treťom tisícročí - seminár venovaný 45. výročiu výučby a výskumu na Katedre anorganickej chémie PF UPJŠ (Inorganic Chemistry in the 3$^{rd}$ Millennium - Seminar

Dedicated to 45th Anniversary of Teaching and Research at the Department of Inorganic Chemistry PF UPJS), Strbske Pleso, Slovakia (06/2010).

- talk: P. Štarha, L. Dvořák, Z. Dvořák, Z. Trávníček: *In vitro cytotoxicita Pt(II) a Pd(II) oxalato a cyklobutan-1,1-dikarboxylato komplexů s N-donorovými ligandy na bázi N6-benzyl-9-isopropyladeninu [In Vitro Cytotoxicity of Pt(II) and Pd(II) Oxalato and Cyclobutan-1,1-dicarboxylato Complexes with N6-benzyl-9-isopropyladenine-based N-donor Ligands],* 62. sjezd asociací českých a slovenských chemických společností (62nd Congress of Czech and Slovak Chemical Societies Associations), Pardubice (06/2010).
- poster: P. Štarha, L. Dvořák, I. Popa, Z. Trávníček, Z. Dvořák: *Platinum(II) Cyclobutane-1,1-dicarboxylato Complexes Involving N6-benzyl-9-isopropyladenine-based Ligands with Promising In Vitro Cytotoxicity,* 39th International Conference of Coordination Chemistry (ICCC 39), Adelaide, Australia (07/2010).

**OTHER CONFERENCE CONTRIBUTIONS:**

- poster: P. Štarha, R. Vrzal, P. Štarha, A. Klanicová, Z. Dvořák, Z. Trávníček: *Cytotoxicity of Cu(II), Pd(II) and Pt(II) Complexes Involving N6-benzyladenine Derivatives in Selected Human Cancer Cell Lines and Primary Human Hepatocytes,* 61. sjezd asociací českých a slovenských chemických společností (60th Congress of Czech and Slovak Chemical Societies Associations), Vysoke Tatry, Slovakia (09/2009).
- talk: I. Popa, P. Štarha, Z. Trávníček: *NMR studium platnatých komplexů odvozených od cisplatiny, karboplatiny a oxaliplatiny obsahující N-donorové ligandy odvozené od 2,6,9-trisubstituovaných purinů [NMR Study of Platinum Complexes Derived from Cisplatin, Carboplatin and Oxaliplatin Involving N-donor Ligands Derived form 2,6,9-trisubstituted Purines],* Anorganická chémia v treťom tisícročí - seminár venovaný 45. výročiu výučby a výskumu na Katedre anorganickej chémie PF UPJŠ (Inorganic Chemistry in the 3rd Millennium - Seminar Dedicated to 45th Anniversary of Teaching and Research at the Department of Inorganic Chemistry PF UPJS), Strbske Pleso, Slovakia (06/2010).
- poster: Z. Dvořák, R. Vrzal, P. Štarha, I. Popa, Z. Trávníček: *Evaluation of In Vitro Cytotoxic Activity of [Pt(ox)($L_n$)$_2$] Complexes Involving Adenine-based N-donor Ligands,* 39th International Conference of Coordination Chemistry, Adelaide, Australia (07/2010).

**AWARDS:**

- 3rd place in the competitive work "O cenu děkana 2010" of the Ph.D. students of the study programme Chemistry at the Faculty of Science, Palacky University, with a lecture given in English called *Platinum(II) and Palladium(II) Oxalato Complexes Involving N6-benzyladenine-based N-donor Ligands: Synthesis, Characterization and In Vitro Cytotoxicity.*

# 8. APPENDIX

An appendix consists of five papers related to the thesis theme, which were already published by the author of the thesis together with co-authors (sorted by date):

***APPENDIX I:***

P. Štarha, Z. Trávníček and I. Popa: *Synthesis, characterization and in vitro cytotoxicity of the first palladium(II) oxalato complexes involving adenine-based ligands*. J. Inorg. Biochem. *103* (**2009**) 978–988.

***APPENDIX II:***

P. Štarha, I. Popa and Z. Trávníček: *Palladium(II) oxalato complexes involving N6-(benzyl)-9-isopropyladenine-based N-donor carrier ligands: synthesis, general properties,* $^{1}H$, $^{13}C$ *and* $^{15}N\{^{1}H\}$ *NMR characterization and in vitro cytotoxicity.* Inorg. Chim. Acta *363* (**2010**) 1469–1478.

***APPENDIX III:***

P. Štarha, Z. Trávníček and I. Popa: *Platinum(II) oxalato complexes with adenine-based carrier ligands showing significant in vitro antitumor activity.* J. Inorg. Biochem. *104* (**2010**) 639–647.

***APPENDIX IV:***

Z. Trávníček, P. Štarha, I. Popa, R. Vrzal and Z. Dvořák: *Potent Roscovitine-based CDK inhibitors acting as N-donor ligands in the platinum(II) oxalato complexes: complex preparations, characterization and in vitro antitumor activity.* Eur. J. Med. Chem. *In press, corrected proof* (**2010**) doi:10.1016/j.ejmech.2010.07.025.

***APPENDIX V:***

R. Vrzal, P. Štarha, Z. Dvořák and Z. Trávníček: *Evaluation of in vitro anticancer activity of platinum(II) and palladium(II) oxalato complexes with adenine derivatives as carrier ligands.* J. Inorg. Biochem. Short Commun. *104* (**2010**) 1130–1132.

# APPENDIX I

Journal of Inorganic Biochemistry 103 (2009) 978–988

Contents lists available at ScienceDirect

Journal of Inorganic Biochemistry

journal homepage: www.elsevier.com/locate/jinorgbio

# Synthesis, characterization and *in vitro* cytotoxicity of the first palladium(II) oxalato complexes involving adenine-based ligands

Pavel Štarha, Zdeněk Trávníček *, Igor Popa

*Department of Inorganic Chemistry, Faculty of Science, Palacký University, Křížkovského 10, CZ-771 47 Olomouc, Czech Republic*

ARTICLE INFO

*Article history:*
Received 7 November 2008
Received in revised form 27 February 2009
Accepted 20 April 2009
Available online 4 May 2009

*Keywords:*
Palladium(II) complexes
Oxalate
Adenine derivatives
*In vitro* cytotoxicity
X-ray structure

ABSTRACT

The first $[Pd(L^n)_2(ox)]$ $xH_2O$ oxalato(ox) complexes involving 2-chloro-N6-(benzyl)-9-isopropyladenine ($L^1$; complex **1**), 2-chloro-N6-(4-methoxybenzyl)-9-isopropyladenine ($L^2$; **2**), 2-chloro-N6-(2,3-dimethoxybenzyl)-9-isopropyladenine ($L^3$; **3**), 2-chloro-N6-(2,4-dimethoxybenzyl)-9-isopropyladenine ($L^4$; **4**), and 2-chloro-N6-(4-methylbenzyl)-9-isopropyladenine ($L^5$; **5**) have been synthesized by the reactions of potassium bis(oxalato)palladate(II) dihydrate, $[K_2Pd(ox)_2]\cdot 2H_2O$, with the mentioned organic compounds ($H_2ox$ = oxalic acid; $x = 0$ for **1**–**3** and **5** or 2 for **4**). Elemental analyses (C, H, N), FTIR, Raman and NMR ($^1H$, $^{13}C$, $^{15}N$) spectroscopies, conductivity measurements and thermal studies (thermogravimetric and differential thermal analyses, TG/DTA) have been used to characterize the prepared complexes. The molecular structures of $[Pd(L^2)_2(ox)]$ (**2**) and $[Pd(L^5)_2(ox)]\cdot L^5\cdot Me_2CO$ (**5**·$L^5$·$Me_2CO$) have been determined by a single crystal X-ray analysis. The geometry of these complexes is slightly distorted square-planar with two appropriate $L^n$ ($n = 2$ or 5) molecules mutually arranged in the head-to-head (**2**) or head-to-tail (**5**) orientation. The $L^n$ ligands are coordinated to the central Pd(II) ion *via* the N7 atoms. The same conclusions regarding the binding properties of $L^1$–$L^5$ ligands can be made based on multinuclear NMR spectra. *In vitro* cytotoxicity of the complexes **1**–**5** has been evaluated against human chronic myelogenous leukaemia (K562) and human breast adenocarcinoma (MCF7) cancer cell lines. Significant cytotoxicity has been determined for the complexes **3** ($IC_{50}$ = 6.2 μM) and **5** ($IC_{50}$ = 6.8 μM) on the MCF7 cell line, which is even better than that found for the well-known and widely-used platinum-bearing antineoplastic drugs, i.e. oxaliplatin and cisplatin.



## 1. Introduction

The preparations of metallocomplexes with potential antitumor activity has been one of the main targets of transition metal chemistry since Rosenberg's discovery of cisplatin {*cis*-diamminedichloridoplatinum(II), *cis*-$[Pt(NH_3)_2Cl_2]$} cytotoxic activity in the 1960s [1]. In 1978, cisplatin was approved as the first platinum-based drug for the oncology treatment, although several negative side-effects (nephrotoxicity, neurotoxicity, nausea, etc.) had been induced on treated patients [2]. Nevertheless, cisplatin was followed by carboplatin [3] {*cis*-diammine-1,1-cyclobutanedicarboxylateplatinum(II), $[Pt(NH_3)_2(cbdc)]$, approved in 1985} and oxaliplatin [4] {*1R*,*2R*-diamminocyclohexaneoxalatoplatinum(II), [Pt(dach)(ox)], approved in 1996}, which met requirements of improving antitumor activity and reducing disadvantages of cisplatin. carboplatin and oxaliplatin represent the second, and third platinum-based drug generations, respectively [5].

Nowadays, not only platinum-bearing complexes are extensively studied with the aim to broaden a spectrum of transition metal-based complexes which could be used in the treatment of cancer. Mainly due to the similar structural properties, palladium(II) complexes were tested on various cancer cells among the first of the non-platinum metallocomplexes. The simple analogues of effective antitumor platinum(II) complexes, such as *cis*-$[Pd(NH_3)_2Cl_2]$ and $[Pd(dach)_2Cl_2]$, have been prepared and tested, however, they were found to be inactive on a Sarcoma 180 tumour cell line [6].

Up to now, many mono-, di-, or polynuclear palladium(II) complexes with various N-donor or S-donor ligands have been reported as agents with promising properties for the cancer therapy [7,8]. For instance, the *trans*-$[Pd(dmnp)_2Cl_2]$ complex (dmnp = 2,6-dimethyl-4-nitropyridine) exceeds the antitumor activity of cisplatin in *in vitro* testing on the adenocarcinoma of the rectum (SW707), breast cancer (T47D) and bladder cancer (HCV29T) human cell lines, with the $IC_{50}$ (the drug concentrations lethal for 50% of the tumour cells) values of 1.1, 1.0, and 1.1 μM, respectively, compared to 6.1, 20.0 and 8.1 μM (converted from μg $mL^{-1}$ to μM) as determined for cisplatin on the

* Corresponding author. Tel.: +420 585 634 944; fax: +420 585 634 954.
*E-mail address:* zdenek.travnicek@upol.cz (Z. Trávníček).

0162-0134/$ - see front matter © 2009 Elsevier Inc. All rights reserved.
doi:10.1016/j.jinorgbio.2009.04.008

same cell lines [9]. The *trans*-[Pd(bbiy)$_2$Cl$_2$] complex (bbiy = 1-benzyl-3-*tert*-butylimidazol-2-ylidene) has been recently reported as a compound, whose cytotoxicity exceeds cisplatin in *in vitro* tests on the HeLa (cervical cancer), MCF7 and HCT 116 (colon adenocarcinoma) human cell lines [10]. Its $IC_{50}$ values (for cisplatin in parentheses) were determined to be 4.0 (8.0), 0.8 (16.0) and 1.0 (15.0) μM on the named cell lines. In our laboratory, other cytotoxic active *trans*-palladium(II) complexes with a $PdN_2Cl_2$ donor set {*trans*-[Pd(L)$_2$Cl$_2$]·H$_2$O; L = 2-[(*R*)-(1-ethyl-2-hydroxyethylamino)]-N6-(3-hydroxybenzyl)-9-isopropyladenine or 2-[(1-isopropyl-2-hydroxyethylamino)]-N6-(3-hydroxybenzyl)-9-isopropyladenine} were prepared [11]. These complexes were found to be even more active than both cisplatin ($IC_{50}$ = 11 μM) and oxaliplatin ($IC_{50}$ = 18 μM) on the MCF7 human cancer cell line, since their $IC_{50}$ values equalled 3 μM in both cases.

It has been proved for platinum(II) cytotoxic complexes that the oxalato group as well as the chlorido ligands may be considered to be very suitable leaving groups in such complexes [12,13]. Considering this finding, it is quite surprising that only a few monomeric palladium(II) oxalato complexes with a $PdN_2O_2$ donor set, e.g. [Pd(NH$_3$)$_2$(ox)] [14], [Pd(mi)$_2$(ox)]·2H$_2$O (mi = N-methylimidazole), [Pd(ei)$_2$(ox)] (ei = N-ethylimidazole), [Pd(pi)$_2$(ox)] (pi = N-propylimidazole) [15], [Pd(mi)$_2$(ox)]·H$_2$O [16], [Pd(hoen)$_2$(ox)]·½H$_2$O (hoen = *N,N′*-bis(hydroxyethyl)ethylenediamine) and [Pd(clen)$_2$(ox)] (clen = *N,N′*-bis(chloroethyl)ethylenediamine) [17], [Pd(py)$_2$(ox)] (py = pyridoxine, pyridoxial, or pyridoxamine) [18], [Pd(dach)$_2$(ox)] [19], [Pd(phen)(ox)]·H$_2$O (phen = 1,10-phenanthroline) [20], or [Pd(pda)(ox)]·H$_2$O (pda = propane-1,3-diamine) [21] have been reported up to now. To date, twenty X-ray structures with a Pd(ox) motive have been deposited at the Crystallographic Structural Database (CSD ver. 5.29, August 2008 update) [22]. Among them, there are only five monomeric palladium(II) oxalato complexes with a $PdN_2O_2$ chromophore, i.e. [Pd(NH$_3$)$_2$(ox)] [14], [Pd(mi)$_2$(ox)]·H$_2$O [16], [Pd(py)$_2$(ox)] (py = pyridoxine) [18], [Pd(phen)(ox)]·H$_2$O [20] and [Pd(pda)(ox)]·H$_2$O [21]. With respect to these statements we report the structures of **2** and **5**·L$^5$·Me$_2$CO as the first examples of palladium(II) complexes involving combination of an oxalate dianion and adenine-based derivative. The above mentioned complexes [Pd(hoen)$_2$(ox)]·½H$_2$O and [Pd(clen)$_2$(ox)] were tested for their antitumour activity, but they were found inactive on P388 (mice leukaemia) cells with the $IC_{50}$ values equal to 200 μM. Finally, it is necessary to mention some of the mononuclear palladium(II) complexes with purine-based N-donor ligands, such as *trans*-[Pd(nuo)$_2$X$_2$]·*x*H$_2$O (nuo = adenosine, guanosine, inosine, or xanthosine, X = Cl$^-$ or Br$^-$) [23], *cis*-[Pd(pen)$_2$Cl$_2$] (pen = 2-amino-9-[4-hydroxy-3-(hydroxymethyl)-butyl]-6,9-dihydro-3*H*-purin-6-one, penciclovir) [24], *trans*-[Pd(ade)$_2$-(bup)$_2$] (AdeH = adenine, bup = tri-*n*-butylphosphine) [25], or [Pd(guo)$_2$(en)] 9H$_2$O (en = ethylene-1,2-diamine) [26].

This paper reports the first palladium(II) oxalato complexes bearing the adenine-based compounds (L$^1$–L$^5$) of the general formula [Pd(L$^n$)$_2$(ox)] ·*x*H$_2$O (**1**–**5**) (*x* = 0 or 2). The compounds L$^1$–L$^5$ stand for the derivatives of the aromatic cytokinin 6-(benzylamino)purine [N6-(benzyl)adenine, Bap] [27] and represent the cytotoxic inactive precursors for the preparation of cyclin dependent kinase (CDK) inhibitors, such as e.g. 2-[(*R*)-(1-ethyl-2-hydroxyethylamino)]-N6-(benzyl)-9-isopropyladenine, *R*-Roscovitine (Seliciclib, CYC202), that is presently tested in 2b-phase of clinical trials on patients with non-small cell lung cancer (NSCLC) [28,29]. The prepared complexes **1**–**5** have been fully characterized by various physical techniques. The single crystal X-ray analysis of [Pd(L$^2$)$_2$(ox)] (**2**) and [Pd(L$^5$)$_2$(ox)]·L$^5$·Me$_2$CO (**5**·L$^5$·Me$_2$CO) revealed a slightly distorted square-planar geometry in the vicinity of the central atom. Moreover, *in vitro* cytotoxicity of the prepared complexes against two human cancer cell lines (K562 and MCF7) has been evaluated and the results are discussed within the text.

## 2. Experimental

### 2.1. Materials

Chemicals and solvents were purchased from Sigma–Aldrich Co., Acros Organics Co., Lachema Co. or Fluka Co. They were used as received, except for dimethyl sulfoxide (DMSO), which was dried using $MgSO_4$.

### 2.2. Physical measurements

Elemental analyses (C, H, N) were performed on a Flash EA-1112 Elemental Analyser (Thermo Finnigan). Conductivity measurements were carried out on a Cond 340i/SET (WTW) in *N,N′*-dimethylformamide (DMF; $10^{-3}$ M) and acetone ($10^{-3}$ M) solutions at 25 °C. FTIR spectra were recorded on a Nexus 670 FT-IR (ThermoNicolet) using KBr (400–4000 cm$^{-1}$) and Nujol (150–600 cm$^{-1}$) techniques. Raman spectroscopy measurements were performed on a NXR FT-Raman Module (ThermoNicolet) in the range of 150–3750 cm$^{-1}$. The intensity of reported FTIR and Raman signals are defined as w = weak, m = medium, s = strong and vs = very strong. $^1$H, $^{13}$C and $^{15}$N NMR spectra [$^1$H–$^1$H gs-COSY, $^1$H–$^{13}$C gs-HMQC, $^1$H–$^{13}$C gs-HMBC and $^1$H–$^{15}$N gs-HMBC (obtained at natural abundance) at 300 K, and $^1$H and $^1$H–$^{15}$N gs-HMBC also at 340 K in case of all complexes; gs = gradient selected, COSY = correlation spectroscopy, HMQC = Heteronuclear Multiple Quantum Coherence, HMBC = Heteronuclear Multiple Bond Coherence] of DMF-$d_7$ solutions of L$^1$–L$^5$ and **1**–**5** were measured on a Bruker Avance 300 MHz NMR spectrometer at 300.13 MHz, 75.47 MHz and 30.42 MHz for $^1$H, $^{13}$C, and $^{15}$N, respectively. Spectra were calibrated against the signals of tetramethylsilane (an internal standard for $^1$H and $^{13}$C NMR spectra) and against the residual signals of the solvent (an internal reference for $^{15}$N adjusted to 104.7 ppm). Simultaneous thermogravimetric (TG) and differential thermal (DTA) analyses were carried out using a thermal analyzer Exstar TG/DTA 6200 (Seiko Instruments Inc.). TG/DTA studies were performed in ceramic pans from laboratory temperature to 650 °C (**2** and **3**) or 1000 °C (**1**, **4** and **5**) with a 2.5 °C min$^{-1}$ temperature gradient in dynamic air atmosphere (150 mL min$^{-1}$).

### 2.3. Single crystal X-ray analysis of [Pd(L$^2$)$_2$(ox)] (**2**) and [Pd(L$^5$)$_2$(ox)]·L$^5$·Me$_2$CO (**5**·L$^5$·Me$_2$CO)

X-ray measurements of selected crystals of **2** and **5**·L$^5$·Me$_2$CO were collected on an Xcalibur™2 diffractometer (Oxford Diffraction Ltd.) with Mo Kα (Monochromator Enhance, Oxford Diffraction Ltd.) and Sapphire2 CCD detector at 120 K, and 105 K, respectively. Data collection and reduction were performed using CrysAlis software (Version 1.171.24) [30]. The structure was solved by direct methods using SHELXS-97 [31] and refined on $F^2$ using the full-matrix least-squares procedure (SHELXL-97) [32]. Non-hydrogen atoms were refined anisotropically and hydrogen atoms were located in a difference map and refined by using the riding model with C–H = 0.95 and 0.99 Å, N–H = 0.88 Å and $U_{iso}$(H) = 1.2$U_{eq}$(CH, CH$_2$, NH) or 1.5$U_{eq}$(CH$_3$). The isopropyl group of **2**, involving the C(16), C(17) and C(18) atoms, was refined as disordered over two positions with occupancy factors 63% and 37%, while the C(23) atom of acetone molecule of crystallization of **5**·L$^5$·Me$_2$CO was refined with the occupancy of 50% for each of two components. The molecular graphics were drawn and additional structural parameters were interpreted using DIAMOND [33].

### 2.4. In vitro cytotoxicity

*In vitro* cytotoxicity of the complexes **1**–**5** was determined by a calcein acetoxymethyl (AM) assay on the chronic myelogenous leukaemia (K562) and breast adenocarcinoma (MCF7) human cancer cell lines, which were maintained in plastic tissue culture flasks and grown (37 °C, 5% $CO_2$ atmosphere, 100% humidity) on Dulbecco's modified Eagle's cell culture medium (DMEM). The suspension of cancer cells (*ca* $1.25 \times 10^5$ cells $mL^{-1}$) was reattributed into 96-well microtitre plates (Nunc) and preincubated for 12 h. The tested palladium(II) complexes, which were pre-dissolved in DMF (DMF was used instead of DMSO in connection with high ability of DMSO to coordinate to Pd(II) ion which could cause the substitution of $L^n$ ligands in the tested complexes) and then diluted with deionised water to the final DMF concentration of 0.6%, were added in the concentration range of 0.2–25 μM. After the incubation lasting 72 h, the cells were incubated with calcein AM for 1 h. The fluorescence of the live cells was measured at 485/538 nm (excitation/emission) with Fluoroscan Ascent (Labsystems). Each experiment was repeated three times and the discussed $IC_{50}$ values represent an arithmetic mean. The maximal deviation did not exceed 17% related to an arithmetic mean.

### 2.5. Syntheses

#### 2.5.1. Syntheses of starting compounds

*2.5.1.1. Potassium Bis(oxalato)palladate(II) Dihydrate, $K_2[Pd(ox)_2]\cdot 2H_2O$.* $K_2[Pd(ox)_2]\cdot 2H_2O$ was synthesized using a slightly modified and previously published procedure [34]. Both potassium tetrachloropalladate(II), $K_2PdCl_4$, and potassium oxalate monohydrate, $K_2(ox)\cdot H_2O$, were dissolved separately in a minimum volume of distilled water (25 °C) in a 1:2 molar ratio. Then, both solutions were mixed together and stirred in the dark at laboratory temperature for 1 h. Orange precipitate, which formed, was filtered off and washed with cold distilled water and ethanol. The product was dissolved in a minimum volume of hot distilled water (50 °C), and then cooled down in the fridge to give the orange-brown needle-like crystals of $K_2[Pd(ox)_2]\cdot 2H_2O$ in very good yields (>90%). The compound was characterized by elemental analyses and FTIR, Raman and $^{13}C$ NMR spectroscopies. *Note: $K_2[Pd(ox)_2]\cdot 2H_2O$ should be stored in the dark and cool place to avoid its decomposition induced by light and heat.* Anal. Calc. for $PdK_2C_4O_8\cdot 2H_2O$ ($M_r$ = 396.7): C, 12.1; H, 1.0. Found: C, 12.3; H, 1.0%. IR (Nujol; $cm^{-1}$): 562m, 492w, 413w, 372m, 350vs, 291w, 236m, 215m. IR (KBr; $cm^{-1}$): 3559m, 3469m, 1702vs, 1679vs, 1660s, 1393s, 1236m, 1051w, 897w, 822m, 559m, 471m, 420m. Raman ($cm^{-1}$): 3492w, 3416w, 1717s, 1663m, 1420m, 1255m, 900w, 847w, 804w, 567m, 243vs. $^{13}C$ NMR ($D_2O$, ppm): $\delta$ 166.95 (Cox).

*2.5.1.2. 2-Chloro-N6-(benzyl)-9-isopropyladenine ($L^1$), 2-chloro-N6-(4-methoxybenzyl)-9-isopropyladenine ($L^2$), 2-chloro-N6-(2,3-dimethoxybenzyl)-9-isopropyladenine ($L^3$), 2-chloro-N6-(2,4-dimethoxybenzyl)-9-isopropyladenine ($L^4$) and 2-chloro-N6-(4-methylbenzyl)-9-isopropyladenine ($L^5$).* Modification of a formerly reported procedure [35] has been used for the preparation of organic molecules which are summarized in Scheme 1. Briefly, the first step included alkylation of the N9 position of 2,6-dichloropurine by 2-bromopropane provided in dried DMSO at laboratory temperature. Prepared 2,6-dichloro-9-isopropylpurine (DCIP) reacted in ethyl acetate (80 °C; 5 h) with an equimolar amount of benzylamine or its corresponding derivative. The mixture was stirred overnight at laboratory temperature. The solvent was evaporated under vacuum and the formed solid was filtered off, washed by ethyl acetate, distilled water and diethyl ether and dried in the air at the temperature of 40 °C. The results of elemental analyses, FTIR, Raman and NMR ($^1H$, $^{13}C$, $^{15}N$) spectral data and structural formulas of $L^1$–$L^5$ compounds are summarized in Appendix A in Supplementary material.

*2.5.2. Preparation of $[Pd(L^1)_2(ox)]$ (**1**), $[Pd(L^2)_2(ox)]$ (**2**), $[Pd(L^3)_2(ox)]$ (**3**), $[Pd(L^4)_2(ox)]\cdot 2H_2O$ (**4**) and $[Pd(L^5)_2(ox)]$ (**5**)*

The corresponding organic compound, $L^1$–$L^5$, (2 mmol) was dispersed in 5 mL of acetone and added to a water solution (5 mL) of $K_2[Pd(ox)_2]\cdot 2H_2O$ (1 mmol). The reaction mixture was stirred for ca. 24 h at 40 °C. The obtained solid, representing the palladium(II) complexes **1**–**5**, was filtered off, washed with warm and cold distilled water, and *iso*propanol, and dried in the air at 40 °C. Single crystals of **2** were obtained from the acetone solution of **2** in 4 weeks. In the case of **5**, well developed single crystals of $[Pd(L^5)_2(ox)]\cdot L^5\cdot Me_2CO$ (**5**·$L^5$·$Me_2CO$) formed in the mother liquor in a few weeks. The results of FTIR, Raman and NMR spectroscopies are summarized in Appendix A in Supplementary material.

**1**: Yield: 500 mg (63%). Anal. Calc. for $PdC_{32}H_{32}N_{10}O_4Cl_2$ ($M_r$ = 798.0): C, 48.2; H, 4.0; N, 17.6. Found: C, 48.1; H, 3.9; N, 17.1%.

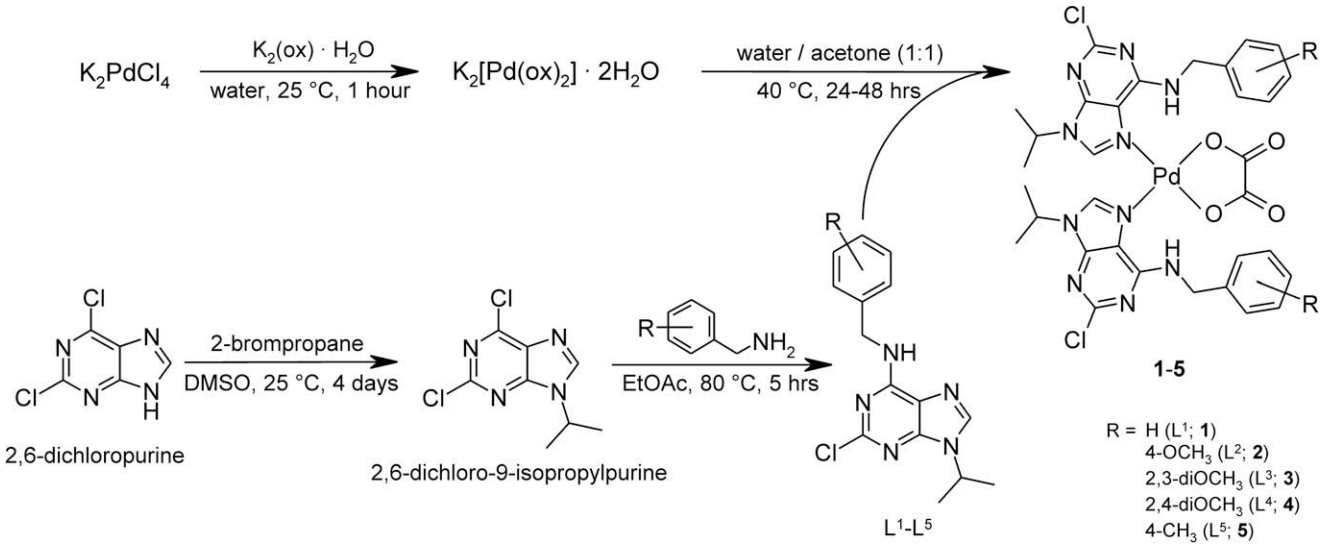


**Scheme 1.** Synthetic pathways for the preparation of starting compounds, i.e. $K_2[Pd(ox)_2]\cdot 2H_2O$ and $L^1$–$L^5$, and palladium(II) complexes (**1**–**5**).

**2**: Yield: 704 mg (82%). Anal. Calc. for $PdC_{34}H_{36}N_{10}O_6Cl_2$ ($M_r$ = 858.0): C, 47.6; H, 4.2; N, 16.3. Found: C, 47.8; H, 4.2; N, 15.8%.

**3**: Yield: 740 mg (81%). Anal. Calc. for $PdC_{36}H_{40}N_{10}O_8Cl_2$ ($M_r$ = 918.1): C, 47.1; H, 4.4; N, 15.3. Found: C, 47.5; H, 4.7; N, 15.0%.

**4**: Yield: 640 mg (70%). Anal. Calc. for $PdC_{36}H_{40}N_{10}O_8Cl_2\ 2H_2O$ ($M_r$ = 954.1): C, 45.3; H, 4.6; N, 14.7. Found: C, 45.5; H, 4.8; N, 15.0%.

**5**: Yield: 550 mg (67%). Anal. Calc. for $PdC_{34}H_{36}N_{10}O_4Cl_2$ ($M_r$ = 826.0): C, 49.4; H, 4.4; N, 17.0. Found: C, 48.9, H, 4.3; N, 17.3%.

## 3. Results and discussion

### 3.1. General properties

Pale yellow palladium(II) complexes $[Pd(L^n)_2(ox)]\cdot xH_2O$ (**1**–**5**) have been synthesized by the reactions of $K_2[Pd(ox)_2]\cdot 2H_2O$ with the corresponding organic derivative ($L^1$–$L^5$) in a distilled water/acetone mixture (1:1, v/v) in the 1:2 molar ratio, with quite good yields (63–82%). The complexes **1**–**5** have been found to be very well soluble in DMF, DMSO and acetone, whereas, relatively low solubility has been observed in ethanol, methanol and distilled water at laboratory temperature. The determined values of molar conductivity ranged from 1.1 to 3.8 S cm$^2$ mol$^{-1}$ (for $10^{-3}$ M DMF solutions) and from 0.1 to 1.4 S cm$^2$ mol$^{-1}$ (for $10^{-3}$ M acetone solutions) (Table 6), and confirmed that the prepared palladium(II) complexes behave as non-electrolytes [36]. The values of molar conductivity were determined as slightly higher after 4 weeks (3.1–8.3 S cm$^2$ mol$^{-1}$ for DMF solutions and from 2.3–4.0 S cm$^2$ mol$^{-1}$ for acetone solutions) which can be caused by a partial dissociation of the complexes in the solvents used.

### 3.2. FTIR and Raman spectroscopy

The presence of both the $L^1$–$L^5$ ligands and oxalate dianion in the palladium(II) complexes **1**–**5** has been clearly proved by FTIR and Raman spectroscopy. The bands of very strong intensity detected in the 1614–1619 cm$^{-1}$ region (see Table 2) in the FTIR spectra may be assigned to the $\nu$(C=N) vibration of a purine ring [37]. These bands are shifted by 3–30 cm$^{-1}$ compared with those observed in free $L^1$–$L^5$ compounds, showing on coordination of these organic molecules as ligands. The other vibrations characterizing $L^2$–$L^4$ ligands (involved in the complexes **2**–**4**) with methoxy-substituted benzyl ring, were observed at 1033–1062 cm$^{-1}$ and 1229–1243 cm$^{-1}$, which can be assigned to [$\nu$(C–O)$_{met}$, and $\nu$(C–O)$_{ar}$], respectively. The bands observed at 1157–1176 cm$^{-1}$,

**Table 1**
Crystal data and structure refinements for **2** and **5**·$L^5$·$Me_2CO$.

| Compound | **2** | **5**·$L^5$·$Me_2CO$ |
|---|---|---|
| Empirical formula | $C_{34}H_{36}Cl_2N_{10}O_6Pd$ | $C_{53}H_{60}Cl_3N_{15}O_5Pd$ |
| Formula weight | 858.03 | 1199.91 |
| Temperature (K) | 120(2) | 105(2) |
| Wavelength (Å) | 0.71073 | 0.71073 |
| Crystal system, space group | Triclinic, $P\bar{1}$ | Triclinic, $P\bar{1}$ |
| *Unit cell dimensions* | | |
| $a$ (Å) | 9.3315(2) | 10.8200(3) |
| $b$ (Å) | 13.9014(4) | 15.0532(4) |
| $c$ (Å) | 16.0228(5) | 17.6293(4) |
| $\alpha$ (°) | 64.671(3) | 89.068(2) |
| $\beta$ (°) | 85.916(2) | 75.599(2) |
| $\gamma$ (°) | 73.535(2) | 83.676(2) |
| $V$ (Å$^3$) | 1798.62(9) | 2764.05(12) |
| $Z$, $D_{calc}$ (g cm$^{-3}$) | 2, 1.584 | 2, 1.442 |
| Absorption coefficient (mm$^{-1}$) | 0.725 | 0.542 |
| Crystal size (mm) | 0.25 × 0.20 × 0.20 | 0.25 × 0.20 × 0.15 |
| $F$ (0 0 0) | 876 | 1240 |
| $\theta$ range for data collection (°) | $2.60 \leqslant \theta \leqslant 25.00$ | $2.68 \leqslant \theta \leqslant 25.00$ |
| Index ranges ($h$, $k$, $l$) | $-11 \leqslant h \leqslant 11$ | $-12 \leqslant h \leqslant 11$ |
| | $-12 \leqslant k \leqslant 16$ | $-17 \leqslant k \leqslant 17$ |
| | $-17 \leqslant l \leqslant 19$ | $-20 \leqslant l \leqslant 17$ |
| Reflections collected/unique ($R_{int}$) | 15041/6302 (0.0244) | 23281/9674 (0.0439) |
| Max. and min. transmission | 0.8686 and 0.8395 | 0.9231 and 0.8763 |
| Data/restraints/parameters | 6302/0/504 | 9674/0/707 |
| Goodness-of-fit on $F^2$ | 1.109 | 1.020 |
| Final $R$ indices [$I>2\sigma(I)$] | $R_1$ = 0.0383, w$R_2$ = 0.0915 | $R_1$ = 0.0474, w$R_2$ = 0.0961 |
| $R$ indices (all data) | $R_1$ = 0.0537, w$R_2$ = 0.1028 | $R_1$ = 0.0783, w$R_2$ = 0.1030 |
| Largest peak and hole (e Å$^{-3}$) | 0.741, −0.587 | 0.631, −0.815 |

**Table 2**
Important FTIR and Raman (in parentheses) data for $K_2[Pd(ox)_2]\cdot 2H_2O$ and complexes **1**–**5** given in cm$^{-1}$.

| Complex | $\nu$(Pd–N) | $\nu$(Pd–O) | $\nu$(C–Cl) | $\nu$(C=C) | $\nu$(C=N) | $\nu_a$(C=O)$_{ox}$ | $\nu$(C–H)$_{aliphatic}$ |
|---|---|---|---|---|---|---|---|
| $K_2[Pd(ox)_2]\cdot 2H_2O$ | – | 562 (567) | – | – | – | 1702, 1679 (1717, 1663) | – |
| **1** | 521 (523) | 560 (558) | 1164 (1160) | 1581, 1486 (1579, 1488) | 1617 (1606) | 1705, 1676 (1691, 1671) | 3060, 2941 (3063, 2943) |
| **2** | 521 (523) | 564 (562) | 1157 (1157) | 1580, 1483 (1576, 1486) | 1614 (1610) | 1708, 1676 (1695, 1660) | 3061, 2935 (3060, 2950) |
| **3** | 516 (515) | 559 (560) | 1169 (1170) | 1581, 1480 (1580, 1489) | 1619 (1614) | 1709, 1677 (1695, 1676) | 3068, 2936 (3053, 2935) |
| **4** | 517 (526) | 565 (562) | 1157 (1159) | 1588, 1485 (1583, 1489) | 1618 (1610) | 1714, 1672 (1706, 1668) | 3062, 2937 (3072, 2933) |
| **5** | 522 (526) | 562 (571) | 1163 (1157) | 1581, 1483 (1579, 1486) | 1617 (1614) | 1716, 1674 (1702, 1670) | 3057, 2930 (3053, 2941) |

**Table 3**
Selected coordination shifts ($\Delta\delta = \delta_{complex} - \delta_{ligand}$) observed for complexes **1**–**5** in $^{1}$H, $^{13}$C NMR and $^{1}$H-$^{15}$N gs-HMBC spectra.

| Complex | $^{1}$H NMR | | $^{13}$C NMR | | | | | | $^{15}$N NMR | | | | |
|---|---|---|---|---|---|---|---|---|---|---|---|---|---|
| | N6H | C8H | C2 | C4 | C5 | C6 | C8 | Cox | N1 | N3 | N6 | N7 | N9 |
| **1** | 0.57 | 0.49 | 0.12 | −0.25 | −2.42 | −0.93 | 3.82 | −1.07 | 4.4 | 0.1 | 7.1 | −92.4 | 7.1 |
| **2** | 0.46 | 0.41 | −0.02 | −0.26 | −2.46 | −0.84 | 3.84 | −0.98 | 5.9 | 2.0 | 8.3 | −91.2 | 9.0 |
| **3** | 0.63 | 0.47 | −0.13 | −0.25 | −2.44 | −0.97 | 3.80 | −1.28 | 4.0 | −0.3 | 6.5 | −92.4 | 6.2 |
| **4** | 0.63 | 0.42 | 0.11 | −0.24 | −2.43 | −1.00 | 3.84 | −1.52 | 2.5 | −1.3 | 7.7 | −94.0 | 6.1 |
| **5** | 0.54 | 0.47 | 0.07 | −0.24 | −2.45 | −0.91 | 3.82 | −1.18 | 4.4 | [a] | 7.3 | −92.8 | 6.9 |

[a] N3 atom was not observed in the $^{1}$H–$^{15}$N gs-HMBC spectrum of $L^5$.

**Table 4**
Selected bond lengths (Å) and angles (°) for complexes **2** and **5**·$L^5$·$Me_2CO$.

| Compound | $[Pd(L^2)_2(ox)]$ (**2**) | $[Pd(L^5)_2(ox)]\cdot L^5\cdot Me_2CO$ (**5**?$L^5\cdot Me_2CO$) | |
|---|---|---|---|
| *Bond lengths* | | [a] | [b] |
| Pd(1)–N(7) | 2.012(3) | 2.023(3) | – |
| Pd(1)–N(7A) | 2.024(3) | 2.021(3) | – |
| Pd(1)–O(1) | 1.992(2) | 1.971(2) | – |
| Pd(1)–O(2) | 1.987(2) | 1.983(2) | – |
| O(1)–C(21) | 1.302(4) | 1.332(4) | – |
| O(2)–C(20) | 1.289(4) | 1.282(4) | – |
| O(3)–C(21) | 1.215(4) | 1.239(4) | – |
| O(4)–C(20) | 1.222(4) | 1.230(4) | – |
| C(20)–C(21) | 1.549(5) | 1.471(5) | – |
| N(1)–C(2) | 1.321(5)/1.328(5) | 1.328(4)/1.315(4) | 1.332(4) |
| N(1)–C(6) | 1.355(4)/1.358(4) | 1.349(4)/1.345(4) | 1.351(4) |
| C(2)–Cl(1) | 1.755(4)/1.756(4) | 1.757(4)/1.754(4) | 1.751(4) |
| C(2)–N(3) | 1.315(5)/1.303(5) | 1.311(4)/1.317(4) | 1.309(4) |
| N(3)–C(4) | 1.348(4)/1.350(5) | 1.344(4)/1.346(4) | 1.353(4) |
| C(4)–C(5) | 1.384(5)/1.382(5) | 1.380(5)/1.376(5) | 1.381(5) |
| C(4)–N(9) | 1.378(5)/1.352(5) | 1.371(4)/1.384(4) | 1.375(4) |
| C(5)–C(6) | 1.403(5)/1.417(5) | 1.406(5)/1.422(5) | 1.408(5) |
| C(5)–N(7) | 1.394(4)/1.390(4) | 1.397(4)/1.392(4) | 1.397(4) |
| C(6)–N(6) | 1.339(4)/1.319(4) | 1.330(4)/1.333(4) | 1.335(4) |
| N(7)–C(8) | 1.327(4)/1.319(4) | 1.316(4)/1.327(4) | 1.313(4) |
| C(8)–N(9) | 1.341(5)/1.347(5) | 1.351(4)/1.344(4) | 1.363(4) |
| *Bond angles* | | | |
| O(1)–Pd(1)–N(7A) | 93.09(10) | 89.86(10) | – |
| O(1)–Pd(1)–N(7) | 174.96(10) | 173.26(10) | – |
| O(1)–Pd(1)–O(2) | 84.46(9) | 84.20(10) | – |
| O(2)–Pd(1)–N(7) | 91.12(10) | 89.38(10) | – |
| O(2)–Pd(1)–N(7A) | 177.10(10) | 171.75(10) | – |
| N(7)–Pd(1)–N(7A) | 91.39(11) | 96.32(11) | – |
| Pd(1)–O(1)–C(21) | 111.8(2) | 110.6(2) | – |
| Pd(1)–O(2)–C(20) | 111.8(2) | 111.5(2) | – |
| O(1)–C(21)–O(3) | 125.2(3) | 121.1(3) | – |
| O(2)–C(20)–O(4) | 124.9(3) | 123.0(3) | – |
| O(1)–C(21)–C(20) | 115.3(3) | 116.3(3) | – |
| O(2)–C(20)–C(21) | 115.9(3) | 117.4(3) | – |
| O(3)–C(21)–C(20) | 119.5(3) | 122.5(3) | – |
| O(4)–C(20)–C(21) | 119.3(3) | 119.6(3) | – |
| Pd(1)–N(7)–C(5) | 127.9(2)/129.8(2) | 135.8(2)/129.9(2) | – |
| Pd(1)–N(7)–C(8) | 126.9(2)/124.8(2) | 119.2(2)/119.6(2) | – |
| C(2)–N(1)–C(6) | 117.4(3)/117.5(3) | 116.9(3)/117.4(3) | 117.0(3) |
| N(1)–C(2)–N(3) | 131.5(3)/132.1(3) | 132.3(3)/132.4(3) | 132.1(3) |
| C(2)–N(3)–C(4) | 109.7(3)/109.7(3) | 109.4(3)/109.0(3) | 109.6(3) |
| N(3)–C(4)–C(5) | 126.4(3)/126.5(4) | 126.4(3)/127.2(3) | 126.2(3) |
| N(3)–C(4)–N(9) | 127.2(3)/126.4(3) | 126.1(3)/126.2(3) | 127.5(3) |
| C(4)–C(5)–C(6) | 116.8(3)/117.2(3) | 117.5(3)/116.5(3) | 117.4(3) |
| C(4)–C(5)–N(7) | 108.8(3)/108.2(3) | 108.2(3)/108.9(3) | 110.5(3) |
| C(5)–C(6)–N(1) | 117.7(3)/116.9(3) | 117.5(3)/117.5(3) | 117.7(3) |
| C(5)–C(6)–N(6) | 123.7(3)/123.7(3) | 122.3(3)/124.5(3) | 122.4(3) |
| N(1)–C(6)–N(6) | 118.6(3)/119.4(3) | 120.2(3)/118.0(3) | 119.9(3) |
| C(6)–N(6)–C(9) | 122.5(3)/124.8(3) | 125.9(3)/122.7(3) | 124.0(3) |
| N(6)–C(9)–C(10) | 110.2(3)/111.9(3) | 111.8(3)/113.2(3) | 114.9(3) |
| C(5)–N(7)–C(8) | 105.2(3)/105.4(3) | 105.0(3)/105.3(3) | 103.1(3) |
| N(7)–C(8)–N(9) | 112.6(3)/112.2(3) | 113.4(3)/112.6(3) | 114.8(3) |
| C(8)–N(9)–C(4) | 107.1(3)/107.2(3) | 105.8(3)/106.6(6) | 105.3(3) |

[a] data for both coordinated $L^5$ molecules (N7 atom involving molecule/N7A atom involving molecule). The values given behind the slash belong to the equivalent interatomic parameter.
[b] Data for $L^5$ molecule of crystallization assigned to the equivalent interatomic parameter.

3103–3138 cm$^{-1}$ and 3269–3385 cm$^{-1}$ can be assigned to $\nu$(C–Cl), $\nu$(C–H)$_{ar}$, and (N–H), respectively. The maxima of the $\nu$(C–H)$_{aliphatic}$ vibrations were detected in the 2835–3068 cm$^{-1}$ region. The medium to strong $\nu_{as}$(C=O)$_{ox}$ bands of an oxalato group were observed

**Table 5**
Hydrogen bond parameters (Å, °) for complexes **2** and **5**?$L^5{\cdot}Me_2CO$.

| D–H···A | d(D–H) | d(H···A) | d(D···A) | < (DHA) |
|---|---|---|---|---|
| $[Pd(L^2)_2(ox)]$ (**2**) | | | | |
| N(6)–H(6)···O(4)$^{i}$ | 0.88 | 2.12 | 2.805(3) | 133.7 |
| $[Pd(L^5)_2(ox)]{\cdot}L^5{\cdot}Me_2CO$ (**5**·$L^5{\cdot}Me_2CO$) | | | | |
| N(6)–H(6)···O(4)$^{i}$ | 0.88 | 2.07 | 2.786(4) | 138.4 |
| N(6A)–H(6A)···O(4)$^{i}$ | 0.88 | 1.97 | 2.788(4) | 154.4 |
| N(6B)–H(6B)···N(7B)$^{ii}$ | 0.88 | 2.30 | 3.073(4) | 146.2 |

Symmetry codes: (i) $1-x, 1-y, 1-z$; (ii) $1-x, 1-y, -z$.

in both 1672–1676 $cm^{-1}$ and 1705–1716 $cm^{-1}$ regions, supporting a bidentate coordination of this dianion [38]. The bands connected with the $\nu_{sym}(C{-}O)_{ox}$ vibration were found between 1373 and 1389 $cm^{-1}$. The maxima observed in the far-FTIR spectra of the complexes **1**–**5** at 559–565 $cm^{-1}$ can be assigned to the $\nu$(Pd–O) vibration. These values correlated very well with those observed for $K_2[Pd(ox)_2]{\cdot}2H_2O$ at 562 $cm^{-1}$ (this work) and 556 $cm^{-1}$ (as reported in the literature [39]). The bands observed at 516–522 $cm^{-1}$ may be assignable to $\nu$(Pd–N) (see Table 2) [40].

Very similar conclusions regarding the presence and coordination mode of the ligands within the complexes **1**–**5** may be drawn from the Raman spectra (Table 2). The most intensive bands, which may be assigned to the stretching vibration of the purine skeleton, appeared in the 1340–1351 $cm^{-1}$ region [41]. They were shifted by 1–17 $cm^{-1}$ as compared with the free $L^1$–$L^5$ molecules. The vibrations of medium to strong intensity assignable to $\nu(C{-}H)_{aliphatic}$ $\nu_{sym}(C{-}O)_{ox}$ and $\nu$(Pd–O) were observed in the range of 2933–3072 $cm^{-1}$, 1404–1413 $cm^{-1}$, and 558–571 $cm^{-1}$, respectively. The split maxima at 1660–1706 $cm^{-1}$ and sharp peaks at 1606–1614 $cm^{-1}$ belong to $\nu_{as}(C{=}O)_{ox}$, and $\nu$(C=N), respectively. It is quite surprising, that maxima of the $\nu$(C=N) vibration were not shifted by more than two $cm^{-1}$ in the case of complexes **1**–**5** as compared to free ligands $L^1$–$L^5$. The weak $\nu$(Pd–N) vibrations, which were found in the Raman spectra of **1**–**5** around 520 $cm^{-1}$, correlated well with those detected in the FTIR spectra.

### 3.3. $^1H$, $^{13}C$, $^{15}N$ NMR spectroscopy

$^1H$, $^{13}C$, $^1H$–$^1H$ gs-COSY, $^1H$–$^{13}C$ gs-HMQC, $^1H$–$^{13}C$ gs-HMBC and $^1H$–$^{15}N$ gs-HMBC NMR experiments were performed for both free $L^1$–$L^5$ and complexes **1**–**5**. The comparison of chemical shifts ($\delta$) observed in the NMR spectra of free compounds $L^1$–$L^5$ and palladium(II) complexes, which are interpreted and discussed as coordination shifts $\Delta\delta = \delta_{complex} - \delta_{ligand}$, provided relevant information not only about the composition of the prepared complexes **1**–**5** but also about the coordination mode of the $L^1$–$L^5$ ligands to the Pd(II) centre.

The most relevant conclusions may be drawn from $^1H$–$^{15}N$ gs-HMBC spectra, which clearly proved the coordination of the $L^1$–$L^5$ molecules to the Pd(II) ion through the N7 atom of the purine moiety. This statement is based on coordination shift values ($\Delta\delta$), ranging from −94.0 ppm to −91.2 ppm for the N7 atoms, compared to $|\Delta\delta| < 9.0$ of the others nitrogen atoms (Table 3). The same conclusion may be deduced from the results of $^{13}C$ NMR and $^1H$ NMR experiments. The most significant coordination shifts, $|\Delta\delta|$, were observed for C8 (shifted by 3.80–3.84 ppm downfield as compared to free $L^1$–$L^5$ compounds) and C5 (shifted by 2.42–2.46 ppm upfield) in $^{13}C$ NMR spectra and for N6H ($\Delta\delta$ ranged from 0.46–0.63 ppm) and C8H ($\Delta\delta$ = 0.41–0.49 ppm) in $^1H$ NMR spectra. Larger $\Delta\delta$ values of N6H compared to those of C8H may be caused by the different orientation of the benzyl group of $L^n$ ligands within the complexes compared to free organic molecules. Moreover, the presence of non-bonding contacts (e.g. hydrogen bonds), in which the N6H group should be involved in the DMF-$d_7$ solutions, could affect the chemical shift values as well. It should be noted that such interactions were observed in the solid state in the X-ray structures of the complexes **2** and **5** (see Section 3.4).

The signal of the oxalate dianion carbons (Cox), that was found in the $^{13}C$ NMR spectra ($D_2O$ solutions) of $K_2[Pd(ox)_2]{\cdot}2H_2O$ at 166.95 ppm, was also found between 165.43–165.97 ppm in the case of $^{13}C$ NMR spectra of palladium(II) complexes **1**–**5**. Moreover, these signals were not observed by measuring of $^1H$–$^{13}C$ gs-HMQC and $^1H$–$^{13}C$ gs-HMBC experiments. The mentioned experiments clearly supported the statement that these signals belong to bidentate coordinated oxalato dianion present in the complexes **1**–**5**.

### 3.4. X-ray structures of $[Pd(L^2)_2(ox)]$ (**2**) and $[Pd(L^5)_2(ox)]{\cdot}L^5{\cdot}Me_2CO$ (**5**·$L^5{\cdot}Me_2CO$)

The molecular structures of **2** and **5**·$L^5{\cdot}Me_2CO$ were determined by a single crystal X-ray analysis and are depicted in Figs. 1 and 3, respectively. The crystal data and structure refinements are given in Table 1, the selected bond lengths and angles are listed in Table 4, while the hydrogen bond parameters are summarized in Table 5.

The Pd(II) centre of **2** is four-coordinated by two N(7) atoms of two $L_2$ molecules, and the O(1) and O(2) atoms of the bidentate oxalato group ($PdN_2O_2$ chromophore). The geometry is slightly distorted square-planar (Fig. 1, Table 4). Both $L^2$ molecules were found to be mutually arranged in head-to-head orientation.

The Pd(1) atom is situated 0.0109(3) Å out of the least-square plane formed by two N-atoms, originating from two $L^2$ ligands, and by two O-atoms, originating from the bidentate coordinated oxalate dianion. Two purine rings containing N(7) and N(7A) atoms form a dihedral angle being 86.27(6)°. The dihedral angles formed by the corresponding purine moiety and benzene ring of $L^2$ ligands were found to be 82.26(8)° for $L^2_{N(7)}$ [$L^2_{N(7)}$ = $L^2$ molecule involving N(7) atom] and 74.07(9)° for $L^2_{N(7A)}$ [$L^2_{N(7A)}$ = $L^2$ molecule involving

**Table 6**
Molar conductivity and selected TG/DTA data of complexes **1**–**5**.

| Complex | Conductivity data[a] | | TG/DTA thermal studies | | | | | |
|---|---|---|---|---|---|---|---|---|
| | | | $[Pd(L_n)_2(ox)]{\cdot}xH_2O \rightarrow PdO$ | | | PdO → Pd | | |
| | DMF | $Me_2CO$ | T (°C) | Δm (%)[b] | DTA (°C)[c] | T (°C) | Δm (%)[b] | DTA (°C) |
| $[Pd(L^1)_2(ox)]$ (**1**) | 3.8 (8.3) | 1.1 (4.0) | 168–444 | 84.7/84.2 | 205 exo, 422 exo | 809–840 | 2.0/1.8 | 816 endo |
| $[Pd(L^2)_2(ox)]$ (**2**) | 1.8 (5.4) | 0.1 (2.6) | 177–437 | 85.7/86.8 | 197 exo, 413 exo | [d] | [d] | [d] |
| $[Pd(L^3)_2(ox)]$ (**3**) | 1.8 (8.1) | 0.4 (2.3) | 166–434 | 86.7/87.4 | 181 exo, 393 exo | [d] | [d] | [d] |
| $[Pd(L^4)_2(ox)]{\cdot}2H_2O$ (**4**) | 1.1 (5.6) | 0.1 (2.5) | 66–450 | 87.2/86.2 | 100 endo, 134 endo, 178 exo, 423 exo | 808–834 | 1.6/1.6 | 820 endo |
| $[Pd(L^5)_2(ox)]$ (**5**) | 1.6 (3.1) | 1.5 (2.5) | 174–444 | 85.2/84.3 | 199 exo, 429 exo | 819–839 | 1.9/1.8 | 830 endo |

[a] $10^{-3}$ M solutions; values determined after 28 days in parentheses.
[b] Calc./Found.
[c] Stands for maximum of exothermic effect or minimum of endothermic effect.
[d] Measured up to 650 °C only.

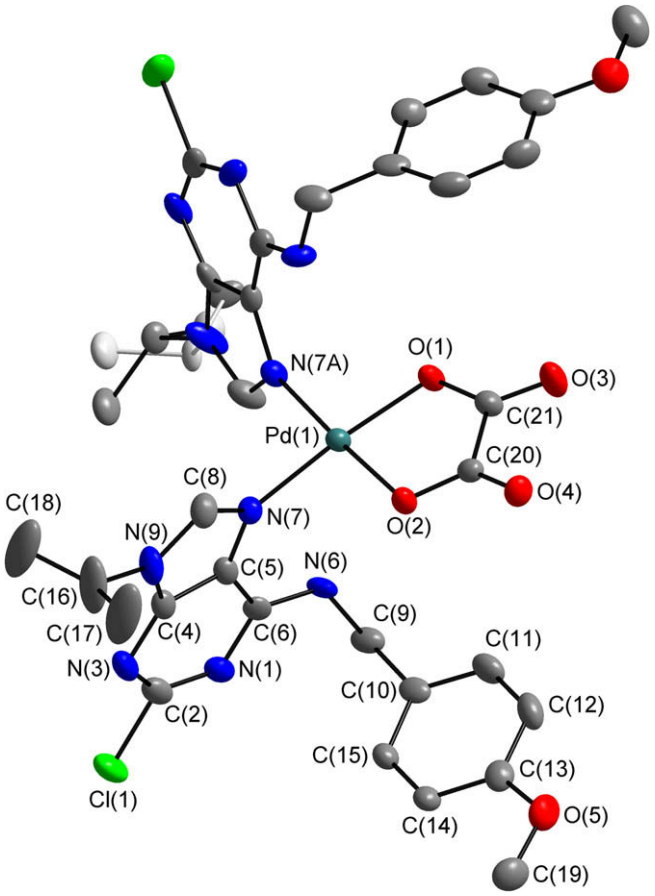


**Fig. 1.** The molecular structure of $[Pd(L^2)_2(ox)]$ (**2**) with non-hydrogen atoms drawn as thermal ellipsoids at 50% probability level, showing the atom numbering scheme. The C-atoms of isopropyl group distorted over two positions are displayed in light grey colour. H-toms are omitted for clarity.

N(7A) atom]. Moreover, the purine moieties form the dihedral angles of 85.90(7)° ($L^5_{N(7)}$) and 66.18(6)° ($L^5_{N(7A)}$) with a least-square plane formed by atoms of the $PdN_2O_2$ chromophore.

The oxalate dianion is coordinated through two O-atoms, O(1) and O(2), which are −0.006(2) Å for O(1) and −0.038(3) Å for O(2) out of the least-square $PdO_2C_2$ plane formed by the Pd(1), O(1), O(2), C(20) and C(21) atoms. A quite different situation was observed for the non-coordinated O-atoms of the oxalato group, since O(3) is −0.122(3) Å and O(4) 0.246(3) Å out of the above-mentioned plane. This is most likely caused by the intermolecular N–H···O hydrogen bonds in which the O(4) atoms are involved, as discussed below.

Two molecules of the complex **2** form centrosymmetric dimers which are linked together by the N(6A)–H···O(4) hydrogen bonds (Fig. 2). Both basal planes, formed by the atoms of $PdN_2O_2$ moieties, are coplanar with the dihedral angle being 0.000(85)°. None of the O(3) atoms in the crystal structure of **2** is involved in the hydrogen bond system. Except for the N–H···O hydrogen bonds, the non-bonding intermolecular interactions of the C–H···O and C···Cl type have been found to stabilize the crystal structure of **2** (for detailed information see Appendix A in Supplementary material).

The asymmetric unit of **5**·$L^5$·$Me_2CO$ consists of one molecule of the complex $[Pd(L^5)_2(ox)]$, and $L^5$ and $Me_2CO$ molecules of crystallization. The central Pd(II) ion is four-coordinated ($PdN_2O_2$ chromophore) in a slightly distorted square-planar geometry with both $L^5$ molecules mutually arranged in head-to-tail orientation (Fig. 3). However, several relevant differences were observed between the two discussed complexes, which are most probably caused by the different mutual orientation of both $L_n$ ligands within the complexes **2** (head-to-head) and **5** (head-to-tail).

The Pd(1) atom was found to be more deviated [0.0717(3) Å] from the least-square plane formed by the N(7), N(7A), O(1) and O(2) atoms than in case of complex **2**. The $L^5$ ligands are coordinated through the N(7) atoms of the purine moieties. The significant increase of the C(5)–N(7)–C(8) angle in the coordinated $L^5_{N(7)}$ and ($L^5_{N(7A)}$) molecules [105.0(3)°, and 105.3(3)°, respectively] as compared to that found in the uncoordinated $L^5$ molecule of crystallization [103.1(3)°]. Moreover, the values of C(5)–N(7)–C(8) angles determined for **2** [105.2(3)° for $L^2_{N(7)}$ and 105.4(3)° for $L^2_{N(7A)}$] correlated very well with those of **5** (Table 4).

Both purine rings form a dihedral angle of 89.03(6)°. The dihedral angle between the purine moiety and benzene ring within each of the coordinated $L_5$ molecules is 87.72(10)° for $L^5_{N(7)}$, and 84.25(8)° for ($L^5_{N(7A)}$), respectively, which is significantly higher compared to those of **2**. However, the most significant difference between the complexes **2** and **5** was determined for the dihedral angles, 52.85(7)° ($L^5_{N(7)}$) and 58.63(6)° ($L^5_{N(7A)}$), formed by the purine moieties with a least-square plane formed by the atoms of the $PdN_2O_2$ chromophore, which is caused by the different mutual orientation of $L^2$ (head-to-head) and $L^5$ (head-to-tail) molecules in the complexes **2** and **5**.

The O(3) atom is situated 0.027(3) Å and O(4) atom −0.048(2) Å out of the least-square $PdO_2C_2$ plane. As in the case of **2**, it is due to the N–H···O hydrogen bonds system, in which only the O(4) of the oxalate group is involved.

Similarly to the complex **2**, two molecules of the complex **5** form centrosymmetric dimers with both $PdN_2O_2$ basal planes nearly coplanar with the dihedral angle being 0.000(75)° (Fig. 4). However, due to the different mutual orientation of two coordinated $L^n$ molecules within the complex **5**, as compared to **2**, the N(6)–H···O(4) and N(6A)–H···O(4) hydrogen bonds are present within the crystal structure of **5** (Table 5). None of the O(3) atoms in the crystal structure of **5**·$L^5$·$Me_2CO$ is involved in the hydrogen bond system. Except for the N–H···O hydrogen bonds, the non-bonding intermolecular interactions of the C–H···Cl, C–H···N and C–H···O type have been found to stabilize the crystal structure of **5** (for detailed information see Appendix A in Supplementary material). Similarly to two complex molecules, two $L^5$ molecules of crystallization also form centrosymmetric dimers which are bonded together by a pair of the hydrogen bonds N(6B)–H···N(7B).

The only monomeric palladium(II) oxalato complexes with unidentate N-donor heterocyclic imine, which are deposited in the CSD, are $[Pd(mi)_2(ox)]\cdot H_2O$ [16] and $[Pd(py)_2(ox)]$ [18]. The Pd–O and Pd–N bond lengths and O–Pd–N angles were determined to be 1.997(3) Å, 1.995(3) Å and 174.85(14)° for $[Pd(mi)_2(ox)]\cdot H_2O$ and 2.010(2) Å, 2.015(2) Å and 175.06(9)° for $[Pd(py)_2(ox)]$. These parameters do not differ significantly from those determined for the complexes **2** and **5**·$L^5$·$Me_2CO$, which are given in Table 4. As of complexes **2** and **5**·$L^5$·$Me_2CO$, the differences in their Pd–O and Pd–N bond lengths can be considered to be non-significant (0.003–0.021 Å). Moreover, O(1)–Pd(1)–O(2) angle is quite comparable for these two palladium(II) complexes, but all the other angles around the central Pd(II) ion, which involve N7 atom, differ by 1.70–5.35°. This is most likely caused by the opposite arrangement of $L^n$ molecules within these complexes, as mentioned above.

### 3.5. TG/DTA thermal studies

The complexes $[Pd(L^n)_2(ox)]\cdot xH_2O$ (**1**–**5**) were studied by a simultaneous TG/DTA analysis and the results are summarized in Table 6.

TG curves clearly proved that the complexes **1**–**3** and **5** are non-solvated, because the named compounds have been found to be

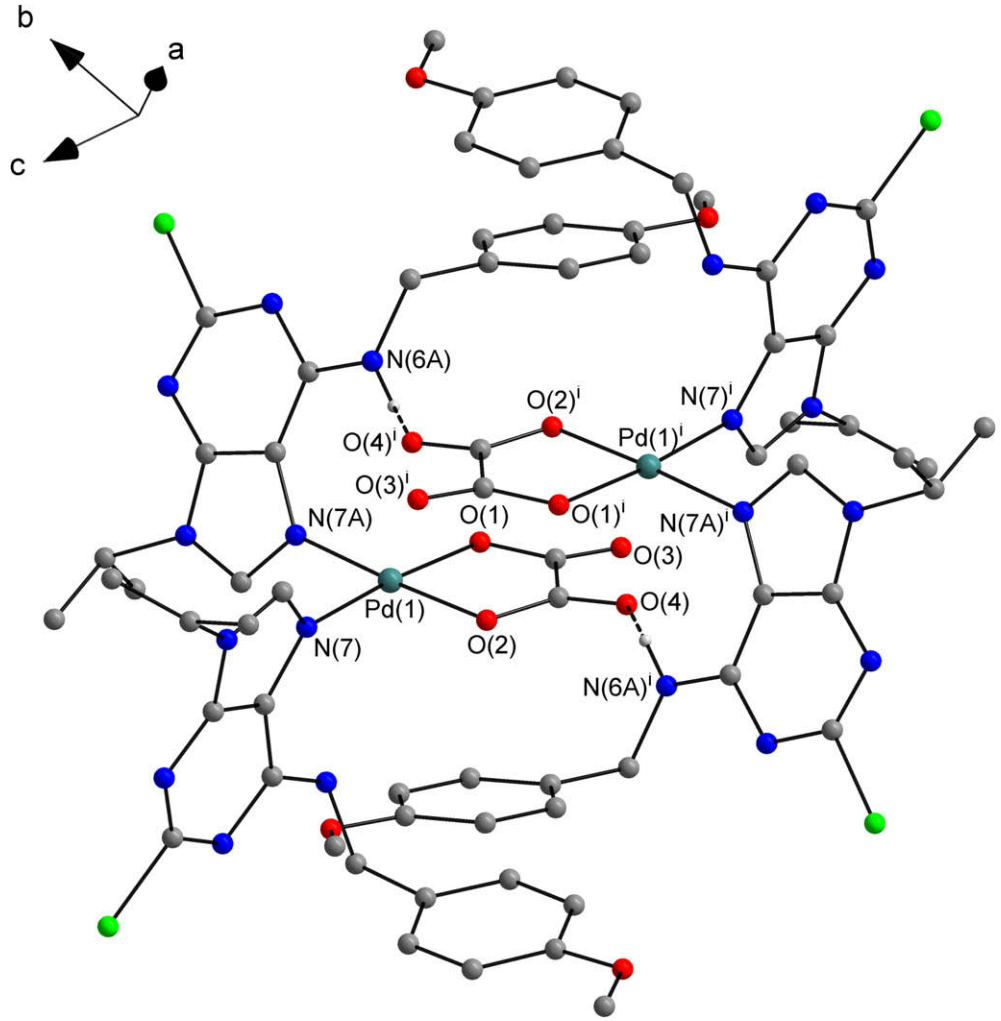


**Fig. 2.** Part of the crystal structure of $[Pd(L^2)_2(ox)]$ (**2**), showing the N–H···O hydrogen bonds (dashed lines). H-toms not involved into hydrogen bonding are omitted for clarity. Symmetry code: (i) $1-x$, $1-y$, $1-z$.

thermally stable up to 166–177 °C (Fig. 5). Complex **4** has been determined as a dihydrate. The thermal decomposition of this complex started at 66 °C by the loss of the first of the two water molecules of crystallization. The process continued by the elimination of the second water molecule and finished at 145 °C. The loss of both water molecules was accompanied by a weight loss on TG curve (Calc./Found: 3.8/4.0%) and by two *endo*-effects with minima at 100 °C and 134 °C on the DTA curve. The courses of thermal degradations of non-solvated complexes **1**–**5** were nearly identical. The decomposition processes started at 145–177 °C and proceeded without formation of any thermally stable products up to ca. 440 °C, and they were accompanied by two subsequent *exo*-effects on the DTA curves. The differences between the overall weight losses determined by the thermal analyses and those calculated to PdO as the final product of thermal degradation did not differ by more than 1.1% (Table 6).

It should be noted that one more weight loss was observed on the TG curve in case of **1**, **4** and **5**, for which the TG/DTA study was performed up to 1000 °C. The process started at about 810 °C and it was accompanied by a weak *endo*-effect on the DTA curve. This may be attributed to the decomposition of PdO to Pd, as proved by the values of weight loss (Calc./Found: **1**, 2.0/1.8; **4**, 1.7/1.6; **5**, 1.9/1.8%). Thus, PdO and Pd can be considered to be the final products of thermal degradation of $[Pd(L^n)_2(ox)]\cdot xH_2O$ complexes **1**–**5** depending on the temperature range of the experiment.

### 3.6. In vitro cytotoxicity

All of the prepared palladium(II) oxalato complexes **1**–**5** have been tested on their *in vitro* cytotoxicity against human chronic myelogenous leukaemia (K562) and human breast adenocarcinoma (MCF7) cancer cell lines. The results are expressed as the $IC_{50}$ values and are summarized in Table 7. The tests were performed with the solutions of the complex concentrations up to 25 μM. Significant *in vitro* cytotoxicity has been found for the complexes **3** and **5** on the MCF7 cancer cell line. The determined $IC_{50}$ values of these complexes, 6.2 μM for **3** and 6.8 μM for **5**, are considerably lower than those of the commercially used antineoplastic drugs cisplatin ($IC_{50}$ = 11 μM) and oxaliplatin ($IC_{50}$ = 18 μM) on the same cell line. As for the K562 cancer cell line, the lowest $IC_{50}$ value (16.2 μM) was determined for complex **5**. All the remaining results showed the prepared palladium(II) complexes to be inactive against the mentioned cell line within the evaluated concentration interval, i.e. up to 25 μM.

Nevertheless, the discussed $IC_{50}$ values regarding *in vitro* cytotoxicity of complex **3** against the MCF7 cell line and those of complex **5** against both MCF7 and K562 cell lines are significantly lower than those of *cis*- or *trans*-$[Pd(L)_2Cl_2]$ complexes involving the 2-chloro-N6-(benzyl)-9-isopropyladenine skeleton which were previously prepared in our laboratory [11,42]. Based on these results it is possible to support the positive role of an oxalate anion

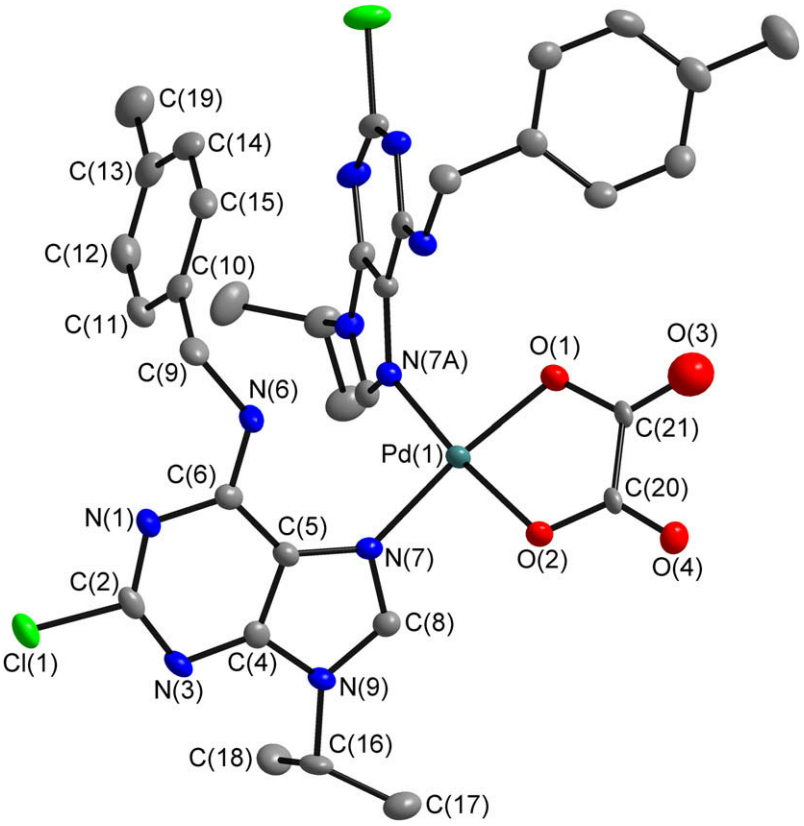


**Fig. 3.** The molecular structure of $[Pd(L^5)_2(ox)]\cdot L^5\cdot Me_2CO$ (**5**·$L^5$·$Me_2CO$) with non-hydrogen atoms drawn as thermal ellipsoids at 50% probability level, showing the atom numbering scheme. The $L^5$ and $Me_2CO$ molecules of crystallization and H-atoms are omitted for clarity.

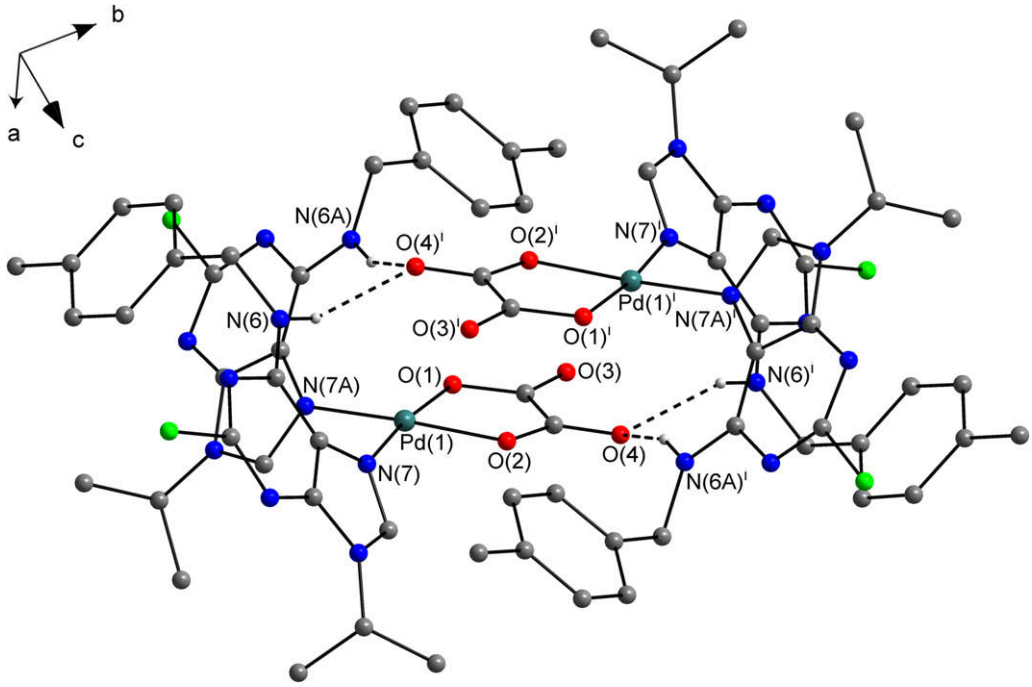


**Fig. 4.** Part of the crystal structure of $[Pd(L^5)_2(ox)]\cdot L^5\cdot Me_2CO$ (**5**·$L^5$·$Me_2CO$), showing the N–H···O hydrogen bonds (dashed lines). The $L^5$ and $Me_2CO$ molecules of crystallization and H-atoms not involved in hydrogen bonds are omitted for clarity. Symmetry code: (i) $1-x, 1-y, 1-z$.

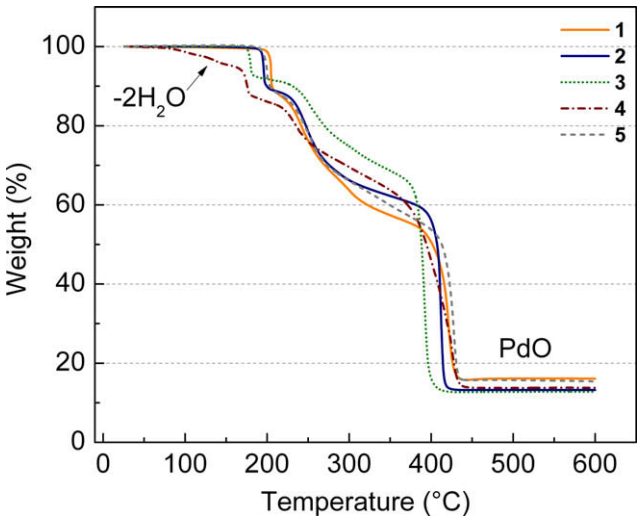


**Fig. 5.** TG curves of the palladium(II) complexes **1**–**5**.

**Table 7**
Results of *in vitro* cytotoxicity testing of complexes **1**–**5**.

| Complex | $IC_{50}$ (μM) | |
|---|---|---|
| | K562[a] | MCF7[b] |
| $[Pd(L^1)_2(ox)]$ (**1**) | >25 | >25 |
| $[Pd(L^2)_2(ox)]$ (**2**) | >12.5 | >12.5 |
| $[Pd(L^3)_2(ox)]$ (**3**) | >25 | 6.2 |
| $[Pd(L^4)_2(ox)]\cdot 2H_2O$ (**4**) | >12.5 | >12.5 |
| $[Pd(L^5)_2(ox)]$ (**5**) | 16.2 | 6.8 |
| cisplatin | 4.7 | 10.9 |
| oxaliplatin | 8.8 | 18.2 |

[a] Human chronic myelogenous leukaemia.
[b] Human breast adenocarcinoma.

as a leaving group on cytotoxic properties of the palladium(II) complexes.

## 4. Conclusions

The first square-planar palladium(II) oxalato complexes of the composition $[Pd(L^n)_2(ox)]\cdot xH_2O$ ($x = 0$ or 2) (**1**–**5**), bearing adenine-based ligands involving the N6-(benzyl)adenine moiety ($L^n$), have been prepared by the reactions of $[K_2Pd(ox)_2]\cdot 2H_2O$ with the corresponding $L^n$ compound. Two $L^n$ ligands are coordinated to Pd(II) ion through the N7 atoms of the purine moiety, while the oxalate dianion is coordinated as a bidentate O-donor ligand, as proved by a single crystal X-ray analysis and multinuclear NMR study. The mutual arrangement of two $L^n$ ligands was determined by a single crystal X-ray analysis as head-to-head and head-to-tail orientation in the case of complexes **2**, and **5**, respectively. The *in vitro* cytotoxicity results, expressed as $IC_{50}$ values, obtained for the complexes **3** ($IC_{50} = 6.2$ μM) and **5** ($IC_{50} = 6.8$ μM) on the MCF7 human cancer cell line are significantly lower than those of cisplatin ($IC_{50} = 11$ μM) and oxaliplatin ($IC_{50} = 18$ μM) for the same cancer cell line.

## Acknowledgements

The authors gratefully thank the Ministry of Education, Youth and Sports of the Czech Republic for financial support (a Grant No. MSM6198959218), Dr. Miroslava Matíková-Malarová for FTIR and Raman spectra measurements, Mr. Lukáš Dvořák for performing CHN elemental analyses, and Dr. Vladimír Kryštof and Mrs. Dita Parobková for *in vitro* cytotoxicity testing.

## Appendix A. Supplementary material

Additional crystallographic data are deposited as CCDC 716051 {$[Pd(L^2)_2(ox)]$ (**2**)} and CCDC 716052 {$[Pd(L^5)_2(ox)]\cdot L^5\cdot Me_2CO$ (**5**$\cdot L^5\cdot Me_2CO$)} and can be obtained free of charge from the Cambridge Crystallographic Data Centre, 12 Union Road, Cambridge CB2 1EZ, UK; fax: (+44) 1223 336 033; email: deposit@ccdc.cam.ac.uk, or at http://www.ccdc.cam.ac.uk. The results of elemental analyses and FTIR, Raman and NMR ($^1H$, $^{13}C$, $^{15}N$) spectral data of $L^1$–$L^5$ organic compounds, the results of FTIR, Raman and NMR ($^1H$, $^{13}C$, $^{15}N$) spectroscopies of the complexes **1**–**5**, as well as the figures of crystal packing of the complexes **2** and **5**$\cdot L^5\cdot Me_2CO$ together with the tables of its selected parameters are deposited. Supplementary material associated with this article can be found, in the online version, at doi:10.1016/j.jinorgbio.2009.04.008.

## References

[1] B. Rosenberg, L. Van Camp, T. Krigas, Nature 205 (1965) 698–699.
[2] L.R. Kelland, N.P. Farrell, Platinum-Based Drugs in Cancer Therapy, Humana, Totowa, 2000.
[3] K.R. Harrap, Cancer Treat. Rev. 12 (1985) 21–33.
[4] Y. Kidani, K. Inagaki, J. Med. Chem. 21 (1978) 1315–1318.
[5] L.M. Pasetto, R.M. DAndrea, A.A. Brandes, E. Rossi, S. Monfardini, Crit. Rev. Oncol. Hematom. 60 (2006) 59–75.
[6] J.L. Butour, S. Wimmer, F. Wimmer, P. Castan, Chem. Biol. Interact. 104 (1997) 165–178.
[7] M. Gielen, E.R.T. Tiekink, Metallotherapeutic Drugs and Metal-Based Diagnostic Agents, Willey, London, 2005. pp. 399–419.
[8] A. Garoufis, S.K. Hadjikakou, N. Hadjiliadis, Coord. Chem. Rev. (2008), doi:10.1016/j.ccr.2008.09.011.
[9] J. Kuduk-Jaworska, A. Puszko, M. Kubiak, M. Pełczyńska, J. Inorg. Biochem. 98 (2004) 1447–1456.
[10] S. Ray, R. Mohan, J.K. Singh, M.K. Samantaray, M.M. Shaikh, D. Panda, P. Ghosh, J. Am. Chem. Soc. 129 (2007) 15042–15053.
[11] L. Szüčová, Z. Trávníček, M. Zatloukal, I. Popa, Bioorg. Med. Chem. 14 (2006) 479–491.
[12] M.J. Cleare, Coord. Chem. Rev. 12 (1974) 349–405.
[13] E. Monti, M. Gariboldi, A. Maiocchi, E. Marengo, C. Cassino, E. Gabano, D. Osella, J. Med. Chem. 48 (2005) 857–866.
[14] F.G. Mann, D. Crowfoot, D.C. Gattiker, N. Wooster, J. Chem. Soc. (1935) 1642–1652.
[15] G. Devoto, M. Biddau, M. Massacesi, R. Pinna, G. Ponticelli, L.V. Tatjanenko, I.A. Zakharova, J. Inorg. Biochem. 19 (1983) 311–318.
[16] Z. Zhou, G. Hu, K. Yu, L. Liu, W.T. Robinson, L. Zhang, Q. Yang, G. Li, Chinese J. Struct. Chem. 6 (1987) 119–121.
[17] K.I. Lee, T. Tashiro, M. Noji, Chem. Pharm. Bull. 42 (1994) 702–703.
[18] S. Dey, P. Banerjee, S. Gangopadhyay, P. Vojtíšek, Transit. Met. Chem. 28 (2003) 765–771.
[19] A.S. Abu-Surrah, T.A.K. Al-Allaf, M. Klinga, M. Ahlgren, Polyhedron 22 (2003) 1529–1534.
[20] M. Odoko, Y. Wang, N. Okabe, Acta Crystallogr. Sect. E 60 (2004) m1825–m1827.
[21] M. Odoko, N. Okabe, Acta Crystallogr. Sect. E 63 (2007) m628–m630.
[22] F.A. Allen, Acta Crystallogr. Sect. B: Struct. Sci. 58 (2002) 380–388.
[23] M. Quirós, J.M. Salas, M. Purificación Sánchez, A.L. Beauchamp, X. Solans, Inorg. Chim. Acta 203 (1994) 213–220.
[24] A. Garoufis, K. Karidi, N. Hadjiliadis, S. Kasselouri, J. Kobe, J. Balzarini, E. De Clercq, Met. Based Drugs 8 (2001) 57–63.
[25] W.M. Beck, J.C. Calabrese, N.D. Kottmair, Inorg. Chem. 18 (1979) 176–182.
[26] K.J. Barnham, C.J. Bauer, M.I. Djuran, M.A. Mazid, T. Rau, P.J. Sadler, Inorg. Chem. 34 (1995) 2826–2832.
[27] P.J. Davies, Plant Hormones, third ed., Springer, Dordrecht, 1997.
[28] L. Meijer, A. Borgne, O. Mulner, J.P. J Chong, J.J. Blow, N. Inagaki, M. Inagaki, J.G. Delcros, J.P. Moulinoux, Eur. J. Biochem. 243 (1997) 527–536.
[29] C. Benson, S. Kaye, P. Workman, M. Garret, M. Walton, J. de Bono, Br. J. Cancer 92 (2005) 7–12.
[30] CrysAlis RED and CrysAlis CCD software (Ver.1.171.23), Oxford Diffraction: Oxford, UK, 2003.
[31] G.M. Sheldrick, SHELXS 97, Acta Cryst. A 46 (1990) 467.
[32] G.M. Sheldrick, SHELXL 97, Program for Crystal Structure Refinement, University of Göttingen, Göttingen, Germany, 1997.
[33] K. Brandenburg, DIAMOND, Relase 3.1f, Crystal Impact GbR, Bonn, Germany, 2006.
[34] K. Torigoe, K. Esumi, Langmuir 9 (1993) 1664–1667.

[35] C.H. Oh, S.C. Lee, K.S. Lee, E.R. Woo, C.Y. Hong, B.S. Yang, D.J. Baek, J.H. Cho, Arch. Pharm. Pharm. Med. Chem. 332 (1999) 187–190.
[36] W.J. Geary, Coord. Chem. Rev. 7 (1971) 81–122.
[37] C.J. Pouchert, in: The Aldrich Library of Infrared Spectra, Aldrich Chemical Company Press, Milwaukee, 1981.
[38] D.M. de Faria, M.I. Yoshida, C.B. Pinheiro, K.J. Guedes, K. Krambrock, R. Diniz, L.F.C. de Oliveira, F.C. Machalo, Polyhedron 26 (2007) 4525–4532.
[39] J. Fujita, A.E. Martell, K. Nakamoto, J. Chem. Phys. 36 (1962) 324–331.
[40] K. Nakamoto, Infrared and Raman Spectra of Inorganic and Coordination Compounds, Part B: Applications in Coordination, Organometallic and Bioinorganic Chemistry, fifth ed., Willey, New York, 1997.
[41] Z. Dhaouadi, M. Ghomi, J.C. Austin, R.B. Girling, R.E. Hester, P. Mojzes, L. Chinsky, P.Y. Turpin, C. Coulombeau, H. Jobic, J. Tomkinson, J. Phys. Chem. 97 (1993) 1074–1084.
[42] Z. Trávníček, L. Szüčová, I. Popa, J. Inorg. Biochem. 101 (2007) 477–492.

**Supplementary Material**

# Synthesis, characterization and *in vitro* cytotoxicity of the first palladium(II) oxalato complexes involving adenine-based ligands

Pavel Štarha, Zdeněk Trávníček*, Igor Popa

*Department of Inorganic Chemistry, Faculty of Science, Palacký University, Křížkovského 10, CZ–771 47 Olomouc, Czech Republic*

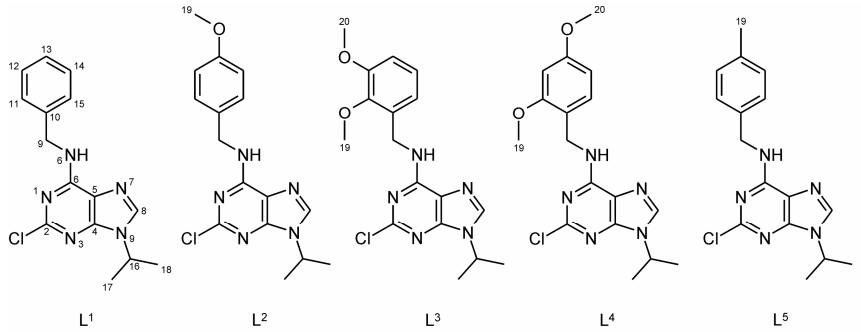


**Scheme 1.** 2-Chloro-N6-(benzyl)-9-isopropyladenine ($L^1$) and its derivatives ($L^2$–$L^5$) used for the synthesis of palladium(II) complexes **1**–**5**.

The results of elemental analyses, FTIR, Raman and NMR ($^1$H, $^{13}$C, $^{15}$N) spectroscopies of 2-chloro-N6-(benzyl)-9-isopropyladenine ($L^1$), 2-chloro-N6-(4-methoxybenzyl)-9-isopropyl-adenine ($L^2$), 2-chloro-N6-(2,3-dimethoxybenzyl)-9-isopropyladenine ($L^3$), 2-chloro-N6-(2,4-dimethoxybenzyl)-9-isopropyladenine ($L^4$) and 2-chloro-N6-(4-methylbenzyl)-9-isopropyl-adenine ($L^5$).

2-Chloro-N6-(benzyl)-9-isopropyladenine, $L_1$ (see Scheme 1): Anal. Calc. for $C_{15}H_{16}N_5Cl$ ($M_r$ = 301.8): C, 59.7; H, 5.3; N, 23.2. Found: C, 59.7; H, 5.4; N, 23.6%. IR (Nujol; $cm^{-1}$): 594m, 535s, 482vs, 463m, 428w, 387w, 343w, 228m, 215m. IR (KBr; $cm^{-1}$): 3266m, 3222m, 3125m, 2978m, 2939m, 2739w, 2677m, 2623m, 2604m, 2530w, 2495m, 1625vs, 1571s, 1537m, 1497w, 1474m, 1453m, 1424m, 1398m, 1354s, 1311s, 1292s, 1253m, 1223s, 1202m, 1172w, 1134w, 1101w, 1068m, 1037m, 967w, 930m, 883w, 860w, 850w, 808w, 789w, 744w, 724m, 696m, 679w, 660m, 642w, 607w, 536w, 484w. Raman ($cm^{-1}$): 3125m, 3060s, 2979vs, 2942vs, 2918s, 2787w, 2764w, 2729w, 2623w, 2497w, 1605w, 1569m, 1475s, 1400m, 1384m, 1356vs, 1314m, 1291w, 1252w, 1186w, 1163m, 1104w, 1080w, 1028w, 1001s, 903w, 884w, 803m, 762w, 615w, 536w, 462w, 430w, 390m, 231m, 217m, 152s. $^1$H

* Corresponding author. Tel.: +420 585 634 944; fax: +420585 634 954; e-mail: zdenek.travnicek@upol.cz (Zdeněk Trávníček).

NMR (DMF–$d_7$, ppm): δ 8.67 (t, 6.2, N6H, 1H), 8.28 (s, C8H, 1H), 7.46 (dd, 7.3, 1.6, C11H, C15H, 2H), 7.34 (tt, 7.3, 1.6, C12H, C14H, 2H), 7.23 (tt, 7.3, 1.6, C13H, 1H), 4.82 (d, 6.2, C9H, 2H), 4.76 (sep, 6.8, C16H, 1H), 1.58 (d, 6.8, C17H, C18H, 6H). $^{13}$C NMR (DMF–$d_7$, ppm): δ 156.11 (C6), 153.96 (C2), 150.57 (C4), 140.39 (C10), 140.04 (C8), 128.98 (C12, C14), 128.28 (C11, C15), 127.56 (C13), 119.68 (C5), 47.90 (C16), 44.22 (C9), 22.41 (C17, C18). $^{15}$N NMR (DMF–$d_7$, ppm): δ 239.76 (N7), 227.30 (N1), 223.94 (N3), 178.60 (N9), 93.56 (N6).

2-Chloro-N6-(4-methoxybenzyl)-9-isopropyladenine, $L_2$: Anal. Calc. for $C_{16}H_{18}N_5OCl$ ($M_r$ = 331.8): C, 57.9; H, 5.5; N, 21.1. Found: C, 57.5; H, 5.3; N, 20.7%. IR (Nujol; cm$^{-1}$): 567w, 534vs, 517s, 428w, 418w, 390w, 337w, 312w, 266w. IR (KBr; cm$^{-1}$): 3269m, 3223m, 3194m, 3151m, 3086m, 2998m, 2974m, 2933m, 2835w, 1644vs, 1612s, 1576s, 1541m, 1513vs, 1471s, 1416m, 1389w, 1363m, 1310vs, 1291vs, 1251vs, 1227vs, 1200s, 1176s, 1158m, 1134w, 1099w, 1074m, 1034m, 971w, 935m, 919m, 882w, 816m, 787w, 755w, 739m, 676w, 660m, 640m, 611w, 571w, 534m, 517w, 417w. Raman (cm$^{-1}$): 3123w, 3062s, 2999s, 2969s, 2938s, 2913s, 2835m, 2729w, 1610m, 1577s, 1477s, 1441m, 1411m, 1361vs, 1312m, 1291m, 1247m, 1200w, 1177m, 1161m, 1073w, 1016w, 917w, 882w, 838m, 818m, 796m, 727w, 636m, 611w, 569w, 531w, 481w, 418w, 391s, 347w, 292w, 247m, 187m. $^1$H NMR (DMF–$d_7$; ppm): δ 8.59 (t, 6.1, N6H, 1H), 8.25 (s, C8H, 1H), 7.39 (dd, 8.8, 1.8, C11H, C15H, 2H), 6.91 (dd, 8.8, 1.8, C12H, C14H, 2H), 4.75 (sep, 6.8, C16H, 1H), 4.74 (d, 6.8, C9H, 2H), 3.78 (s, C19H, 3H), 1.57 (d, 6.8, C17H, C18H, 6H). $^{13}$C NMR (DMF–$d_7$; ppm): δ 159.52 (C13), 156.01 (C6), 153.96 (C2), 150.52 (C4), 139.96 (C8), 132.26 (C10), 129.64 (C11, C15), 119.66 (C5), 114.36 (C12, C14), 55.52 (C19), 47.89 (C16), 43.71 (C9), 22.41 (C17, C18). $^{15}$N NMR (DMF–$d_7$; ppm): δ 238.43 (N7), 225.69 (N1), 221.95 (N3), 176.93 (N9), 94.20 (N6).

2-Chloro-N6-(2,3-dimethoxybenzyl)-9-isopropyladenine, $L_3$: Anal. Calc. for $C_{17}H_{20}N_5O_2Cl$ ($M_r$ = 361.8): C, 56.4; H, 5.6; N, 19.4. Found: C, 56.6; H, 5.6; N, 18.9 %. IR (Nujol; cm$^{-1}$): 535vs, 495w, 461w, 428w, 422w, 389w, 343w, 320w, 259w, 220w. IR (KBr; cm$^{-1}$): 3259m, 3217m, 3186m, 3144m, 3072m, 2970m, 2938m, 2839w, 1622vs, 1573s, 1544m, 1476vs, 1425s, 1396m, 1353s, 1341s, 1313vs, 1292s, 1261s, 1228vs, 1202s, 1165m, 1105w, 1084m, 1061s, 999s, 978m, 932m, 890w, 852w, 803w, 785m, 754m, 703w, 680w, 664m, 641m, 606w, 535w, 494w, 430w. Raman (cm$^{-1}$): 3125w, 3079m, 2986m, 2937s, 2839m, 1613w, 1572m, 1478m, 1405w, 1382m, 1352vs, 1315m, 1289m, 1266m, 1168w, 1087m, 999w, 891w, 799m, 734w, 705w, 627w, 604w, 533w, 389m, 219m, 158m. $^1$H NMR (DMF–$d_7$, ppm): δ 8.49 (t, 6.8, N6H, 1H), 8.29 (s, C8H, 1H), 6.99 (m, C13H, C14H, C15H, 3H), 4.85 (d, 5.9, C9H, 2H), 4.76 (sep, 6.8, C16H, 1H), 3.91 (s, C19, 3H), 3.88 (s, C20, 3H), 1.58 (d, 6.8, C17H, C18H, 6H). $^{13}$C NMR (DMF–$d_7$, ppm): δ 156.19 (C6), 153.99 (C11), 153.44 (C2), 150.54 (C4), 147.53 (C12), 140.05 (C8), 133.54 (C10), 124.40 (C14), 120.71 (C15), 119.77 (C5), 112.42 (C13), 60.57 (C19), 56.14 (C20), 47.92 (C16), 39.17 (C9), 22.42 (C17, C18). $^{15}$N NMR (DMF–$d_7$, ppm): δ 240.1 (N7), 227.8 (N1), 224.3 (N3), 179.8 (N9), 92.3 (N6).

2-Chloro-N6-(2,4-dimethoxybenzyl)-9-isopropyladenine, $L_4$: Anal. Calc. for $C_{17}H_{20}N_5O_2Cl$ ($M_r$ = 361.8): C, 56.4; H, 5.6; N, 19.4. Found: C, 56.4; H, 5.9; N, 19.0%. IR (Nujol; cm$^{-1}$): 567m, 534vs, 510s, 455m, 409w, 390w, 347w. IR (KBr; cm$^{-1}$): 3261m, 3219m, 3184m, 3140w, 3108w, 3072w, 2993m, 2970m, 2941m, 2916m, 2835w, 1616vs, 1587vs, 1572s, 1537m, 1504s, 1468s, 1452s, 1435m, 1415m, 1355s, 1309vs, 1293s, 1266s, 1227vs, 1208vs, 1158s, 1120s, 1074m, 1040s, 1009w, 975w, 933m, 913m, 889w, 862w, 831m, 779m, 721w, 682w, 665m, 644m, 603w, 569w, 534w, 510w, 455w. Raman (cm$^{-1}$): 3109w, 3077m, 2990s, 2943s, 2919s, 2838w, 1612m, 1569m, 1474s, 1460m, 1401m, 1386m, 1352vs, 1308s, 1259w, 1204w, 1181w, 1159m, 1119w, 1037w, 916w, 888w, 795m, 776w, 720w, 666w,

605w, 568w, 531w, 441w, 391m, 330w, 296w, 268m, 155s. $^{1}$H NMR (DMF–$d_7$, ppm): δ 8.28 (s, 1H, C8H), 8.23 (t, 6.8, N6H, 1H), 7.23 (d, 8.2, C15H, 1H), 6.62 (d, 2.4, C12H, 1H), 6.49 (dd, 8.2, 2.4, C14H, 1H), 4.76 (sep, 6.8, C16H, 1H), 4.72 (d, 5.9, C9H, 2H), 3.89 (s, C11H, 1H), 3.80 (s, C13H, 1H), 1.58 (d, 6.8, C17H, C18H, 6H). $^{13}$C NMR (DMF–$d_7$, ppm): δ 161.03 (C13), 158.99 (C11), 156.27 (C6), 154.01 (C2), 150.49 (C4), 139.96 (C8), 129.37 (C15), 120.32 (C10), 119.71 (C5), 104.90 (C14), 98.93 (C12), 55.88 (C19), 55.65 (C20), 47.90 (C16), 39.36 (C9), 22.42 (C17, C18). $^{15}$N NMR (DMF–$d_7$, ppm): δ 241.1 (N7), 228.5 (N1), 224.1 (N3), 179.6 (N9), 91.8 (N6).

2-Chloro-N6-(4-methylbenzyl)-9-isopropyladenine, $L_5$: Anal. Calc. for $C_{16}H_{18}N_5Cl$ ($M_r$ = 315.8): C, 60.9; H, 5.8; N, 22.2. Found: C, 60.6; H, 5.7; N, 21.7%. IR (Nujol; cm$^{-1}$): 572m, 520vs, 479s, 415w, 388w, 357w, 322w. IR (KBr; cm$^{-1}$): 3268m, 3223m, 3194m, 3149m, 3081w, 3045w, 2987m, 2968m, 2928w, 2875w, 1643vs, 1575s, 1541m, 1515m, 1476m, 1432m, 1407m, 1358s, 1344m, 1313vs, 1293s, 1252s, 1230vs, 1201m, 1180w, 1161m, 1102w, 1078m, 1019w, 975w, 944w, 925m, 882w, 836w, 809m, 787w, 756w, 700w, 677w, 662m, 639m, 607w, 571w, 521w, 479w, 418w. Raman (cm$^{-1}$): 3134w, 3051m, 2988s, 2973s, 2925vs, 2872m, 2734w, 1613m, 1577s, 1478s, 1442w, 1379m, 1357vs, 1318m, 1291w, 1248w, 1195w, 1180m, 1164m, 1077w, 1022w, 920w, 883w, 834m, 812m, 792w, 639w, 607w, 571w, 518w, 479w. $^{1}$H NMR (DMF–$d_7$; ppm): δ 8.62 (t, 6.6, N6H, 1H), 8.26 (s, C8H, 1H), 7.34 (d, 7.9, C11H, C15H, 2H), 7.14 (d, 7.9, C12H, C14H, 2H), 4.77 (d, 6.8, C9H, 2H), 4.76 (sep, 6.8, C16H, 1H), 2.28 (s, C19H, 3H), 1.58 (d, 6.8, C17H, C18H, 6H). $^{13}$C NMR (DMF–$d_7$; ppm): δ 156.09 (C6), 153.97 (C2), 150.54 (C4), 139.99 (C8), 137.30 (C10), 136.96 (C13), 129.57 (C12, C14), 128.23 (C11, C15), 119.68 (C5), 47.90 (C16), 43.99 (C9), 22.41 (C17, C18), 20.95 (C19). $^{15}$N NMR (DMF–$d_7$; ppm): δ 238.43 (N7), 225.69 (N1), 221.95 (N3), 176.93 (N9), 94.20 (N6).

The results of FTIR, Raman and NMR ($^{1}$H, $^{13}$C, $^{15}$N) spectroscopies of $[Pd(L^1)_2(ox)]$ (**1**), $[Pd(L^2)_2(ox)]$ (**2**), $[Pd(L^3)_2(ox)]$ (**3**), $[Pd(L^4)_2(ox)] \cdot 2H_2O$ (**4**) and $[Pd(L^5)_2(ox)]$ (**5**).

$[Pd(L^1)_2(ox)]$ (**1**): IR (Nujol; cm$^{-1}$): 560vs, 540s, 521s, 490s, 432m, 391m, 347w, 318w, 268w, 202w. IR (KBr; cm$^{-1}$): 3369m, 3133w, 3060w, 2980w, 2941w, 2884w, 1705s, 1676m, 1617vs, 1581s, 1538w, 1486m, 1455w, 1387m, 1348m, 1319s, 1230m, 1164w, 1138w, 1109w, 1070w, 1057w, 1029w, 976w, 935w, 889w, 800w, 785w, 750w, 699w, 666w, 637w, 602w, 561w, 540w, 521w. Raman (cm$^{-1}$): 3063s, 2984m, 2943s, 1691w, 1671w, 1606w, 1579s, 1539w, 1488m, 1448m, 1411s, 1348vs, 1307m, 1223w, 1160m, 1031w, 1003s, 888w, 811m, 735w, 620w, 558s, 523w, 407m, 304w, 245m. $^{1}$H NMR (DMF–$d_7$, ppm): δ (300 K)/δ (340 K) 9.24 (t, 6.2, N6H, 1H)/9.13 (t, 6.2, N6H, 1H), 8.77 (s, C8H, 1H)/8.68 (s, C8H, 1H), 7.51 (dd, 7.3, 1.6, C11H, C15H, 2H)/7.51 (dd, 7.3, 2.0, C11H, C15H, 2H), 7.32 (tt, 7.3, 1.6, C12H, C14H, 2H)/7.32 (tt, 7.3, 2.0, C12H, C14H, 2H), 7.26 (tt, 7.3, 1.6, C13H, 1H)/7.27 (tt, 7.3, 2.0, C13H, 1H), 4.88 (d, 6.2, C9H, 2H)/4.88 (d, 6.2, C9H, 2H), 4.80 (sep, 6.8, C16H, 1H)/4.82 (sep, 6.8, C16H, 1H), 1.53 (d, 6.8, C17H, C18H, 6H)/1.54 (d, 6.8, C17H, C18H, 6H). $^{13}$C NMR (DMF–$d_7$, ppm): δ 165.88 (Cox), 155.18 (C6), 154.08 (C2), 150.32 (C4), 143.86 (C8), 139.27 (C10), 128.99 (C12, C14), 128.42 (C11, C15), 127.64 (C13), 117.26 (C5), 49.70 (C16), 45.19 (C9), 21.95 (C17, C18). $^{15}$N NMR (DMF–$d_7$, 340 K, ppm): δ 231.7 (N1), 224.1 (N3), 185.7 (N9), 147.3 (N7), 100.7 (N6).

$[Pd(L^2)_2(ox)]$ (**2**): IR (Nujol; cm$^{-1}$): 578vs, 564vs, 535vs, 522vs, 459m, 420m, 393s, 372m, 365m, 320m, 278w, 266w, 246m, 203w. IR (KBr; cm$^{-1}$): 3355w, 3305w, 3109w, 3061w, 2981w, 2935w, 2837w, 1709s, 1677m, 1614vs, 1580s, 1539w, 1513s, 1483m, 1464m, 1389m, 1346m, 1316s, 1243s, 1176m, 1110w, 1068w, 1033m, 974w, 923w, 889w, 800m, 785w, 756w, 667w, 638w, 579w, 563w, 521w, 457w. Raman (cm$^{-1}$): 3060m, 2994m, 2950s, 2840w, 1695w, 1660w, 1610m, 1576m, 1541w, 1486m, 1441m, 1414m, 1351vs, 1304m, 1252w, 1218w, 1178w, 1157w, 1109w, 890w, 847m, 817m, 734w, 638w, 562m, 523w,

476w, 405m, 375w, 320w, 244w, 167m. $^{1}$H NMR (DMF–$d_7$, ppm): δ (300 K)/δ (340 K) 9.11 (t, 6.0, N6H, 1H)/9.05 (t, 5.8, N6H, 1H), 8.69 (s, C8H, 1H)/8.66 (s, C8H, 1H), 7.39 (dd, 8.8, 2.0, C11H, C15H, 2H)/7.44 (dd, 8.6, 2.0, C11H, C15H, 2H), 6.83 (dd, 8.8, 2.0, C12H, C14H, 2H)/6.89 (dd, 8.6, 2.0, C12H, C14H, 2H), 4.75 (sep, 6.8, C16H, 1H)/4.81 (sep, 6.8, C16H, 1H), 4.75 (d, 5.9, C9H, 2H)/4.80 (d, 5.8, C9H, 2H), 3.76 (s, C19H, 3H)/3.82 (s, C19H, 3H), 1.48 (d, 6.8, C17H, C18H, 6H)/1.54 (d, 6.8, C17H, C18H, 6H). $^{13}$C NMR (DMF–$d_7$, ppm): δ 165.97 (Cox), 159.55 (C13), 155.17 (C6), 153.94 (C2), 150.26 (C4), 143.80 (C8), 131.10 (C10), 129.88 (C11, C15), 117.20 (C5), 114.34 (C12, C14), 55.53 (C19), 49.68 (C16), 44.68 (C9), 21.91 (C17, C18). $^{15}$N NMR (DMF–$d_7$, 340 K, ppm): δ 231.9 (N1), 223.9 (N3), 185.9 (N9), 147.2 (N7), 102.5 (N6).

[Pd($L^3$)$_2$(ox)] (**3**): IR (Nujol; cm$^{-1}$): 559vs, 536vs, 516m, 458m, 434s, 399w, 388m, 315m, 267m, 214m. IR (KBr; cm$^{-1}$): 3407m, 3269w, 3138w, 3068w, 2978w, 2936w, 2835w, 1708m, 1676m, 1619vs, 1581m, 1541w, 1480m, 1428w, 1389m, 1348m, 1316m, 1272m, 1229m, 1169w, 1084w, 1062m, 1001w, 934w, 889w, 802w, 785w, 751w, 668w, 640w, 605w, 561w, 536w, 517w, 467w, 432w. Raman (cm$^{-1}$): 3085w, 3053w, 3000m, 2982m, 2935s, 2836w, 1695m, 1676w, 1657w, 1614w, 1580s, 1545m, 1489m, 1464m, 1404s, 1351vs, 1309m, 1262m, 1170m, 1089w, 1016w, 997w, 889w, 801w, 735w, 709w, 692w, 607w, 560m, 515w, 434w, 403w, 390m, 341w, 312m, 266m. $^{1}$H NMR (DMF–$d_7$, ppm): δ (300 K)/δ (340 K) 9.12 (t, 6.0, N6H, 1H)/9.00 (t, 6.0, N6H, 1H), 8.76 (s, C8H, 1H)/8.67 (s, C8H, 1H), 6.99 (m, C13H, C14H, C15H, 3H)/7.00 (m, C13H, C14H, C15H, 3H), 4.92 (d, 6.0, C9H, 2H)/4.92 (d, 6.0, C9H, 2H), 4.82 (sep, 6.4, C16H, 1H)/4.83 (sep, 6.8, C16H, 1H), 3.98 (s, C19H, 3H)/3.99 (s, C19H, 3H), 3.90 (s, C20H, 3H)/3.91 (s, C20H, 3H), 1.53 (d, 6.4, C17H, C18H, 6H)/1.55 (d, 6.8, C17H, C18H, 6H). $^{13}$C NMR (DMF–$d_7$, ppm): δ 165.67 (Cox), 155.22 (C6), 154.10 (C11), 153.31 (C2), 150.29 (C4), 147.46 (C12), 143.85 (C8), 132.57 (C10), 124.56 (C14), 120.87 (C15), 117.33 (C5), 112.58 (C13), 60.65 (C19), 56.17 (C20), 49.69 (C16), 40.12 (C9), 21.96 (C17, C18). $^{15}$N NMR (DMF–$d_7$, 340 K, ppm): δ 231.8 (N1), 224.0 (N3), 186.0 (N9), 147.7 (N7), 98.8 (N6).

[Pd($L^4$)$_2$(ox)] · 2H$_2$O (**4**): IR (Nujol; cm$^{-1}$): 565vs, 539vs, 517s, 492m, 474s, 419m, 405m, 390m, 353m, 320w, 255w, 202w. IR (KBr; cm$^{-1}$): 3385m, 3103w, 3062w, 2984w, 2937w, 2836w, 1714s, 1672s, 1618vs, 1588s, 1540w, 1508m, 1485m, 1464m, 1439w, 1417w, 1387w, 1348m, 1317s, 1234m, 1208s, 1157m, 1129w, 1068w, 1036m, 936w, 889w, 824w, 800w, 785w, 667w, 637w, 565w, 538w, 517w, 471w. Raman (cm$^{-1}$): 3072m, 2989s, 2933vs, 2837m, 1706m, 1668w, 1610m, 1583vs, 1541w, 1489m, 1454m, 1410vs, 1349vs, 1305s, 1159m, 1101w, 1036w, 935w, 881w, 801w, 725w, 622w, 562m, 526w, 469m, 409m, 302m, 161vs. $^{1}$H NMR (DMF–$d_7$, ppm): δ (300 K)/δ (340 K) 8.86 (t, 5.9, N6H, 1H)/(t, 5.9, N6H, 1H), 8.70 (s, C8H, 1H)/(s, C8H, 1H), 7.31 (d, 8.2, C15H, 1H)/(d, 8.2, C15H, 1H), 6.64 (d, 2.2, C12H, 1H)/(d, 2.2, C12H, 1H), 6.45 (dd, 8.2, 2.2, C14H, 1H)/(dd, 8.2, 2.2, C14H, 1H), 4.80 (sep, 6.8, C16H, 1H)/(sep, 6.8, C16H, 1H), 4.79 (d, 5.9, C9H, 2H)/(d, 5.9, C9H, 2H), 3.92 (s, C19H, 3H)/(s, C19H, 3H), 3.82 (s, C20H, 3H)/(s, C20H, 3H), 1.52 (d, 6.8, C17H, C18H, 6H)/(d, 6.8, C17H, C18H, 6H). $^{13}$C NMR (DMF–$d_7$, ppm): δ 165.43 (Cox), 161.16 (C13), 159.05 (C11), 155.27 (C6), 154.12 (C2), 150.25 (C4), 143.80 (C8), 129.81 (C15), 118.76 (C10), 117.28 (C5), 105.05 (C14), 99.00 (C12), 56.04 (C19), 55.65 (C20), 49.61 (C16), 40.20 (C9), 21.97 (C17, C18). $^{15}$N NMR (DMF–$d_7$, 300 K, ppm): δ 231.0 (N1), 222.8 (N3), 185.7 (N9), 147.1 (N7), 99.5 (N6).

[Pd($L^5$)$_2$(ox)] (**5**): IR (Nujol; cm$^{-1}$): 587vs, 562vs, 542vs, 522vs, 463m, 424m, 397w, 355m, 324m. IR (KBr; cm$^{-1}$): 3374m, 3098w, 3057w, 2980w, 2930w, 2879w, 1716s, 1674m, 1617vs, 1581s, 1538w, 1515w, 1483m, 1462m, 1373m, 1347s, 1317s, 1232s, 1163w, 1136w, 1071w, 1022w, 925w, 889w, 801w, 785w, 667w, 636w, 572w, 520w, 473w. Raman (cm$^{-1}$): 3053s, 3030m, 3010m, 2988s, 2941s, 2875m, 1702m, 1670m, 1614m, 1579s, 1537m, 1486m, 1413s, 1340vs, 1302s, 1204m, 1157m, 887m, 844s, 811m, 642m, 571m, 526w, 429m, 406m,

313m, 263m. $^{1}$H NMR (DMF–$d_7$, ppm): δ (300 K)/δ (340 K) 9.16 (t, 6.0, N6H, 1H)/9.07 (t, 6.0, N6H, 1H), 8.73 (s, C8H, 1H)/8.67 (s, C8H, 1H), 7.38 (dd, 8.1, 1.8, C11H, C15H, 2H)/7.38 (d, 7.7, C11H, C15H, 2H), 7.12 (dd, 8.1, 1.8, C12H, C14H, 2H)/7.12 (d, 7.7, C12H, C14H, 2H), 4.81 (d, 6.0, C9H, 2H)/4.82 (d, 6.0, C9H, 2H), 4.80 (sep, 6.8, C16H, 1H)/4.81 (sep, 6.8, C16H, 1H), 2.31 (s, C19H, 3H)/2.32 (s, C19H, 3H), 1.52 (d, 6.8, C17H, C18H, 6H)/1.54 (d, 6.8, C17H, C18H, 6H). $^{13}$C NMR (DMF–$d_7$, ppm): δ 165.92 (Cox), 155.18 (C6), 154.04 (C2), 150.30 (C4), 143.81 (C8), 137.05 (C13), 136.18 (C10), 129.60 (C12, C14), 128.42 (C11, C15), 117.23 (C5), 49.71 (C16), 44.95 (C9), 21.94 (C17, C18), 21.04 (C19). $^{15}$N NMR (DMF–$d_7$, 340 K, ppm): δ 231.9 (N1), 224.0 (N3), 185.7 (N9), 147.3 (N7), 101.6 (N6).

**Table 1.** Selected interatomic parameters (Å, °) of the non–bonding interactions of complexes **2** and **5** · $L_5$ · $Me_2CO$

| D−H···A | *d*(D−H) | *d*(H···A) | *d*(D···A) | < (DHA) |
|---|---|---|---|---|
| *[Pd(L$_2$)$_2$(ox)] (**2**)* | | | | |
| C(2)−Cl(1)$^{i}$ | | | 3.417(4) | |
| C(8)−H(8A)···O(4)$^{ii}$ | 0.950 | 2.402(3) | 3.150(5) | 135.44(26) |
| C(8A)−H(8AA)···O(3)$^{iii}$ | 0.950 | 2.559(3) | 3.237(6) | 128.53(26) |
| C(9)−H(9A)···O(1)$^{iii}$ | 0.990 | 2.574(2) | 3.435(4) | 145.35(18) |
| C(9)−H(9A)···O(3)$^{iii}$ | 0.990 | 2.655(2) | 3.235(4) | 117.61(21) |
| C(17)−H(17H)···O(3)$^{ii}$ | 0.980 | 2.503(3) | 3.430(7) | 157.87(34) |
| C(17)−H(17I)···O(5A)$^{ii}$ | 0.980 | 2.650(2) | 3.571(5) | 156.89(35) |
| C(17A)−H(17C)···O(5)$^{iv}$ | 0.980 | 2.497(3) | 3.405(9) | 154.03(46) |
| C(17B)−H(17D)···O(5)$^{iv}$ | 0.980 | 2.630(3) | 3.348(14) | 130.32(74) |
| C(18A)−H(18B)···O(4)$^{iii}$ | 0.980 | 2.664(3) | 3.326(15) | 125.14(74) |
| C(18B)−H(18E)···O(4)$^{iii}$ | 0.980 | 2.464(3) | 3.230(20) | 134.7(10) |
| C(19)−H(19E)···O(5A)$^{v}$ | 0.980 | 2.640(3) | 3.478(5) | 143.66(25) |
| O(2)−C(20)$^{ii}$ | | | 3.124(5) | |
| O(4)−Pd(1)$^{ii}$ | | | 3.056(3) | |
| *[Pd(L$_5$)$_2$(ox)] · L$_5$ · Me$_2$CO (**5** · L$_5$ · Me$_2$CO)* | | | | |
| C(8)−H(8A)···O(5) | 0.950 | 2.654(3) | 3.059(5) | 106.23(22) |
| C(8A)−H(8AA)···Cl(1)$^{vi}$ | 0.950 | 2.9082(9) | 3.426(3) | 115.45(19) |
| C(8A)−H(8AA)···O(5) | 0.950 | 2.380(3) | 3.221(5) | 147.15(22) |
| C(11)−H(11A)···N(3)$^{vi}$ | 0.950 | 2.679(3) | 3.557(4) | 153.75(20) |
| C(12A)−H(12B)···Cl(1A)$^{vii}$ | 0.950 | 2.7336(8) | 3.537(3) | 142.81(21) |
| C(12B)−H(12C)···O(4)$^{viii}$ | 0.950 | 2.552(3) | 3.439(5) | 155.78(25) |

| | | | | |
|---|---|---|---|---|
| C(14B)−H(14C)···O(1)$^{vii}$ | 0.950 | 2.439(2) | 3.334(4) | 156.94(24) |
| C(18)−H(18F)···N(3B)$^{ix}$ | 0.980 | 2.632(3) | 3.502(5) | 147.99(22) |
| O(2)···C(20)$^{ii}$ | | | 3.184(4) | |
| O(2)···C(21)$^{ii}$ | | | 3.133(5) | |
| O(4)···Pd(1)$^{ii}$ | | | 3.081(3) | |

Symmetry codes: (i) – x, 1 – y, 2 – z; (ii) 1 – x, 1 – y, 1 – z; (iii) – x, 1 – y, 1 – z; (iv) x – 1, y +1, z; (v) x, y – 1, z + 1; (vi) 1 – x, – y, 1 – z; (vii) 2 – x, 1 – y, – z; (viii) x, y, z – 1; (ix) x, y, 1 + z.

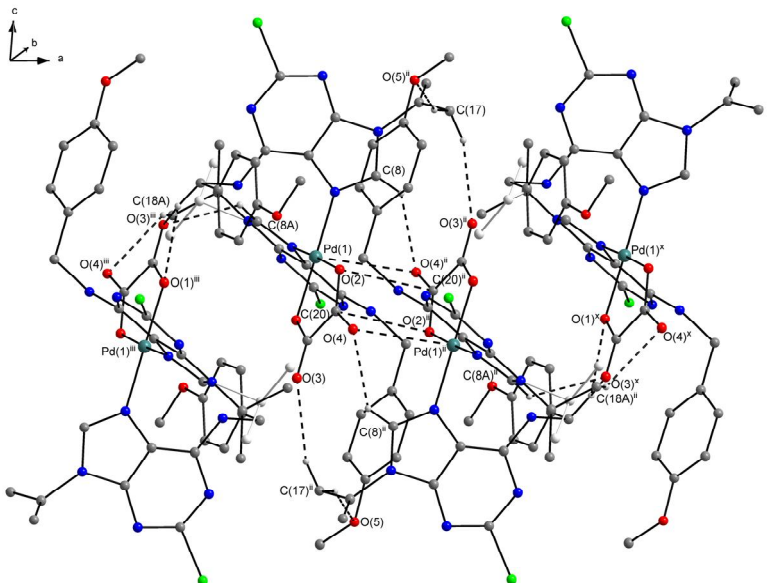


**Figure 1.** Part of the crystal structure of [Pd($L_2$)$_2$(ox)] (**2**), showing the C−H···O, C···O and Pd···O non–bonding contacts (dashed lines). H–atoms not involved in the interactions are omitted for clarity. Symmetry codes: (ii) 1 – x, 1 – y, 1 – z; (iii) – x, 1 – y, 1 – z; (x) 1 + x, y, z.

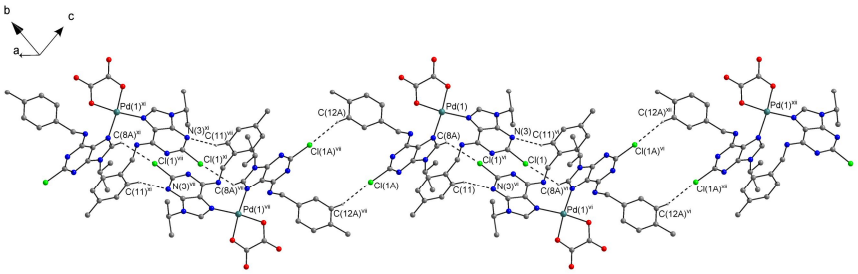


**Figure 2.** Part of the crystal structure of $[Pd(L_5)_2(ox)] \cdot L_5 \cdot Me_2CO$ (**5** $\cdot L_5 \cdot Me_2CO$), showing the C−H···Cl and C−H···N non–bonding interactions (dashed lines). The $L_5$ and $Me_2CO$ molecules of crystallization and H–atoms not involved in the interactions are omitted for clarity. Symmetry codes: (vi) 1 – x, – y, 1 – z; (vii) 2 – x, 1 – y, – z; (xi) 1 + x, 1 + y, z – 1; (xii) x – 1, y – 1, 1 + z.

# APPENDIX II

Inorganica Chimica Acta 363 (2010) 1469–1478

Contents lists available at ScienceDirect

Inorganica Chimica Acta

journal homepage: www.elsevier.com/locate/ica

# Palladium(II) oxalato complexes involving N6-(benzyl)-9-isopropyladenine-based N-donor carrier ligands: Synthesis, general properties, $^{1}H$, $^{13}C$ and $^{15}N\{^{1}H\}$ NMR characterization and *in vitro* cytotoxicity

Pavel Štarha, Igor Popa, Zdeněk Trávníček *

*Department of Inorganic Chemistry, Faculty of Science, Palacký University, Tř. 17. listopadu 12, CZ-771 46 Olomouc, Czech Republic*

ARTICLE INFO

*Article history:*
Received 7 December 2009
Received in revised form 15 January 2010
Accepted 22 January 2010
Available online 29 January 2010

*Keywords:*
Palladium(II) complexes
Oxalate
Adenine derivatives
CDK inhibitors
*In vitro* cytotoxicity

ABSTRACT

Reactions of potassium bis(oxalato)palladate dihydrate, $K_2[Pd(ox)_2]\cdot 2H_2O$, with two molar equivalents of N6-(benzyl)-9-isopropyladenine-based organic molecules ($L_{1-7}$), i.e. 2-chloro-N6-(2-methoxybenzyl)-9-isopropyladenine ($L_1$), 2-chloro-N6-(3-methoxybenzyl)-9-isopropyladenine ($L_2$), 2-chloro-N6-(3,5-dimethoxybenzyl)-9-isopropyladenine ($L_3$), 2-(1-ethyl-2-hydroxyethylamino)-N6-(benzyl)-9-isopropyladenine ($L_4$), 2-(1-ethyl-2-hydroxyethylamino)-N6-(2-methoxybenzyl)-9-isopropyladenine ($L_5$), 2-(1-ethyl-2-hydroxyethylamino)-N6-(3-methoxybenzyl)-9-isopropyladenine ($L_6$) and 2-(1-ethyl-2-hydroxyethylamino)-N6-(4-methoxybenzyl)-9-isopropyladenine ($L_7$), provided a series of seven palladium(II) oxalato (ox) complexes of the general formula $[Pd(ox)(L_{1-7})_2]\cdot nH_2O$ (**1**–**7**; $n = 0$ for **4**, **5** and **7**, ¾ for **1** and **2**, 1 for **6**, and 3 for **3**). The compounds were characterized by elemental analysis, IR, Raman, $^{1}H$, $^{13}C$ and $^{15}N\{^{1}H\}$ NMR spectroscopy, ESI+ mass spectrometry, molar conductivity and TG/DTA thermal analysis. The geometry of $[Pd(ox)(L_2)_2]$ (**2**) was optimized on the B3LYP/6-311G*/LANL2DZ level of theory. The complexes **4**–**7** represent the first palladium(II) oxalato complexes with a $PdN_2O_2$ donor set, which involve highly potent purine-based cyclin-dependent kinase (CDK) inhibitors ($L_{4-7}$) as carrier N-donor ligands. The selected complexes **1**, **3**–**5** and **7** were tested by an MTT assay for their *in vitro* cytotoxic activity against human osteosarcoma (HOS) cancer cell line. The highest activity was found for the complexes **5** ($IC_{50} = 34.9$ μM) and **7** ($IC_{50} = 39.2$ μM).



## 1. Introduction

The plant hormone N6-(benzyl)adenine [6-(benzylamino)-purine] [1] and its derivatives were found to be suitable N-donor ligands of transition metal complexes. In the field of palladium(II) complexes, the *cis*-$[PdCl_2(L)_2]$, *trans*-$[PdCl_2(L)_2]$, $[PdCl_3(L^+)]$, $[PdCl_2(H_2O)(L)]$, $[PdCl(H_2O)_2(L^-)]$ and $[Pd(ox)(L)_2]$ types of compounds were prepared in our laboratory (see lit. [2–5] and the reference cited therein), where L, $L^+$ and $L^-$ stand for an electroneutral, protonated, and deprotonated N6-(benzyl)adenine derivative, respectively, and ox symbolizes an oxalate dianion.

Talking about the $[Pd(ox)(L)_2]$ compounds in more detail, five complexes with 2-chloro-N6-(benzyl)-9-isopropyladenine, or its analogues with the substituted benzyl group, have recently been published [3]. The molecular and crystal structures of two complexes involving 2-chloro-N6-(4-methoxybenzyl)-9-isopropyladenine ($L_I$; complex **I**) and 2-chloro-N6-(4-methylbenzyl)-9-isopropyladenine ($L_{II}$; complex **II**), were determined by a single-crystal X-ray analysis. The mentioned complexes **I** and **II** have the tetra-coordinated central Pd(II) ion which is surrounded by one bidentate-coordinated oxalate dianion and by two monodentate bonded adenine-based molecules ($L_I$ or $L_{II}$) in a $PdN_2O_2$ donor set. Moreover, these complexes were tested by a calcein acetoxymethyl (AM) assay for their *in vitro* cytotoxic activity against breast adenocarcinoma (MCF-7) and chronic myelogenous leukaemia (K562) human cancer cell lines. Two of the tested substances showed promising *in vitro* cytotoxicity ($IC_{50}$ values of 6.2 and 6.8 μM), which is higher than those of the commercially used platinum-based anticancer drugs *Cisplatin* ($IC_{50} = 10.9$ μM) and *Oxaliplatin* ($IC_{50} = 18.2$ μM). To our best knowledge, only the $[Pd(ox)(Hoen)_2]\cdot 0.5H_2O$ and $[Pd(ox)(Clen)_2]$ complexes (Hoen = *N,N′*-bis(hydroxyethyl)ethylenediamine, Clen = *N,N′*-bis(chloroethyl)ethylenediamine) [6], besides the above-mentioned $[Pd(ox)(L)_2]$ compounds prepared in our laboratory, were tested for their *in vitro* cytotoxicity within a group of monomeric palladium(II) oxalato complexes, however, these substances were inactive against mice leukaemia (P388) cells. On the other hand, the results obtained in the case of $[Pd(ox)(L)_2]$ showed that this type of complexes represents a promising group of compounds in

* Corresponding author. Tel.: +420 585 634 352; fax: +420 585 634 954.
*E-mail address:* zdenek.travnicek@upol.cz (Z. Trávníček).

0020-1693/$ - see front matter © 2010 Elsevier B.V. All rights reserved.
doi:10.1016/j.ica.2010.01.035

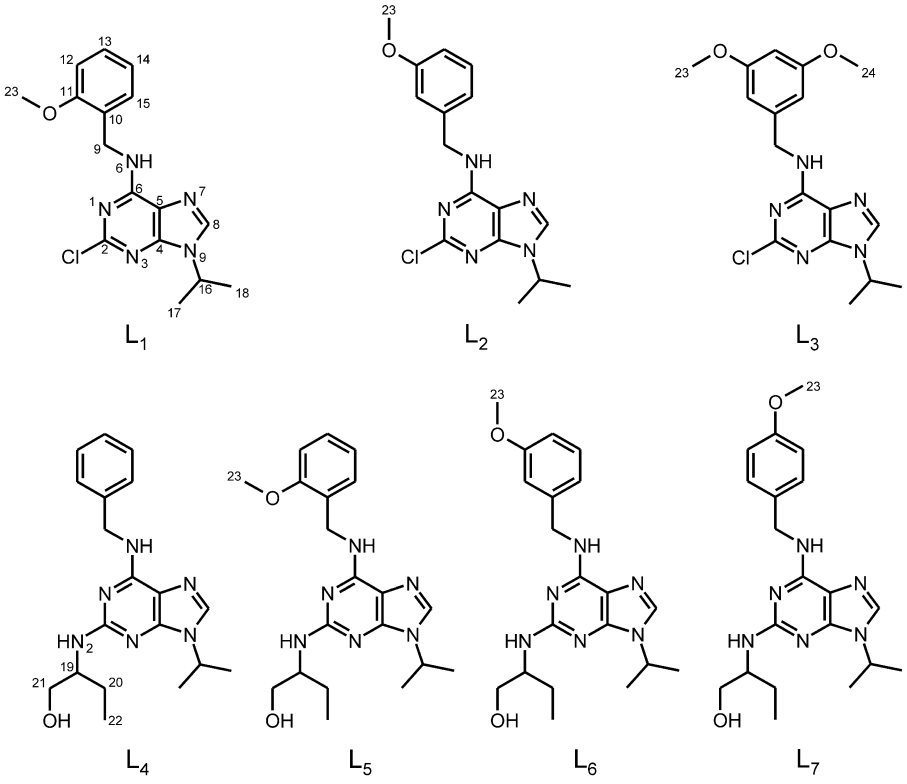


**Scheme 1.** The derivatives of N6-(benzyl)-9-isoropyladenine ($L_{1-7}$) used for the preparation of the $[Pd(ox)(L_{1-7})]\cdot nH_2O$ palladium(II) oxalato complexes.

connection with their *in vitro* cytotoxicity. For comparison, other types of biologically active palladium complexes have been reviewed in the literature [2,4].

In this paper, we present results following from our ongoing research of palladium(II) oxalate complexes involving N6-(benzyl)-9-isopropyladenine-based N-donor carrier ligands. We prepared and characterized seven $[Pd(ox)(L)_2]\cdot nH_2O$ complexes of which the compounds **1**–**3** represent analogues of recently reported palladium(II) oxalato complexes [3] varying in the substitution on a benzene ring of the 2-chloro-N6-(benzyl)-9-isopropyladenine moiety ($L_{1-3}$; see Scheme 1). On the other hand, the complexes **4**–**7** involve differently substituted type of N6-(benzyl)adenine derivatives with 2-amino-1-butanol at the C2 position of a purine ring instead of the chlorine atom, namely 2-(1-ethyl-2-hydroxyethylamino)-N6-(benzyl)-9-isopropyladenine (*Roscovitine*, $L_4$) [7] and its benzyl-substituted analogues ($L_{5-7}$; Scheme 1). It is known that *Roscovitine* and its derivatives belong to the group of highly potent cyclin-dependent kinase (CDK) inhibitors, and thus the presented complexes **4**–**7** represent the first palladium(II) oxalato complexes with purine-based CDK inhibitors acting as N-donor carrier ligands.

Based on the above-mentioned statements, we decided to carry out an *in vitro* cytotoxicity screening of the prepared complexes against human osteosarcoma cancer cell line (HOS). The obtained results showed that the complexes **5** and **7**, involving the potent CDK inhibitors, have *in vitro* cytotoxicity comparable with *Cisplatin*, as discussed below. These findings motivated us to evaluate deeply the *in vitro* cytotoxicity of these complexes, and thus, the named palladium(II) oxalato complexes are currently tested against a variety of human cancer cell lines, e.g. MCF-7, lung carcinoma (A549), cervix epithelioid carcinoma (HeLa), ovarian carcinoma (A2780), *Cisplatin*-resistant ovarian carcinoma (A2780*cis*) or malignant melanoma (G-361).

## 2. Experimental

### 2.1. Starting materials

Chemicals and solvents were purchased from the commercial sources (Sigma-Aldrich Co., Acros Organics Co., Lachema Co. or Fluka Co.) and they were used as received. Dimethyl sulfoxide (DMSO) was dried using $MgSO_4$.

Potassium bis(oxalato)palladate(II) dihydrate, $K_2[Pd(ox)_2]\cdot 2H_2O$, was prepared from potassium tetrachloropalladate(II), $K_2[PdCl_4]$, as formerly described [3,8]. Syntheses of 2-chloro-N6-(2-methoxybenzyl)-9-isopropyladenine ($L_1$), 2-chloro-N6-(3-methoxybenzyl)-9-isopropyladenine ($L_2$), 2-chloro-N6-(3,5-dimethoxybenzyl)-9-isopropyladenine ($L_3$), 2-(1-ethyl-2-hydroxyethylamino)-N6-(benzyl)-9-isopropyladenine ($L_4$), 2-(1-ethyl-2-hydroxyethylamino)-N6-(2-methoxybenzyl)-9-isopropyladenine ($L_5$), 2-(1-ethyl-2-hydroxyethylamino)-N6-(3-methoxybenzyl)-9-isopropyladenine ($L_6$) and 2-(1-ethyl-2-hydroxyethylamino)-N6-(4-methoxybenzyl)-9-isopropyladenine ($L_7$) were inspired by several literature sources, and their structures are depicted in Scheme 1 [9–12]. A scheme of the synthetic pathway of the $L_{1-7}$ compounds, as well as the results of IR, Raman and NMR spectroscopies, are given in Appendix A in Supplementary material.

### 2.2. Preparation of $[Pd(ox)(L_1)_2]\cdot{}^3\!/_4H_2O$ (**1**), $[Pd(ox)(L_2)_2]\cdot{}^3\!/_4H_2O$ (**2**), $[Pd(ox)(L_3)_2]\cdot 3H_2O$ (**3**), $[Pd(ox)(L_4)_2]$ (**4**), $[Pd(ox)(L_5)_2]$ (**5**), $[Pd(ox)(L_6)_2]\cdot H_2O$ (**6**) and $[Pd(ox)(L_7)_2]$ (**7**)

The palladium(II) oxalato complexes **1**–**7** were prepared according to a general synthetic procedure recently published and depicted in Scheme 2 [3]. Briefly, a $K_2[Pd(ox)_2]\cdot 2H_2O$ distilled water solution (15 mL, 40 °C) was mixed together with an acetone solu-

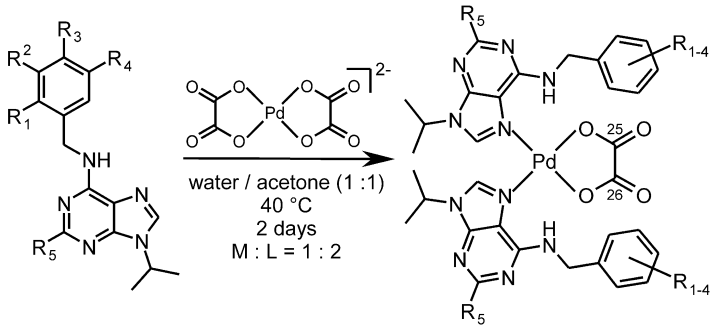


| | $R_1$ | $R_2$ | $R_3$ | $R_4$ | $R_5$ |
|---|---|---|---|---|---|
| **1** | OMe | H | H | H | Cl |
| **2** | H | OMe | H | H | Cl |
| **3** | H | OMe | H | OMe | Cl |
| **4** | H | H | H | H | 2-amino-1-butanol |
| **5** | OMe | H | H | H | 2-amino-1-butanol |
| **6** | H | OMe | H | H | 2-amino-1-butanol |
| **7** | H | H | OMe | H | 2-amino-1-butanol |

**Scheme 2.** A schematic representation of the preparation pathway of the palladium(II) oxalato complexes **1**–**7**.

tion (15 mL, 25 °C) of the appropriate organic molecule $L_{1-7}$ in a 1:2 molar ratio. The product, which formed during two days of stirring at the temperature of 40 °C, was filtered off, washed with hot (5 mL) and cold (5 mL) distilled water and acetone (5 mL) and dried in the air at 40 °C.

**1**: Yield: 580 mg (67%). *Anal.* Calc. for $C_{34}H_{36}N_{10}O_6Cl_2Pd\cdot{}^3/_4H_2O$: C, 46.9; H, 4.3; N, 16.1. Found: C, 46.8; H, 4.5; N, 15.9%. m.p. 169–171 °C (decomp.). $\Lambda_M$ (DMF solution, S cm$^2$ mol$^{-1}$): 5.8. ESI+ MS (methanol, *m/z*) $[Pd(ox)(L_1)_3 + H]^+$ 1189.5, $[Pd(ox)(L_1)_2 + K]^+$ 897.0, $[Pd(ox)(L_1)_2 + Na]^+$ 880.9, $[Pd(ox)(L_1)_2 + H]^+$ 858.8, $[Pd(ox)(L_1) + K]^+$ 566.0, $[Pd(ox)(L_1) + Na]^+$ 549.8, $[Pd(ox)(L_1) + H]^+$ 527.9, $[L_1 + H]^+$ 332.1. IR (Nujol; cm$^{-1}$): 559vs $\nu$(Pd–O), 518 $\nu$(Pd–N). IR (KBr; cm$^{-1}$): 3130w, 3113w, 3066w $\nu$(C–H)$_{ar}$, 2981w, 2939w, 2836w $\nu$(C–H)$_{al}$; 1707vs, 1671s $\nu$(C=O)$_{ox}$; 1622vs $\nu$(C=N); 1539w, 1491s $\nu$(C=C)$_{ar}$; 1364vs $\nu$(C–O)$_{ox}$; 1242vs $\nu$(C–O)$_{ar}$; 1163w $\nu$(C–Cl); 560w $\nu$(Pd–O). $^1$H NMR (DMF-$d_7$, ppm): $\delta$ 8.99 (t, 6.2, N$^6$H, 1H), 8.76 (s, C$^8$H, 1H), 7.40 (dd, 7.3, 1.7, C$^{15}$H, 1H), 7.28 (tt, 7.9, 1.7, C$^{14}$H, 1H), 7.05 (dd, 8.2, 1.1, C$^{12}$H, 1H), 6.86 (tt, 7.5, 1.1, C$^{13}$H, 1H), 4.88 (d, 6.2, C$^9$H, 2H), 4.81 (sp, 6.8, C$^{16}$H, 1H), 3.94 (s, C$^{23}$H, 3H), 1.53 (d, 6.8, C$^{17}$H, C$^{18}$H, 6H). $^{13}$C NMR (DMF-$d_7$, ppm): $\delta$ 165.57 (C$^{25}$, C$^{26}$), 157.95 (C$^{11}$), 155.27 (C$^6$), 154.25 (C$^2$), 150.31 (C$^4$), 143.85 (C$^8$), 129.02 (C$^{13}$), 128.72 (C$^{15}$), 126.66 (C$^{10}$), 120.98 (C$^{14}$), 117.31 (C$^5$), 111.14 (C$^{12}$), 55.95 (C$^{23}$), 49.67 (C$^{16}$), 40.51 (C$^9$), 21.97 (C$^{17}$, C$^{18}$). $^{15}$N NMR (DMF-$d_7$, ppm): $\delta$ 230.1 (N$^1$), 223.0 (N$^3$), 185.8 (N$^9$), 147.3 (N$^7$), 97.5 (N$^6$).

**2**: Yield: 590 mg (69%). *Anal.* Calc. for $C_{34}H_{36}N_{10}O_6Cl_2Pd\cdot{}^3/_4H_2O$: C, 46.9; H, 4.3; N, 16.1. Found: C, 46.9; H, 4.4; N, 16.5%. m.p. 178–181 °C (decomp.). $\Lambda_M$ (DMF solution, S cm$^2$ mol$^{-1}$): 0.3. ESI+ MS (methanol, *m/z*): $[Pd(ox)(L_2)_3 + H]^+$ 1189.4, $[Pd(ox)(L_2)_2 + H]^+$ 858.7, $[Pd(ox)(L_2) + H]^+$ 527.8, $[L_2 + H]^+$ 332.2. IR (Nujol; cm$^{-1}$): 558vs $\nu$(Pd–O), 506s $\nu$(Pd–N). IR (KBr; cm$^{-1}$): 3114w, 3053w $\nu$(C–H)$_{ar}$, 2977w, 2938w, 2836w $\nu$(C–H)$_{al}$; 1711s, 1675s $\nu$(C=O)$_{ox}$; 1618vs $\nu$(C=N); 1537w, 1488s $\nu$(C=C)$_{ar}$; 1373w $\nu$(C–O)$_{ox}$; 1265s $\nu$(C–O)$_{ar}$; 1165w $\nu$(C–Cl); 559w $\nu$(Pd–O). Raman (cm$^{-1}$): 3370w $\nu$(N–H); 3139w, 3059w $\nu$(C–H)$_{ar}$; 2990s, 2939s, 2838w $\nu$(C–H)$_{al}$; 1703w, 1659s $\nu$(C=O)$_{ox}$; 1537w, 1485s $\nu$(C=C)$_{ar}$; 1167w $\nu$(C–Cl); 559s $\nu$(Pd–O). $^1$H NMR (DMF-$d_7$, ppm): $\delta$ 9.22 (t, 6.2, N$^6$H, 1H), 8.77 (s, C$^8$H, 1H), 7.23 (t, 8.0, C$^{14}$H, 1H), 7.10 (t, 2.2, C$^{11}$H, 1H), 7.09 (d, 7.8, C$^{15}$H, 1H), 6.84 (dd, 8.2, 2.6, C$^{13}$H, 1H), 4.85 (d, 6.2, C$^9$H, 2H), 4.81 (sp, 6.8, C$^{16}$H, 1H), 3.82 (s, C$^{23}$H, 3H), 1.53 (d, 6.8, C$^{17}$H, C$^{18}$H, 6H). $^{13}$C NMR (DMF-$d_7$, ppm): $\delta$ 165.72 (C$^{25}$, C$^{26}$), 160.48 (C$^{12}$), 155.13 (C$^2$), 154.05 (C$^6$), 150.32 (C$^4$), 143.81 (C$^8$), 140.85 (C$^{10}$), 130.04 (C$^{14}$), 120.62 (C$^{15}$), 117.26 (C$^5$), 113.91 (C$^{11}$), 113.31 (C$^{13}$), 55.50 (C$^{23}$), 49.64 (C$^{16}$), 45.19 (C$^9$), 21.96 (C$^{17}$, C$^{18}$). $^{15}$N NMR (DMF-$d_7$, ppm): $\delta$ 227.6 (N$^1$), 217.6 (N$^3$), 181.5 (N$^9$), 143.4 (N$^7$), 97.2 (N$^6$).

**3**: Yield: 610 mg (63%). *Anal.* Calc. for $C_{36}H_{40}N_{10}O_8Cl_2Pd\cdot 3H_2O$: C, 44.5; H, 4.8; N, 14.4. Found: C, 44.1; H, 4.7; N, 13.9%. m.p. 176–179 °C (decomp.). $\Lambda_M$ (DMF solution, S cm$^2$ mol$^{-1}$): 0.1. ESI+ MS (methanol, *m/z*): $[Pd(ox)(L_3)_3 + H]^+$ 1279.4, $[Pd(ox)(L_3)_2 + H]^+$ 918.6, $[Pd(ox)(L_3) + K]^+$ 596.8, $[Pd(ox)(L_3) + H]^+$ 557.9, $[L_3 + H]^+$ 362.1. IR (Nujol; cm$^{-1}$): 560vs $\nu$(Pd–O); 521s $\nu$(Pd–N). IR (KBr; cm$^{-1}$): 3137w, 3111w, 3057w $\nu$(C–H)$_{ar}$, 2982w, 2941w, 2838w $\nu$(C–H)$_{al}$; 1712vs, 1676s $\nu$(C=O)$_{ox}$; 1619vs $\nu$(C=N); 1539w, 1470s $\nu$(C=C)$_{ar}$; 1378s $\nu$(C–O)$_{ox}$; 1229w $\nu$(C–O)$_{ar}$; 1156s $\nu$(C–Cl); 560w $\nu$(Pd–O); 521w $\nu$(Pd–N). Raman (cm$^{-1}$): 3333w $\nu$(N–H); 3137w, 3076w, 3014w $\nu$(C–H)$_{ar}$; 2985s, 2945s, 2838w $\nu$(C–H)$_{al}$; 1697s, 1657w $\nu$(C=O)$_{ox}$; 1535w, 1486w $\nu$(C=C)$_{ar}$; 1166w $\nu$(C–Cl); 560s $\nu$(Pd–O); 521w $\nu$(Pd–N). $^1$H NMR (DMF-$d_7$, ppm): $\delta$ 9.18 (t, 6.2, N$^6$H, 1H), 8.76 (s, C$^8$H, 1H), 6.72 (d, 2.4, C$^{11}$H, C$^{15}$H, 2H), 6.41 (t, 2.4, C$^{13}$H, 1H), 4.82 (d, 6.2, C$^9$H, 2H), 4.79 (sp, 6.8, C$^{16}$H, 1H), 3.81 (s, C$^{23}$H, C$^{24}$H, 6H), 1.53 (d, 6.8, C$^{17}$H, C$^{18}$H, 6H). $^{13}$C NMR (DMF-$d_7$, ppm): $\delta$ 165.59 (C$^{25}$, C$^{26}$), 161.67 (C$^{12}$, C$^{14}$), 155.14 (C$^6$), 154.10 (C$^2$), 150.36 (C$^4$), 143.80 (C$^8$), 141.65 (C$^{10}$), 117.32 (C$^5$), 106.48 (C$^{11}$, C$^{15}$), 99.75 (C$^{13}$), 55.66 (C$^{23}$, C$^{24}$), 49.64 (C$^{16}$), 45.39 (C$^9$), 21.99 (C$^{17}$, C$^{18}$). $^{15}$N NMR (DMF-$d_7$, ppm): $\delta$ 231.2 (N$^1$), 223.8 (N$^3$), 185.8 (N$^9$), 147.5 (N$^7$), 100.4 (N$^6$).

**4**: Yield: 320 mg (71%). *Anal.* Calc. for $C_{40}H_{52}N_{12}O_6Pd$: C, 53.2; H, 5.8; N, 18.6. Found: C, 52.7, H, 6.1; N, 18.5%. m.p. 164–166 °C (decomp.). $\Lambda_M$ (DMF solution, S cm$^2$ mol$^{-1}$): 0.3. ESI+ MS (methanol, *m/z*): $[Pd(ox)(L_4)_3 + H]^+$ 1257.0, $[Pd(ox)(L_4)_2 + Na]^+$ 925.2, $[Pd(L_4)_2 + H]^+$ 813.1, $[Pd(L_4) + Na]^+$ 571.1, $[Pd(L_4) + H]^+$ 461.2, $[L_4 + H]^+$ 355.3. IR (Nujol; cm$^{-1}$): 559vs $\nu$(Pd–O); 524vs $\nu$(Pd–N). IR (KBr; cm$^{-1}$): 3131w, 3062w, 3030w $\nu$(C–H)$_{ar}$, 2965s, 2932s, 2875s $\nu$(C–H)$_{al}$; 1706vs, 1674s $\nu$(C=O)$_{ox}$; 1610vs $\nu$(C=N); 1545vs, 1493vs $\nu$(C=C)$_{ar}$; 1376vs $\nu$(C–O)$_{ox}$; 1058s $\nu$(C–O)$_{al}$; 560w $\nu$(Pd–O); 523w $\nu$(Pd–N). Raman (cm$^{-1}$): 3148w, 3057vs $\nu$(C–H)$_{ar}$; 2979s, 2935vs, 2877s $\nu$(C–H)$_{al}$; 1692w, $\nu$(C=O)$_{ox}$; 1606vs $\nu$(C–N); 1491s $\nu$(C=C)$_{ar}$; 561w $\nu$(Pd–O). $^1$H NMR (DMF-$d_7$, ppm): $\delta$ 8.43 (br, N$^6$H, 1H), 8.38 (s, C$^8$H, 1H), 7.50 (dd, 7.2, 1.6, C$^{11}$H, C$^{15}$H, 2H), 7.31 (tt, 7.2, 1.6, C$^{12}$H, C$^{14}$H, 2H), 7.23 (tt, 7.2, 1.6, C$^{13}$H, 1H), 6.32 (br, N$^2$H, 1H), 4.80 (d, 6.0, C$^9$H, 2H), 4.70 (m, O$^{20}$H, 1H), 4.67 (sp, 6.8, C$^{16}$H, 1H), 3.97 (sx, 6.8, C$^{19}$H, 1H), 3.66 (sx, 6.8, C$^{20}$H$^a$, 1H), 3.59 (sx, C$^{20}$H$^b$, 1H), 1.75 (sp, 6.8, C$^{21}$H$^a$, 1H), 1.56 (m, C$^{21}$H$^b$, 1H), 1.50 (d, 6.8, C$^{17}$H, C$^{18}$H, 6H), 0.93 (t, 6.8, C$^{22}$H, 3H). $^{13}$C NMR (DMF-$d_7$, ppm): $\delta$ 166.20 (C$^{25}$, C$^{26}$), 160.44 (C$^2$), 153.50 (C$^6$), 151.43 (C$^4$), 140.57 (C$^{10}$), 139.24 (C$^8$), 128.80 (C$^{12}$, C$^{14}$), 128.32 (C$^{11}$, C$^{15}$), 127.21 (C$^{13}$), 111.84 (C$^5$), 64.12 (C$^{20}$), 55.35 (C$^{19}$), 48.39 (C$^{16}$), 44.61 (C$^9$), 24.76 (C$^{21}$), 21.84 (C$^{17}$), 21.80 (C$^{18}$), 10.93 (C$^{22}$). $^{15}$N NMR (DMF-$d_7$, ppm): $\delta$ 199.8 (N$^1$), 181.0 (N$^9$), 144.3 (N$^7$), 96.7 (N$^2$), 91.6 (N$^6$).

**5**: Yield: 240 mg (50%). *Anal.* Calc. for $C_{42}H_{56}N_{12}O_8Pd$: C, 52.4; H, 5.9; N, 17.4. Found: C, 51.9, H, 5.8; N, 17.6%. m.p. 159–160 °C (decomp.). $\Lambda_M$ (DMF solution, S cm$^2$ mol$^{-1}$): 3.0. ESI+ MS (methanol, *m/z*): $[Pd(ox)(L_5)_3 + H]^+$ 1347.2, $[Pd(L_5) + H]^+$ 491.1, $[L_5 + H]^+$ 385.3. IR (Nujol; cm$^{-1}$): 559vs $\nu$(Pd–O); 527vs $\nu$(Pd–N). IR (KBr; cm$^{-1}$): 3116w, 3072w $\nu$(C–H)$_{ar}$, 2964w, 2933w, 2875w, 2837w $\nu$(C–H)$_{al}$; 1708s, 1676s $\nu$(C=O)$_{ox}$; 1609vs $\nu$(C=N); 1541s, 1492s

$\nu$(C=C)$_{ar}$; 1371s $\nu$(C–O)$_{ox}$; 1243s $\nu$(C–O)$_{ar}$; 1050w $\nu$(C–O)$_{al}$; 556w $\nu$(Pd–O); 526w $\nu$(Pd–N). Raman (cm$^{-1}$): 3345w $\nu$(N–H); 3069s $\nu$(C–H)$_{ar}$; 2974s, 2936vs, 2878s, 2842w $\nu$(C–H)$_{al}$; 1705w, 1672w, $\nu$(C=O)$_{ox}$; 1606vs $\nu$(C–N); 1536w, 1491s $\nu$(C=C)$_{ar}$; 1251s $\nu$(C–O)$_{ar}$; 1049 $\nu$(C–O)$_{al}$; 560w $\nu$(Pd–O); 526w $\nu$(Pd–N). $^1$H NMR (DMF-$d_7$, ppm): $\delta$ 8.34 (s, C$^8$H, 1H), 8.23 (br, N$^6$H, 1H), 7.40 (d, 7.5, C$^{15}$H, 1H), 7.24 (tt, 7.9, 1.6, C$^{13}$H, 1H), 7.02 (d, 8.2, C$^{12}$H, 1H), 6.85 (t, 7.5, C$^{14}$H, 1H), 6.29 (br, N$^2$H, 1H), 4.80 (d, 7.3, C$^9$H, 2H), 4.70 (br, O$^{20}$H, 1H), 4.68 (sp, 6.8, C$^{16}$H, 1H), 3.94 (m, C$^{19}$H, 1H), 3.91 (s, C$^{23}$H, 3H), 3.64 (m, C$^{20}$H$^a$, 1H), 3.56 (m, C$^{20}$H$^b$, 1H), 1.72 (sp, 7.4, C$^{21}$H$^a$, 1H), 1.55 (sp, 7.4, C$^{21}$H$^b$, 1H), 1.50 (d, 6.8, C$^{17}$H, C$^{18}$H, 6H), 0.91 (br, C$^{22}$H, 3H). $^{13}$C NMR (DMF-$d_7$, ppm): $\delta$ 165.94 (C$^{25}$, C$^{26}$), 160.49 (C$^2$), 157.95 (C$^{11}$), 153.64 (C$^6$), 151.40 (C$^4$), 139.28 (C$^8$), 128.87 (C$^{13}$), 128.61 (C$^{15}$), 127.90 (C$^{10}$), 120.87 (C$^{14}$), 112.07 (C$^5$), 110.92 (C$^{12}$), 64.05 (C$^{20}$), 55.83 (C$^{23}$), 55.38 (C$^{19}$), 48.36 (C$^{16}$), 39.75 (C$^9$), 24.78 (C$^{21}$), 21.86 (C$^{17}$), 21.82 (C$^{18}$), 10.96 (C$^{22}$). $^{15}$N NMR (DMF-$d_7$, ppm): $\delta$ 200.0 (N$^1$), 181.8 (N$^9$), 180.0 (N$^3$), 145.4 (N$^7$), 96.9 (N$^2$), 89.7 (N$^6$).

**6**: Yield: 370 mg (77%). *Anal.* Calc. for $C_{42}H_{56}N_{12}O_8Pd{\cdot}H_2O$: C, 51.4; H, 6.0; N, 17.1. Found: C, 51.0, H, 6.1; N, 17.2%. m.p. 155–158 °C (decomp.). $\Lambda_M$ (DMF solution, S cm$^2$ mol$^{-1}$): 2.4. ESI+ MS (methanol, *m/z*): [Pd(ox)(L$_6$)$_3$ + H]$^+$ 1347.0, [Pd(L$_6$) + H]$^+$ 491.2, [L$_6$ + H]$^+$ 385.3. IR (Nujol; cm$^{-1}$): 557vs $\nu$(Pd–O); 524vs $\nu$(Pd–N). IR (KBr; cm$^{-1}$): 3120w $\nu$(C–H)$_{ar}$, 2965w, 2934w, 2875w, 2834w $\nu$(C–H)$_{al}$; 1708s, 1676s $\nu$(C=O)$_{ox}$; 1609vs $\nu$(C=N); 1544s, 1491s $\nu$(C=C)$_{ar}$; 1374s $\nu$(C–O)$_{ox}$; 1265s $\nu$(C–O)$_{ar}$; 1047w $\nu$(C–O)$_{al}$; 558w $\nu$(Pd–O). Raman (cm$^{-1}$): 3061w $\nu$(C–H)$_{ar}$; 2975s, 2937vs, 2876s, 2833w $\nu$(C–H)$_{al}$; 1701w, 1669w, $\nu$(C=O)$_{ox}$; 1608vs $\nu$(C–N); 1542w, 1488w $\nu$(C=C)$_{ar}$; 1266s $\nu$(C–O)$_{ar}$; 559s $\nu$(Pd–O); 526w $\nu$(Pd–N). $^1$H NMR (DMF-$d_7$, ppm): $\delta$ 8.46 (br, N$^6$H, 1H), 8.36 (s, C$^8$H, 1H), 7.21 (t, 7.9, C$^{14}$H, 1H), 7.13 (t, 2.1, C$^{11}$H, 1H), 7.08 (d, 7.6, C$^{15}$H, 1H), 6.81 (dd, 8.2, 2.6, C$^{13}$H, 1H), 6.34 (br, N$^2$H, 1H), 4.82 (br, O$^{20}$H, 1H), 4.76 (d, 6.8, C$^9$H, 2H), 4.68 (sp, 6.8, C$^{16}$H, 1H), 3.95 (sx, 5.5, C$^{19}$H, 1H), 3.80 (s, C$^{23}$H, 3H), 3.66 (sp, 5.5, C$^{20}$H$^a$, 1H), 3.55 (m, C$^{20}$H$^b$, 1H), 1.74 (sp, 7.4, C$^{21}$H$^a$, 1H), 1.55 (sp, 7.4, C$^{21}$H$^b$, 1H), 1.50 (d, 6.8, C$^{17}$H, C$^{18}$H, 6H), 0.92 (t, 7.5, C$^{22}$H, 3H). $^{13}$C NMR (DMF-$d_7$, ppm): $\delta$ 166.04 (C$^{25}$, C$^{26}$), 160.54 (C$^{12}$), 160.44 (C$^2$), 153.53 (C$^6$), 151.46 (C$^4$), 142.32 (C$^{10}$), 139.32 (C$^8$), 129.85 (C$^{14}$), 120.60 (C$^{15}$), 113.67 (C$^{11}$), 113.11 (C$^{13}$), 111.87 (C$^5$), 64.12 (C$^{20}$), 55.47 (C$^{23}$), 55.36 (C$^{19}$), 48.34 (C$^{16}$), 44.68 (C$^9$), 24.77 (C$^{21}$), 21.88 (C$^{17}$), 21.84 (C$^{18}$), 10.96 (C$^{22}$). $^{15}$N NMR (DMF-$d_7$, ppm): $\delta$ 199.6 (N$^1$), 181.1 (N$^9$), 144.7 (N$^7$), 96.8 (N$^2$), 91.7 (N$^6$).

**7**: Yield: 320 mg (66%). *Anal.* Calc. for $C_{42}H_{56}N_{12}O_8Pd$: C, 52.4; H, 5.9; N, 17.4. Found: C, 52.2, H, 6.4; N, 17.3%. mp 165–167 °C (decomp.). $\Lambda_M$ (DMF solution, S cm$^2$ mol$^{-1}$): 3.2. ESI+ MS (methanol, *m/z*): [Pd(ox)(L$_7$)$_3$ + H]$^+$ 1347.0, [Pd(L$_7$) + H]$^+$ 491.1, [L$_7$ + H]$^+$ 385.3. IR (Nujol; cm$^{-1}$): 560vs $\nu$(Pd–O); 522vs $\nu$(Pd–N). IR (KBr; cm$^{-1}$): 3132w $\nu$(C–H)$_{ar}$, 2964s, 2933s, 2875s, 2835w $\nu$(C–H)$_{al}$; 1707vs, 1675s $\nu$(C=O)$_{ox}$; 1608vs $\nu$(C=N); 1543vs, 1493s $\nu$(C=C)$_{ar}$; 1374vs $\nu$(C–O)$_{ox}$; 1249vs $\nu$(C–O)$_{ar}$; 1057w $\nu$(C–O)$_{al}$; 561w $\nu$(Pd–O); 525w $\nu$(Pd–N). Raman (cm$^{-1}$): 3335w $\nu$(N–H); 3058s $\nu$(C–H)$_{ar}$; 2976s, 2936vs, 2876s, 2842w $\nu$(C–H)$_{al}$; 1711w, 1672w, $\nu$(C=O)$_{ox}$; 1610vs $\nu$(C–N); 1549w $\nu$(C=C)$_{ar}$; 1255w $\nu$(C–O)$_{ar}$; 561w $\nu$(Pd–O). $^1$H NMR (DMF-$d_7$, ppm): $\delta$ 8.36 (br, N$^6$H, 1H), 8.33 (s, C$^8$H, 1H), 7.45 (dd, 8.6, 2.0, C$^{12}$H, C$^{14}$H, 2H), 6.87 (dd, 8.6, 2.0, C$^{11}$H, C$^{15}$H, 2H), 6.35 (br, N$^2$H, 1H), 4.77 (t, 6.0, O$^{20}$H, 1H), 4.71 (d, 5.5, C$^9$H, 2H), 4.67 (sp, 6.6, C$^{16}$H, 1H), 3.99 (br, C$^{19}$H, 1H), 3.78 (s, C$^{23}$H, 3H), 3.69 (m, C$^{20}$H$^a$, 1H), 3.57 (m, C$^{20}$H$^b$, 1H), 1.77 (sp, 6.8, 1.5, C$^{21}$H$^a$, 1H), 1.58 (sp, 6.8, C$^{21}$H$^b$, 1H), 1.49 (d, 6.8, C$^{17}$H, C$^{18}$H, 6H), 0.94 (tt, 7.5, 2.5, C$^{22}$H, 3H). $^{13}$C NMR (DMF-$d_7$, ppm): $\delta$ 166.10 (C$^{25}$, C$^{26}$), 160.48 (C$^2$), 159.31 (C$^{13}$), 153.48 (C$^6$), 151.42 (C$^4$), 139.30 (C$^8$), 132.45 (C$^{10}$), 129.83 (C$^{12}$, C$^{14}$), 114.24 (C$^{11}$, C$^{15}$), 111.87 (C$^5$), 64.19 (C$^{20}$), 55.48 (C$^{23}$), 55.40 (C$^{19}$), 48.42 (C$^{16}$), 44.14 (C$^9$), 24.81 (C$^{21}$), 21.81 (C$^{17,18}$), 10.97 (C$^{22}$). $^{15}$N NMR (DMF-$d_7$, ppm): $\delta$ 200.0 (N$^1$), 181.2 (N$^9$), 144.4 (N$^7$), 97.3 (N$^2$), 93.3 (N$^6$).

### 2.3. Physical measurements

Elemental analyses (C, H, N) were performed on a Fisons EA-1108 CHNS-O Elemental Analyzer (Thermo Scientific). The yields were calculated and based on palladium. Melting point determinations were performed on a Melting Point B-540 apparatus (Büchi) with 5 °C min$^{-1}$ gradient and the obtained values were uncorrected. Conductivity measurements were carried out on a Cond 340i/SET (WTW) in *N,N′*-dimethylformamide (DMF; 10$^{-3}$ M) solution at the temperature of 25 °C. Infrared spectra were recorded on a Nexus 670 FT-IR (ThermoNicolet) by KBr (400–4000 cm$^{-1}$) and Nujol (150–600 cm$^{-1}$) techniques. Raman spectroscopy was performed on an NXR FT-Raman Module (ThermoNicolet) in the 150–3750 cm$^{-1}$ region; the Raman spectrum was not obtained in case of **1** (the sample burnt under laser beam). The reported IR and Raman signal intensities have been defined as w = weak, s = strong and vs = very strong. $^1$H and $^{13}$C spectra and $^1$H–$^1$H gs-COSY, $^1$H–$^{13}$C gs-HMQC, $^1$H–$^{13}$C gs-HMBC and $^1$H–$^{15}$N gs-HMBC (gs = gradient selected, COSY = correlation spectroscopy, HMQC = Heteronuclear Multiple Quantum Coherence, HMBC = Heteronuclear Multiple Bond Coherence) correlation experiments (DMF-$d_7$ solutions of L$_{1-7}$ and **1**–**7**) were measured on a Varian 400 MHz NMR device at 400.00 MHz ($^1$H), 100.58 MHz ($^{13}$C) and 40.53 MHz ($^{15}$N). Spectra were obtained at natural abundance at 300 K ($^1$H and $^1$H–$^{15}$N gs-HMBC also at 340 K) and were calibrated against the signals of tetramethylsilane (an internal standard for $^1$H and $^{13}$C NMR spectra) and against the residual signals of the solvent (an internal reference for $^{15}$N adjusted to 104.7 ppm). The splitting of proton resonances in the reported $^1$H spectra is defined as s = singlet, d = doublet, t = triplet, sx = sextuplet, sp = septuplet, br = broad band, dd = doublet of doublets, tt = triplet of triplets, m = multiplet. Mass spectra (MS) of the methanol solutions of **1**–**7** were obtained using a LCQ Fleet ion trap mass spectrometer by the positive mode electrospray ionization (ESI+) technique (Thermo Scientific). Simultaneous thermogravimetric (TG) and differential thermal (DTA) analyses were carried out using a thermal analyzer Exstar TG/DTA 6200 (Seiko Instruments Inc.). TG/DTA studies were performed in ceramic pans from laboratory temperature to 900 °C with a 2.5 °C min$^{-1}$ temperature gradient in dynamic air atmosphere (100 mL min$^{-1}$). Geometry of the complex **2** was fully optimized at the B3LYP level with the 6-311G$^*$/LANL2DZ basis set, where the LANL2DZ pseudo-potential was applied for the Pd(II) ion. Theoretical calculations were performed with SPARTAN06 program package [13]. The molecular graphic was drawn by DIAMOND, the structural parameters and calculations were interpreted using the same software [14].

### 2.4. In vitro cytotoxic activity

*In vitro* cytotoxicity of the complexes **1**, **3**–**5** and **7** was evaluated by an MTT assay against the human osteosarcoma cancer cell line (HOS); [MTT = 3-(4,5-dimethylthiazol-2-yl)-2,5-diphenyltetrazolium bromide] [15].

The suspension of 2.5 × 10$^4$ cells/well was stabilized in 96-well microplates in the culture medium enriched by fetal calf serum for 16 h at the temperature of 37 °C in 5% $CO_2$ atmosphere. The tested complexes were dissolved in DMF up to concentration of 50 μM, and then diluted with the cell culture medium to the final DMF concentration of 0.1%. This mixture was added to microplates with the cancer cells instead of the above-mentioned culture medium. The cancer cells were incubated for the period of 24 h. After this period, the cells were washed with sterile phosphate buffer saline (PBS), and 100 μL of MTT (0.3 mg mL$^{-1}$) were poured in. The medium including the complexes was removed after 2 h. 100 μL of DMSO with 1% $NH_3$ were added to dissolve the purple formazane, whose absorbance was measured at 630 nm (an automatic

microplate ELISA reader). The obtained results are discussed as $IC_{50}$ values.

## 3. Results and discussion

### 3.1. General features

The palladium(II) oxalato complexes of the general composition $[Pd(ox)(L_{1-7})_2]\cdot nH_2O$ (**1**–**7**; $n$ = 0 for **4**, **5** and **7**, ¾ for **1** and **2**, 1 for **6** and 3 for **3**) have been prepared by a one-step synthesis using the reaction of $K_2[Pd(ox)_2]\cdot 2H_2O$ with two molar equivalents of the appropriate N6-(benzyl)-9-isopropyladenine-based organic molecule ($L_{1-7}$; specified in Section 2.1 and Scheme 1). The pale yellow powder complexes **1**–**7** were isolated after two days of stirring at 40 °C by filtration from the reaction mixture (Scheme 2).

The complexes **1**–**7** were determined to be non-electrolytes, since the molar conductivity values of their $10^{-3}$ M DMF solutions ranged from 0.1 to 5.8 S cm$^2$ mol$^{-1}$, and these values are typical for non-electrolytes in DMF [16].

The prepared palladium(II) oxalato complexes **1**–**7** are well soluble in various solvents (e.g. DMF, DMSO, chloroform, ethanol, methanol, acetone) and less soluble in water. However, the attempts to prepare crystals suitable for a single-crystal X-ray analysis have been unsuccessful to date in all the above-mentioned solvents or their combinations. That is why the composition and structure of complexes **1**–**7** were deduced from the obtained results of physical techniques (mainly from NMR and mass spectra) and based on similarity with the previously published $[Pd(ox)(L_I)_2]$ (**I**) and $[Pd(ox)(L_{II})_2]\cdot L_{II}\cdot Me_2CO$ (**II**) complexes whose structures were determined by a single-crystal X-ray analysis; $L_I$ = 2-chloro-N6-(4-methoxybenzyl)-9-isopropyladenine and $L_{II}$ = 2-chloro-N6-(4-methylbenzyl)-9-isopropyladenine [3]. For the lack of single crystals suitable for a crystallographic study, the geometry of the complex **2** was optimized using DFT calculations (see Section 3.5).

### 3.2. IR and Raman spectroscopy

The title $[Pd(ox)(L_{1-7})_2]\cdot nH_2O$ complexes (**1**–**7**) involve two types of ligands, i.e. the N-donor ligands ($L_{1-7}$) derived from N6-(benzyl)-9-isopropyladenine, and O-donor bidentate-coordinated oxalate dianion (ox). Characteristic vibrations of both ligand types were unambiguously detected in the IR (150–4000 cm$^{-1}$) and Raman (150–3750 cm$^{-1}$) spectra.

The $L_{1-7}$ organic molecules coordinated to the central Pd(II) ion in the complexes **1**–**7** showed characteristic and the most intensive $\nu$(C=N) bands at 1608–1622 cm$^{-1}$ [17,18]. It should be pointed out, that the maxima values differ between the groups of complexes **1**–**3** (1618–1622 cm$^{-1}$) and **4**–**7** (1608–1610 cm$^{-1}$), which may be connected with a different substitution of N6-(benzyl)-9-isopropyladenine skeleton at the C2 position. The peaks of the $\nu(C–H)_{ar}$ and $\nu(C–H)_{al}$ vibrations were detected at 3030–3137 and 2834–2982 cm$^{-1}$, respectively [17–19]. The $\nu(C{=}C)_{ar}$ bands showed two maxima at ~1470 and ~1545 cm$^{-1}$. The bands observed in the 1229–1265 cm$^{-1}$ region are assignable to the $\nu(C–O)_{ar}$ vibration of the methoxy substituent of a benzyl group (it was not found in case of **4**, which does not have the methoxy-substituted benzene ring). The presence of the $\nu$(C–Cl) (for **1**–**3**) and $\nu(C–O)_{al}$ (for **4**–**7**) vibrations at ~1050 and ~1160 cm$^{-1}$, respectively, is a consequence of a different substitution of the C2 atom of the adenine derivatives $L_{1-3}$ and $L_{4-7}$ involved in the complexes **1**–**3** and **4**–**7**. A broad peak was observed in IR spectra of all the complexes between ca. 3300 and 3500 cm$^{-1}$, and thus, the maxima belonging to both the $\nu$(N–H) and $\nu$(O–H) vibrations could not be assigned unambiguously.

An oxalate dianion, which is bidentate-coordinated to the Pd(II) ion in complexes **1**–**7**, showed two bands of the $\nu_{as}(C{=}O)_{ox}$ vibration at 1671–1676 and 1706–1712 cm$^{-1}$ [20]. Other peaks of an oxalato group, assignable to the $\nu_s(C–O)_{ox}$ vibration, were found in the 1364–1378 cm$^{-1}$ region. The coordination of both ligand types to the metal centre was indirectly proved by detection of the $\nu$(Pd–N) and $\nu$(Pd–O) vibrations in the far-IR spectra. The bands of the $\nu$(Pd–O) were observed at 557–560 cm$^{-1}$, while the maxima observed between 506 and 527 cm$^{-1}$ are assignable to the $\nu$(Pd–N) vibration [19–21].

Most of the above-described vibrations detected by the IR spectroscopy of **1**–**7** were observed in the corresponding Raman spectra of the complexes **2**–**7** (complex **1** burnt up in the light of laser beam). The maxima belonging to the $\nu(C–H)_{ar}$, $\nu(C–H)_{al}$, and $\nu$(Pd–O) stretching vibrations were found in Raman spectra of all the complexes **2**–**7** at 3057–3148, 2833–2990, and at 559–561 cm$^{-1}$, respectively. Two maxima of the $\nu_{as}(C{=}O)_{ox}$ vibrations were detected at 1692–1711 and 1657–1672 cm$^{-1}$, while the maxima of the $\nu(C{=}C)_{ar}$ were observed at 1535–1549 and 1454–1485 cm$^{-1}$. However, the other vibrations discussed for IR spectroscopy, i.e. $\nu(C{=}N)_{ar}$, $\nu_s(C–O)_{ox}$, $\nu(C–O)_{ar}$ and $\nu$(Pd–N), were observed only in Raman spectra of some of the palladium(II) oxalato complexes **2**–**7** (see Section 2.2). In case of the $\nu(C{=}N)_{ar}$ vibration, it could be connected with decrease in intensity of the named band, as recently experimentally observed and theoretically calculated for this vibration in adenine [18]. Nevertheless, in the cases that these bands were observed, the positions of their maxima correlated well with those observed in the IR spectra (see Section 2.2 for more details). The band of a very strong intensity at about 1320 cm$^{-1}$, which was not detected in the IR spectra, can be assigned to the skeletal stretching vibrations of a purine ring, as formerly reported [18,22]. Contrary to the IR spectra, the $\nu$(N–H) bands were detected in the Raman spectra of **2**, **3**, **5** and **7** (not for **4** and **6**). However, the maxima of the peaks connected with this vibration, observed within the 3333–3370 cm$^{-1}$ region, were of very low intensity, which is in accordance with results given for non-substituted adenine [18].

### 3.3. NMR spectroscopy

Multinuclear and two dimensional (2D) NMR experiments (see Section 2.3) were performed for all the complexes **1**–**7** as well as for the free organic compounds $L_{1-7}$ involved in **1**–**7** as N-donor ligands. The chemical shifts ($\delta$; ppm) are given in Section 2.2, while the coordination shifts ($\Delta\delta = \delta_{complex} - \delta_{ligand}$; ppm) are summarized in Tables 1–3.

All the signals detected in the $^1$H and $^{13}$C NMR spectra of the free $L_{1-7}$ molecules were also found in the appropriate spectra of complexes **1**–**7**. The highest $|\Delta\delta|$ values in the $^1$H NMR spectra were observed for the hydrogen atoms bound to the N$^6$ (0.34–0.95 ppm downfield) and C$^8$ (0.28–0.61 ppm downfield) atoms (see Table 1). In the case of complexes **4**–**7**, the N$^2$H signals are significantly shifted downfield as well, but less than the mentioned N$^6$H and C$^8$H signals. The coordination shifts of the other proton signals were insignificant.

The highest coordination shifts of carbon atoms were determined for the C$^8$ atom (3.50–3.94 ppm downfield), followed by the C$^5$ (1.24–3.12 ppm upfield), C$^6$ (0.93–2.22 ppm upfield) and C$^{16}$ (1.31–1.75 ppm downfield) ones (Table 2). It can be pointed out, that the C$^5$, C$^6$ and C$^8$ coordination shifts of **1**–**3** and **4**–**7** differ significantly within the group of complexes **1**–**7**, which is most likely caused by various compositions and structures of the appropriate adenine derivatives involved in these two types of compounds. It has to be noted, that there was one more signal detected at ~166 ppm in the $^{13}$C NMR spectra of the complexes **1**–**7**, which was not observed in the spectra of free $L_{1-7}$ molecules,

**Table 1**
Coordination shifts ($\Delta\delta = \delta_{complex} - \delta_{ligand}$) determined from the $^{1}H$ NMR spectra for the complexes **1**–**7**.

| | $N^2H$ | $N^6H$ | $C^8H$ | $C^9H$ | $C^{11}H$ | $C^{12}H$ | $C^{13}H$ | $C^{14}H$ | $C^{15}H$ | $C^{16}H$ | $C^{17}H$, $C^{18}H$ | $C^{19}H$ | $C^{20}H^a$ | $C^{20}H^b$ | $O^{20}H$ | $C^{21}H^a$ | $C^{21}H^b$ | $C^{22}H$ | $C^{23}H$ | $C^{24}H$ |
|---|---|---|---|---|---|---|---|---|---|---|---|---|---|---|---|---|---|---|---|---|
| **1** | | 0.61 | 0.40 | 0.08 | | 0.02 | −0.03 | 0.03 | 0.12 | 0.05 | −0.05 | | | | | | | | 0.04 | |
| **2** | | 0.34 | 0.28 | 0.05 | 0.02 | | 0.00 | −0.03 | 0.07 | 0.01 | −0.06 | | | | | | | | 0.03 | |
| **3** | | 0.52 | 0.47 | 0.07 | 0.07 | | −0.01 | | 0.07 | 0.03 | −0.04 | | | | | | | | 0.03 | 0.03 |
| **4** | 0.46 | 0.71 | 0.61 | −0.03 | 0.05 | 0.01 | 0.01 | 0.01 | 0.05 | 0.06 | −0.02 | −0.01 | 0.00 | −0.07 | −0.09 | 0.01 | −0.18 | −0.01 | | |
| **5** | 0.49 | 0.95 | 0.54 | 0.02 | | 0.00 | 0.01 | −0.02 | 0.06 | 0.06 | −0.03 | −0.01 | 0.00 | 0.00 | −0.07 | 0.00 | −0.04 | −0.01 | 0.01 | |
| **6** | 0.48 | 0.77 | 0.56 | 0.01 | 0.06 | | 0.00 | −0.02 | 0.06 | 0.07 | −0.04 | −0.02 | −0.02 | −0.03 | 0.06 | 0.00 | −0.03 | 0.01 | 0.03 | |
| **7** | 0.49 | 0.76 | 0.55 | 0.01 | −0.01 | 0.07 | | 0.07 | −0.01 | 0.06 | −0.03 | 0.01 | 0.02 | 0.00 | −0.01 | 0.02 | 0.00 | −0.01 | 0.01 | |

**Table 2**
Coordination shifts ($\Delta\delta = \delta_{complex} - \delta_{ligand}$) determined from the $^{13}C$ NMR spectra for the complexes **1**–**7**.

| | $C^2$ | $C^4$ | $C^5$ | $C^6$ | $C^8$ | $C^9$ | $C^{10}$ | $C^{11}$ | $C^{12}$ | $C^{13}$ | $C^{14}$ | $C^{15}$ | $C^{16}$ | $C^{17}$ | $C^{18}$ | $C^{19}$ | $C^{20}$ | $C^{21}$ | $C^{22}$ | $C^{23}$ | $C^{24}$ | $C^{25,26}$ |
|---|---|---|---|---|---|---|---|---|---|---|---|---|---|---|---|---|---|---|---|---|---|---|
| **1** | 0.24 | −0.21 | −2.44 | −1.09 | 3.77 | 0.92 | −0.94 | 0.05 | 0.08 | 0.24 | 0.18 | 0.58 | 1.75 | −0.46 | −0.46 | | | | | 0.16 | | −1.38 |
| **2** | 0.80 | −0.06 | −1.24 | −1.60 | 3.94 | 0.95 | −0.86 | −0.23 | −0.03 | 0.43 | −0.01 | 0.24 | 1.31 | −0.37 | −0.37 | | | | | 0.06 | | −1.23 |
| **3** | 0.19 | −0.21 | −2.37 | −0.93 | 3.70 | 1.08 | −1.03 | 0.11 | 0.01 | 0.70 | 0.01 | 0.11 | 1.74 | −0.41 | −0.41 | | | | | 0.12 | 0.12 | −1.36 |
| **4** | 0.13 | −0.42 | −3.12 | −2.20 | 3.50 | 0.68 | −1.15 | 0.08 | 0.02 | 0.01 | 0.02 | 0.08 | 1.55 | −0.54 | −0.54 | 0.02 | −0.44 | −0.19 | −0.10 | | | −0.75 |
| **5** | 0.21 | −0.28 | −2.97 | −2.22 | 3.53 | 0.67 | −0.97 | 0.07 | 0.04 | 0.36 | 0.17 | 0.16 | 1.52 | −0.51 | −0.51 | 0.12 | −0.39 | −0.13 | −0.03 | 0.12 | | −1.01 |
| **6** | 0.18 | −0.34 | −3.09 | −2.12 | 3.58 | 0.93 | −1.06 | −0.36 | 0.13 | 0.61 | 0.06 | 0.17 | 1.54 | −0.48 | −0.49 | 0.06 | −0.39 | −0.15 | −0.05 | 0.11 | | −0.91 |
| **7** | 0.20 | −0.30 | −3.08 | −2.14 | 3.63 | 0.95 | −1.18 | 0.07 | 0.23 | 0.06 | 0.23 | 0.07 | 1.63 | −0.50 | −0.46 | 0.09 | −0.38 | −0.13 | −0.06 | 0.02 | | −0.85 |

**Table 3**
$^{15}N$ coordination shifts ($\Delta\delta = \delta_{complex} - \delta_{ligand}$) determined from the $^{1}H–^{15}N$ gs-HMBC NMR spectra for the complexes **1**–**7**.

| | $N^1$ | $N^2$ | $N^3$ | $N^6$ | $N^7$ | $N^9$ |
|---|---|---|---|---|---|---|
| **1** | 2.7 | | −0.9 | 8.2 | −93.0 | 7.3 |
| **2** | 1.5 | | −5.5 | 1.6 | −98.2 | 1.9 |
| **3** | 3.6 | | −0.9 | 6.5 | −92.7 | 6.4 |
| **4** | 2.0 | 2.6 | n.o. | 4.0 | −96.5 | 6.7 |
| **5** | −1.3 | −1.3 | −4.5 | 5.7 | −99.0 | 3.7 |
| **6** | −0.3 | 3.6 | n.o. | 8.8 | −94.5 | 7.3 |
| **7** | −2.8 | −3.4 | n.o. | 12.6 | −102.6 | 1.5 |

n.o. – signals were not observed in the $^{1}H–^{15}N$ gs-HMBC spectra of the appropriate complexes.

as well as in any of 2D carbon experiments. This signal unambiguously belongs to the $C^{25}$ and $C^{26}$ atoms of an oxalate dianion bidentate-coordinated to the metal centre. The signals of these atoms are shifted by 0.75–1.38 ppm upfield as compared with the corresponding $^{13}C$ NMR signal of the starting compound $K_2[Pd(ox)_2]\cdot 2H_2O$ dissolved in $D_2O$ and detected at 166.95 ppm. As in the case of the $C^5$, $C^6$ and $C^8$ atoms, the $|\Delta\delta|$ of $C^{25}$ and $C^{26}$ are different for the complexes **1**–**3** as compared with **4**–**7**.

In the case of $^{1}H–^{15}N$ gs-HMBC 2D correlation experiments, coordination shifts of the $N^7$ atoms [$\Delta\delta = -92.7 - (-102.6)$ ppm] were found to be significantly higher as compared with those of the remaining nitrogen atoms ($|\Delta\delta| < 12.6$ ppm) involved in $L_{1-7}$ molecules (Table 3). The analogical NMR spectroscopy results were recently published for palladium(II) oxalato [3] and dichlorido [5] complexes involving N6-(benzyl)-9-isopropyladenine-based N-donor ligands, whose structures were crystallographically determined. It is caused by a coordination of $L_{1-7}$ molecules to the Pd(II) ion through the mentioned $N^7$ atom of the adenine moiety within the structure of the complexes **1**–**7**. In connection with this statement, we can focus back on the results of $^{1}H$ and $^{13}C$ NMR spectroscopy, where we discuss the $C^8H$, $N^6H$, $C^8$ and $C^5$ atoms as those with the highest $\Delta\delta$. As it can be seen from Schemes 1 and 2, the above-mentioned hydrogen and carbon atoms neighbour to the coordination site, i.e. the $N^7$ atom, which indirectly support discussed conclusion regarding coordination.

### 3.4. ESI+ mass spectrometry

The ESI+ MS of the complexes **1**–**7** dissolved in methanol were measured and the results are given in Section 2.2. All the observed isotopic distribution representations correspond very well with the theoretic ones (QUALBROWSER software, version 2.0.7, Thermo Fischer Scientific).

In case of the complexes **1**–**3**, involving 2-chloro-N6-(benzyl)-9-isopropyladenine-based molecules $L_{1-3}$, the $[Pd(ox)(L_{1-3})_2 + H]^+$ molecular peaks were found in the appropriate spectra at 858.8 *m/z* (**1**), 858.7 *m/z* (**2**) and 918.6 *m/z* (**3**), which indirectly confirmed the composition of discussed palladium(II) oxalato complexes. Moreover, the $[Pd(ox)(L_1)_2 + Na]^+$ (for **1**), $[Pd(ox)(L_1)_2 + K]^+$ (for **1**) and $[Pd(ox)(L_{1-3})_3 + H]^+$ (for **1**–**3**) adducts were observed as well. The $[Pd(ox)(L_{1-3}) + H]^+$ and $[(L_{1-3}) + H]^+$ fragments of the studied compounds were also detected in the mass spectra of **1**–**3**; $[(L_{1-3}) + H]^+$ fragment, detected at 332.1 *m/z* for **1**, 332.2 *m/z* for **2** and 362.1 *m/z* for **3**, is unambiguously assignable to the adenine derivative ($L_{1-3}$) involved in the structures of **1**–**3**. Fig. 1 depicts the $[Pd(ox)(L_1) + H]^+$ and $[Pd(ox)(L_1)_2 + K]^+$ peaks found in ESI+ mass spectrum of the complex **1** and their comparison with the theoretic ones.

Quite different results were obtained for the complexes **4**–**7**, since any of the $[Pd(ox)(L_{4-7})_2 + H]^+$, $[Pd(L_{5-7})_2 + H]^+$, or $[Pd(ox)(L_{4-7}) + H]^+$ peaks were not found in their mass spectra, except for $[Pd(L_4)_2 + H]^+$ observed at 813.1 *m/z*; the $[Pd(ox)(L_4)_2 + Na]^+$ and $[Pd(ox)(L_4) + Na]^+$ adducts were detected for this compound as well. On the other hand, the $[Pd(L_{4-7}) + H]^+$ fragment, whose analogue was not detected in any spectrum of **1**–**3**, was clearly observed for the compounds **4**–**7** *m/z* at 461.2, 491.1, 491.2, and 491.1, respectively. Similarly as in the case of complexes **1**–**3**, the $[Pd(ox)(L_{4-7})_3 + H]^+$ and $[(L_{4-7}) + H]^+$ peaks were found in the mass spectra of **4**–**7**.

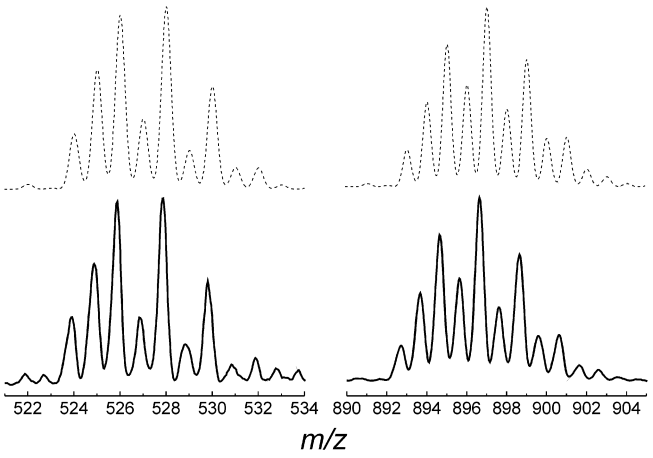


**Fig. 1.** Observed (full line) and calculated (dashed line) isotopic distribution representation of $[Pd(ox)(L_1) + H]^+$ (left) and $[Pd(ox)(L_1)_2 + K]^+$ (right) peaks as obtained by an ESI+ mass spectrometry of the complex **1**.

### 3.5. DFT calculations

The molecular structures of $[Pd(ox)(L_I)_2]$ (**I**) and $[Pd(ox)(L_{II})_2]\cdot L_{II}\cdot Me_2CO$ (**II**) complexes were determined by a single-crystal X-ray analysis, as it was reported in our previous work describing the palladium(II) oxalato complexes with N6-(benzyl)-9-isopropy-

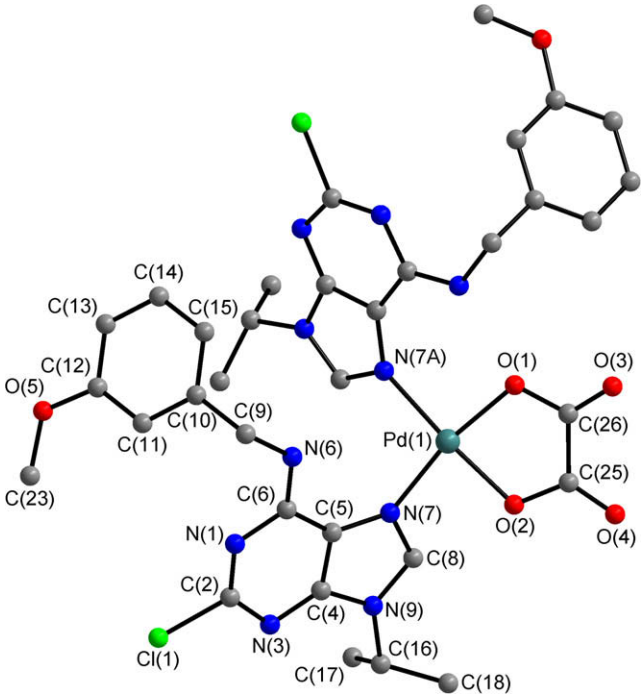


**Fig. 2.** Geometry of the $[Pd(ox)(L_2)_2]$ (**2**) complex optimized on the B3LYP/6-311G*/LANL2DZ level of theory.

ladenine-based N-donor ligands; $L_I$ = 2-chloro-N6-(4-methoxybenzyl)-9-isopropyladenine, $L_{II}$ = 2-chloro-N6-(4-methylbenzyl)-9-isopropyladenine [3]. In present work, partially due to a lack of single crystals suitable for a crystallographic study, we decided to perform theoretical calculations relating to the geometry of the complex $[Pd(ox)(L_2)_2]$ (**2**) on the B3LYP/6-311G*/LANL2DZ level, whose optimized structure is depicted in Fig. 2. The selected bond lengths and angles of the complexes **2**, **I** and **II** are given in Table 4.

The central Pd(II) ion of the complex **2** is tetra-coordinated by two 2-chloro-N6-(3-methoxybenzyl)-9-isopropyladenine ($L_2$) molecules bound to the metal centre through their N(7) atoms of the adenine moieties and by one bidentate-coordinated oxalate dianion. Geometry in the vicinity of the central Pd(II) ion is distorted square-planar. The deviations from a least-square plane defined by atoms of the $PdN_2O_2$ chromophore are: 0.027 Å for Pd(1), 0.070 Å for O(1), −0.089 Å for O(2), 0.064 Å for N(7) and −0.072 Å for N(7A). For the complex **II**, the above-discussed deviations were determined to be: 0.0005(3) Å [Pd(1)], −0.0305(22) Å [O(1)], 0.0276(27) Å [O(2)], −0.0513(29) Å [N(7)] and 0.0259(29) Å [N(7A)]. In case of the complex **II** they equalled, in the given order, 0.0032(3), −0.0202(23), −0.0643(23), −0.0530(32), and −0.1318(32) Å, respectively. Two $L_2$ molecules are, similarly to the complex **II**, mutually arranged in the head-to-tail arrangement within the structure of the complex **2**; the complex **I** has its $L_I$ molecules arranged in the head-to-head orientation.

All the calculated Pd–N and Pd–O bands of **2** are slightly longer as compared with those determined for the complexes **I** and **II** (Table 4). As for bond angles, it has to be noted that in some cases [e.g. O(1)–Pd(1)–N(7)], the values observed for the complex **2** differ significantly from those of **I** and **II**. But differences of the same order can be found even between some angles of **I** and **II** [e.g. O(2)–Pd(1)–N(7A) angle], which is caused by a variedness of the structures of the studied complexes (see Table 4).

**Table 4**
Selected bond lengths (Å) and angles (°) for the complex $[Pd(ox)(L_2)_2]$ (**2**) optimized on the B3LYP/6-311G* /LANL2DZ level of theory, and for the complexes $[Pd(ox)(L_I)_2]$ (**I**) and $[Pd(ox)(L_{II})_2]\cdot L_{II}\cdot Me_2CO$ (**II**) as determined by a single-crystal X-ray analysis (see Ref. [3]); $L_2$ = 2-chloro-N6-(3-methoxybenzyl)-9-isopropyladenine, $L_I$ = 2-chloro-N6-(4-methoxy-benzyl)-9-isopropyladenine and $L_{II}$ = 2-chloro-N6-(4-methylbenzyl)-9-isopropyladenine.

| Compound | 2 | I | II |
|---|---|---|---|
| *Bond lengths* | | | |
| Pd(1)–N(7) | 2.078 | 2.012(3) | 2.023(3) |
| Pd(1)–N(7A) | 2.110 | 2.024(3) | 2.021(3) |
| Pd(1)–O(1) | 2.017 | 1.992(2) | 1.971(2) |
| Pd(1)–O(2) | 2.011 | 1.987(2) | 1.983(2) |
| O(1)–C(26) | 1.355 | 1.302(4) | 1.332(4) |
| O(2)–C(25) | 1.351 | 1.289(4) | 1.282(4) |
| O(3)–C(26) | 1.234 | 1.215(4) | 1.239(4) |
| O(4)–C(25) | 1.233 | 1.222(4) | 1.230(4) |
| C(25)–C(26) | 1.540 | 1.549(5) | 1.471(5) |
| *Bond angles* | | | |
| O(1)–Pd(1)–N(7A) | 95.37 | 93.09(10) | 89.86(10) |
| O(1)–Pd(1)–N(7) | 168.73 | 174.96(10) | 173.26(10) |
| O(1)–Pd(1)–O(2) | 82.28 | 84.46(9) | 84.20(10) |
| O(2)–Pd(1)–N(7) | 86.83 | 91.12(10) | 89.38(10) |
| O(2)–Pd(1)–N(7A) | 173.54 | 177.10(10) | 171.75(10) |
| N(7)–Pd(1)–N(7A) | 95.76 | 91.39(11) | 96.32(11) |
| Pd(1)–O(1)–C(26) | 114.48 | 111.8(2) | 110.6(2) |
| Pd(1)–O(2)–C(25) | 114.67 | 111.8(2) | 111.5(2) |
| O(1)–C(26)–O(3) | 122.62 | 125.2(3) | 121.1(3) |
| O(2)–C(25)–O(4) | 123.38 | 124.9(3) | 123.0(3) |
| O(1)–C(26)–C(25) | 114.02 | 115.3(3) | 116.3(3) |
| O(2)–C(25)–C(26) | 114.33 | 115.9(3) | 117.4(3) |
| O(3)–C(26)–C(25) | 123.36 | 119.5(3) | 122.5(3) |
| O(4)–C(25)–C(26) | 122.30 | 119.3(3) | 119.6(3) |
| Pd(1)–N(7)–C(5) | 134.37 | 127.9(2) | 135.8(2) |
| Pd(1)–N(7)–C(8) | 118.18 | 126.9(2) | 119.2(2) |
| C(5)–N(7)–C(8) | 106.45 | 105.2(3) | 105.0(3) |
| Pd(1)–N(7A)–C(5A) | 134.31 | 129.8(2) | 129.9(2) |
| Pd(1)–N(7A)–C(8A) | 119.50 | 124.8(2) | 119.6(2) |
| C(5A)–N(7A)–C(8A) | 106.11 | 105.4(3) | 105.3(3) |

### 3.6. Thermal analysis

The TG and DTA methods of a thermal analysis of **1**–**7** indicated two types of thermal behaviour of the complexes **1**–**3** and **4**–**7**. As representatives of both groups, the complexes **3** and **4** were chosen for detailed interpretation and their TG/DTA curves are depicted in Fig. 3. All the important thermal characteristics of the studied complexes are given in Table 5.

The dehydration of **3** began right after the start of the analysis at 28 °C, and this first step is finished at 132 °C. The endothermic effects (*endo*-effects), anticipated for the dehydration process, were found on the DTA curve with minima at 40 and 124 °C. The compound existed in its dehydrated form of $[Pd(ox)(L_3)_2]$ between 132 and 149 °C. Consequently, the decay proceeded in three waves without formation of thermally stable intermediates up to 480 °C. This process is accompanied by two exothermic effects (*exo*-effects) on the DTA curve (Table 5) with maxima at 182, and 368 °C, respectively. A plateau, which may be connected with the formation of a thermally stable intermediate palladium(II) oxide (PdO), occurred on the TG curve from 480 up to 808 °C. The PdO further decomposed to Pd (with the minimum of *endo*-effect at 816 °C), which formed as a final product of the thermal degradation of **3**. No weight changes were observed on the TG curve from 820 °C to the final temperature of the experiment (900 °C). The observed weight losses of described partial processes of the thermal decomposition of **3** differ insignificantly from the calculated ones (Table 5).

The anhydrous complex $[Pd(ox)(L_3)_2]$ (**4**) is thermally stable up to 128 °C (Fig. 3). The process of thermal degradation proceeded from this temperature, with three steps observable on the TG curve, without formation of any thermally stable intermediates up to 544 °C, when it is finished by a formation of PdO. As it is given in Table 5, four *exo*-effects and two *endo*-effects were detected on the DTA curve in connection with this process. The second weak *endo*-effect, whose minimum is lying at 163 °C, is most likely connected with melting and simultaneous decomposition of the complex **4** (melting temperature determined by a melting point apparatus was found to be 164–166 °C). The PdO was thermally stable in the 544–803 °C range. Its decomposition to Pd was observed at 803–837 °C and it was accompanied by *endo*-effect on

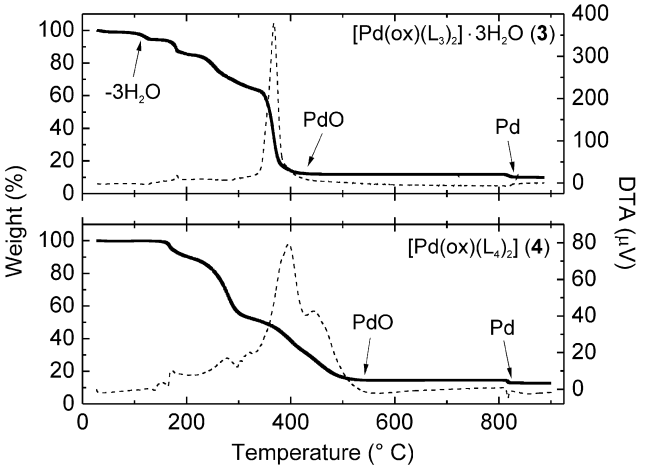


**Fig. 3.** TG/DTA curves of the complexes **3** and **4** as obtained in the dynamic air atmosphere in the 25–900 °C temperature range.

**Table 5**
Results of TG/DTA thermal analyses of the palladium(II) oxalato complexes **1**–**7**.

| Complex | Dehydration | | $[Pd(ox)(L_n)_2]$ | $[Pd(ox)(L_{1-7})_2] \rightarrow PdO$ | | PdO | $PdO \rightarrow Pd$ | | DTA (°C)[d] | |
|---|---|---|---|---|---|---|---|---|---|---|
| | $T$ (°C)[a] | $\Delta m$ (%)[b] | $T$ (°C)[c] | $T$ (°C)[a] | $\Delta m$ (%)[b] | $T$ (°C)[c] | $T$ (°C)[a] | $\Delta m$ (%)[b] | *endo*-effect | *exo*-effect |
| $[Pd(ox)(L_1)_2]\cdot{}^3/_4H_2O$ (**1**) | 61–149 | 1.6/1.6 | | 149–445 | 84.4/83.5 | 445–816 | 816–845 | 1.8/1.8 | 828 | 171, 416 |
| $[Pd(ox)(L_2)_2]\cdot{}^3/_4H_2O$ (**2**) | 28–145 | 1.6/1.5 | | 145–475 | 84.4/83.5 | 475–821 | 821–851 | 1.8/1.6 | 824 | 178, 419 |
| $[Pd(ox)(L_3)_2]\cdot 3H_2O$ (**3**) | 28–145 | 5.6/5.7 | 132–149 | 145–480 | 81.9/82.5 | 480–808 | 808–835 | 1.6/1.6 | 40, 124, 816 | 182, 368 |
| $[Pd(ox)(L_4)_2]$ (**4**) | | | 29–128 | 128–544 | 86.5/85.3 | 544–803 | 803–837 | 1.8/1.6 | 138, 163, 817 | 170, 278, 396, 444 |
| $[Pd(ox)(L_5)_2]$ (**5**) | | | 30–109 | 109–569 | 87.3/86.0 | 569–809 | 809–831 | 1.7/1.7 | 158, 823 | 170, 301, 353, 407 |
| $[Pd(ox)(L_6)_2]\cdot H_2O$ (**6**) | 28–130 | 1.8/1.6 | | 130–578 | 85.7/85.4 | 578–806 | 806–821 | 1.7/1.7 | 156, 815 | 173, 300, 429 |
| $[Pd(ox)(L_7)_2]$ (**7**) | | | 28–133 | 133–552 | 87.3/85.9 | 552–811 | 811–836 | 1.7/1.6 | 164, 825 | 172, 287, 411 |

[a] The temperature range of the corresponding transformation process.
[b] Weight losses; calcd./found.
[c] The temperature range of a thermally stable intermediate.
[d] Positions of minima of endothermic effects (*endo*-effect) and maxima of exothermic effects (*exo*-effect).

the DTA curve with a minimum at 817 °C. A plateau of thermally stable palladium can be seen above 837 °C to the final temperature of 900 °C. Again, the obtained and calculated weight losses correlated well with each other (see Table 5).

### 3.7. In vitro cytotoxicity

Promising *in vitro* cytotoxicity (tested by an AM assay) results of several palladium(II) oxalato complexes with 2-chloro-N6-(benzyl)-9-isopropyladenine-based derivatives against K562 and MCF-7 human cancer cell lines were reported in our previous paper [3]. That is why we decided to test several representatives (namely the complexes **1**, **3**–**5** and **7**) of a new series of palladium(II) oxalato complexes involving mentioned N-donor ligands. However, an MTT assay was used instead of an AM one, which reduces comparability of both groups of results.

The tested complexes showed the following *in vitro* cytotoxic activities against HOS cancer cells: >50.0 μM for **1**, >5.0 μM for **3**, >25.0 μM for **4**, 34.9 ± 11.0 μM for **5**, and 39.2 ± 6.0 μM for **7**. The obtained values were compared with that of platinum-based anticancer drug *Cisplatin*, whose $IC_{50}$ value was found to be 34.2 ± 6.4 μM, as determined by an MTT test. It can be seen that *in vitro* cytotoxicity of tested complexes **5** and **7** is comparable with that of *Cisplatin*. The results presented herein as well as in our previous paper [3] encourage us to continue with the biological testing and to test these complexes by an MTT assay for their *in vitro* cytotoxicity against some other human cancer cell lines, which is currently in progress. Moreover, the DNA interaction study, as well as the *in vivo* testing will be carried out for the palladium(II) oxalato complexes involving N6-(benzyl)-9-isopropyladenine-based derivatives in the near future.

## 4. Conclusions

A series of $[Pd(ox)(L_{1-7})_2]\cdot nH_2O$ (**1**–**7**; $n$ = 0 for **4**, **5** and **7**, ¾ for **1** and **2**, 1 for **6** and 3 for **3**) palladium(II) oxalato complexes was synthesized by reactions of $K_2[Pd(ox)_2]\cdot 2H_2O$ with two molar equivalents of the appropriate $L_{1-7}$ organic compound. The pale yellow powder products were isolated in good yields and characterized by various physical methods. Within the complexes **1**–**7**, compounds **1**–**3** represent analogues of recently published palladium(II) oxalato complexes with 2-chloro-N6-(benzyl)-9-isopropyladenine derivatives [3] similar to $L_{1-3}$ molecules, but with differently substituted benzyl group. On the other hand, we report here the substances **4**–**7** as the first palladium(II) oxalato complexes involving the highly potent CDK inhibitors, namely 2-(1-ethyl-2-hydroxyethylamnio)-N6-(benzyl)-9-isopropyladenine (*Roscovitine*; $L_4$) or its analogues with the substituted benzyl group ($L_{5-7}$), as N-donor carrier ligands.

Based on the obtained results, the complexes **1**–**7** have been characterized as square–planar compounds with the central Pd(II) ion tetra-coordinated by one bidentate O-donor oxalate dianion and two adenine derivatives bound to the metal centre through N7 atoms of their adenine moieties, thus giving a $PdN_2O_2$ chromophore. The prepared complexes **1**, **3**–**5** and **7** were tested *in vitro* for their antitumour activity against human osteosarcoma cancer cell line, HOS. The obtained results showed the complexes **5** and **7** as the substances with *in vitro* cytotoxicity comparable with commercially used platinum-based drug *Cisplatin*.

## Acknowledgements

The financial support from the Ministry of Education, Youth and Sports of the Czech Republic is gratefully acknowledged (a Grant No. MSM6198959218). The authors also thank Mrs. Pavla Richterová for performing CHN elemental analyses, Ms. Radka Novotná for infrared and Raman spectra measurements, Ms. Alena Klanicová for mass spectra measurements and Dr. Radim Vrzal and Prof. Zdeněk Dvořák for *in vitro* cytotoxicity testing.

## Appendix A. Supplementary material

A scheme of the synthetic pathway of $L_{1-7}$ organic compounds, as well as their IR, Raman and NMR ($^1H$, $^{13}C$, $^{15}N$) spectral data, are deposited. Supplementary data associated with this article can be found, in the online version, at doi:10.1016/j.ica.2010.01.035.

## References

[1] P.J. Davies, Plant Hormones, 3rd ed., Springer, Dordrecht, 1997.
[2] M. Gielen, E.R.T. Tiekink, Metallotherapeutic Drugs and Metal-based Diagnostic Agents, Willey, London, 2005.
[3] P. Štarha, Z. Trávníček, I. Popa, J. Inorg. Biochem. 103 (2009) 978.
[4] A. Garoufis, S.K. Hadjikakou, N. Hadjiliadis, Coord. Chem. Rev. 253 (2008) 1384.
[5] Z. Trávníček, L. Szüčová, I. Popa, J. Inorg. Biochem. 101 (2007) 477.
[6] K.I. Lee, T. Tashiro, M. Noji, Chem. Pharm. Bull. 42 (1994) 702.
[7] L. Meijer, A. Borgne, O. Mulner, J.P.J. Chong, J.J. Blow, N. Inagaki, M. Inagaki, J.G. Delcros, J.P. Moulinoux, Eur. J. Biochem. 243 (1997) 527.
[8] K. Torigoe, K. Esumi, Langmuir 9 (1993) 1664.
[9] M. Legraverend, O. Ludwig, E. Bisagni, S. Leclerc, L. Meijer, N. Giocanti, R. Sadri, V. Favaudon, Bioorg. Med. Chem. 7 (1999) 1281.
[10] C.H. Oh, S.C. Lee, K.S. Lee, E.R. Woo, C.Y. Hong, B.S. Yang, D.J. Baek, J.H. Cho, Arch. Pharm. Pharm. Med. Chem. 332 (1999) 187.
[11] J.W. Daly, B.E. Christensen, J. Org. Chem. 21 (1956) 177.
[12] P. Imbach, H.G. Capraro, P. Furet, H. Mett, T. Meyer, J. Zimmermann, Bioorg. Med. Chem. Lett. 9 (1999) 91.
[13] SPARTAN06 (Version 1.1.2), Wavefunction Inc., 18401 Von Karman Avenue, Suite 370, Irvine, CA 92612, USA.
[14] K. Brandenburg, DIAMOND, Release 3.1f, Crystal Impact GbR, Bonn, Germany, 2006.
[15] J. Ulrichová, Z. Dvořák, J. Vičar, J. Lata, J. Smržová, A. Šedo, V. Šimánek, Toxicol. Lett. 125 (2001) 125.

[16] W.J. Geary, Coord. Chem. Rev. 7 (1971) 81.
[17] C.J. Pouchert, The Aldrich Library of Infrared Spectra, 3rd ed., Aldrich Chemical Co., Milwaukee, 1981.
[18] T.A. Mohamed, I.A. Shabaan, W.M. Zoghaib, J. Husband, R.S. Farag, A.E.M.A. Alajhaz, J. Mol. Struct. 938 (2009) 263.
[19] V. Montoya, J. Pons, J. García-Antón, X. Solans, M. Font-Bardia, J. Ros, Inorg. Chim. Acta 360 (2007) 625.
[20] K. Nakamoto, Infrared and Raman Spectra of Inorganic and Coordination Compounds, 5th ed., Willey-Interscience, New York, 1997.
[21] M. Espinal, J. Pons, J. García-Antón, X. Solans, M. Font-Bardia, J. Ros, Inorg. Chim. Acta 361 (2008) 2648.
[22] Z. Dhaouadi, M. Ghomi, J.C. Austin, R.B. Girling, R.E. Hester, P. Mojzes, L. Chinsky, P.Y. Turpin, C. Coulombeau, H. Jobic, J. Tomkinson, J. Phys. Chem. 97 (1993) 1074.

**Supplementary Material**

# Palladium(II) oxalato complexes involving N6-(benzyl)-9-isopropyladenine-based N-donor carrier ligands: synthesis, general properties, $^{1}H$, $^{13}C$ and $^{15}N\{^{1}H\}$ NMR characterization and *in vitro* cytotoxicity

Pavel Štarha, Igor Popa, Zdeněk Trávníček*

*Department of Inorganic Chemistry, Faculty of Science, Palacký University,*

*Tř. 17. listopadu 12, CZ-771 46 Olomouc, Czech Republic*

* Corresponding author. Tel.: +420 585 634 944; fax: +420585 634 954; e-mail: zdenek.travnicek@upol.cz (Zdeněk Trávníček).

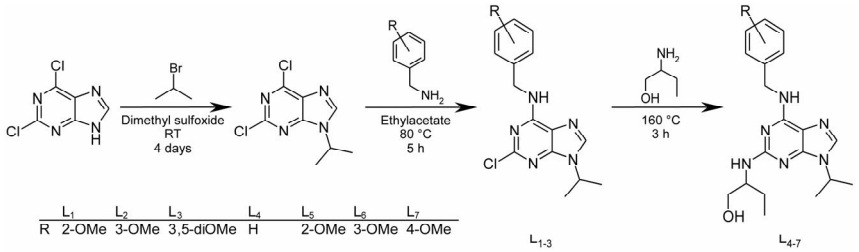


**Scheme 1.** A synthetic pathway for the preparation of the N6-(benzyl)-9-isopropyladenine derivatives $L_{1–7}$.

The results of IR, Raman and $^{1}H$, $^{13}C$ and $^{15}N$ NMR spectroscopy of 2-chloro-N6-(2-methoxybenzyl)-9-isopropyladenine ($L_1$), 2-chloro-N6-(3-methoxybenzyl)-9-isopropyladenine ($L_2$), 2-chloro-N6-(3,5-dimethoxybenzyl)-9-isopropyladenine ($L_3$), 2-(1-ethyl-2-hydroxyethylamino)-N6-(benzyl)-9-isopropyladenine ($L_4$), 2-(1-ethyl-2-hydroxyethylamino)-N6-(2-methoxybenzyl)-9-isopropyladenine ($L_5$), 2-(1-ethyl-2-hydroxyethylamino)-N6-(3-methoxybenzyl)-9-isopropyladenine ($L_6$) and 2-(1-ethyl-2-hydroxyethylamino)-N6-(4-methoxybenzyl)-9-isopropyladenine ($L_7$).

2-chloro-N6-(2-methoxybenzyl)-9-isopropyladenine, $L_1$: IR (Nujol; $cm^{-1}$): 582w, 544w, 529vs, 493s, 446s, 418w, 388w, 343w, 323w. IR (KBr; $cm^{-1}$): 3271s, 3225s, 3149w, 3129s, 3074w, 2976s, 2929w, 2844w, 1633vs, 1600s, 1586s, 1574vs, 1539s, 1493s, 1464s, 1439s, 1423s, 1371s, 1352s, 1311vs, 1291vs, 1244vs, 1223vs, 1201s, 1155s, 1114w, 1098w, 1073s, 1051w, 1025s, 973w, 939w, 916w, 882w, 849w, 814w, 789w, 757vs, 710w, 679w, 660s, 643w, 607w, 528w, 492w, 445w. Raman ($cm^{-1}$): 3125w, 3073w, 3030w, 2979vs, 2943vs, 2846w, 2785w, 2762w, 2723w, 2626w, 1599w, 1578w, 1471s, 1403w, 1356vs, 1318w,

1292w, 1248w, 1166w, 1077w, 1051w, 907w, 880w, 855w, 798w, 769w, 612w, 530w, 465w, 391w, 274w, 199w, 165w. $^{1}$H NMR (DMF-$d_7$; ppm): δ 8.38 (t, 6.8, $N^{6}$H, 1H), 8.30 (s, $C^{8}$H, 1H), 7.28 (d, 8.1, $C^{15}$H, 1H), 7.25 (tt, 8.1, 2.0, $C^{14}$H, 1H), 7.03 (d, 8.4, $C^{12}$H, 1H), 6.89 (d, 8.4, $C^{13}$H, 1H), 4.80 (d, 5.8, $C^{9}$H, 2H), 4.76 (sp, 7.0, $C^{16}$H, 1H), 3.90 (s, $C^{23}$H, 3H), 1.58 (d, 7.0, $C^{17}$H, $C^{18}$H, 6H). $^{13}$C NMR (DMF-$d_7$; ppm): δ 157.90 ($C^{11}$), 156.36 ($C^{6}$), 154.01 ($C^{2}$), 150.52 ($C^{4}$), 140.08 ($C^{8}$), 128.78 ($C^{13}$), 128.14 ($C^{15}$), 127.60 ($C^{10}$), 120.80 ($C^{14}$), 119.75 ($C^{5}$), 111.06 ($C^{12}$), 55.79 ($C^{23}$), 47.92 ($C^{16}$), 39.59 ($C^{9}$), 22.43 ($C^{17}$, $C^{18}$). $^{15}$N NMR (DMF-$d_7$, ppm): δ 240.3 ($N^{7}$), 227.4 ($N^{1}$), 223.9 ($N^{3}$), 178.5 ($N^{9}$), 89.3 ($N^{6}$).

2-Chloro-N6-(3-methoxybenzyl)-9-isopropyladenine, $L_2$: IR (Nujol; cm$^{-1}$): 572s, 552w, 529s, 503w, 470s, 463s, 445w, 410w, 388w, 363w, 342s, 314s, 291w, 269w, 237s, 179vs, 166vs. IR (KBr; cm$^{-1}$): 3266s, 3217w, 3124s, 3066s, 2978vs, 2937vs, 2739s, 2676vs, 2623vs, 2604vs, 2531s, 2497vs, 1623vs, 1571s, 1534s, 1491s, 1475vs, 1445s, 1425s, 1398vs, 1384s, 1342s, 1311vs, 1291s, 1267s, 1247s, 1227vs, 1201s, 1172s, 1149w, 1073w, 1038s, 974w, 930w, 885w, 851w, 807w, 788w, 773w, 723w, 692w, 679w, 660w, 642w, 606w, 572w, 530w, 463w. Raman (cm$^{-1}$): 3122w, 3080w, 3053w, 2999s, 2979vs, 2941vs, 2837w, 2787w, 2763w, 2725w, 2621w, 2497w, 1610w, 1572w, 1464s, 1402w, 1356s, 1313w, 1291w, 1267w, 1248w, 1163w, 1078w, 1036w, 997w, 931w, 904w, 885w, 854w, 800w, 762w, 665w, 627w, 553w, 530w, 461w, 391w, 299w, 256w, 226w, 179w. $^{1}$H NMR (DMF-$d_7$; ppm): δ 8.88 (t, 6.8, $N^{6}$H, 1H), 8.49 (s, $C^{8}$H, 1H), 7.26 (t, 7.8, $C^{14}$H, 1H), 7.08 (t, 1.9, $C^{11}$H, 1H), 7.02 (d, 7.8, $C^{15}$H, 1H), 6.84 (dd, 7.8, $C^{13}$H, 1H), 4.80 (sp, 6.9, $C^{16}$H, 1H), 4.80 (d, 6.6, $C^{9}$H, 2H), 3.79 (s, $C^{23}$H, 3H), 1.59 (d, 6.9, $C^{17}$H, $C^{18}$H, 6H). $^{13}$C NMR (DMF-$d_7$; ppm): δ 160.51 ($C^{12}$), 155.65 ($C^{6}$), 154.33 ($C^{2}$), 150.38 ($C^{4}$), 141.71 ($C^{10}$), 139.87 ($C^{8}$), 130.05 ($C^{14}$), 120.38 ($C^{15}$), 118.50 ($C^{5}$), 114.14 ($C^{11}$), 112.88 ($C^{13}$), 55.44 ($C^{23}$), 48.33 ($C^{16}$), 44.24 ($C^{9}$), 22.33 ($C^{17}$, $C^{18}$). $^{15}$N NMR (DMF-$d_7$, ppm): δ 241.6 ($N^{7}$), 226.1 ($N^{1}$), 223.1 ($N^{3}$), 179.6 ($N^{9}$), 95.6 ($N^{6}$).

2-Chloro-N6-(3,5-dimethoxybenzyl)-9-isopropyladenine, $L_3$: IR (Nujol; cm$^{-1}$): 544vs, 526s, 487w, 459w, 436w, 417w, 387w, 345w, 318w, 214w. IR (KBr; cm$^{-1}$): 3269s, 3225s, 3131w, 3084w, 2977s, 2939w, 2843w, 1644vs, 1600vs, 1577s, 1539s, 1463vs, 1431s, 1422s, 1351vs, 3111vs, 1296vs, 1268w, 1240vs, 1205vs, 1158vs, 1144s, 1102w, 1065s, 1047s, 1015w, 932s, 911s, 881w, 826s, 787w, 735w, 694w, 678w, 665s, 650w, 635w, 604w, 545w. Raman (cm$^{-1}$): 3130w, 3103w, 3014s, 2976vs, 2937vs, 2918vs, 2871w, 2844w, 1595s, 1576s, 1537w, 1479s, 1383s, 1356vs, 1294w, 1232w, 1201w, 1186w, 1163w, 1097w, 1074w, 1043w, 1016w, 993vs, 931w, 908w, 881w, 796s, 731w, 650w, 623w, 604w, 542w, 526w, 484w, 457w, 434w, 391s, 310w, 256s, 229s, 202w, 172s. $^{1}$H NMR (DMF-$d_7$; ppm): δ 8.66 (t, 6.4, $N^{6}$H, 1H), 8.29 (s, $C^{8}$H, 1H), 6.65 (d, 2.2, $C^{11}$H, $C^{15}$H, 2H), 6.42 (d, 2.2, $C^{13}$H, 1H), 4.76 (sp, 6.8, $C^{16}$H, 1H), 4.75 (d, 6.8, $C^{9}$H, 2H), 3.78 (s, $C^{23}$H, $C^{24}$H, 6H), 1.57 (d, 6.8, $C^{17}$H, $C^{18}$H, 6H). $^{13}$C NMR (DMF-$d_7$; ppm): δ 161.66 ($C^{12}$, $C^{14}$), 156.07 ($C^{6}$), 153.91 ($C^{2}$), 150.57 ($C^{4}$), 142.68 ($C^{10}$), 140.10 ($C^{8}$), 119.69 ($C^{5}$), 106.37 ($C^{11}$, $C^{15}$), 99.05 ($C^{13}$), 55.54 ($C^{23}$, $C^{24}$), 47.90 ($C^{16}$), 44.31 ($C^{9}$), 22.40 ($C^{17}$, $C^{18}$). $^{15}$N NMR (DMF-$d_7$, ppm): δ 240.2 ($N^{7}$), 227.6 ($N^{1}$), 224.7 ($N^{3}$), 179.4 ($N^{9}$), 93.9 ($N^{6}$).

2-(1-ethyl-2-hydroxyethylamino)-N6-(benzyl)-9-isopropyladenine ($L_4$): IR (Nujol; cm$^{-1}$): 553vs, 542vs, 531vs, 518s, 490s, 474s, 460vs, 436s, 413w, 371s, 315vs, 303s, 291s, 266s, 240s. IR (KBr; cm$^{-1}$): 3273vs, 3211s, 3084s, 3030s, 2968s, 2914s, 2873, 1608vs, 1546vs, 1485s, 1453vs, 1429s, 1388s, 1376s, 1345s, 1293s, 1263s, 1241s, 1219s, 1166w, 1131w, 1103w, 1070s, 1031w, 976w, 839w, 787s, 745w, 731w, 696s, 638s, 600w, 544w, 531w, 461w. Raman (cm$^{-1}$): 3123w, 3061s, 2968s, 2937s, 2913s, 2875s, 1610vs, 1584w, 1537w, 1475s, 1450w, 1414w, 1378s, 1340w, 1311vs, 1264s, 1215w, 1183w, 1127w, 1100w, 1028w, 1002s, 884w, 842w, 800w, 736w, 706w, 643w, 619w, 593w, 539w, 508w, 459w, 415w, 352w, 296w, 220w, 198w, 172s. $^{1}$H NMR (DMF-$d_7$, ppm): δ 7.79 (s, $C^{8}$H, 1H), 7.72 (br, $N^{6}$H, 1H), 7.45 (dd, 7.8, 2.5, $C^{11}$, $C^{15}$H, 2H), 7.31 (tt, 7.8, 2.5, $C^{12}$, $C^{14}$H, 2H), 7.22 (tt, 7.8,

2.5, $C^{13}H$, 1H), 5.86 (d, 5.9, $N^{2}H$, 1H), 4.78 (br, $C^{9}H$, 2H), 4.75 (br, $O^{20}H$, 1H), 4.61 (sp, 7.0, $C^{16}H$, 1H), 3.97 (sx, 5.5, $C^{19}H$, 1H), 3.66 (m, $C^{20}H^{a}$, 1H), 3.56 (m, $C^{20}H^{b}$, 1H), 1.74 (spsp, 7.4, 0.5, $C^{21}H^{a}$, 1H), 1.58 (spsp, 7.4, 0.5, $C^{21}H^{b}$, 1H), 1.54 (d, 6.8, $C^{17}H$, $C^{18}H$, 6H), 0.93 (t, 7.4, $C^{22}H$, 3H). $^{13}C$ NMR (DMF-$d_7$, ppm): δ 160.27 ($C^{2}$), 155.66 ($C^{6}$), 151.74 ($C^{4}$), 147.75 ($C^{10}$), 135.73 ($C^{8}$), 128.78 ($C^{12}$, $C^{14}$), 128.24 ($C^{11}$, $C^{15}$), 127.19 ($C^{13}$), 114.93 ($C^{5}$), 64.51 ($C^{20}$), 55.29 ($C^{19}$), 46.79 ($C^{16}$), 43.77 ($C^{9}$), 24.91 ($C^{21}$), 22.37 ($C^{17}$), 22.30 ($C^{18}$), 11.03 ($C^{22}$). $^{15}N$ NMR (DMF-$d_7$, ppm): δ 241.1 ($N^{7}$), 198.0 ($N^{1}$), 181.3 ($N^{3}$), 174.3 ($N^{9}$), 93.4 ($N^{2}$), 88.6 ($N^{6}$).

2-(1-ethyl-2-hydroxyethylamino)-N6-(2-methoxybenzyl)-9-isopropyladenine ($L_5$): IR (Nujol; $cm^{-1}$): 581s, 549vs, 532vs, 496vs, 459w, 445s, 422w, 408s, 388w, 368w, 340w, 295vs, 255w. IR (KBr; $cm^{-1}$): 3264vs, 3203s, 315s, 3067s, 2956s, 2927s, 2868s, 2850s, 1601vs, 1538vs, 1491vs, 1459vs, 1437vs, 1424s, 1389s, 1369s, 1352s, 1328s, 1290s, 1240vs, 1170w, 1133w, 1104w, 1068s, 1049w, 1031s, 988w, 970w, 885w, 835w, 788s, 748s, 706w, 638w, 608w, 582w, 550w, 532w, 496w. Raman ($cm^{-1}$): 3269w, 3199w, 3130w, 3069s, 3003w, 2980s, 2963s, 2926vs, 2868s, 2849s, 1603vs, 1543w, 1479s, 1455s, 1422w, 1365s, 1326vs, 1291s, 1239w, 1223w, 1188w, 1160w, 1112w, 1049w, 1029w, 888w, 841w, 771s, 715w, 700w, 647w, 582w, 526w, 458w, 388w, 280w, 262w, 227w, 182s. $^{1}H$ NMR (DMF-$d_7$, ppm): δ 7.80 (s, $C^{8}H$, 1H), 7.34 (dd, 7.5, 1.2, $C^{15}H$, 1H), 7.28 (br, $N^{6}H$, 1H), 7.23 (tt, 7.8, 1.6, $C^{13}H$, 1H), 7.02 (dd, 8.3, 0.8, $C^{12}H$, 1H), 6.87 (tt, 7.5, 0.8, $C^{14}H$, 1H), 5.80 (d, 8.2, $N^{2}H$, 1H), 4.78 (br, $C^{9}H$, 2H), 4.77 (br, $O^{20}H$, 1H), 4.62 (sp, 6.8, $C^{16}H$, 1H), 3.95 (m, $C^{19}H$, 1H), 3.90 (s, $C^{23}H$, 3H), 3.64 (m, $C^{20}H^{a}$, 1H), 3.56 (m, $C^{20}H^{b}$, 1H), 1.72 (spsp, 7.4, 1.2, $C^{21}H^{a}$, 1H), 1.59 (spsp, 7.4, 1.2, $C^{21}H^{b}$, 1H), 1.53 (d, 6.8, $C^{17}H$, $C^{18}H$, 6H), 0.92 (t, 7.4, $C^{22}H$, 3H). $^{13}C$ NMR (DMF-$d_7$, ppm): δ 160.28 ($C^{2}$), 157.88 ($C^{11}$), 155.86 ($C^{6}$), 151.68 ($C^{4}$), 135.75 ($C^{8}$), 128.87 ($C^{10}$), 128.51 ($C^{13}$), 128.45 ($C^{15}$), 120.70 ($C^{14}$), 115.04 ($C^{5}$), 110.88 ($C^{12}$), 64.44 ($C^{20}$), 55.71 ($C^{23}$), 55.26 ($C^{19}$), 46.84 ($C^{16}$), 39.07 ($C^{9}$), 24.91 ($C^{21}$), 22.37 ($C^{17}$), 22.33 ($C^{18}$), 10.99 ($C^{22}$). $^{15}N$ NMR (DMF-$d_7$, ppm): δ 244.4 ($N^{7}$), 201.3 ($N^{1}$), 184.5 ($N^{3}$), 178.1 ($N^{9}$), 98.2 ($N^{2}$), 84.0 ($N^{6}$).

2-(1-ethyl-2-hydroxyethylamino)-N6-(3-methoxybenzyl)-9-isopropyladenine ($L_6$): IR (Nujol; $cm^{-1}$): 555vs, 530w, 497s, 472s, 446w, 430w, 409w, 390w, 368w, 311w, 298w, 268w, 234w. IR (KBr; $cm^{-1}$): 3425s, 3261s, 3209s, 3145w, 3076w, 2965s, 2929s, 2873w, 1604vs, 1543vs, 1490s, 1461s, 1434s, 1416w, 1391w, 1369s, 1350s, 1291w, 1264s, 1222w, 1164w, 1106w, 1064w, 1042w, 975w, 882w, 855w, 787w, 743w, 692w, 668w, 640w, 554w, 472. Raman ($cm^{-1}$): 3265w, 3205w, 3126w, 3068, 3052w, 2993s, 2971s, 2925vs, 2875s, 2853w, 2728w, 1610vs, 1547w, 1476s, 1455s, 1418w, 1394w, 1367s, 1316vs, 1292s, 1264s, 1223w, 1160w, 1107w, 1078w, 1029w, 995vs, 973w, 923w, 88w, 840w, 787w, 747s, 703w, 650w, 584w, 556w, 527w, 495w, 451w, 429w, 407w. $^{1}H$ NMR (DMF-$d_7$, ppm): δ 7.80 (s, $C^{8}H$, 1H), 7.69 (br, $N^{6}H$, 1H), 7.23 (t, 7.8, $C^{14}H$, 1H), 7.07 (s, $C^{11}H$, 1H), 7.02 (d, 7.8, $C^{15}H$, 1H), 6.81 (dd, 8.2, 2.0, $C^{13}H$, 1H), 5.86 (d, 7.0, $N^{2}H$, 1H), 4.76 (br, $O^{20}H$, 1H), 4.75 (br, $C^{9}H$, 2H), 4.61 (sp, 6.7, $C^{16}H$, 1H), 3.97 (sx, 5.5, $C^{19}H$, 1H), 3.77 (s, $C^{23}H$, 3H), 3.68 (m, $C^{20}H^{a}$, 1H), 3.58 (m, $C^{20}H^{b}$, 1H), 1.74 (spsp, 7.4, 1.2, $C^{21}H^{a}$, 1H), 1.58 (spsp, 7.4, 1.2, $C^{21}H^{b}$, 1H), 1.54 (d, 7.0, $C^{17}H$, $C^{18}H$, 6H), 0.93 (t, 7.4, $C^{22}H$, 3H). $^{13}C$ NMR (DMF-$d_7$, ppm): δ 160.41 ($C^{12}$), 160.26 ($C^{2}$), 155.65 ($C^{6}$), 151.80 ($C^{4}$), 143.38 ($C^{10}$), 135.74 ($C^{8}$), 129.79 ($C^{14}$), 120.43 ($C^{15}$), 114.96 ($C^{5}$), 114.03 ($C^{11}$), 112.50 ($C^{13}$), 64.51 ($C^{20}$), 55.36 ($C^{23}$), 55.30 ($C^{19}$), 46.80 ($C^{16}$), 43.75 ($C^{9}$), 24.92 ($C^{21}$), 22.36 ($C^{17}$), 22.33 ($C^{18}$), 11.01 ($C^{22}$). $^{15}N$ NMR (DMF-$d_7$, ppm): δ 239.2 ($N^{7}$), 199.9 ($N^{1}$), 180.7 ($N^{3}$), 173.8 ($N^{9}$), 93.2 ($N^{2}$), 82.9 ($N^{6}$).

2-(1-ethyl-2-hydroxyethylamino)-N6-(4-methoxybenzyl)-9-isopropyladenine ($L_7$): IR (Nujol; $cm^{-1}$): 594s, 569s, 536vs, 525vs, 470w, 454w, 429s, 420s, 364w, 339w, 324s. IR (KBr; $cm^{-1}$): 3279s, 3209s, 3127s, 3070w, 2961s, 2931s, 2874w, 2837w, 1611vs, 1545vs, 1514vs, 1468s, 1419s, 1392s, 1376s, 1350s, 1297w, 1255vs, 1215w, 1181w, 1172w, 1059w, 1034w, 970w, 838w, 817w, 789w, 641w, 536w, 525w, 428w. Raman ($cm^{-1}$): 3293w, 3125w,

3068s, 2976s, 2935vs, 2875s, 2837w, 1608vs, 1549w, 1463s, 1384s, 1351s, 1309vs, 1255s, 1213w, 1172w, 1096w, 848s, 710w, 636w, 595w, 534w, 457w, 418w, 337w. $^{1}$H NMR (DMF-$d_7$, ppm): δ 7.78 (s, $C^{8}H$, 1H), 7.60 (br, $N^{6}H$, 1H), 7.38 (d, 8.0, $C^{12}H$, $C^{14}H$, 2H), 6.88 (d, 8.0, $C^{11}H$, $C^{15}H$, 2H), 5.86 (d, 7.7, $N^{2}H$, 1H), 4.78 (br, $O^{20}H$, 1H), 4.70 (br, $C^{9}H$, 2H), 4.61 (sp, 6.8, $C^{16}H$, 1H), 3.98 (q, 5.9, $C^{19}H$, 1H), 3.77 (s, $C^{23}H$, 3H), 3.67 (m, $C^{20}H^{a}$, 1H), 3.57 (m, $C^{20}H^{b}$, 1H), 1.75 (spsp, 7.7, 1.5, $C^{21}H^{a}$, 1H), 1.58 (m, $C^{21}H^{b}$, 1H), 1.52 (d, 6.8, $C^{17}H$, $C^{18}H$, 6H), 0.95 (t, 7.5, $C^{22}H$, 3H). $^{13}$C NMR (DMF-$d_7$, ppm): δ 160.28 ($C^{2}$), 159.25 ($C^{13}$), 155.62 ($C^{6}$), 151.72 ($C^{4}$), 135.67 ($C^{8}$), 133.63 ($C^{10}$), 129.60 ($C^{12}$, $C^{14}$), 114.95 ($C^{5}$), 114.17 ($C^{11}$, $C^{15}$), 64.57 ($C^{20}$), 55.46 ($C^{23}$), 55.31 ($C^{19}$), 46.79 ($C^{16}$), 43.19 ($C^{9}$), 24.94 ($C^{21}$), 22.37 ($C^{17}$), 22.33 ($C^{18}$), 11.03 ($C^{22}$). $^{15}$N NMR (DMF-$d_7$, ppm): δ 247.0 ($N^{7}$), 202.8 ($N^{1}$), 187.3 ($N^{3}$), 179.7 ($N^{9}$), 100.7 ($N^{2}$), 80.7 ($N^{6}$).

# APPENDIX III

Journal of Inorganic Biochemistry 104 (2010) 639–647

Contents lists available at ScienceDirect

Journal of Inorganic Biochemistry

journal homepage: www.elsevier.com/locate/jinorgbio

# Platinum(II) oxalato complexes with adenine-based carrier ligands showing significant *in vitro* antitumor activity

Pavel Štarha, Zdeněk Trávníček *, Igor Popa

*Department of Inorganic Chemistry, Faculty of Science, Palacký University, Třída 17. listopadu 12, CZ-771 46 Olomouc, Czech Republic*

ARTICLE INFO

*Article history:*
Received 18 January 2010
Received in revised form 16 February 2010
Accepted 19 February 2010
Available online 3 March 2010

*Keywords:*
Platinum(II) complexes
Oxalate
Adenine derivatives
Crystal structures
*In vitro* cytotoxicity

ABSTRACT

[Pt(L)$_2$(ox)] (**1**), [Pt(*2-OMe*L)$_2$(ox)] (**2**), [Pt(*3-OMe*L)$_2$(ox)] (**3**), [Pt(*2,3-diOMe*L)$_2$(ox)] (**4**), [Pt(*2,4-diOMe*L)$_2$(ox)] (**5**), [Pt(*3,4-diOMe*L)$_2$(ox)] (**6**) and [Pt(*3,5-diOMe*L)$_2$(ox)]·4H$_2$O (**7**) platinum(II) oxalato (ox) complexes were synthesized using the reaction of potassium bis(oxalato)platinate(II) dihydrate with 2-chloro-N6-(benzyl)-9-isopropyladenine or its benzyl-substituted analogues (*n*L). The complexes **1**–**7**, which represent the first platinum(II) oxalato complexes involving adenine-based ligands, were fully characterized by various physical methods including multinuclear and two dimensional NMR spectroscopy. A single-crystal X-ray analysis of [Pt(*2,4-diOMe*L)$_2$(ox)]·2DMF (**5**·2DMF; DMF = *N,N′*-dimethylformamide), proved the slightly distorted square–planar geometry in the vicinity of the Pt(II) ion with one bidentate-coordinated oxalate dianion and two adenine derivatives (*n*L) coordinated to the Pt(II) centre through the N7 atom of an adenine moiety, thereby giving a PtN$_2$O$_2$ donor set. *In vitro* cytotoxicity of the prepared complexes was tested by an MTT assay against osteosarcoma (HOS) and breast adenocarcinoma (MCF7) human cancer cell lines. The best results were achieved for the complexes **2** and **5** in the case of both cell lines, whose IC$_{50}$ values equalled 3.6 ± 1.0, and 4.3 ± 2.1 μM (for **2**), and 5.4 ± 3.8, and 3.6 ± 2.1 μM (for **5**), respectively. The IC$_{50}$ equals 9.2 ± 1.5 μM against MCF7 cells in the case of **1**. The *in vitro* cytotoxicity of the mentioned complexes significantly exceeded commercially used platinum-based anticancer drugs cisplatin (34.2 ± 6.4 μM and 19.6 ± 4.3 μM) and oxaliplatin (>50.0 μM for both cancer cell lines).



## 1. Introduction

Platinum(II) oxalato complexes are an important group of compounds mainly due to (*1R,2R*-diaminocyclohexane)oxalatoplatinum(II) complex (oxaliplatin), which belongs, together with *cis*-diamminedichloridoplatinum(II) complex (cisplatin), diammine-1,1′-cyclobutanedicarboxylatoplatinum(II) complex (carboplatin), diammine-glycolatoplatinum(II) complex (nedaplatin) and (1,2-diaminomethylcyclobutane)lactatoplatinum(II) complex (lobaplatin), to the group of the platinum-based drugs recently used in treatment of cancer [1–3].

Since the discovery of oxaliplatin and its anticancer properties [4], plenty of its derivatives have been prepared and tested for their both *in vitro* and *in vivo* cytotoxicity. Basically, the platinum(II) oxaliplatin derivatives can be divided into two groups. The first one involves dach-based platinum(II) complexes containing various isomers and derivatives of 1,2-diaminocyclohexane (dach) as N-donor carrier ligands, while a leaving group differs from the oxalate dianion [5–7]. The second one comprises the platinum(II) oxalato complexes with bidentate oxalate dianion as a leaving group, and on the other hand, the carrier N-donor ligand differs from dach [8–13]. The prepared complexes **1**–**7** belong to the second group of the oxaliplatin derivatives. Moreover, compounds **1**–**7** represent the first platinum(II) oxalato complexes of the PtN$_2$(ox) motive involving an adenine derivative as an N-donor carrier ligand (SciFinder Scholar, 2004 ed.; Cambridge Structural Database ver. 5.30, September 2009 update [14]).

The oxalate dianion, together with the chloride anions, had been predicted by Cleare and Hoeschele to be a suitable leaving group of platinum(II) complexes [15]. This hypothesis was proven by the studies of the platinum(II) oxalato complexes involving dach [16], *trans*-3,4-diamino-2,2,6,6-tetramethylpiperidine-l-oxyl [9], or 1-methyl-4-(methylamino)piperidine [10], where the platinum(II) oxalato complexes showed higher *in vitro* cytotoxic activity compared to the analogues with a different leaving group.

Except for the mentioned platinum(II) oxalato complexes, several platinum(II) compounds of a different type have been recently prepared and tested for their *in vitro* cytotoxicity. Among them, [Pt(dpaOH)$X_2$] complexes ($X_2$ = 2Cl$^-$, ox, malonate, cyclobutane-1,1′-dicarboxylate or 3-hydroxycyclobutane-1,1′-dicarboxylate; dpaOH = 2-hydroxy-1,3-diaminopropane) showed higher *in vitro* cytotoxicity against the gastric cancer cell line (SGC-7901), human prostate cancer cell line (LNcap) cancer cells and both sensitive and resistant human lung cancer cell line (A549 and A549/ATCC) as compared to carboplatin [17]. The complex *trans*-[Pt(tce)$_2$(pta)$_2$], involving the thiocarbamate ester of the SC

* Corresponding author. Tel.: +420 585 634 352; fax: +420585 634 954.
*E-mail address:* zdenek.travnicek@upol.cz (Z. Trávníček).

0162-0134/$ – see front matter © 2010 Elsevier Inc. All rights reserved.
doi:10.1016/j.jinorgbio.2010.02.005

(OMe) = $NC_6H_4Cl$ composition (tce) and 1,3,5-triaza-7-phosphaadamantane (pta), was determined to be more active than cisplatin against human ovarian carcinoma cells (SK-OV-3) and human colon carcinoma (HT29) [18]. In the case of [Pt(pyrr)$Cl_2$] complex, where pyrr stands for both 2(S)-aminomethylpyrrolidine and 2(R)-aminomethylpyrrolidine enantiomers, the *in vitro* cytotoxicity against human ovarian carcinoma cells (A2780) is comparable with cisplatin, while it was determined as higher than that of cisplatin against A2780R cells (a cisplatin-resistant counterpart of A2780) [19]. Finally, spermidine-bridged dinuclear platinum(II) complexes represent an alternative to the known platinum-based drugs, since these compounds showed promising biological properties (*in vitro* cytotoxicity testing against ovarian carcinoma cells both sensitive and resistant to cisplatin) [20].

Recently, platinum(II) and platinum(IV) complexes involving N6-(benzyl)adenine-based N-donor ligands have been synthesized and their *in vitro* cytotoxic activity has been evaluated against several human cancer cell lines (lit. [21,22] and the references cited therein). The best results have been obtained for *cis*-[Pt(ros)$_2$$Cl_2$] in the case of the malignant melanoma (G-361), osteosarcoma (HOS) and chronic myelogenous leukaemia (K562) human cancer cell lines, with the $IC_{50}$ values of 1.0 μM against the mentioned cells [23]; ros stands for cyclin dependent kinases (CDK) inhibitor 2-[(*R*)-(1-ethyl-2-hydroxyethylamino)]-N6-(benzyl)-9-isopropyladenine (*R*-roscovitine) [24]. *R*-roscovitine, cisplatin and oxaliplatin have not been found as cytotoxic as the mentioned platinum(II) complex, since their $IC_{50}$ equalled 19.0, 20.0, and 50.0 μM for *R*-roscovitine, 3.0, 3.0 and 5.0 μM for cisplatin, and 7.0, 7.0 and 8.0 μM for oxaliplatin, respectively.

This work describes the platinum(II) oxalato complexes, [Pt(*n*L)$_2$(ox)]·*n*$H_2O$ (**1**–**7**; *n* = 0 for **1**–**6** and *n* = 4 for **7**), involving the adenine-based N-donor ligands: 2-chloro-N6-(benzyl)-9-isopropyladenine (L; complex **1**), 2-chloro-N6-(2-methoxybenzyl)-9-isopropyladenine (*2-OMe*L; **2**), 2-chloro-N6-(3-methoxybenzyl)-9-isopropyladenine (*3-OMe*L; **3**), 2-chloro-N6-(2,3-dimethoxybenzyl)-9-isopropyladenine (*2,3-diOMe*L; **4**), 2-chloro-N6-(2,4-dimethoxybenzyl)-9-isopropyladenine (*2,4-diOMe*L; **5**), 2-chloro-N6-(3,4-dimethoxybenzyl)-9-isopropyladenine (*3,4-diOMe*L; **6**) and 2-chloro-N6-(3,5-dimethoxybenzyl)-9-isopropyladenine (*3,5-diOMe*L; **7**). The complexes **1**–**7** have been prepared by a synthetic method using potassium bis(oxalato)platinate(II) dihydrate, $K_2$[Pt(ox)$_2$]·$2H_2O$, reacting with the corresponding organic molecule (Scheme 1). The molecular structure of [Pt(*2,4-diOMe*L)$_2$(ox)]·2DMF (**5**·2DMF; DMF = *N,N′*-dimethylformamide) has been determined by a single-crystal X-ray analysis, which proved a slightly distorted square–planar geometry in the vicinity of the Pt(II) centre. *In vitro* cytotoxic activity of the complexes **1**–**7** has been tested against the osteosarcoma (HOS) and breast adenocarcinoma (MCF7) human cancer cell lines. The $IC_{50}$ values showed promising cytotoxicity for the prepared platinum(II) oxalato complexes, which are in the case of the complexes **1**, **2** and **5** even better as compared to cisplatin and oxaliplatin.

## 2. Experimental section

### 2.1. Starting materials

Chemicals and solvents were used as received from commercial sources (Sigma-Aldrich Co., Acros Organics Co., Lachema Co. and Fluka Co.). DMSO was dried using $MgSO_4$. Organic compounds 2-chloro-N6-(benzyl)-9-isopropyladenine (L), 2-chloro-N6-(2-methoxybenzyl)-9-isopropyladenine (*2-OMe*L), 2-chloro-N6-(3-methoxybenzyl)-9-isopropyladenine (*3-OMe*L), 2-chloro-N6-(2,3-dimethoxybenzyl)-9-isopropyladenine (*2,3-diOMe*L), 2-chloro-N6-(2,4-dimethoxybenzyl)-9-isopropyladenine (*2,4-diOMe*L), 2-chloro-N6-(3,4-dimethoxybenzyl)-9-isopropyladenine (*3,4-diOMe*L) and 2-chloro-N6-(3,5-dimethoxybenzyl)-9-isopropyladenine (*3,5-diOMe*L) were prepared following formerly reported procedure (Scheme 1) [25], and characterized by elemental analysis, IR, Raman and NMR spectroscopies (summarized in Appendix A in Supplementary material).

### 2.2. General physical measurements

Elemental analyses were performed on a Flash EA-1112 Elemental Analyzer (Thermo Finnigan). Conductivity measurements of $10^{-3}$ M

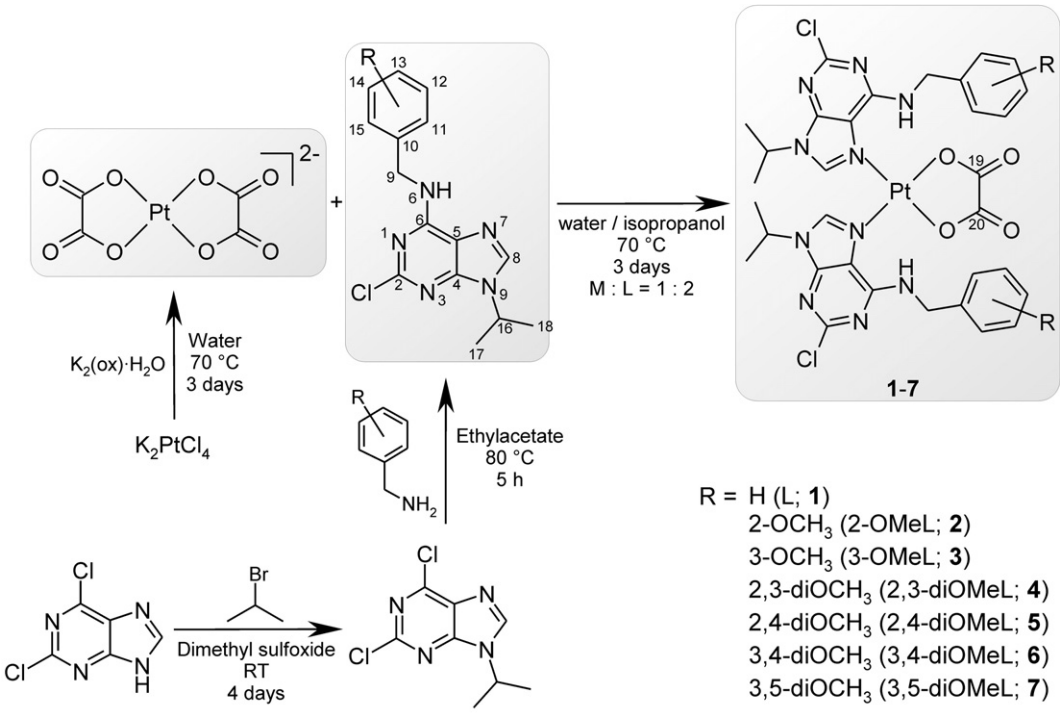


**Scheme 1.** A representation of the synthetic pathways leading to the preparation of the complexes **1**–**7**.

DMF solutions were done using a Cond 340i/SET (WTW) conductometer at a temperature of 25 °C. IR spectra were recorded on a Nexus 670 FT-IR spectrometer (Thermo Nicolet) in the 400–4000 $cm^{-1}$ (KBr pellets) and 150–600 $cm^{-1}$ (Nujol technique) regions. Raman spectroscopy measurements were performed using an NXR FT-Raman Module (Thermo Nicolet) in the 150–3750 $cm^{-1}$ region. The reported IR and Raman signal intensities have been defined as w = weak, s = strong and vs = very strong. Mass spectra (MS) of the methanol solutions of **1**–**7** were obtained by an LCQ Fleet ion trap mass spectrometer by the positive mode electrospray ionization (ESI+) technique (Thermo Scientific). The theoretic values were calculated by QualBrowser software (version 2.0.7, Thermo Fischer Scientific). Simultaneous thermogravimetric (TG) and differential thermal (DTA) analyses were performed using an Exstar TG/DTA 6200 thermal analyzer (Seiko Instruments Inc.) in a ceramic crucible in dynamic air atmosphere (150 mL $min^{-1}$) from laboratory temperature to 700 °C (gradient 2.5 °C $min^{-1}$). Melting point determinations were performed on a Melting Point B-540 apparatus (Büchi) with 5 °C $min^{-1}$ gradient, and the obtained values were uncorrected.

### 2.3. NMR measurements

$^{1}H$, $^{13}C$ and $^{195}Pt$ NMR spectra and 2D correlation experiments ($^{1}H$–$^{1}H$ gs-COSY, $^{1}H$–$^{13}C$ gs-HMQC, $^{1}H$–$^{13}C$ gs-HMBC and $^{1}H$–$^{15}N$ gs-HMBC; gs = gradient selected, COSY = correlation spectroscopy, HMQC = heteronuclear multiple quantum coherence and HMBC = heteronuclear multiple bond coherence) of the DMF-$d_7$ solutions were measured at 300 K on a Varian 400 device at 400.00 MHz ($^{1}H$; **2**–**7**), 100.58 MHz ($^{13}C$; **2**–**7**), 40.53 MHz ($^{15}N$; **2**–**7**) and 86.00 MHz ($^{195}Pt$; **2**–**7**) and on a Bruker Avance 300 device at 300.00 MHz ($^{1}H$), 75.43 MHz ($^{13}C$), 30.40 MHz ($^{15}N$) and 64.50 MHz ($^{195}Pt$) for **1**. $^{1}H$ and $^{13}C$ spectra were calibrated against the signals of tetramethylsilane ($Me_4Si$). $^{195}Pt$ NMR was adjusted against potassium hexachloroplatinate, $K_2[PtCl_6]$, in $D_2O$ found at 0 ppm. $^{1}H$–$^{15}N$ gs-HMBC experiments were obtained at natural abundance and calibrated against the residual signals of the DMF adjusted to 104.7 ppm. The splitting of proton resonances in the reported proton spectra is defined as s = singlet, d = doublet, t = triplet, sp = septuplet, dd = doublet of doublets, tt = triplet of triplets and m = multiplet.

### 2.4. Single-crystal X-ray analysis of [Pt(2,4-diOMeL)$_2$(ox)]·2DMF (**5**·2DMF)

X-ray measurements of selected crystals of **5**·2DMF were collected on an Xcalibur™2 diffractometer (Oxford Diffraction Ltd.) with Sapphire2 CCD detector, and with Mo Kα (Monochromator Enhance, Oxford Diffraction Ltd.) and at 110 K. Data collection and reduction were performed using CrysAlis software (Version 1.171.32.11) [26]. The same software was used for data correction for an absorption effect by the empirical absorption correction using spherical harmonics, implemented in SCALE3 ABSPACK scaling algorithm. The structure was solved by direct methods using SHELXS-97 [27] and refined on $F^2$ using the full-matrix least-squares procedure (SHELXL-97). Non-hydrogen atoms were refined anisotropically and hydrogen atoms were located in a difference map and refined by using the riding model with C–H = 0.95 and 0.99 Å, N–H = 0.88 Å and $U_{iso}(H) = 1.2U_{eq}(CH, CH_2, NH)$ or $1.5U_{eq}(CH_3)$. A part of one DMF molecule of crystallization was refined as disordered over two positions with the occupancy factors for the corresponding components of 53%, and 47%, respectively. The crystal data and structure refinements are given in Table 1. The molecular graphics as well as additional structural calculations were drawn and interpreted using DIAMOND [28].

**Table 1**
Crystal data and structure refinement for **5**·2DMF.

| | |
|---|---|
| Empirical formula | $C_{42}H_{54}Cl_2N_{12}O_{10}Pt$ |
| Formula weight | 1152.96 |
| Temperature (K) | 110(2) |
| Wavelength (Å) | 0.71073 |
| Crystal system, space group | Orthorhombic, $P_{bca}$ |
| Unit cell dimensions | |
| $a$ (Å) | 22.9961(7) |
| $b$ (Å) | 14.9474(6) |
| $c$ (Å) | 27.3667(9) |
| $\alpha$ (°) | 90.00 |
| $\beta$ (°) | 90.00 |
| $\gamma$ (°) | 90.00 |
| $V$ (Å$^3$) | 9406.8(6) |
| $Z$, $D_{calc}$ (g $cm^{-3}$) | 8, 1.628 |
| Absorption coefficient ($mm^{-1}$) | 3.166 |
| Crystal size (mm) | 0.30×0.30×0.25 |
| $F$ (000) | 4656 |
| $\theta$ range for data collection (°) | $2.69 \le \theta \le 25.00$ |
| Index ranges ($h$, $k$, $l$) | $-27 \le h \le 26$<br>$-17 \le k \le 16$<br>$-32 \le l \le 32$ |
| Reflections collected/unique ($R_{int}$) | 75679/8275 (0.0226) |
| Data/restraints/parameters | 8275/0/646 |
| Goodness-of-fit on $F^2$ | 1.186 |
| Final $R$ indices [$I>2\sigma(I)$] | $R_1 = 0.0265$, $wR_2 = 0.0532$ |
| $R$ indices (all data) | $R_1 = 0.0412$, $wR_2 = 0.0557$ |
| Largest peak and hole (e Å$^{-3}$) | 1.055, −0.601 |

### 2.5. In vitro cytotoxicity testing

*In vitro* cytotoxic activity of the prepared platinum(II) complexes was determined against the human osteosarcoma (HOS; ECACC No. 87070202) and human breast adenocarcinoma (MCF7; ECACC No. 86012803) cancer cell lines by an MTT assay [MTT = 3-(4,5-dimethylthiazol-2-yl)-2,5-diphenyltetrazolium bromide]. The suspension of $2.5 \times 10^4$ cells/well was stabilized in culture medium enriched by fetal calf serum in 96-well microplates (16 h, 37 °C, 5% $CO_2$ atmosphere). The medium was replaced by a fresh one containing DMF solutions of **1**–**7** up to a concentration of 50 μM (complexes were dissolved in DMF and then diluted with cell culture medium to the final DMF concentration of 0.1%). After incubation lasting 24 h, the cells were washed (sterile phosphate buffered saline, PBS) and incubated with MTT (100 μL; 0.3 mg $mL^{-1}$) for 2 h. Thereafter, the medium including dissolved tested complexes was removed and 100 μL of DMSO with 1% $NH_3$ were added to dissolve the purple formazane. The absorbance of formazane solution was measured at 630 nm with an automatic microplate ELISA reader. The discussed results expressed as $IC_{50}$ values represent an arithmetic mean. *Note:* DMSO, a solvent usually used during *in vitro* cytotoxicity testing, was not used because of its well-known ability to coordinate the Pt(II) ion which could lead to the replacement of *n*L ligands in the tested platinum(II) complexes. For that reason, all the prepared complexes as well as cisplatin and oxaliplatin were tested using DMF instead of DMSO.

### 2.6. Synthesis of potassium bis(oxalato)platinate(II) dihydrate, $K_2[Pt(ox)_2]\cdot 2H_2O$

$K_2[Pt(ox)_2]\cdot 2H_2O$ was prepared using a modification of a formerly described method [29] as follows: to a solution of $K_2[PtCl_4]$ (5 mmol) in 20 mL of hot distilled water (70 °C), 25 mmol of potassium oxalate monohydrate, $K_2(ox)\cdot H_2O$, was added. The mixture was stirred at 70 °C for 3 days. The light green powder product was filtered off, washed with hot, and cold distilled water, and re-crystallized from hot (70 °C) distilled water. Green needle-like crystals of $K_2[Pt(ox)_2]\cdot 2H_2O$ which formed, were filtered off, and washed with cold distilled water and ethanol, and dried in the air at 40 °C.

Yield: 80%. Anal. Calcd for $C_4O_8K_2Pt \cdot 2H_2O$: C, 9.9; H, 0.8. Found: C, 10.1; H, 0.9%. IR ($\nu_{Nujol}/cm^{-1}$): $\nu$(PtO), 568 m. IR ($\nu_{KBr}/cm^{-1}$): $\nu(OH_w)$, 3563 s, 3479 s; $\nu(CO_{ox})$, 1709vs, 1673vs, 1386vs, 1235 s, 901 m, 826 s; $\nu$(PtO), 570 s. Raman ($cm^{-1}$): $\nu(OH_w)$, 3480w; $\nu(CO_{ox})$, 1708vs, 1672 m, 1395vs, 1251w, 908w, 843w; $\nu$(PtO), 577w. $^{13}$C NMR (75.43 MHz, $D_2O$, ppm): $\delta$ ($SiMe_4$) 167.87 (C19, C20).

### 2.7. Synthesis of [Pt(L)$_2$(ox)] (**1**), [Pt(2-OMeL)$_2$(ox)] (**2**), [Pt(3-OMeL)$_2$(ox)] (**3**), [Pt(2,3-diOMeL)$_2$(ox)] (**4**), [Pt(2,4-diOMeL)$_2$(ox)] (**5**), [Pt(3,4-diOMeL)$_2$(ox)] (**6**) and [Pt(3,5-diOMeL)$_2$(ox)]·4H$_2$O (**7**)

The distilled water solution (20 mL, 50 °C) of $K_2[Pt(ox)_2] \cdot 2H_2O$ (1 mmol) was added to an *iso*propanol solution (20 mL, 50 °C) of the corresponding 2-chloro-N6-(benzyl)-9-isopropyladenine derivative (*n*L; 2 mmol). The reaction mixture was stirred at 70 °C for 3 days (see Scheme 1). Light grey solid formed gradually during this period. It was filtered off, washed with hot (5 mL, 50 °C) and cold (5 mL, 20 °C) distilled water, and hot (5 mL, 50 °C) and cold (5 mL, 20 °C) *iso*propanol. The product was dried in the air at 40 °C. In the case of **5**, crystals of [Pt(*2,4-diOMe*L)$_2$(ox)]·2DMF (**5**·2DMF), suitable for a single-crystal X-ray analysis, were obtained by re-crystallization of **5** from hot (70 °C) DMF during two weeks.

[Pt(L)$_2$(ox)] (**1**). Yield: 56%. mp 295–297 °C (decomp.). Anal. Calcd for $C_{32}H_{32}N_{10}O_4Cl_2Pt$: C, 43.4; H, 3.6; N, 15.8. Found: C, 43.0; H, 3.5; N, 15.5%. TG/DTA data: decomposition began at 230 and finished at 574 °C with a weight loss of 77.4% (calc. to PtO residue: 76.2%), endothermic peaks at 292 °C and 294 °C and exothermic peaks at 380, 462, 487 and 507 °C. $\Lambda_M$ (DMF solution, S cm$^2$ mol$^{-1}$): 0.4. ESI+ mass spectra (methanol): *m/z* 302.3 (calc. 302.1) $[L+H]^+$. IR ($\nu_{Nujol}/cm^{-1}$): $\nu$(PtO), 570vs; $\nu$(PtN), 541vs. IR ($\nu_{KBr}/cm^{-1}$): $\nu(CH_{ar})$, 3102w, 3063w; $\nu(CH_{aliph})$, 2981w, 2937w, 2881w; $\nu(CO_{ox})$, 1713 s, 1672 m; $\nu$(CN), 1618vs; $\nu(CC_{phen})$, 1540w, 1488 s; $\nu$(CCl), 1164w; $\nu$(PtO), 572w; $\nu$(PtN), 542w. Raman ($cm^{-1}$): $\nu(CH_{ar})$, 3061 s; $\nu(CH_{aliph})$, 2983 m, 2943 m; $\nu(CO_{ox})$, 1700 m, 1672w; $\nu$(CN), 1606w; $\nu(CC_{phen})$, 1541w, 1487 m; $\nu$(CCl), 1159w; $\nu$(PtO), 569 s. $^1$H NMR (300.00 MHz, DMF-$d_7$, ppm): $\delta$ ($SiMe_4$) 9.14 (t, 6.2, N6H, 1H), 9.00 (s, C8H, 1H), 7.48 (dd, 8.1, 1.6, C11H, C15H, 2H), 7.29 (m, C12H, C13H, C14H, 3H), 4.89 (d, 6.4, C9H, 2H), 4.84 (sp, 6.8, C16H, 1H), 1.57 (d, 6.8, C17H, C18H, 6H). $^{13}$C NMR (75.43 MHz, DMF-$d_7$, ppm): $\delta$ ($SiMe_4$) 165.94 (C19, C20), 155.23 (C6), 153.96 (C2), 149.94 (C4), 144.31 (C8), 139.27 (C10), 129.00 (C12, C14), 128.16 (C11, C15), 127.62 (C13), 116.87 (C5), 49.84 (C16), 45.07 (C9), 21.99 (C17, C18). $^{15}$N NMR (30.40 MHz, DMF-$d_7$, ppm): $\delta$ (DMF-$d_7$) 232.2 (N1), 224.3 (N3), 185.5 (N9), 128.2 (N7), 99.1 (N6). $^{195}$Pt NMR (64.50 MHz, DMF-$d_7$, ppm): $\delta$ ($K_2PtCl_6$) −1685.

[Pt(*2-OMe*L)$_2$(ox)] (**2**). Yield: 55%. mp 235–237 °C (decomp.). Anal. Calcd for $C_{34}H_{36}N_{10}O_6Cl_2Pt$: C, 43.1; H, 3.8; N, 14.8. Found: C, 42.8; H, 3.9; N, 14.4%. TG/DTA data: decomposition began at 219 °C and finished at 456 °C with a weight loss of 78.6% (calc. to PtO residue: 77.7%), endothermic peak at 234 °C and exothermic peaks at 238, 264, 334 and 415 °C. $\Lambda_M$ (DMF solution, S cm$^2$ mol$^{-1}$): 0.1. ESI+ mass spectra (methanol): *m/z* 332.3 (calc. 332.1) $[2\text{-}OMeL+H]^+$, 947.0 (947.2) $[Pt(2\text{-}OMeL)_2(ox)+H]^+$, 969.1 (969.2) $[Pt(2\text{-}OMeL)_2(ox)+Na]^+$. IR ($\nu_{Nujol}/cm^{-1}$): $\nu$(PtO), 565vs; $\nu$(PtN), 542vs. IR ($\nu_{KBr}/cm^{-1}$): $\nu(CH_{ar})$, 3109w, 3057w; $\nu(CH_{aliph})$, 2980w, 2939w, 2832w; $\nu(CO_{ox})$, 1723vs, 1670 m; $\nu$(CN), 1621vs; $\nu(CC_{phen})$, 1540w, 1492 m; $\nu$(CCl), 1165w; $\nu$(PtO), 575w. Raman ($cm^{-1}$): $\nu(CH_{ar})$, 3130w, 3065 m; $\nu(CH_{aliph})$, 2988 m, 2937 m, 2881w, 2838w; $\nu(CO_{ox})$, 1710w, 1674w; $\nu$(CN), 1602w; $\nu(CC_{phen})$, 1540w, 1485w; $\nu$(CCl), 1164w; $\nu$(PtO), 574w. $^1$H NMR (400.00 MHz, DMF-$d_7$, ppm): $\delta$ ($SiMe_4$) 8.95 (s, C8H, 1H), 8.93 (t, 6.2, N6H, 1H), 7.35 (dd, 7.6, 1.5, C15H, 1H), 7.28 (tt, 7.7, 1.6, C13H, 1H), 7.05 (d, 7.8, C12H, 1H), 6.85 (t, 7.3, C14H, 1H), 4.87 (d, 6.3, C9H, 2H), 4.84 (sp, 6.9, C16H, 1H), 3.92 (s, C21H, 3H), 1.55 (d, 6.9, C17H, C18H, 6H). $^{13}$C NMR (100.58 MHz, DMF-$d_7$, ppm): $\delta$ ($SiMe_4$) 165.69 (C19, C20), 157.92 (C11), 155.33 (C6), 154.07 (C2), 149.91 (C4), 144.33 (C8), 129.05 (C13), 128.43 (C15), 126.58 (C10), 120.97 (C14), 116.88 (C5), 111.14 (C12), 55.93 (C21), 49.81 (C16), 40.57 (C9), 21.99 (C17, C18). $^{15}$N NMR (40.53 MHz, DMF-$d_7$, ppm): $\delta$ (DMF-$d_7$) 231.2 (N1), 223.1 (N3), 185.5 (N9), 128.7 (N7), 97.0 (N6). $^{195}$Pt NMR (86.00 MHz, DMF-$d_7$, ppm): $\delta$ ($K_2PtCl_6$) −1691.

[Pt(*3-OMe*L)$_2$(ox)] (**3**). Yield: 48%. mp 223–224 °C (decomp.). Anal. Calcd for $C_{34}H_{36}N_{10}O_6Cl_2Pt$: C, 43.1; H, 3.8; N, 14.8. Found: C, 43.3; H, 3.9; N, 14.5%. TG/DTA data: decomposition began at 206 °C and finished at 490 °C with a weight loss of 78.6% (calc. to PtO residue: 77.7%), endothermic peak at 222 °C and exothermic peaks at 226, 333 and 433 °C. $\Lambda_M$ (DMF solution, S cm$^2$ mol$^{-1}$): 1.7. ESI+ mass spectra (methanol): *m/z* 332.2 (calc. 332.1) $[3\text{-}OMeL+H]^+$, 946.9 (947.2) $[Pt(3\text{-}OMeL)_2(ox)+H]^+$, 969.1 (969.2) $[Pt(3\text{-}OMeL)_2(ox)+Na]^+$. IR ($\nu_{Nujol}/cm^{-1}$): $\nu$(PtO), 572vs; $\nu$(PtN), 538 s. IR ($\nu_{KBr}/cm^{-1}$): $\nu(CH_{ar})$, 3103w, 3059w; $\nu(CH_{aliph})$, 2980w, 2939w, 2837w; $\nu(CO_{ox})$, 1706 s, 1673 m; $\nu$(CN), 1615vs; $\nu(CC_{phen})$, 1540w, 1488 m; $\nu$(CCl), 1162w; $\nu$(PtO), 572w; $\nu$(PtN), 540w. Raman ($cm^{-1}$): $\nu(CH_{ar})$, 3057 m; $\nu(CH_{aliph})$, 2990 m, 2943 m, 2841w; $\nu(CO_{ox})$, 1698 m, 1668w; $\nu$(CN), 1606 m; $\nu(CC_{phen})$, 1541w, 1485 m; $\nu$(CCl), 1165w; $\nu$(PtO), 569w; $\nu$(PtN), 534w. $^1$H NMR (400.00 MHz, DMF-$d_7$, ppm): $\delta$ ($SiMe_4$) 9.15 (t, 6.7, N6H, 1H), 9.03 (s, C8H, 1H), 7.22 (t, 8.2, C14H, 1H), 7.05 (d, 8.2, C15H, 1H), 7.04 (s, C11H, 1H), 6.84 (dd, 8.2, 2.6, C13H, 1H), 4.87 (d, 6.3, C9H, 2H), 4.83 (sp, 6.8, C16H, 1H), 3.81 (s, C21H, 3H), 1.56 (d, 6.8, C17H, C18H, 6H). $^{13}$C NMR (100.58 MHz, DMF-$d_7$, ppm): $\delta$ ($SiMe_4$) 165.92 (C19, C20), 160.50 (C12), 155.19 (C6), 153.93 (C2), 149.94 (C4), 144.21 (C8), 140.89 (C10), 130.04 (C14), 120.32 (C15), 116.83 (C5), 113.61 (C11), 113.20 (C13), 55.50 (C21), 49.76 (C16), 45.02 (C9), 22.01 (C17, C18). $^{15}$N NMR (40.53 MHz, DMF-$d_7$, ppm): $\delta$ (DMF-$d_7$) 232.7 (N1), 224.6 (N3), 185.0 (N9), 127.6 (N7), 98.5 (N6). $^{195}$Pt NMR (86.00 MHz, DMF-$d_7$, ppm): $\delta$ ($K_2PtCl_6$) −1689.

[Pt(*2,3-diOMe*L)$_2$(ox)] (**4**). Yield: 62%. mp 223–224 °C (decomp.). Anal. Calcd for $C_{36}H_{40}N_{10}O_8Cl_2Pt$: C, 43.0; H, 4.0; N, 13.9. Found: C, 42.9; H, 4.0; N, 13.5%. TG/DTA data: decomposition began at 206 °C and finished at 447 °C with a weight loss of 79.1% (calc. to PtO residue: 79.0%), endothermic peak at 222 °C and exothermic peaks at 227 and 381 °C. $\Lambda_M$ (DMF solution, S cm$^2$ mol$^{-1}$): 1.9. ESI+ mass spectra (methanol): *m/z* 362.2 (calc. 362.1) $[2,3\text{-}diOMeL+H]^+$, 646.0 (646.1) $[Pt(2,3\text{-}diOMeL)(ox)+H]^+$, 1007.0 (1007.2) $[Pt(2,3\text{-}diOMeL)_2(ox)+H]^+$, 1029.1 (1029.2) $[Pt(2,3\text{-}diOMeL)_2(ox)+Na]^+$. IR ($\nu_{Nujol}/cm^{-1}$): $\nu$(PtO), 574vs; $\nu$(PtN), 538 m. IR ($\nu_{KBr}/cm^{-1}$): $\nu(CH_{ar})$, 3118w, 3063w; $\nu(CH_{aliph})$, 2980w, 2938w, 2835w; $\nu(CO_{ox})$, 1722 s, 1670 m; $\nu$(CN), 1621vs; $\nu(CC_{phen})$, 1539w, 1483 s; $\nu$(CCl), 1169w; $\nu$(PtO), 574w; $\nu$(PtN), 540w. Raman ($cm^{-1}$): $\nu(CH_{ar})$, 3086 m, 3053 m; $\nu(CH_{aliph})$, 2983 m, 2936 s, 2883 m, 2837 m; $\nu(CO_{ox})$, 1710 m, 1675 m; $\nu(CC_{phen})$, 1543 m, 1489 s; $\nu$(CCl), 1168 m; $\nu$(PtO), 573w; $\nu$(PtN), 538w. $^1$H NMR (400.00 MHz, DMF-$d_7$, ppm): $\delta$ ($SiMe_4$) 9.05 (t, 6.4, N6H, 1H), 8.97 (s, C8H, 1H), 7.03 (dd, 9.5, 2.0, C15H, 1H), 7.02 (dd, 9.5, 2.0, C13H, 1H), 6.95 (t, 7.7, C14H, 1H), 4.92 (d, 6.2, C9H, 2H), 4.84 (sp, 6.7, C16H, 1H), 3.95 (s, C21H, 3H), 3.89 (s, C22H, 3H), 1.56 (d, 6.7, C17H, C18H, 6H). $^{13}$C NMR (100.58 MHz, DMF-$d_7$, ppm): $\delta$ ($SiMe_4$) 165.82 (C19, C20), 155.26 (C6), 153.95 (C2), 153.30 (C12), 149.88 (C4), 147.27 (C11), 144.31 (C8), 132.59 (C10), 124.56 (C14), 120.33 (C15), 116.90 (C5), 112.47 (C13), 60.51 (C21), 56.11 (C22), 49.76 (C16), 40.09 (C9), 21.99 (C17, C18). $^{15}$N NMR (40.53 MHz, DMF-$d_7$, ppm): $\delta$ (DMF-$d_7$) 231.7 (N1), 223.3 (N3), 185.1 (N9), 128.6 (N7), 97.4 (N6). $^{195}$Pt NMR (86.00 MHz, DMF-$d_7$, ppm): $\delta$ ($K_2PtCl_6$) −1689.

[Pt(*2,4-diOMe*L)$_2$(ox)] (**5**). Yield: 68%. mp 210–212 °C (decomp.). Anal. Calcd for $C_{36}H_{40}N_{10}O_8Cl_2Pt$: C, 43.0; H, 4.0; N, 13.9. Found: C, 42.9; H, 3.8; N, 13.8%. TG/DTA data: decomposition began at 205 °C and finished at 478 °C with a weight loss of 79.8% (calc. to PtO residue: 79.0%), endothermic peak at 209 °C and exothermic peaks at 211, 232 and 357 °C. $\Lambda_M$ (DMF solution, S cm$^2$ mol$^{-1}$): 2.1. ESI+ mass spectra (methanol): *m/z* 361.9 (calc. 362.1) $[2,4\text{-}diOMeL+H]^+$, 1006.8 (1007.2) $[Pt(2,4\text{-}diOMeL)_2(ox)+H]^+$, 1029.1 (1029.2) $[Pt(2,4\text{-}diOMeL)_2(ox)+Na]^+$, 1045.0 (1045.2) $[Pt(2,4\text{-}diOMeL)_2(ox)+K]^+$. IR ($\nu_{Nujol}/cm^{-1}$): $\nu$(PtO), 571vs; $\nu$(PtN), 540 s. IR ($\nu_{KBr}/cm^{-1}$):

$\nu(CH_{ar})$, 3127w, 3064w; $\nu(CH_{aliph})$, 2978w, 2933w, 2852w, 2838w; $\nu(CO_{ox})$, 1720 s, 1670 m; $\nu$(CN), 1619vs; $\nu(CC_{phen})$, 1539w, 1486 m; $\nu$(CCl), 1158 m; $\nu$(PtO), 573w. Raman ($cm^{-1}$): $\nu(CH_{ar})$, 3079 m; $\nu(CH_{aliph})$, 2996 s, 2943 s, 2838 m; $\nu(CO_{ox})$, 1709 m, 1674w; $\nu$(CN), 1613 m; $\nu(CC_{phen})$, 1541w, 1491 m; $\nu$(CCl), 1160w; $\nu$(PtO), 570 s; $\nu$(PtN), 537w. $^1$H NMR (400.00 MHz, DMF-$d_7$, ppm): $\delta$ ($SiMe_4$) 8.88 (s, C8H, 1H), 8.81 (t, 6.2, N6H, 1H), 7.27 (d, 8.6, C15H, 1H), 6.63 (d, 2.2, C12H, 1H), 6.44 (dd, 8.4, 2.2, C14H, 1H), 4.83 (sp, 6.8, C16H, 1H), 4.79 (d, 6.0, C9H, 2H), 3.91 (s, C21H, 3H), 3.82 (s, C22H, 3H), 1.54 (d, 6.8, C17H, C18H, 6H). $^{13}$C NMR (100.58 MHz, DMF-$d_7$, ppm): $\delta$ ($SiMe_4$) 165.58 (C19, C20), 161.19 (C13), 159.03 (C11), 155.33 (C6), 153.93 (C2), 149.84 (C4), 144.33 (C8), 129.57 (C15), 118.65 (C10), 116.86 (C5), 105.01 (C14), 99.02 (C12), 56.04 (C21), 55.65 (C22), 49.76 (C16), 40.28 (C9), 21.98 (C17, C18). $^{15}$N NMR (40.53 MHz, DMF-$d_7$, ppm): $\delta$ (DMF-$d_7$) 230.9 (N1), 222.4 (N3), 185.3 (N9), 128.0 (N7), 98.6 (N6). $^{195}$Pt NMR (86.00 MHz, DMF-$d_7$, ppm): $\delta$ ($K_2PtCl_6$) −1685. ESI+ mass spectra (methanol): *m/z* 361.9 [*2,4-diOME*L + H]$^+$, 1006.8 [Pt(*2,4-diOME*L)$_2$(ox) + H]$^+$.

[Pt(*3,4-diOME*L)$_2$(ox)] (**6**). Yield: 59%. mp 192–194 °C (decomp.). Anal. Calcd for $C_{36}H_{40}N_{10}O_8Cl_2Pt$: C, 43.0; H, 4.0; N, 13.9. Found: C, 43.0; H, 4.2; N, 13.9%. TG/DTA data: decomposition began at 190 °C and finished at 447 °C with a weight loss of 79.4% (calc. to PtO residue: 79.0%), endothermic peaks at 191 and 207 °C and exothermic peaks at 217 and 378 °C. $\Lambda_M$ (DMF solution, S cm$^2$ mol$^{-1}$): 1.6. ESI+ mass spectra (methanol): *m/z* 362.1 (calc. 362.1) [*3,4-diOME*L + H]$^+$, 1007.0 (1007.2) [Pt(*3,4-diOME*L)$_2$(ox) + H]$^+$. IR ($\nu_{Nujol}$/$cm^{-1}$): $\nu$(PtO), 568vs; $\nu$(PtN), 543vs. IR ($\nu_{KBr}$/$cm^{-1}$): $\nu(CH_{ar})$, 3123w, 3062w; $\nu(CH_{aliph})$, 2979w, 2937w, 2836w; $\nu(CO_{ox})$, 1724 s, 1669 m; $\nu$(CN), 1620vs; $\nu(CC_{phen})$, 1538w, 1485 m; $\nu$(CCl), 1158 m; $\nu$(PtO), 572w. Raman ($cm^{-1}$): $\nu(CH_{ar})$, 3109w, 3077w; $\nu(CH_{aliph})$, 2996 m, 2941 s, 2866w, 2839w; $\nu(CO_{ox})$, 1722w, 1692w; $\nu$(CN), 1608 m; $\nu(CC_{phen})$, 1537w; $\nu$(CCl), 1165w; $\nu$(PtO), 572w. $^1$H NMR (400.00 MHz, DMF-$d_7$, ppm): $\delta$ ($SiMe_4$) 9.04 (t, 6.3, N6H, 1H), 8.94 (s, C8H, 1H), 7.22 (d, 2.0, C11H, 1H), 7.02 (dd, 8.2, 2.0, C15H, 1H), 6.89 (d, 8.2, C14H, 1H), 4.83 (sp, 6.8, C16H, 1H), 4.82 (d, 6.5, C9H, 2H), 3.85 (s, C21H, 3H), 3.81 (s, C22H, 3H), 1.54 (d, 6.8, C17H, C18H, 6H). $^{13}$C NMR (100.58 MHz, DMF-$d_7$, ppm): $\delta$ ($SiMe_4$) 165.80 (C19, C20), 155.18 (C6), 153.85 (C2), 149.96 (C4), 149.88 (C12), 149.20 (C13), 144.30 (C8), 131.57 (C10), 120.79 (C15), 116.95 (C5), 112.76 (C11), 112.35 (C14), 56.07 (C21, C22), 49.72 (C16), 45.04 (C9), 22.00 (C17, C18). $^{15}$N NMR (40.53 MHz, DMF-$d_7$, ppm): $\delta$ (DMF-$d_7$) 231.6 (N1), 223.1 (N3), 185.8 (N9), 128.7 (N7), 101.0 (N6). $^{195}$Pt NMR (86.00 MHz, DMF-$d_7$, ppm): $\delta$ ($K_2PtCl_6$) −1688.

[Pt(*3,5-diOME*L)$_2$(ox)]·4$H_2O$ (**7**). Yield: 62%. mp 231–233 °C (decomp.). Anal. Calcd for $C_{36}H_{40}N_{10}O_8Cl_2Pt \cdot 4H_2O$: C, 40.1; H, 4.5; N, 13.0. Found: C, 40.0; H, 4.4; N, 13.4%. TG/DTA data: weight loss of 6.8% found in the 128–174 °C region with endothermic peak at 164 °C (6.7% calcd. for 4$H_2O$); decomposition began at 201 °C and finished at 456 °C with a weight loss of 74.5% (calc. 73.8%), endothermic peak at 234 °C and exothermic peaks at 238 and 383 °C; total weight loss of 81.3% (calc. to PtO residue: 80.4%). $\Lambda_M$ (DMF solution, S cm$^2$ mol$^{-1}$): 1.9. ESI+ mass spectra (methanol): *m/z* 362.2 (calc. 362.1) [*3,5-diOME*L + H]$^+$, 1007.0 (1007.2) [Pt(*3,5-diOME*L)$_2$(ox) + H]$^+$, 1029.1 (1029.2) [Pt(*3,5-diOME*L)$_2$(ox) + Na]$^+$. IR ($\nu_{Nujol}$/$cm^{-1}$): $\nu$(PtO), 568vs; $\nu$(PtN), 540 m. IR ($\nu_{KBr}$/$cm^{-1}$): $\nu(CH_{ar})$, 3097w; $\nu(CH_{aliph})$, 2978w, 2937 m, 2839w; $\nu(CO_{ox})$, 1712vs, 1677 s; $\nu$(CN), 1620vs; $\nu(CC_{phen})$, 1539w; $\nu$(CCl), 1156 s; $\nu$(PtO), 568w; $\nu$(PtN), 540w. Raman ($cm^{-1}$): $\nu(CH_{ar})$, 3094w; $\nu(CH_{aliph})$, 2990w, 2944 m, 2879w, 2839w; $\nu(CO_{ox})$, 1702 m, 1666w; $\nu(CC_{phen})$, 1537w, 1491 m; $\nu$(CCl), 1166w; $\nu$(PtO), 567w. $^1$H NMR (400.00 MHz, DMF-$d_7$, ppm): $\delta$ ($SiMe_4$) 9.12 (t, 6.2, N6H, 1H), 9.02 (s, C8H, 1H), 6.64 (d, 2.3, C11H, C15H, 2H), 6.40 (t, 2.3, C13H, 1H), 4.85 (sp, 6.8, C16H, 1H), 4.83 (d, 6.8, C9H, 2H), 3.80 (s, C21H, C22H, 6H), 1.56 (d, 6.8, C17H, C18H, 6H). $^{13}$C NMR (100.58 MHz, DMF-$d_7$, ppm): $\delta$ ($SiMe_4$) 165.89 (C19, C20), 161.66 (C12, C14), 155.18 (C6), 153.94 (C2), 149.96 (C4), 144.17 (C8), 141.68 (C10), 116.84 (C5), 106.08 (C11, C15), 99.56 (C13), 55.63 (C21, C22), 49.76 (C16), 45.17 (C9), 22.00 (C17, C18). $^{15}$N NMR (40.53 MHz, DMF-$d_7$, ppm): $\delta$ (DMF-$d_7$) 231.3 (N1), 223.1 (N3), 185.2 (N9), 127.8 (N7), 97.8 (N6). $^{195}$Pt NMR (86.00 MHz, DMF-$d_7$, ppm): $\delta$ ($K_2PtCl_6$) −1694.

## 3. Results and discussion

### 3.1. Synthesis and general properties

The platinum(II) oxalato complexes of the general composition [Pt(*n*L)$_2$(ox)]·*x*$H_2O$ (*x* = 0 for **1**–**6** and 4 for **7**) involving 2-chloro-N6-(benzyl)-9-isopropyladenine or its benzyl-substituted analogues (*n*L) were synthesized by a synthetic strategy using potassium bis(oxalato) platinate(II) dihydrate, $K_2[Pt(ox)_2]\cdot 2H_2O$, as a key intermediate (Scheme 1). According to accessible literature data, $K_2[Pt(ox)_2]\cdot 2H_2O$ was used for the first time to prepare platinum(II) oxalato complexes involving the $PtN_2O_2$ chromophore. Reactions were carried out in a mixture of distilled water and *iso*propanol (1:1, v/v) at the temperature of 70 °C. The pale grey powder products formed during 3 days in very good yields.

Prepared complexes **1**–**7** were found to be well soluble in *N*,*N*′-dimethylformamide, and acetone, soluble in ethanol, methanol and chloroform, and partially soluble in water. Measurements of the molar conductivity of $10^{-3}$ M DMF solutions proved that the complexes behave as non-electrolytes, since the molar conductivity values did not exceed the value of 2.1 S cm$^2$ mol$^{-1}$ [30].

The TG/DTA thermal study proved the complexes **1**–**6** to be non-solvated and **7** as a tetrahydrate. The results are given in Section 2.7. The thermal decomposition proceeds in two waves (three in the case of **7**, due to its dehydration; see Fig. S1 in Supplementary material) and it is finished by the formation of platinum(II) oxide (PtO). The total observed weight losses for **1**–**7** are in a good agreement with the calculated ones and both values differ by 0.1–1.2%. The endo-effects observed on the DTA curve with minima between 190 °C (for **6**) and 230 (for **1**) may be connected with melting of unstable intermediates during the degradation process.

The presence of the [Pt(*n*L)$_2$(ox) + H]$^+$ peaks in the ESI+ mass spectra of **2**–**7** indirectly proved the composition of these complexes. In several cases its adducts with sodium and potassium ions, i.e. [Pt(*n*L)$_2$(ox) + Na]$^+$ and [Pt(*n*L)$_2$(ox) + K]$^+$, were also detected (see Section 2.7) for the complex **5** (depicted in Fig. S2 in Supplementary material). The [Pt(*2,3-diOME*L)(ox) + H]$^+$ fragment was observed at 646.0 *m/z* in the mass spectra of **4**. All the mass spectra of **1**–**7** contain the fragment corresponding to the appropriate ligand, i.e. [*n*L + H]$^+$. The observed isotopic distribution representations correlated well with those calculated by QualBrowser software (version 2.0.7, Thermo Fischer Scientific), as it can be seen in Section 2.7.

### 3.2. Spectroscopic characterization

All the $^1$H, $^{13}$C and $^{15}$N NMR signals of the free 2-chloro-N6-(benzyl)-9-isopropyladenine and its derivatives (*n*L) were found in the corresponding spectra of **1**–**7**. The most significant changes of $^1$H NMR chemical shifts ($\delta$), discussed as coordination shifts, $\Delta\delta$, ($\Delta\delta = \delta_{complex} - \delta_{ligand}$), were determined for C8H and N6H signals, which are shifted by 0.54–0.73, and 0.27–0.58 ppm downfield, respectively (Table 2). In the case of $^{13}$C NMR spectra, a signal at 165.58–165.94 ppm was found only in the spectra of the platinum(II) complexes **1**–**7** contrary to free organic adenine derivatives (*n*L). Based on this finding, it may be concluded that these signals unambiguously belong to an oxalate dianion (C19 and C20 atoms) coordinated to the Pt(II) centre, which correlate well with that of $K_2[Pt(ox)_2]\cdot 2H_2O$ ($D_2O$ solutions) found at 167.87 ppm. Moreover, the discussed signals were not found in any of the carbon 2D NMR experiments. Further, the most shifted carbon signals of the *n*L molecules are those of the C8 and C5 atoms, whose coordination

**Table 2**
$^{1}$H, $^{13}$C and $^{15}$N NMR coordination shifts, $\Delta\delta$, ($\Delta\delta = \delta_{complex} - \delta_{ligand}$; ppm) and $^{195}$Pt NMR chemical shifts ($\delta$; ppm) observed for **1**–**7**.

| Complex | $^{1}$H NMR | | $^{13}$C NMR | | | | | $^{15}$N NMR | | | | | $^{195}$Pt |
|---|---|---|---|---|---|---|---|---|---|---|---|---|---|
| | N6H | C8H | C2 | C4 | C5 | C6 | C8 | N1 | N3 | N6 | N7 | N9 | NMR |
| **1** | 0.47 | 0.72 | 0.00 | −0.63 | −2.81 | −0.88 | 4.27 | 4.9 | 0.3 | 5.5 | −111.5 | 6.9 | −1685 |
| **2** | 0.55 | 0.65 | 0.07 | −0.61 | −2.87 | −1.02 | 4.25 | 3.8 | −0.8 | 7.7 | −111.6 | 7.0 | −1691 |
| **3** | 0.27 | 0.54 | −0.41 | −0.44 | −1.67 | −0.46 | 4.34 | 6.6 | 1.5 | 2.9 | −114.0 | 5.4 | −1689 |
| **4** | 0.56 | 0.68 | 0.51 | −0.66 | −2.87 | −0.93 | 4.26 | 3.9 | −1.0 | 5.1 | −111.5 | 5.3 | −1689 |
| **5** | 0.58 | 0.60 | −0.08 | −0.65 | −2.85 | −0.94 | 4.37 | 2.4 | −1.7 | 6.8 | −113.1 | 5.7 | −1685 |
| **6** | 0.44 | 0.67 | −0.07 | −0.55 | −2.73 | −0.81 | 4.31 | 3.8 | −0.6 | 5.1 | −111.6 | 6.5 | −1688 |
| **7** | 0.46 | 0.73 | 0.04 | −0.61 | −2.85 | −0.89 | 4.07 | 3.7 | −1.6 | 3.9 | −112.4 | 5.8 | −1694 |

shifts, $|\Delta\delta|$, equal 4.07–4.37 ppm (downfield), and 1.67–2.87 ppm (upfield), respectively (Table 2).

The above-discussed hydrogen and carbon atoms are situated nearby the N7 atom, whose $\Delta\delta$ values, obtained by the $^{1}$H–$^{15}$N gs-HMBC experiments, ranged from −114.0 to −111.5 ppm (Fig. 1). These values are significantly higher in comparison with the other nitrogen atoms, whose $|\Delta\delta|$ did not exceed 7.7 ppm (Table 2). Presented results clearly proved the coordination of the *n*L molecules to the Pt(II) centre through the N7 atom of the adenine moieties.

The $^{195}$Pt signals were detected between −1694 ppm and −1685 ppm (Table 2). These values differ significantly from those of *cis*-[Pt(L)$_2$Cl$_2$] and *trans*-[Pt(L)$_2$Cl$_2$] complexes bearing N6-(benzyl) adenine-based ligands, whose $\delta$ ~−2000 ppm, which indicates a different chromophore type of the mentioned platinum(II) complexes [21,23]. However, $^{195}$Pt signals of the platinum(II) oxalato complexes ($PtN_2O_2$ chromophore) involving unidentate N-donor ligands, e.g. hexamethyleneimine (−1872 ppm), piperidine (−1978 ppm), 3-methylpiperidine (−1965 ppm), 1-methyl-4-(methylamino)piperidine (−2019 ppm), differ significantly from those of **1**–**7** as well [10,31–33]. Nevertheless, it can be assigned to the structural difference of the mentioned ligands from *n*L molecules used in this work.

The complexes **1**–**7** have been characterized by IR spectroscopy in the 150–4000 cm$^{-1}$ range. The oxalate dianion coordinated to the Pt(II) centre showed a characteristic band of the $\nu$(Pt–O) vibration in the 565–574 cm$^{-1}$ range and two bands of the $\nu_{as}$($C_{ox}$–O) between

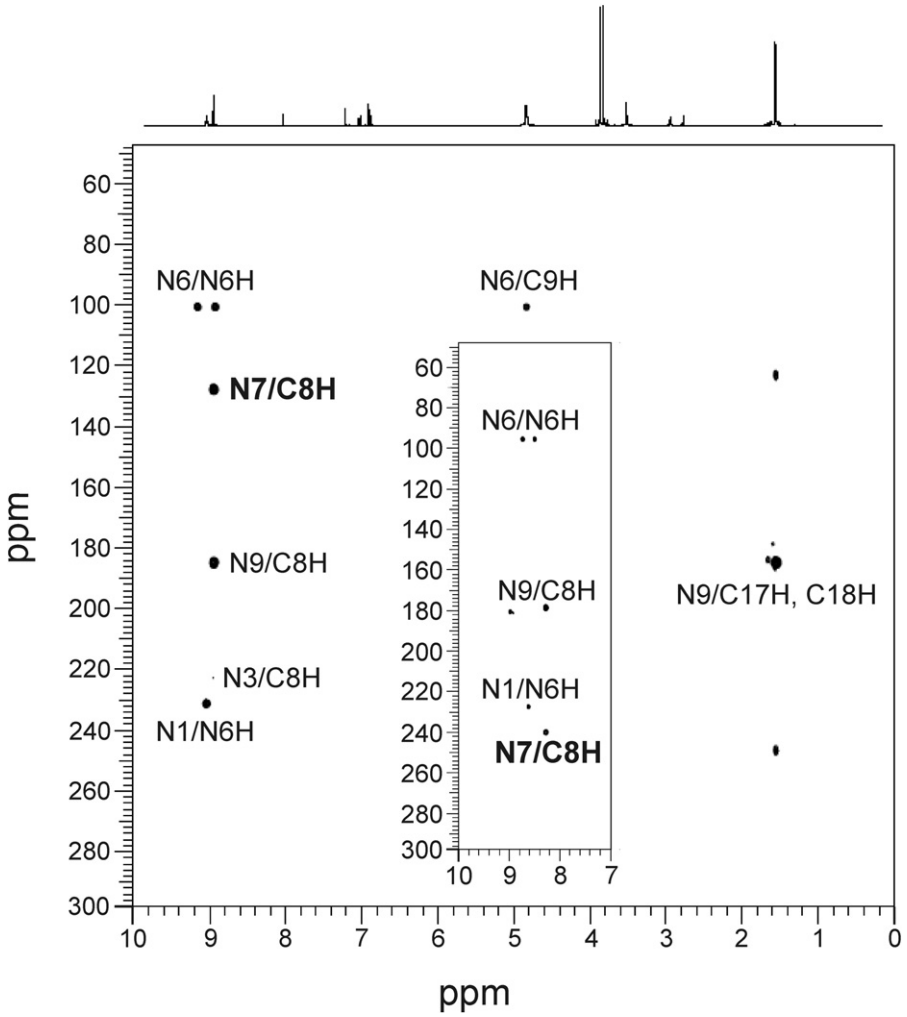


**Fig 1.** $^{1}$H–$^{15}$N gs-HMBC spectrum of [Pt(3,4-*diOMe*L)$_2$(ox)] (**6**) with part of $^{1}$H–$^{15}$N gs-HMBC spectrum of 2-chloro-6-(3,4-dimethoxybenzyl)-9-isopropyladenine (3,4-*diOMe*L; inset).

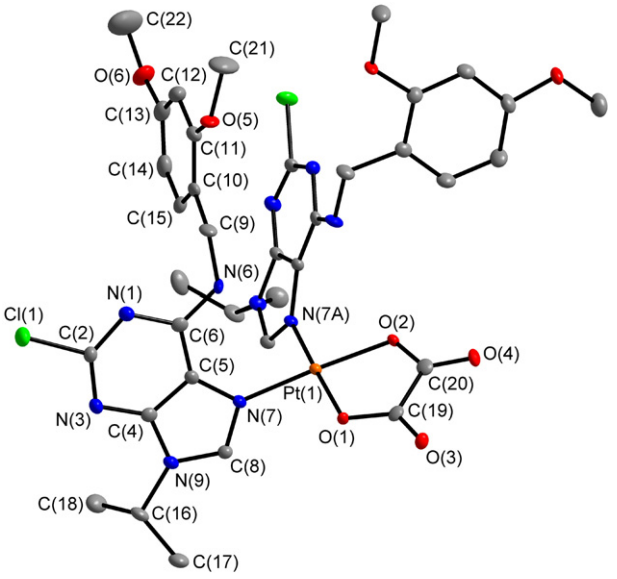


**Fig. 2.** Molecular structure of [Pt(*2,4-diOMe*L)$_2$(ox)]·2DMF (**5**·2DMF) with non-hydrogen atoms drawn as thermal ellipsoids at the 50% probability level and showing the atom numbering scheme; two DMF molecules of crystallization and H-atoms are omitted for clarity.

1669 and 1677 cm$^{-1}$, and 1706–1724 cm$^{-1}$, respectively. These values correlate very well with both in this work determined (568, 1673 and 1709 cm$^{-1}$) and previously reported (575, 1674 and 1709 cm$^{-1}$) values for potassium bis(oxalato)platinate [34]. 2-Chloro-N6-(benzyl)-9-isopropyladenine and its derivatives (*n*L) coordinated in the complexes **1**–**7** showed several bands typical for this type of compounds. The peak of very strong intensity, assignable to the $\nu$(C–N) vibration, appeared at 1615–1621 cm$^{-1}$. The maxima at 1156–1169 cm$^{-1}$ may be assigned to the $\nu$(C–Cl) vibrations. The bands attributable to $\nu$(C–H)$_{aliph}$ were found between 2832 and 2981 cm$^{-1}$, while the maxima at about 3060 cm$^{-1}$ probably belongs to the $\nu$(C–H)$_{ar}$ vibrations. The coordination of the 2-chloro-N6-(benzyl)-9-isopropyladenine derivatives through a nitrogen atom can be proved by a band between 538 and 543 cm$^{-1}$ assignable to the $\nu$(Pt–N) vibration.

The information provided by IR spectroscopy was complemented by the Raman spectral data. The bands describing the above-discussed vibrations were found in the Raman spectra of **1**–**7**, as follows: $\nu$(Pt–O) at 567–574 cm$^{-1}$, $\nu$(C–Cl) at 1159–1168 cm$^{-1}$, $\nu$(C–N) at 1602–1613 cm$^{-1}$ (not observed for **4** and **7**), $\nu_{as}$(C$_{ox}$–O) at 1666–1692 cm$^{-1}$ and 1698–1722 cm$^{-1}$, $\nu$(C–H)$_{aliph}$ at 2836–2996 cm$^{-1}$ and $\nu$(C–H)$_{ar}$ at 3053–3130 cm$^{-1}$. The $\nu$(N–H) bands showed their maxima at ca. 3330 cm$^{-1}$. It should be noted that a very strong band detected at about 1345 cm$^{-1}$ could be assigned to the skeletal stretching vibrations of a purine moiety [35].

### 3.3. X-ray structure of [Pt(2,4-diOMeL)$_2$(ox)]·2DMF (**5**·2DMF)

The molecular structure of the complex, depicted in Fig. 2, was determined by a single-crystal X-ray analysis. The crystal data and structure refinements are given in Table 1 and selected bond lengths and angles are summarized in Table 3.

The central Pt(II) ion is four-coordinated by the O(1) and O(2) oxygen atoms of the bidentate-coordinated oxalate dianion (ox) and by the N(7) and the N(7A) atoms of two 2-chloro-N6-(2,4-dimethoxybenzyl)-9-isopropyladenine (*2,4-diOMe*L) molecules, further labelled as *2,4-diOMe*L$_{N(7)}$ [*2,4-diOMe*L molecule of **5**·2DMF involving the N(7) atom] and *2,4-diOMe*L$_{N(7A)}$ [*2,4-diOMe*L molecule of **5**·2DMF involving the N(7A) atom]. The geometry was found to be slightly distorted square–planar and the *2,4-diOMe*L molecules involved in the structure of the discussed complex are mutually arranged in the head-to-tail orientation (Fig. 2).

The central Pt(II) ion is 0.0217(2) Å out of the least-square plane formed by the N(7), N(7A), O(1) and O(2) atoms of the PtN$_2$O$_2$ donor set. Two purine rings of *2,4-diOMe*L$_{N(7)}$ and *2,4-diOMe*L$_{N(7A)}$ molecules form the dihedral angles of 70.50(7)°, and 53.45(6)°, respectively, with the above mentioned least-square plane. The dihedral angle formed by two purine rings of the two neighbouring *2,4-diOMe*L molecules equals 83.12(6)°. The dihedral angles between a purine moiety and a benzene ring of the respective *2,4-diOMe*L molecules were determined to be 84.24(10)° for *2,4-diOMe*L$_{N(7)}$ and 74.07(9)° for *2,4-diOMe*L$_{N(7A)}$. The benzene, pyrimidine and imidazole rings are nearly planar with maximum deviations from planarity of 0.0208(41) Å (C11), 0.0201(32) Å (C10A), 0.0290(32) Å (C6), 0.0099(31) Å (C6A), 0.0052(32) Å (C8) and 0.0045(31) Å (C8A). The pyrimidine and imidazole rings form the dihedral angle of 1.96(11)° for *2,4-diOMe*L$_{N(7)}$ and 3.47(10)° for *2,4-diOMe*L$_{N(7A)}$. The oxalato group atoms O(1), O(2), O(3), O(4), C(19) and C(20) are 0.0166(24) Å, −0.0138(24) Å, −0.0123(24) Å, 0.0171(25) Å, −0.0083(31) Å, and −0.0016(31) Å, respectively, out of the least-square plane formed by these atoms.

**Table 3**
Selected bond lengths (Å) and angles (°) for **5**·2DMF (data for both coordinated *2,4-diOMe*L molecules given as N7 atom involving molecule/N7A atom involving molecule).

| Bond lengths | | Bond angles | | Bond angles | |
|---|---|---|---|---|---|
| Pt(1)–N(7) | 2.001(3) | O(1)–Pt(1)–N(7) | 92.03(10) | C(2)–N(1)–C(6) | 117.2(3)/117.4(3) |
| Pt(1)–N(7A) | 2.001(3) | O(1)–Pt(1)–N(7A) | 176.98(10) | N(1)–C(2)–N(3) | 132.0(3)/131.6(3) |
| Pt(1)–O(1) | 1.994(2) | O(1)–Pt(1)–O(2) | 83.90(9) | C(2)–N(3)–C(4) | 109.4(3)/110.1(3) |
| Pt(1)–O(2) | 2.010(2) | O(2)–Pt(1)–N(7) | 175.93(10) | N(3)–C(4)–C(5) | 126.3(3)/126.6(4) |
| O(1)–C(19) | 1.303(4) | O(2)–Pt(1)–N(7A) | 94.33(10) | N(3)–C(4)–N(9) | 127.0(3)/126.2(3) |
| O(2)–C(20) | 1.304(4) | N(7)–Pt(1)–N(7A) | 89.74(11) | C(4)–C(5)–C(6) | 117.5(3)/116.9(3) |
| O(3)–C(19) | 1.209(4) | Pt(1)–O(1)–C(19) | 113.2(2) | C(4)–C(5)–N(7) | 108.9(3)/108.1(3) |
| O(4)–C(20) | 1.223(4) | Pt(1)–O(2)–C(20) | 112.1(2) | C(5)–C(6)–N(1) | 117.5(3)/117.4(3) |
| C(19)–C(20) | 1.564(5) | O(1)–C(19)–O(3) | 124.3(3) | C(5)–C(6)–N(6) | 122.4(3)/124.5(3) |
| N(1)–C(2) | 1.323(4)/1.327(5) | O(1)–C(19)–C(20) | 114.8(3) | N(1)–C(6)–N(6) | 120.1(3)/118.0(3) |
| N(1)–C(6) | 1.350(5)/1.357(4) | O(3)–C(19)–C(20) | 120.9(3) | C(6)–N(6)–C(9) | 124.8(3)/122.7(3) |
| C(2)–N(3) | 1.324(5)/1.312(5) | O(2)–C(20)–O(4) | 124.1(3) | Pt(1)–N(7)–C(5) | 128.2(2)/132.3(2) |
| N(3)–C(4) | 1.351(4)/1.345(4) | O(2)–C(20)–C(19) | 115.8(3) | Pt(1)–N(7)–C(8) | 126.2(2)/121.9(2) |
| C(4)–C(5) | 1.375(5)/1.384(5) | O(4)–C(20)–C(19) | 120.1(3) | C(5)–N(7)–C(8) | 105.6(3)/105.5(3) |
| C(4)–N(9) | 1.376(4)/1.377(4) | | | N(7)–C(8)–N(9) | 112.2(3)/112.6(3) |
| C(5)–C(6) | 1.415(5)/1.418(5) | | | N(6)–C(9)–C(10) | 114.3(3)/113.8(3) |
| C(5)–N(7) | 1.388(4)/1.397(4) | | | C(8)–N(9)–C(4) | 106.5(3)/106.6(3) |
| C(6)–N(6) | 1.331(5)/1.335(4) | | | | |
| N(7)–C(8) | 1.318(4)/1.327(4) | | | | |
| C(8)–N(9) | 1.356(4)/1.344(4) | | | | |

**Table 4**
*In vitro* cytotoxicity of the prepared complexes **1**–**7**, cisplatin and oxaliplatin against osteosarcoma (HOS) and breast adenocarcinoma (MCF7) human cancer cell lines; given as $IC_{50}$ values [μM].

| | 1 | 2 | 3 | 4 | 5 | 6 | 7 | Cisplatin | Oxaliplatin |
|---|---|---|---|---|---|---|---|---|---|
| HOS | >10.0 | 3.6 ± 1.0 | >5.0 | >1.0 | 5.4 ± 3.8 | >10.0 | >1.0 | 34.2 ± 6.4 | >50.0 |
| MCF7 | 9.2 ± 1.5 | 4.3 ± 2.1 | >5.0 | >1.0 | 3.6 ± 2.1 | >10.0 | >1.0 | 19.6 ± 4.3 | >50.0 |

The complex is solvated by two *N*,*N*′-dimethylformamide molecules which are involved into a network of hydrogen bonds of the N–H···O type within the crystal structure of **5**·2DMF [N(6A)–H(6A)···O(8)$^{i}$ hydrogen bond; D–H···A parameters: *d*(D–H) 0.88 Å, *d*(H···A) 2.22 Å, *d*(D···A) 2.876(4) Å, <(DHA) 131.33°, symmetry code: (*i*) *x*, 1.5 − *y*, *z* − 0.5] (see Fig. S3 in Supplementary material). Besides the discussed N–H···O hydrogen bonds, the C–H···O, C–H···Cl and C–H···N non-bonding contacts also contribute to the stabilization of the crystal structure of this platinum(II) oxalato complex (see Figs. S4 and S5 in Supplementary material). The interatomic parameters of the last-mentioned contacts are as follows: C(8)–H(8)···O(4)$^{ii}$ [*d*(D–H) 0.950(3) Å, *d*(H···A) 2.284(3) Å, *d*(D···A) 3.012(4) Å, <(DHA) 133.0(2)°, symmetry code: (ii) 1 − *x*, 1 − *y*, − *z*], C(12A)–H(12A)···O(1)$^{iii}$ [*d*(D–H) 0.950(3) Å, *d*(H···A) 2.418(2) Å, *d*(D···A) 3.342(4) Å, <(DHA) 164.5(2)°, symmetry code: (iii) *x* − 0.5, 1.5 − *y*, − *z*], C(21)–H(21F)···Cl(1A)$^{iv}$ [*d*(D–H) 0.981(5) Å, *d*(H···A) 2.7843(9) Å, *d*(D···A) 3.629(5) Å, <(DHA) 144.7(3)°, symmetry code: (iv) 0.5 − *x*, *y* + 0.5, *z*] and C(23)–H(23)···N(3)$^{v}$ [*d*(D–H) 0.950(5) Å, *d*(H···A) 2.628(3) Å, *d*(D···A) 3.447(6) Å, <(DHA) 144.6(3)°, symmetry code: (v) 1 − *x*, *y* − 0.5, 0.5 − *z*]. In the case of one DMF molecule of crystallization, the C(25), C(26) and C(27) atoms as well as hydrogen atoms attached to them were refined as disordered over two positions with occupancy factors of 53% for the main part and 47% for the side one.

### 3.4. In vitro cytotoxicity

The significant *in vitro* cytotoxic activity against HOS and MCF7 human cancer cells was determined for the complexes **2** and **5** against both cancer cell lines and for **1** against MCF7 cells (Table 4). Cytotoxicity evaluation of the other complexes was influenced by the limited solubility of these compounds in the DMF/water mixture, since they were determined to be inactive up to concentrations given in Table 4. Due to objective evaluation of the cytotoxic activity, we also tested platinum-based drugs cisplatin and oxaliplatin on the same cancer cell lines and using the same testing method. $IC_{50}$ of cisplatin equals 34.2 μM (HOS) and 19.6 μM (MCF7); oxaliplatin was found to be inactive up to 50.0 μM against both tested lines. It is quite clear from the obtained results that platinum(II) oxalato complexes **2** and **5** are several times more cytotoxic against HOS and MCF7 cancer cells compared to the mentioned commercially used platinum-based antineoplastic drugs. As for **1**, it is more active than the mentioned substances against MCF7 cells.

## 4. Conclusions

The described platinum(II) oxalato complexes of the general formula $[Pt(nL)_2(ox)]\cdot xH_2O$ (**1**–**7**; *x* = 0 for **1**–**6** and 4 for **7**) represent the first complexes in which both adenine-based ligand (*n*L) and oxalate dianion (ox) are coordinated to the central Pt(II) ion. The mentioned compounds were prepared from $K_2[Pt(ox)_2]\cdot 2H_2O$, as a starting compound, and studied by various physical methods including multinuclear NMR spectroscopy and a single-crystal X-ray analysis, which proved a square–planar geometry in the vicinity of the central Pt(II) ion, with a $PtN_2O_2$ donor set. *In vitro* MTT cytotoxic testing against the HOS and MCF7 cancer cell lines indicated significant cytotoxicity of the complexes **1** (9.2 μM against MCF7), **2** ($IC_{50}$ = 3.6 μM and 4.3 μM) and **5** ($IC_{50}$ = 5.4 μM and 3.6 μM), which is several times higher activity compared to the platinum-based anticancer drugs cisplatin ($IC_{50}$ = 34.2 μM and 19.6 μM) and oxaliplatin ($IC_{50}$ = >50.0 μM and >50.0 μM). These results encourage us to continue in cytotoxicity testing and to test the current set of complexes as well as their suitable substituted analogues against other human cancer cell lines to prove the antitumor properties of these types of compounds, and moreover, to start DNA-interaction studies of such complexes.

## Acknowledgments

The authors thank the Ministry of Education, Youth and Sports of the Czech Republic for financial support (grant no. MSM6198959218), Mr. Lukáš Dvořák and Mrs. Pavla Richterová for performing CHN elemental analyses, Dr. Miroslava Matíková-Malarová and Ms. Radka Novotná for IR and Raman spectra measurements, Ms. Alena Klanicová for mass spectra measurement and Prof. Zdeněk Dvořák and Dr. Radim Vrzal for *in vitro* cytotoxicity testing.

## Appendix A. Supplementary data

Supplementary data associated with this article can be found, in the online version, at doi:10.1016/j.jinorgbio.2010.02.005.

## References

[1] L.R. Kelland, N.P. Farrell, Platinum Based Drugs in Cancer Therapy, Humana Press, Totowa, New Jersey, 2000.
[2] M. Gielen, E.R.T. Tiekink, Metallotherapeutic Drugs and Metal-based Diagnostic Agents, London, Willey, 2005.
[3] L.M. Pasetto, M.R. D'Andrea, A.A. Brandes, E. Rossi, S. Monfardini, Crit. Rev. Oncol. Hemat. 60 (2006) 59–75.
[4] Y. Kidani, K. Inagaki, J. Med. Chem. 21 (1978) 1315–1318.
[5] L. Habala, M. Galanski, A. Yasemi, A.A. Nazarov, N.G. von Keyserlingk, B.K. Keppler, Eur. J. Med. Chem. 40 (2005) 1149–1155.
[6] A.S. Abu-Surrah, M. Kettunen, M. Leskela, Y.Z. Al-Abed, Anorg. Allg. Chem. 634 (2008) 2655–2658.
[7] Y. Yu, L.G. Lou, W.P. Liu, H.J. Zhu, Q.S. Ye, X.Z. Chen, W.G. Gao, S.Q. Hou, Eur. J. Med. Chem. 43 (2008) 1438–1443.
[8] B.E. Bowler, K.J. Ahmed, W.I. Sundquist, L.S. Hollis, E.E. Whang, S.J. Lippard, J. Am. Chem. Soc. 111 (1989) 1299–1306.
[9] V.D. Sen, V.A. Golubev, L.M. Volkova, N.P. Konovalova, J. Inorg. Biochem. 64 (1996) 69–77.
[10] U. Mukhopadhyay, J. Thurston, K.H. Whitmire, Z.H. Siddik, A.R. Khokhar, J. Inorg. Biochem. 94 (2003) 179–185.
[11] K. Meelich, M. Galanski, V.B. Arion, B.K. Keppler, Eur. J. Inorg. Chem. (2006) 2476–2483.
[12] X.Z. Chen, M.J. Xie, W.P. Liu, Q.S. Ye, Y. Yu, S.Q. Hou, W.G. Gao, Y. Liu, Inorg. Chim. Acta 360 (2007) 2851–2856.
[13] X.Z. Chen, O.S. Ye, L.G. Lou, M.J. Xie, W.P. Liu, Y. Yu, S.Q. Hou, Arch. Pharm. 341 (2008) 132–136.
[14] F.A. Allen, Acta Crystallogr., Sect. B: Struct. Sci. 58 (2002) 380–388.
[15] M.J. Cleare, Coord. Chem. Rev. 12 (1974) 349–405.
[16] E. Monti, M. Gariboldi, A. Maiocchi, E. Marengo, C. Cassino, E. Gabano, D.J. Osella, J. Med. Chem. 48 (2005) 857–866.
[17] W. Liu, X. Chen, M. Xie, L. Lou, Q. Ye, S. Hou, J. Inorg. Biochem. 102 (2008) 1942–1946.
[18] D. Dolfen, K. Schottler, S.M. Valiahdi, M.A. Jakupec, B.K. Keppler, E.R.T. Tiekink, F. Mohr, J. Inorg. Biochem. 102 (2008) 2067–2071.
[19] C.I. Diakos, M. Zhang, P.J. Beale, R.R. Fenton, T.W. Hambley, Eur. J. Med. Chem. 44 (2009) 2807–2814.
[20] A. Hegmans, J. Kasparkova, O. Vrana, L.R. Kelland, V. Brabec, N.P. Farrell, J. Med. Chem. 51 (2008) 2254–2260.
[21] L. Szüčová, Z. Trávníček, I. Popa, J. Marek, Polyhedron 27 (2008) 2710–2720.
[22] Z. Trávníček, I. Popa, M. Čajan, R. Herchel, J. Marek, Polyhedron 26 (2007) 5271–5282.
[23] M. Maloň, Z. Trávníček, R. Marek, M. Strnad, J. Inorg. Biochem. 99 (2005) 2127–2138.

[24] L. Meijer, A. Borgne, O. Mulner, J.P.J. Chong, J.J. Blow, N. Inagaki, M. Inagaki, J.G. Delcros, J.P. Moulinoux, Eur. J. Biochem. 243 (1997) 527–536.
[25] C.H. Oh, S.C. Lee, K.S. Lee, E.R. Woo, C.Y. Hong, B.S. Yang, D.J. Baek, J.H. Cho, Arch. Pharm. Pharm. Med. Chem. 332 (1999) 187–190.
[26] CrysAlis RED, CrysAlis CCD, Version 1.171.32.11, Oxford Diffraction Ltd., Abingdon, England, 2006.
[27] G.M. Sheldrick, Acta Cryst. A64 (2008) 112–122.
[28] K. Brandenburg, DIAMOND, Release 3.1f, Crystal Impact GbR, Bonn: Germany, 2006.
[29] K. Krogmann, P. Dodel, Chem. Ber. Recl. 99 (1966) 3402–3408.
[30] W.J. Geary, Coord. Chem. Rev. 7 (1971) 81–122.
[31] M.S. Ali, J.H. Thurston, K.H. Whitmire, A.R. Khokhar, Polyhedron 21 (2002) 2659–2665.
[32] S.R.A. Khan, I. Guzman-Jimenez, K.H. Whitmire, A.R. Khokhar, Polyhedron 19 (2000) 975–981.
[33] S.R.A. Khan, I. Guzman-Jimenez, K.H. Whitmire, A.R. Khokhar, Polyhedron 19 (2000) 983–989.
[34] K. Nakamoto, Infrared and Raman Spectra of Inorganic and Coordination Compounds5th ed., Willey-Interscience, New York, 1997.
[35] Z. Dhaouadi, M. Ghomi, J.C. Austin, R.B. Girling, R.E. Hester, P. Mojzes, L. Chinsky, P.Y. Turpin, C. Coulombeau, H. Jobic, J. Tomkinson, J. Phys. Chem. 97 (1993) 1074–1084.

**Supplementary Material**

# Platinum(II) oxalato complexes with adenine-based carrier ligands showing significant in vitro antitumor activity

Pavel Štarha, Zdeněk Trávníček*, Igor Popa

*Department of Inorganic Chemistry, Faculty of Science, Palacký University,*

*Třída 17. listopadu 12, CZ-771 46 Olomouc, Czech Republic*

* Corresponding author. Tel.: +420 585 634 352; fax: +420585 634 954; e-mail: zdenek.travnicek@upol.cz (Zdeněk Trávníček).



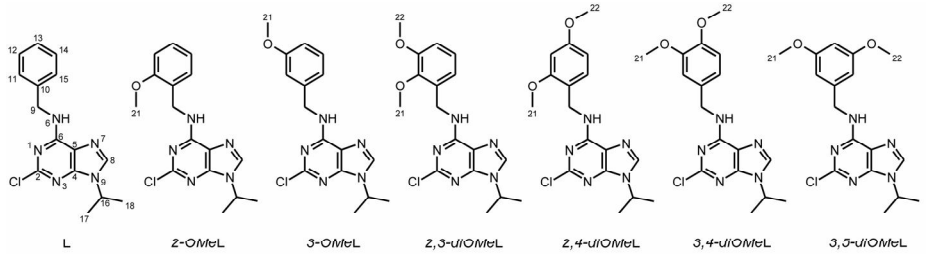


**Scheme S1.** 2-Chloro-N6-(benzyl)-9-isopropyladenine and its derivatives (*n*L) used for the synthesis of platinum(II) complexes **1**–**7**

**The results of elemental analyses and IR, Raman and NMR spectroscopy for *n*L organic compounds.** 2-Chloro-N6-(benzyl)-9-isopropyladenine (L): Anal. Calcd for $C_{15}H_{16}N_5Cl$: C, 59.7; H, 5.3; N, 23.2. Found: C, 59.7; H, 5.4; N, 23.6%. IR ($\nu_{Nujol}$/cm$^{-1}$): 594s, 535vs, 482vs, 463s, 428w, 387w, 343w, 228w, 215m. IR ($\nu_{KBr}$/cm$^{-1}$): 3266s, 3222w, 3125w, 2978s, 2939s, 2739w, 2677s, 2623s, 2604s, 2530w, 2495w, 1625vs, 1571s, 1537w, 1497w, 1474s, 1453s, 1424w, 1398s, 1354s, 1311s, 1292s, 1253s, 1223s, 1202s, 1172w, 1134w, 1101w, 1068w, 1037w, 967w, 930w, 883w, 860w, 850w, 808w, 789w, 744w, 724w, 696w, 679w, 660w, 642w, 607w, 536w, 484w. Raman (cm$^{-1}$): 3125w, 3060s, 2979vs, 2942vs, 2918vs, 2787w, 2764w, 2729w, 1605w, 1569s, 1475s, 1400w, 1384w, 1356vs, 1314w, 1291w, 1252w, 1186w, 1163m, 1104w, 1080w, 1028w, 1001s, 903w, 884w, 803w, 762w, 615w, 536w, 462w, 430w, 390s, 231s, 217s, 152s. $^1$H NMR (300.00 MHz, DMF-$d_7$, ppm): δ ($SiMe_4$) 8.67 (t, 6.2, N6H, 1H), 8.28 (s, C8H, 1H), 7.46 (dd, 7.3, 1.6, C11H, C15H, 2H), 7.34 (tt, 7.3, 1.6, C12H, C14H, 2H), 7.23 (tt, 7.3, 1.6, C13H, 1H), 4.82 (d, 6.2, C9H, 2H), 4.76 (sep, 6.8, C16H, 1H), 1.58 (d, 6.8, C17H, C18H, 6H). $^{13}$C NMR (75.43 MHz, DMF-$d_7$, ppm): δ ($SiMe_4$) 156.11 (C6), 153.96 (C2), 150.57 (C4), 140.39 (C10), 140.04 (C8), 128.98 (C12, C14), 128.28 (C11, C15), 127.56 (C13), 119.68 (C5), 47.90 (C16), 44.22 (C9), 22.41 (C17, C18). $^{15}$N NMR (30.40 MHz, DMF-$d_7$, ppm): δ (DMF-$d_7$) 239.8 (N7), 227.3 (N1), 223.9 (N3), 178.6 (N9), 93.6 (N6).

2-Chloro-N6-(2-methoxybenzyl)-9-isopropyladenine (*2-OMe*L): Anal. Calcd for $C_{16}H_{18}N_5OCl$: C, 57.9; H, 5.5; N, 21.1. Found: C, 57.8; H, 5.5; N, 20.5%. IR ($\nu_{Nujol}$/cm$^{-1}$): 582w, 544w, 529vs, 493s, 446s, 418w, 388w, 343w, 323w. IR ($\nu_{KBr}$/cm$^{-1}$): 3271s, 3225s, 3149w, 3129s, 3074w, 2976s, 2929w, 2844w, 1633vs, 1600s, 1586s, 1574vs, 1539s, 1493s, 1464s, 1439s, 1423s, 1371s, 1352s, 1311vs, 1291vs, 1244vs, 1223vs, 1201s, 1155s, 1114w, 1098w, 1073s, 1051w, 1025s, 973w, 939w, 916w, 882w, 849w, 814w, 789w, 757vs, 710w, 679w, 660s, 643w, 607w, 528w, 492w, 445w. Raman (cm$^{-1}$): 3125w, 3073w, 3030w, 2979vs, 2943vs, 2846w, 2785w, 2762w, 2723w, 2626w, 1599w, 1578w, 1471s, 1403w, 1356vs, 1318w, 1292w, 1248w, 1166w, 1077w, 1051w, 907w, 880w, 855w, 798w, 769w, 612w, 530w, 465w, 391w, 274w, 199w, 165w. $^1$H NMR (400.00 MHz, DMF-$d_7$; ppm): δ ($SiMe_4$) 8.38 (t, 6.8, N6H, 1H), 8.30 (s, C8H, 1H), 7.28 (d, 8.1, C15H, 1H), 7.25 (tt, 8.1, 2.0, C13H, 1H), 7.03 (d, 8.4, C12H, 1H), 6.89 (d, 8.4, C14H, 1H), 4.80 (d, 5.8, C9H, 2H), 4.76 (sep, 7.0, C16H, 1H), 3.90 (s, C21H, 3H), 1.58 (d, 7.0, C17H, C18H, 6H). $^{13}$C NMR (100.58 MHz, DMF-$d_7$; ppm): δ ($SiMe_4$) 157.90 (C11), 156.36 (C6), 154.01 (C2), 150.52 (C4), 140.08 (C8), 128.78 (C13), 128.14 (C15), 127.60 (C10), 120.80 (C14), 119.75 (C5), 111.06 (C12), 55.79 (C21), 47.92 (C16), 39.59 (C9), 22.43 (C17, C18). $^{15}$N NMR (40.53 MHz, DMF-$d_7$, ppm): δ (DMF-$d_7$) 240.3 (N7), 227.4 (N1), 223.9 (N3), 178.5 (N9), 89.3 (N6).

2-Chloro-N6-(3-methoxybenzyl)-9-isopropyladenine (*3-OMe*L): Anal. Calcd for $C_{16}H_{18}N_5OCl$: C, 57.9; H, 5.5; N, 21.1. Found: C, 57.4; H, 5.2; N, 20.7%. IR ($\nu_{Nujol}$/cm$^{-1}$): 572s, 552w, 529s, 503w, 470s, 463s, 445w, 410w, 388w, 363w, 342s, 314s, 291w, 269w, 237s, 179vs, 166vs. IR ($\nu_{KBr}$/cm$^{-1}$): 3266s, 3217w, 3124s, 3066s, 2978vs, 2937vs, 2739s, 2676vs, 2623vs, 2604vs, 2531s, 2497vs, 1623vs, 1571s, 1534s, 1491s, 1475vs, 1445s, 1425s, 1398vs, 1384s, 1342s, 1311vs, 1291s, 1267s, 1247s, 1227vs, 1201s, 1172s, 1149w, 1073w, 1038s, 974w, 930w, 885w, 851w, 807w, 788w, 773w, 723w, 692w, 679w, 660w, 642w, 606w, 572w, 530w, 463w. Raman (cm$^{-1}$): 3122w, 3080w, 3053w, 2999s, 2979vs, 2941vs, 2837w, 2787w, 2763w, 2725w, 2621w, 2497w, 1610w, 1572w, 1464s, 1402w, 1356s, 1313w, 1291w, 1267w, 1248w, 1163w, 1078w, 1036w, 997w, 931w, 904w, 885w, 854w, 800w, 762w, 665w,



627w, 553w, 530w, 461w, 391w, 299w, 256w, 226w, 179w. $^1$H NMR (400.00 MHz, DMF-$d_7$; ppm): δ ($SiMe_4$) 8.88 (t, 6.8, N6H, 1H), 8.49 (s, C8H, 1H), 7.26 (t, 7.8, C14H, 1H), 7.08 (t, 1.9, C11H, 1H), 7.02 (d, 7.8, C15H, 1H), 6.84 (dd, 7.8, C13H, 1H), 4.80 (sep, 6.9, C16H, 1H), 4.80 (d, 6.6, C9H, 2H), 3.79 (s, C21H, 3H), 1.59 (d, 6.9, C17H, C18H, 6H). $^{13}$C NMR (100.58 MHz, DMF-$d_7$; ppm): δ ($SiMe_4$) 160.51 (C12), 155.65 (C6), 154.33 (C2), 150.38 (C4), 141.71 (C10), 139.87 (C8), 130.05 (C14), 120.38 (C5), 118.50 (C5), 114.14 (C11), 112.88 (C13), 55.44 (C21), 48.33 (C16), 44.24 (C9), 22.33 (C17, C18). $^{15}$N NMR (40.53 MHz, DMF-$d_7$, ppm): δ (DMF-$d_7$) 241.6 (N7), 226.1 (N1), 223.1 (N3), 179.6 (N9), 95.6 (N6).

2-Chloro-N6-(2,3-dimethoxybenzyl)-9-isopropyladenine (*2,3-diOMe*L): Anal. Calcd for $C_{17}H_{20}N_5O_2Cl$: C, 56.4; H, 5.6; N, 19.4. Found: C, 56.6; H, 5.6; N, 18.9 %. IR ($\nu_{Nujol}$/cm$^{-1}$): 535vs, 495w, 461w, 428w, 422w, 389w, 343w, 320w, 259w, 220w. IR ($\nu_{KBr}$/cm$^{-1}$): 3259s, 3217s, 3186s, 3144w, 3072w, 2970w, 2938s, 2839w, 1622vs, 1573s, 1544s, 1476vs, 1425vs, 1396w, 1353s, 1341s, 1313vs, 1292vs, 1261s, 1228vs, 1202s, 1165w, 1105w, 1084w, 1061vs, 999s, 978w, 932s, 890w, 852w, 803w, 785s, 754s, 703w, 680w, 664s, 641w, 606w, 535w, 494w, 430w. Raman (cm$^{-1}$): 3125w, 3079w, 2986w, 2937s, 2839w, 1613w, 1572s, 1478s, 1405w, 1382w, 1352vs, 1315w, 1289w, 1266w, 1168w, 1087w, 999w, 891w, 799s, 734w, 705w, 627w, 604w, 533w, 389s, 219w, 158s. $^1$H NMR (300.00 MHz, DMF-$d_7$, ppm): δ ($SiMe_4$) 8.49 (t, 6.8, N6H, 1H), 8.29 (s, C8H, 1H), 6.99 (m, C13H, C14H, C15H, 3H), 4.85 (d, 5.9, C9H, 2H), 4.76 (sep, 6.8, C16H, 1H), 3.91 (s, C19, 3H), 3.88 (s, C20, 3H), 1.58 (d, 6.8, C17H, C18H, 6H). $^{13}$C NMR (75.43 MHz, DMF-$d_7$, ppm): δ ($SiMe_4$) 156.19 (C6), 153.99 (C11), 153.44 (C2), 150.54 (C4), 147.53 (C12), 140.05 (C8), 133.54 (C10), 124.40 (C14), 120.71 (C15), 119.77 (C5), 112.42 (C13), 60.57 (C19), 56.14 (C20), 47.92 (C16), 39.17 (C9), 22.42 (C17, C18). $^{15}$N NMR (30.40 MHz, DMF-$d_7$, ppm): δ (DMF-$d_7$) 240.1 (N7), 227.8 (N1), 224.3 (N3), 179.8 (N9), 92.3 (N6).

2-Chloro-N6-(2,4-dimethoxybenzyl)-9-isopropyladenine (*2,4-diOMe*L): Anal. Calcd for $C_{17}H_{20}N_5O_2Cl$: C, 56.4; H, 5.6; N, 19.4. Found: C, 56.4; H, 5.9; N, 19.0%. IR ($\nu_{Nujol}$/cm$^{-1}$): 567s, 534vs,

510s, 455w, 409w, 390w, 347w. IR ($\nu_{KBr}$/cm$^{-1}$): 3261s, 3219s, 3184w, 3140w, 3108w, 3072w, 2993w, 2970w, 2941w, 2916w, 2835w, 1616vs, 1587vs, 1572s, 1537w, 1504s, 1468s, 1452s, 1435w, 1415s, 1355s, 1309vs, 1293vs, 1266s, 1227vs, 1208vs, 1158s, 1120s, 1074s, 1040s, 1009w, 975w, 933s, 913w, 889w, 862w, 831s, 779w, 721w, 682w, 665s, 644w, 603w, 569w, 534w, 510w, 455w. Raman (cm$^{-1}$): 3109w, 3077w, 2990s, 2943s, 2919s, 2838w, 1612w, 1569s, 1474s, 1460s, 1401w, 1386w, 1352vs, 1308s, 1259w, 1204w, 1181w, 1159w, 1119w, 1037w, 916w, 888w, 795s, 776w, 720w, 666w, 605w, 568w, 531w, 441w, 391s, 330w, 296w, 268w, 155s. $^{1}$H NMR (300.00 MHz, DMF-$d_7$, ppm): δ ($SiMe_4$) 8.28 (s, 1H, C8H), 8.23 (t, 6.8, N6H, 1H), 7.23 (d, 8.2, C15H, 1H), 6.62 (d, 2.4, C12H, 1H), 6.49 (dd, 8.2, 2.4, C14H, 1H), 4.76 (sep, 6.8, C16H, 1H), 4.72 (d, 5.9, C9H, 2H), 3.89 (s, C21H, 3H), 3.80 (s, C22H, 3H), 1.58 (d, 6.8, C17H, C18H, 6H). $^{13}$C NMR (75.43 MHz, DMF-$d_7$, ppm): δ ($SiMe_4$) 161.03 (C13), 158.99 (C11), 156.27 (C6), 154.01 (C2), 150.49 (C4), 139.96 (C8), 129.37 (C15), 120.32 (C10), 119.71 (C5), 104.90 (C14), 98.93 (C12), 55.88 (C19), 55.65 (C20), 47.90 (C16), 39.36 (C9), 22.42 (C17, C18). $^{15}$N NMR (30.40 MHz, DMF-$d_7$, ppm): δ (DMF-$d_7$) 241.1 (N7), 228.5 (N1), 224.1 (N3), 179.6 (N9), 91.8 (N6).

2-Chloro-N6-(3,4-dimethoxybenzyl)-9-isopropyladenine (*3,4-diOMe*L): Anal. Calcd for $C_{17}H_{20}N_5O_2Cl$: C, 56.4; H, 5.6; N, 19.4. Found: C, 56.7; H, 5.9; N, 20.0%. IR ($\nu_{Nujol}$/cm$^{-1}$): 563vs, 542vs, 494w, 459w, 438s, 418w, 363w, 314w, 235s. IR ($\nu_{KBr}$/cm$^{-1}$): 3261s, 3221w, 3190w, 3133w, 3065w, 2989w, 2970w, 2935w, 2906w, 2833w, 1624vs, 1575s, 1514vs, 1463s, 1413s, 1352w, 1314vs, 1294s, 1264vs, 1227vs, 1204w, 1154w, 1135s, 1099w, 1073w, 1030s, 979w, 933w, 906w, 885w, 843w, 796w, 788w, 763w, 681w, 663w, 639w, 600w, 563w, 543. Raman (cm$^{-1}$): 3133w, 3073w, 3030w, 2978s, 2938vs, 2835w, 1606s, 1591w, 1573s, 1472s, 1352vs, 1318s, 1291w, 1253w, 1167w, 1136w, 1074w, 1028w, 935w, 885w, 798w, 763s, 599w, 564w, 541w, 461w, 438w, 393s, 305w, 257w, 180w. $^{1}$H NMR (400.00 MHz, DMF-$d_7$; ppm): δ ($SiMe_4$) 8.60 (t, 6.0, N6H, 1H), 8.27 (s, C8H, 1H), 7.19 (s, C11H, 1H), 6.98 (dd, 8.2, 1.6, C15H, 1H), 6.92 (d, 8.2, C14H, 1H), 4.74 (sep, 6.6, C16H, 1H), 4.71 (d, 6.2, C9H, 2H), 3.82 (s, C21H, 3H), 3.79 (s, C22H, 3H), 1.57 (d, 6.6, C17H, C18H, 6H). $^{13}$C NMR



(100.58 MHz, DMF-$d_7$; ppm): δ ($SiMe_4$) 155.99 (C6), 153.92 (C2), 150.51 (C4), 149.86 (C12), 149.16 (C13), 139.99 (C8), 132.73 (C10), 120.65 (C15), 119.68 (C5), 112.94 (C11), 112.42 (C14), 56.08 (C21), 55.96 (C22), 47.89 (C16), 44.15 (C9), 22.41 (C17, C18). $^{15}$N NMR (40.53 MHz, DMF-$d_7$, ppm): δ (DMF-$d_7$) 240.3 (N7), 227.8 (N1), 223.7 (N3), 179.3 (N9), 95.9 (N6).

2-Chloro-N6-(3,5-dimethoxybenzyl)-9-isopropyladenine (*3,5-diOMe*L): Anal. Calcd for $C_{17}H_{20}N_5O_2Cl$: C, 56.4; H, 5.6; N, 19.4. Found: C, 56.2; H, 5.7; N, 19.2%. IR ($\nu_{Nujol}$/cm$^{-1}$): 544vs, 526s, 487w, 459w, 436w, 417w, 387w, 345w, 318w, 214w. IR ($\nu_{KBr}$/cm$^{-1}$): 3269s, 3225s, 3131w, 3084w, 2977s, 2939w, 2843w, 1644vs, 1600vs, 1577s, 1539s, 1463vs, 1431s, 1422s, 1351vs, 3111vs, 1296vs, 1268w, 1240vs, 1205vs, 1158vs, 1144s, 1102w, 1065s, 1047s, 1015w, 932s, 911s, 881w, 826s, 787w, 735w, 694w, 678w, 665s, 650w, 635w, 604w, 545w. Raman (cm$^{-1}$): 3130w, 3103w, 3014s, 2976vs, 2937vs, 2918vs, 2871w, 2844w, 1595s, 1576s, 1537w, 1479s, 1383s, 1356vs, 1294w, 1232w, 1201w, 1186w, 1163w, 1097w, 1074w, 1043w, 1016w, 993vs, 931w, 908w, 881w, 796s, 731w, 650w, 623w, 604w, 542w, 526w, 484w, 457w, 434w, 391s, 310w, 256s, 229s, 202w, 172s. $^{1}$H NMR (400.00 MHz, DMF-$d_7$; ppm): δ ($SiMe_4$) 8.66 (t, 6.4, N6H, 1H), 8.29 (s, C8H, 1H), 6.65 (d, 2.2, C11H, C15H, 2H), 6.42 (d, 2.2, C13H, 1H), 4.76 (sep, 6.8, C16H, 1H), 4.75 (d, 6.8, C9H, 2H), 3.78 (s, C21H, C22H, 6H), 1.57 (d, 6.8, C17H, C18H, 6H). $^{13}$C NMR (100.58 MHz, DMF-$d_7$; ppm): δ ($SiMe_4$) 161.66 (C12, C14), 156.07 (C6), 153.91 (C2), 150.57 (C4), 142.68 (C10), 140.10 (C8), 119.69 (C5), 106.37 (C11, C15), 99.05 (C13), 55.54 (C21, C22), 47.90 (C16), 44.31 (C9), 22.40 (C17, C18). $^{15}$N NMR (40.53 MHz, DMF-$d_7$, ppm): δ (DMF-$d_7$) 240.2 (N7), 227.6 (N1), 224.7 (N3), 179.4 (N9), 93.9 (N6).

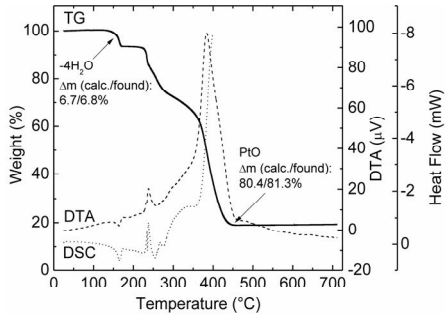


**Figure S1**. TG (full line), DTA (dashed line) and DSC (doted line) curves of thermal decomposition of [Pt(*3,5-diOMe*L)$_2$(ox)] · 4H$_2$O (**7**)



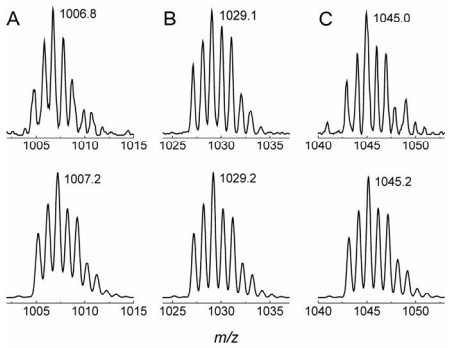


**Figure S2**. The isotopic distribution representation of the [Pt(*2,4-diOMe*L)$_2$(ox)+H]$^+$ (A) molecular peak and its [Pt(*2,4-diOMe*L)$_2$(ox)+Na]$^+$ (B) and [Pt(*2,4-diOMe*L)$_2$(ox)+K]$^+$ (C) adducts as observed (up) and calculated (down) for the complex **5**.

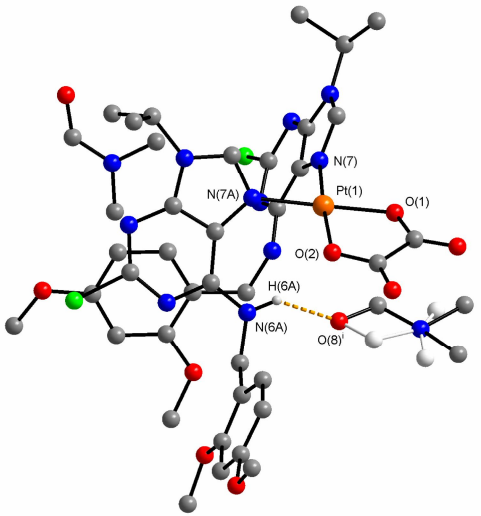


**Figure S3**. Molecular structure of [Pt(*2,4-diOMe*L)$_2$(ox)] · 2DMF (**5** · 2DMF), showing the N(6A)–H(6A)···O(8)$^{i}$ hydrogen bond [dashed orange lines; symmetry code: (i) x, 1.5 – y, z – 0.5] and disordered parts of a DMF molecule (light-grey color). H-atoms not involved into the discussed hydrogen bond are omitted for clarity.



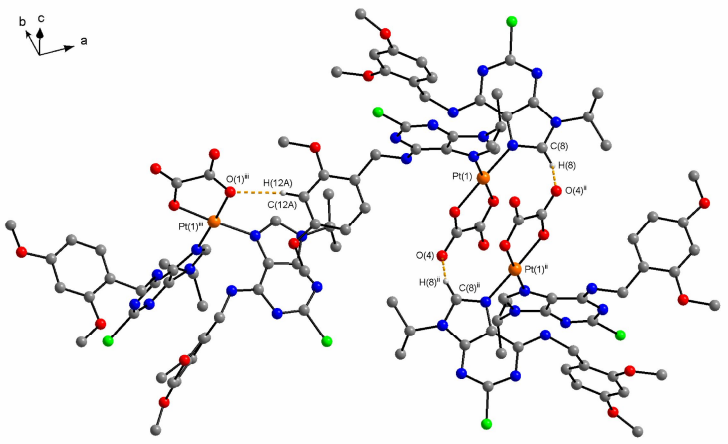


**Figure S4**. Part of the crystal structure of [Pt(*2,4-diOMe*L)$_2$(ox)] · 2DMF (**5** · 2DMF) showing the C(8)–H(8)···O(4)$^{ii}$ and C(12A)–H(12A)···O(1)$^{iii}$ interactions [dashed orange lines; symmetry codes: (ii) 1 – x, 1 – y, –z; (iii) x – 0.5, 1.5 – y, –z]. DMF molecules and H-atoms not involved into the discussed interactions are omitted for clarity.

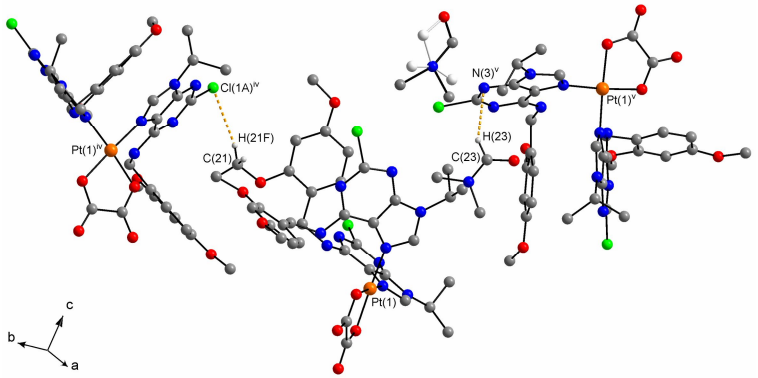


**Figure S5**. Part of the crystal structure of [Pt(*2,4-diOMe*L)$_2$(ox)] · 2DMF (**5** · 2DMF) showing the C(21)−H(21F)···Cl(1A)$^{iv}$ and C(23)−H(23)···N(3)$^{v}$ interactions [dashed orange lines; symmetry codes: (iv) 0.5 – x, y + 0.5, z, (v) 1 – x, y – 0.5, 0.5 – z]. H-atoms not involved into the discussed interactions are omitted for clarity.

# APPENDIX IV

European Journal of Medicinal Chemistry xxx (2010) 1–6

Contents lists available at ScienceDirect

European Journal of Medicinal Chemistry

journal homepage: http://www.elsevier.com/locate/ejmech

Original article

# *Roscovitine*-based CDK inhibitors acting as N-donor ligands in the platinum(II) oxalato complexes: Preparation, characterization and *in vitro* cytotoxicity

Zdeněk Trávníček [a,*], Pavel Štarha [a], Igor Popa [a], Radim Vrzal [b], Zdeněk Dvořák [b]

[a] Department of Inorganic Chemistry, Faculty of Science, Palacký University, Tř. 17. listopadu 12, CZ-771 46 Olomouc, Czech Republic
[b] Department of Cell Biology and Genetics, Faculty of Science, Palacký University, Šlechtitelů 11, CZ-783 71 Olomouc, Czech Republic

ARTICLE INFO

*Article history:*
Received 18 June 2010
Received in revised form
9 July 2010
Accepted 15 July 2010
Available online xxx

*Keywords:*
Platinum(II) complexes
Oxalate
Cytotoxicity
CDK inhibitors
Multinuclear NMR

ABSTRACT

The reactions of potassium bis(oxalato)platinate dihydrate with two molar equivalents of the potent adenine-based cyclin-dependent kinase inhibitor 2-(1-ethyl-2-hydroxyethylamino)-N6-(benzyl)-9-isopropyladenine (*Roscovitine*; Ros) and its benzyl-substituted analogues, i.e. 2-(1-ethyl-2-hydroxyethylamino)-N6-(2-methoxybenzyl)-9-isopropyladenine (2*OMe*Ros), 2-(1-ethyl-2-hydroxyethylamino)-N6-(3-methoxybenzyl)-9-isopropyladenine (3*OMe*Ros) and 2-(1-ethyl-2-hydroxyethylamino)-N6-(4-methoxybenzyl)-9-isopropyladenine (4*OMe*Ros), were performed and the $[Pt(ox)(Ros)_2]\cdot{}^3/_4\ H_2O$ (**1**), $[Pt(ox)(2OMeRos)_2]\cdot H_2O$ (**2**), $[Pt(ox)(3OMeRos)_2]\cdot ½H_2O$ (**3**) and $[Pt(ox)(4OMeRos)_2]\cdot{}^3/_4\ H_2O$ (**4**) platinum(II) oxalato complexes were obtained. The methods of the elemental analysis, IR, Raman and NMR spectroscopy, ESI + mass spectrometry, molar conductivity measurement and TG/DTA thermal analysis were performed to characterize the obtained products. The complexes **1**–**4** involve tetracoordinated central Pt(II) atom with one bidentate-coordinated oxalate dianion (ox) and two monodentate adenine-based molecules (*n*Ros), thus giving the square-planar geometry around the metal centre with a $PtN_2O_2$ donor set. *In vitro* cytotoxic activity of the complexes against ovarian carcinoma (A2780), *cisplatin* resistant ovarian carcinoma (A2780cis), malignant melanoma (G-361), lung carcinoma (A549), cervix epitheloid carcinoma (HeLa), breast adenocarcinoma (MCF7) and osteosarcoma (HOS) human cancer cell lines was evaluated. All the tested complexes exceeded the *in vitro* cytotoxicity of *cisplatin* and *oxaliplatin* against HeLa, A2780cis and, except for **2**, also against HOS cancer cells. The complex **1** was also tested for its cytotoxicity in primary cultures of human hepatocytes and it was not found to be hepatotoxic up to the concentration of 50.0 μM.



## 1. Introduction

2-(1-Ethyl-2-hydroxyethylamino)-N6-(benzyl)-9-isopropyladenine (*Roscovitine*; Ros) is a substance derived from a plant hormone N6-(benzyl)adenine (6-benzylaminopurine) [1]. *Roscovitine* belongs to the group of adenine-based cyclin-dependent kinase inhibitors (CDKI) specifically inhibiting the mentioned proteins, which was recently successfully tested *in vivo* on patients with non-small cell lung cancer [2,3].

Quite a few complexes of diverse transition metals involving variously substituted N6-(benzyl)adenine derivatives as N-donor ligands have been reported to date [4–7]. Among them, a variety of platinum(II) complexes has been recently prepared in our laboratory (see lit. 8, 9 and references cited therein). These complexes were tested for their *in vitro* cytotoxic activity against malignant melanoma (G-361), osteosarcoma (HOS), breast adenocarcinoma (MCF7) and chronic myelogenous leukemia (K-562) human cancer cell lines. The best results were obtained for *cis*-$[PtCl_2(ba)_2]$ and $[Pt(ox)(ba)_2]$; ba symbolizes N6-(benzyl)adenine-based N-donor ligands. The cytotoxic activity of *cis*-$[PtCl_2(Ros)_2]$ ($IC_{50}$ = 1.0 μM against G-361, HOS and K-562 and 2.0 μM against MCF7), *cis*-$[PtCl_2(Boh)_2]$ ($IC_{50}$ = 2.0 μM against HOS, 3.0 μM against G-361 and K-562 and 5.0 μM against MCF7) and *cis*-$[PtCl_2(iOc)_2]$ ($IC_{50}$ = 3.0 μM against HOS and 4.0 μM against G-361, K-562 and MCF7) was found to be comparable or even higher than those of *cisplatin* ($IC_{50}$ = 3.0 μM against HOS and G-361, 5.0 μM against K-562 and 11.0 μM against MCF7), *oxaliplatin* ($IC_{50}$ = 7.0 μM against HOS and G-361, 8.0 μM against K-562 and 18.0 μM against MCF7), and free CDKI *Roscovitine* ($IC_{50}$ = 15.0 μM against MCF7, 19.0 μM against G-361, 20.0 μM against HOS and 50.0 μM against K-562), *Bohemine* [2-(3-hydroxypropylamino)-N6-(benzyl)-9-isopropyladenine, Boh; $IC_{50}$ = 28.0 μM against MCF7, 46.0 μM against G-361, 58.0 μM against HOS and 93.0 μM against K-562] and *isopropyl-Olomoucine* [2-(2-hydroxyethylamino)-N6-(benzyl)-9-isopropyladenine, iOc; $IC_{50}$ = 61.0 μM against MCF7, 118.0 μM against K-562, 120.0 μM against HOS and 135.0 μM against G-361], as determined by an acetoxymethyl (AM) assay [9].

* Corresponding author. Tel.: +420 585 634 352; fax: +420585 634 954.
*E-mail address:* zdenek.travnicek@upol.cz (Z. Trávníček).

0223-5234/$ – see front matter © 2010 Elsevier Masson SAS. All rights reserved.
doi:10.1016/j.ejmech.2010.07.025

Recently, we reported a series of $[Pt(ox)(L)_2]$ complexes with 2-chloro-N6-(benzyl)-9-isopropyladenine derivatives (L) and their *in vitro* cytotoxicity against HOS and MCF7 human cancer cell lines [8]. The complexes $[Pt(ox)(L_1)_2]$, $[Pt(ox)(L_2)_2]$ and $[Pt(ox)(L_3)_2]$ were more *in vitro* cytotoxic ($IC_{50}$ = 9.2, 4.3, and 3.6 μM, respectively) against MCF7 cells as compared with *cisplatin* ($IC_{50}$ = 19.6 μM), two last-mentioned complexes also against HOS cancer cell line with the $IC_{50}$ values of 3.6 and 5.4 μM ($IC_{50}$ = 34.2 μM for *cisplatin*); 2-chloro-N6-(benzyl)-9-isopropyladenine ($L_1$), 2-chloro-N6-(2-methoxybenzyl)-9-isopropyladenine ($L_2$), 2-chloro-N6-(2,4-dimethoxybenzyl)-9-isopropyladenine ($L_3$). The molecular and crystal structures of $[Pt(ox)(L_3)_2]\cdot 2DMF$, a representative of the mentioned complexes, have been crystallographically determined, which showed the slightly distorted square-planar geometry around the central Pt(II) ion with two $L_3$ molecules coordinated through their N7 atoms and one bidentate-coordinated oxalate dianion; DMF stands for *N*,*N*′-dimethylformamide.

Owing to the fact that both the *cis*-$[PtCl_2(ba)_2]$ [9] complexes with N6-(benzyl)adenine-based CDK inhibitor and $[Pt(ox)(L)_2]$ [8] complexes with 2-chloro-N6-(benzyl)-9-isopropyladenine derivatives were previously determined as highly *in vitro* cytotoxic substances, we decided to prepare another series of the platinum (II) oxalato complexes, however now with N6-(benzyl)adenine-based CDK inhibitors, which were found to be antitumour active themselves [2,3]. Because the structure of the prepared complexes **1**–**4** contains Pt(ox) motif, which is suitable in terms of anticancer activity of platinum complexes [10,11], and antitumour active N-donor organic molecule, we expected interesting biological properties of the complexes, which encouraged us to evaluate the *in vitro* cytotoxic activity against a broad spectrum of human cancer cell lines as well as against human hepatocytes.

## 2. Results and discussion

### 2.1. General properties

The platinum(II) oxalato complexes $[Pt(ox)(Ros)_2]\cdot {}^3/_4\,H_2O$ (**1**), $[Pt(ox)(2OMeRos)_2]\cdot H_2O$ (**2**), $[Pt(ox)(3OMeRos)_2]\cdot ½H_2O$ (**3**) and $[Pt(ox)(4OMeRos)_2]\cdot {}^3/_4\,H_2O$ (**4**) were synthesized and characterized by various physical methods. The preparations came out of $K_2[Pt(ox)_2]\cdot 2H_2O$ that reacted with two molar equivalents of the *n*Ros organic compounds (Scheme 1) [8]. The complexes **1**–**4** formed in the period of two days as brown gummy solids after evaporation of the reaction mixture (distilled water/isopropanol), which were subsequently pulverized in diethyl ether to give ocher powder products. The obtained results of elemental analyses determining the percentage contents of carbon, hydrogen and nitrogen are in good agreement with the calculated ones (Section 4.2). The molar conductivity values of the complexes **1**–**4** ($10^{-3}$ M DMF solutions) ranging from 10.5 to 16.7 S $cm^2$ $mol^{-1}$ (see Appendix A, Supplementary data) are significantly lower than the value of 65.0 S $cm^2$ $mol^{-1}$, a value separating non-electrolytes from 1:1 electrolytes in the used solvent [12]. The platinum(II) oxalato complexes **1**–**4** are soluble in DMF, chloroform, ethanol, methanol and acetone, low solubility was observed in the distilled water. Although efforts to prepare crystals suitable for single-crystal X-ray analysis were unsuccessful it may be assumed that the structure of complexes **1**–**4** is very similar to that of $[Pt(ox)(L_3)_2]$, where $L_3$ stands for 2-chloro-N6-(2,4-dimethoxybenzyl)-9-isopropyladenine, in which the platinum(II) atom is coordinated by one oxalate anion and by two $L_3$ ligands in a distorted square-planar arrangement [8].

The water of crystallization content in the prepared $[Pt(ox)(Ros)_2]\cdot xH_2O$ complexes ($x = {}^3/_4$ for **1** and **4**, 1 for **2** and ½ for **3**) was determined by thermogravimetry (TG). The dehydration began right after the start of the analysis (see Appendix A, Supplementary data). This process is accompanied by a very weak endothermic effect (endo-effect) on the differential thermal analysis (DTA) curves of the complexes **2** and **4**; in the case of **1** and **3** no endo-effect was observed. Thermal decomposition of the dehydrated complexes **1**–**4** started at 160–186 °C and it proceeded up to 448–478 °C without formation of any thermally stable intermediates. After that the final product, platinum(II) oxide (PtO), is formed. Four exothermic effects (exo-effects), connected with this degradation, were found on the DTA curves of **1**–**4**. Theoretical total weight losses calculated to PtO (**1**, 79.0%; **2**, 80.3%; **3**, 80.1%; **4**, 80.2%) differ insignificantly from the observed ones (**1**, 80.0%; **2**, 79.8%; **3**, 81.0%; **4**, 80.5%).

### 2.2. IR and Raman spectroscopy

Two bands assignable to the $\nu_{as}$(C=O) vibration of the oxalate dianion coordinated in the complexes **1**–**4** were found at 1670–1673 $cm^{-1}$ and 1711–1720 $cm^{-1}$. The maxima of the $\nu_s$(C–O) vibration were detected between 1353 and 1357 $cm^{-1}$. The ν(Pt–O) band was observed in the 566–571 $cm^{-1}$ region. The bands related to a five-membered ring ($PtO_2C_2$) deformation appeared at 461–468 $cm^{-1}$ [13].

The second type of ligand coordinated to the Pt(II) atom in the complexes **1**–**4**, i.e. 2-(1-ethyl-2-hydroxyethylamino)-N6-(benzyl)-9-isopropyladenine and its benzyl-substituted analogues (*n*Ros), showed several characteristic bands, as well. Namely, the $\nu(C-H)_{ar}$, $\nu(C-H)_{al}$, ν(C=N), ν(C=C) and $\nu(C-O)_{al}$ vibrations were clearly detected in the IR spectra of the complexes **1**–**4**, while the maxima of the $\nu(C-O)_{ar}$ band were found only in the case of **2**–**4** involving substituted phenyl group [14–16]. The most intensive one is the ν

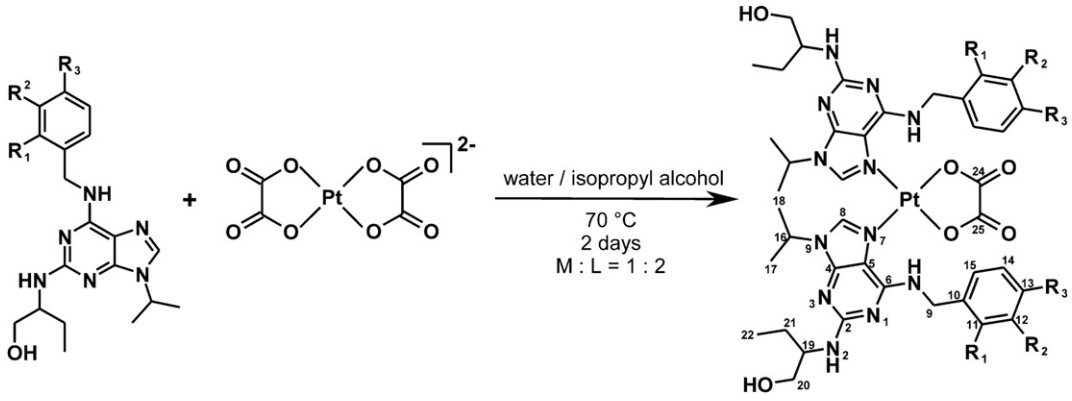


**Scheme 1.** Preparation of the $[Pt(ox)(nRos)_2]\cdot xH_2O$ complexes **1**–**4** given together with the atom numbering.

(C═N) vibration, a typical one for compounds of this type, which was found at 1610–1611 $cm^{-1}$. The maxima of these bands were shifted in the spectra of complexes against free *n*Ros ligands by $|\Delta| = 1–10$ $cm^{-1}$, where Δ is defined as a difference between the maxima position of the complexes **1**–**4** and appropriate *n*Ros molecules. The ν(Pt–N) vibration, that indirectly proved the coordination of the *n*Ros molecules to the metal centre through a nitrogen atom, has its maxima between 520 and 527 $cm^{-1}$.

Most bands detected in the infrared spectra of the platinum(II) oxalato complexes **1**–**4** also appeared in the appropriate Raman spectra. The ν(Pt–N) bands were observed at 523–529 $cm^{-1}$ and the ν(Pt–O) bands between 569 and 570 $cm^{-1}$. The maxima of the ν(C═N) band of a purine ring were found in the 1607–1611 $cm^{-1}$ region. The presence of the oxalate dianion in the structure of **1**–**4** was confirmed by bands assignable to $\nu_{as}$(C═O) appearing at 1677–1681 $cm^{-1}$ and 1710–1713 $cm^{-1}$. The $\nu_s(C–O)_{ox}$ vibration, observed at 1353–1357 $cm^{-1}$ in the IR spectra, was not detected in any Raman spectrum of **1**–**4**, because it is overlaid by a band of very strong intensity at about 1320 $cm^{-1}$, which most likely belongs to the skeletal stretching vibrations of a purine ring [17].

### 2.3. ESI + mass spectrometry

The $[Pt(ox)(nRos)_2 + H]^+$ peaks were detected in the mass spectra at 992.3 (for **1**), 1052.4 (for **2**), 1052.3 (for **3**) and 1052.4 (for **4**) *m*/*z*, which indirectly confirmed the composition of the discussed complexes (Fig. S1 in Supplementary data). Moreover, adducts with the sodium (for **1**) and potassium (**1**–**3**) ions were also detected. The peaks assignable to the $[Pt(ox)(nRos) + H]^+$ fragment also appeared in the mass spectra of the studied compounds at 637.4 (**1**), 667.2 (**2** and **4**) and 667.3 (**3**) *m*/*z*. The mass difference between the values found for the $[Pt(ox)(nRos)_2 + H]^+$ and $[Pt(ox)(nRos) + H]^+$ peaks correlate well the mass of the appropriate *n*Ros molecule, whose peaks, $[nRos + H]^+$, were found at 355.3 *m*/*z* for **1** and 385.3 *m*/*z* for the complexes **2**–**4**.

The $[Pt(nRos^-)_2 + H]^+$ fragments formed by elimination of the oxalic acid from the molecules of the unsolvated complexes **1**–**4** and the peaks assignable to these fragments were also clearly detected. These values differ from those of $[Pt(ox)(nRos)_2 + H]^+$ ones approximately by 90 *m*/*z*, which corresponds to the mass of the mentioned oxalic acid (90.0 *m*/*z* calc. for $C_2H_2O_4$). Similar situation can be discussed also in case of $[Pt(ox)(nRos) + H]^+$ and $[Pt(nRos^{2-}) + H]^+$ fragments, because the peaks of the latter were found in the mass spectra of the prepared complexes **1**–**4** with mass differing by 90 *m*/*z* form the mentioned $[Pt(ox)(nRos) + H]^+$.

The determined values of all the peaks discussed in this section as well as the observed isotopic distribution representation correlated well with the calculated ones. It should be also noted that the other peaks detected between 500 and 600 *m*/*z* were not interpreted, because they represent the mixture of fragments.

### 2.4. NMR spectroscopy

The above mentioned NMR experiments were performed for the complexes **1**–**4** as well as for the free *n*Ros organic compounds. The obtained results gave evidence of the composition of the platinum(II) complexes. The most important coordination shifts ($\Delta\delta = \delta_{complex} - \delta_{ligand}$; ppm) are summarized in Table 1.

All the signals in the $^1H$, $^{13}C$ and $^1H–^{15}N$ gs-HMBC spectra of the *n*Ros molecules were found in the corresponding spectra of **1**–**4**. However, Δδ of the N7 atom of the adenine ring are significantly higher than those of the remaining nitrogen atoms in the $^1H–^{15}N$ gs-HMBC spectra (Table 1). Similarly, the coordination shifts of the carbon atoms at the positions 5 and 8, neighbouring to the mentioned N7 atom, exceeded the rest of the $^{13}C$ signals found in the carbon spectra. The highest changes of the chemical shift in the $^1H$ NMR spectra were observed for the N6H and C8H protons. Based on our extensive experience in the field of platinum(II) complexes involving N6-(benzyl)adenine derivatives [8,9], where the similar NMR results were supported by the molecular structure determined by a single-crystal X-ray analysis, we conclude that both *n*Ros molecules are coordinated to the Pt(II) centre through their N7 atoms of the adenine moieties. One more signal at ~166.2 ppm was detected in the $^{13}C$ NMR spectra of the complexes **1**–**4** that was not observed in the spectra of free *n*Ros compounds. This signal belongs to the carbon atoms (C24, C25) of the oxalate dianion bidentate-coordinated to the Pt(II) atom.

All the chemical shifts in the $^{195}Pt$ NMR spectra of the prepared platinum(II) oxalato complexes were found at −1676 ppm (Fig. S2 in Supplementary data), which is in good agreement with our previous work focusing on similar compounds of the general composition $[Pt(ox)(L)_2]$ complexes [L symbolizes 2-chloro-N6-(benzyl)-9-isopropyladenine or its analogues with substituted benzyl ring], whose signals were observed at ca. −1690 ppm [8].

### 2.5. In vitro cytotoxic activity

Recently, we reported a series of seven platinum(II) oxalato complexes, $[Pt(ox)(L)_2]$, whose *in vitro* cytotoxicity against the HOS and MCF7 human cancer cell lines was found to be in some cases several times higher as compared to *cisplatin*. These complexes involved cytotoxic inactive organic compounds derived from 2-chloro-N6-(benzyl)-9-isopropyladenine (L) as N-donor carrier ligands [8]. Although it is well known that the cytotoxicity of square-planar platinum(II) complexes bears no relation to the N-donor ligand elimination [18], it can be anticipated that the resulting cytotoxicity may be positively affected by an incorporation of biologically active molecule into the structure of such complexes. That is why we decided to substitute this part of the biologically active complexes (i.e. N-donor carrier ligands) by highly *in vitro* cytotoxic organic molecules (*n*Ros) belonging to the group of the adenine-based CDK inhibitors. It has to be noted that the positive finding related with the tested $[Pt(ox)(nRos)_2]$ (**1**–**4**) complexes is the fact that the complexes are well soluble up to the concentration of 50.0 μM, which is significantly better solubility as compared with $[Pt(ox)(L)_2]$ [8].

The obtained results of the *in vitro* cytotoxicity testing are summarized in Section 4.2 and graphically depicted in Fig. 1. The $IC_{50}$ values (μM) of the complexes **1**–**4** were compared with those of the clinically used platinum-based drugs *cisplatin* (A549, >50.0;

**Table 1**
Selected $^1H$, $^{13}C$ and $^{15}N$ NMR coordination shifts ($\Delta\delta = \delta_{complex} - \delta_{ligand}$; ppm) calculated for the prepared complexes **1**–**4**.

| Complex | $^1H$ NMR | | | | $^{13}C$ NMR | | | | | | $^{15}N$ NMR | | | | | |
|---|---|---|---|---|---|---|---|---|---|---|---|---|---|---|---|---|
| | N2H | N6H | C8H | O20H | C2 | C4 | C5 | C6 | C8 | C24, C25 | N1 | N2 | N3 | N6 | N7 | N9 |
| **1** | 0.52 | 0.79 | 0.83 | 0.10 | 0.15 | −0.72 | −3.50 | −2.32 | 3.82 | −1.57 | 6.8 | 4.0 | 7.6 | 1.8 | −115.8 | 5.6 |
| **2** | 0.50 | 1.04 | 0.74 | 0.04 | 0.20 | −0.80 | −3.52 | −2.42 | 3.86 | −1.68 | −2.0 | −1.4 | 2.1 | 4.1 | −119.1 | 1.3 |
| **3** | 0.52 | 0.79 | 0.92 | 0.14 | 0.17 | −0.78 | −3.45 | −2.27 | 3.86 | −1.58 | 4.4 | 3.7 | 10.9 | 6.8 | −114.5 | 6.7 |
| **4** | 0.55 | 0.79 | 0.79 | −0.03 | 0.19 | −0.76 | −3.51 | −2.31 | 3.95 | −1.64 | −1.7 | −3.6 | 3.0 | 11.0 | −121.5 | 0.9 |

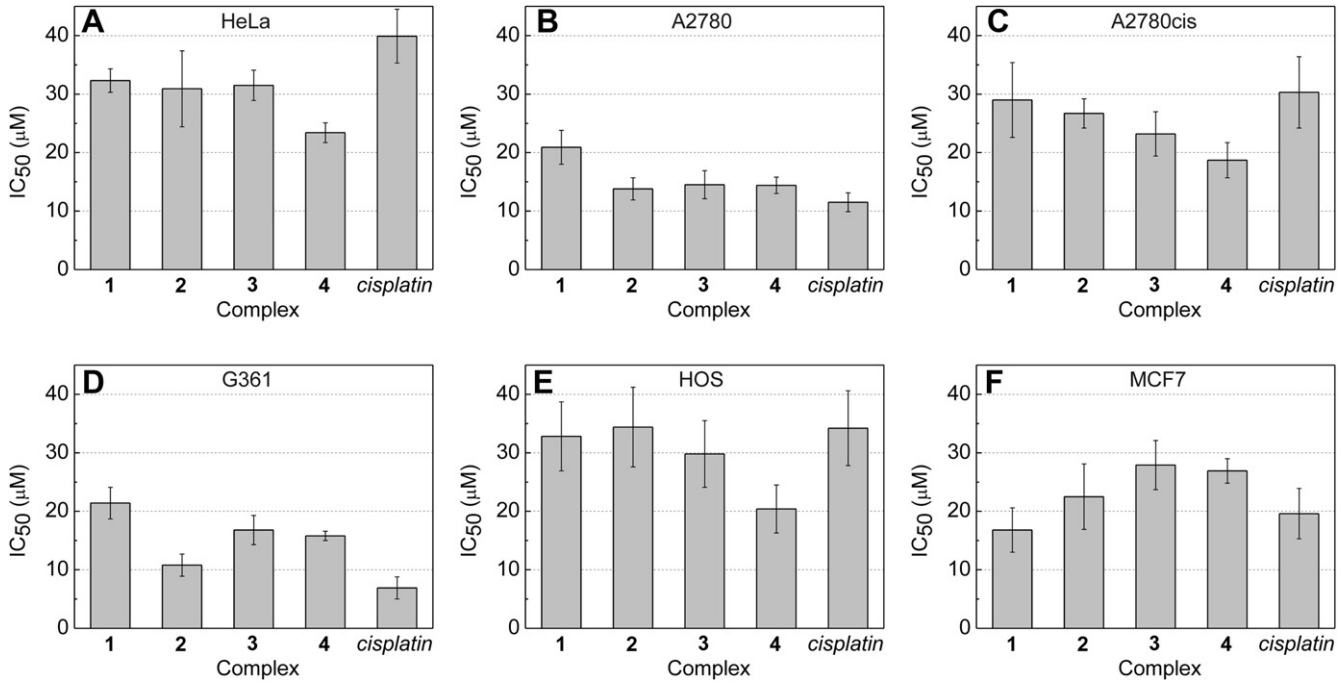


**Fig. 1.** The results of the *in vitro* cytotoxic activity testing of the complexes **1**–**4** and their comparison with the commercially applied platinum-based drug *cisplatin* as determined by an MTT assay against cervix epitheloid carcinoma (HeLa), ovarian carcinoma (A2780), ovarian carcinoma *cisplatin* resistant (A2780cis), malignant melanoma (G-361), osteosarcoma (HOS) and breast adenocarcinoma (MCF7) human cancer cell lines; the results determined for **1**–**4** against lung carcinoma (A549) cells as well as the $IC_{50}$ values of oxaliplatin against all the employed cell lines are not depicted, because the *in vitro* cytotoxicity of the complexes **1**–**4** against A549 as well as that of oxaliplatin against all the human cancer cell lines exceeded the tested concentration range ($IC_{50} > 50$ μM); the cells were exposed to the compounds for 24 h, each experiment was repeated three times and the given $IC_{50}$ (μM) values represent an arithmetic mean.

HeLa, 39.9 ± 4.6; A2780, 11.5 ± 1.6; A2780cis, 30.3 ± 6.1; G-361, 6.9 ± 1.9; HOS, 34.2 ± 6.4; MCF7, 19.6 ± 4.3; LH32, >50.0) and *oxaliplatin* (A549, >50.0; HeLa, >50.0; A2780, >50.0; A2780cis, >50.0; G-361, >50.0; HOS, >50.0; MCF7, >50.0; LH32, >50.0).

The prepared complexes are more cytotoxic than *cisplatin* and *oxaliplatin* against HeLa (Fig. 1A) and A2780cis (Fig. 1C). The complex **4** showed the highest efficiency against both HeLa and A2780cis, with the $IC_{50}$ values of 23.4 μM and 18.7 μM, respectively. The complexes **1**, **3** and **4** exceeded the *in vitro* cytotoxic activity of the mentioned platinum-based drugs against human osteosarcoma cancer cells (Fig. 1E). As for the MCF7 cell line, only **1** was found to be more effective as compared with *cisplatin* and *oxaliplatin* (Fig. 1F). On the other hand, the tested complexes were less active than the positive controls against A2780 and G-361 cancer cell lines (see Fig. 1B and D). All the tested compounds (**1**–**4**, *cisplatin* and *oxaliplatin*) were found to be inactive against A549 cancer cell line up to the concentration of 50.0 μM.

A comparison of the results obtained against A2780 and A2780cis cell lines, which can be expressed as *resistance factor ratios* [calculated as $IC_{50}$(A2780cis)/$IC_{50}$(A2780)] equalling to 1.39 for **1**, 1.93 for **2**, 1.60 for **3**, 1.30 for **4** and 2.63 for *cisplatin*, showed that the tested complexes **1**–**4** can be considered non-cross-resistant with platinum-based drug *cisplatin*.

It has to be mentioned that the free organic compounds (*n*Ros) were not tested for their *in vitro* cytotoxicity within the framework of this study. However, the cytotoxicity of *Roscovitine* and also *cisplatin* was determined previously by a calcein acetoxymethyl (AM) assay against the G-361, HOS and MCF7 human cancer cells with the $IC_{50}$ values of 19.0, 20.0, and 15.0 μM, respectively, for *Roscovitine*, and with the $IC_{50}$ values of 3.0, 3.0, and 11.0 μM, respectively, for *cisplatin* [9]. The ratios, calculated as $IC_{50}$(*Roscovitine*)/$IC_{50}$(*cisplatin*), equal 6.33 (G-361), 6.67 (HOS) and 1.36 (MCF7). From the comparison of these ratio values with those calculated as $IC_{50}$(**1**–**4**)/$IC_{50}$(*cisplatin*), based on the $IC_{50}$ values determined in this work, which are equal to 3.10, 0.96 and 0.86 for **1**, 1.56, 1.00 and 1.15 for **2**, 2.43, 0.87 and 1.42 for **3**, and 2.29, 0.60 and 1.37 for **4** against G-361, HOS, and MCF7, respectively, higher *in vitro* cytotoxicity of the complexes **1**–**4** in comparison with *Roscovitine* can be indirectly demonstrated.

The *in vitro* cytotoxicity against human hepatocytes (LH32) was studied for the complex **1**, *cisplatin* and *oxaliplatin*. These compounds did not affect hepatocytes up to the concentration of 50.0 μM, implying that the complex [Pt(ox)(Ros)$_2$] (**1**) can be considered *in vitro* non-hepatotoxic.

Finally, the mechanism of action of complexes **1**–**4** most likely includes the formation of [Pt(OH$^-$)$_2$(*n*Ros)$_2$] species and their consequent interaction with DNA. In other words, the elimination of *n*Ros ligands is not expected in the case of complexes **1**–**4**. This statement can also be supported by the results of the NMR study of the complexes in a DMF/distilled water mixture, which disproved a presence of the free and uncoordinated *n*Ros molecules in the medium even after the period of more than two months. However, the study of detailed solution behavior of the complexes **1**–**4** exceeds the framework of the present work, it will be a subject of the consecutive study of these platinum(II) complexes.

## 3. Conclusions

Four mononuclear platinum(II) oxalato complexes of the general composition [Pt(ox)(*n*Ros)$_2$]·$x$H$_2$O ($x = {}^3/_4$ for **1** and **4**, 1 for **2** and ½ for **3**) involving *Roscovitine*-based N-donor carrier ligands (*n*Ros) were synthesized from K$_2$[Pt(ox)$_2$]·2H$_2$O and fully characterized by various physical methods. Although any crystals suitable for a single-crystal X-ray analysis have not been prepared, we can conclude that these compounds have a distorted square-planar arrangement around the central Pt(II) atom, which is tetracoordinated by two *n*Ros

Please cite this article in press as: Z. Trávníček, et al., *Roscovitine*-based CDK inhibitors acting as N-donor ligands in the..., European Journal of Medicinal Chemistry (2010), doi:10.1016/j.ejmech.2010.07.025

molecules (bound through their N7 atoms) and by one bidentate-coordinated oxalate dianion, thus giving a $PtN_2O_2$ donor set. The prepared complexes **1**–**4** represent the first examples of platinum(II) oxalato complexes with adenine-based potent CDK inhibitors acting as carrier N-donor ligands. The complexes showed higher *in vitro* anticancer activity against cervix epitheloid carcinoma (**1**, 32.3 ± 2.0 μM; **2**, 30.9 ± 6.5 μM; **3**, 31.5 ± 2.6 μM; **4**, 23.4 ± 1.7 μM) and *cisplatin* resistant ovarian carcinoma (**1**, 29.0 ± 6.4 μM; **2**, 26.7 ± 2.5 μM; **3**, 23.2 ± 3.8 μM; **4**, 18.7 ± 3.0 μM) human cancer cell lines as compared with the commercially used platinum-based drugs *cisplatin* (39.9 ± 4.6 μM against HeLa and 30.3 ± 6.1 μM against A2780cis) and *oxaliplatin* (>50.0 μM against HeLa and >50.0 μM against A2780cis). Moreover, the complex **1** was also tested, as a representative sample, for its cytotoxicity in primary cultures of human hepatocytes and it was found to be non-hepatotoxic up to the concentration of 50.0 μM.

## 4. Experimental

### 4.1. Starting materials

Chemicals and solvents were purchased from Sigma–Aldrich Co., Acros Organics Co., Lachema Co. and Fluka Co. and they were used as received, except for dimethyl sulfoxide (DMSO) that was dried using $MgSO_4$.

Potassium bis(oxalato)platinate(II) dihydrate, $K_2[Pt(ox)_2]\cdot 2H_2O$ [8], 2-(1-ethyl-2-hydroxyethylamino)-N6-(benzyl)-9-isopropyladenine (Ros), 2-(1-ethyl-2-hydroxyethylamino)-N6-(2-methoxybenzyl)-9-isopropyladenine (2*OMe*Ros), 2-(1-ethyl-2-hydroxyethylamino)-N6-(3-methoxybenzyl)-9-isopropyladenine (3*OMe*Ros) and 2-(1-ethyl-2-hydroxyethylamino)-N6-(4-methoxybenzyl)-9-isopropyladenine (4*OMe*Ros) [7] were synthesized as described in the cited literature source. The spectral data (IR, Raman, NMR) of Ros, 2*OMe*Ros, 3*OMe*Ros, and 4*OMe*Ros were given in our previous paper [7].

### 4.2. General procedure for the preparation of the $[Pt(ox)(Ros)_2]\cdot {}^3/_4 H_2O$ (**1**), $[Pt(ox)(2OMeRos)_2]\cdot H_2O$ (**2**), $[Pt(ox)(3OMeRos)_2]\cdot ½H_2O$ (3) and $[Pt(ox)(4OMeRos)_2]\cdot {}^3/_4 H_2O$ (4) complexes

The platinum(II) oxalato complexes of the general composition $[Pt(ox)(n\text{Ros})_2]\cdot xH_2O$ were prepared using the synthetic strategy employing $K_2[Pt(ox)_2]\cdot 2H_2O$ as a starting platinum(II) compound [8]. A hot distilled water solution (20 mL) of this complex (0.75 mmol) was mixed together with the appropriate organic compound (*n*Ros; 1.5 mmol) dissolved in hot isopropanol (20 mL). The clear yellowish mixture was stirred at 70 °C. The colour turned to pale brown in the period of two days. Then the reaction mixture was evaporated to dryness. The brown gummy product was washed with hot distilled water (2 × 5 mL) and hot isopropanol (2 × 5 mL). Finally, the obtained platinum(II) oxalato complexes **1**–**4** were pulverized in diethyl ether, filtered off and dried at the temperature of 40 °C. The described synthesis is schematically shown in Scheme 1.

The experimental data resulting from IR, Raman and NMR spectroscopy, ESI + mass spectrometry, molar conductivity measurements and simultaneous TG/DTA thermal studies are given in Appendix A, Supplementary data.

#### 4.2.1. $[Pt(ox)(Ros)_2]\cdot {}^3/_4 H_2O$ (**1**)

The complex **1** was isolated as light ocher powder product in a yield of 640 mg (86%). Anal. Calc. for $C_{40}H_{52}N_{12}O_6Pt\cdot {}^3/_4 H_2O$: C, 47.78; H, 5.36; N, 16.72. Found: C, 47.89; H, 5.58; N, 16.77. *In vitro* cytotoxicty (μM): A549, >50.0; HeLa, 32.3 ± 2.0; A2780, 20.9 ± 2.9; A2780cis, 29.0 ± 6.4; G-361, 21.4 ± 2.7; HOS, 32.8 ± 5.9; MCF7, 16.8 ± 3.8; LH32, >50.0.

#### 4.2.2. $[Pt(ox)(2OMeRos)_2]\cdot H_2O$ (**2**)

The above described synthetic procedure provided 710 mg (90%) of the desired complex, as dark ocher solid. Anal. Calc. for $C_{42}H_{56}N_{12}O_8Pt\cdot H_2O$: C, 47.14; H, 5.46; N, 15.71. Found: C, 47.02; H, 5.88; N, 15.53. *In vitro* cytotoxicity (μM): A549, >50.0; HeLa, 30.9 ± 6.5 A2780, 13.8 ± 1.9; A2780cis, 26.7 ± 2.5; G-361, 10.8 ± 1.9; HOS, 34.4 ± 6.8; MCF7, 22.5 ± 5.6.

#### 4.2.3. $[Pt(ox)(3OMeRos)_2]\cdot ½H_2O$ (**3**)

490 mg (62%) of the ocher solid were obtained. Anal. Calc. for $C_{42}H_{56}N_{12}O_8Pt\cdot ½H_2O$: C, 47.54; H, 5.41; N, 15.84. Found: C, 47.14; H, 5.56; N, 16.37%. *In vitro* cytotoxicity (μM): A549, >50.0; HeLa, 31.5 ± 2.6; A2780, 14.5 ± 2.4; A2780cis, 23.2 ± 3.8; G-361, 16.8 ± 2.5; HOS, 29.8 ± 5.7; MCF7, 27.9 ± 4.2.

#### 4.2.4. $[Pt(ox)(4OMeRos)_2]\cdot {}^3/_4 H_2O$ (**4**)

The dark ocher powder product was prepared (560 mg, 71%). Anal. Calc. for $C_{42}H_{56}N_{12}O_8Pt\cdot {}^3/_4 H_2O$: C, 47.34; H, 5.44; N, 15.77. Found: C, 47.52; H, 5.37; N, 15.61. *In vitro* cytotoxicity (μM): A549, >50.0; HeLa, 23.4 ± 1.7; A2780, 14.4 ± 1.4; A2780cis, 18.7 ± 3.0; G-361, 15.8 ± 0.8; HOS, 20.4 ± 4.1; MCF7, 26.9 ± 2.1.

### 4.3. Physical methods

Elemental analyses were carried out on a Fisons EA-1108 CHNS-O Elemental Analyzer (Thermo Scientific). Infrared spectra were recorded on a Nexus 670 FT-IR (Thermo Nicolet) in the 400–4000 $cm^{-1}$ (KBr pellets) and 150–600 $cm^{-1}$ (Nujol technique) regions. Raman spectra were recorded using an NXR FT-Raman Module (Thermo Nicolet) between 150 and 3750 $cm^{-1}$. Molar conductivity values of $10^{-3}$ M DMF solutions (25 °C) were determined by a Cond 340i/SET (WTW). Mass spectra of the methanol solutions of complexes were obtained by LCQ Fleet ion trap mass spectrometer using the ESI + technique (Thermo Scientific). All the observed isotopic distribution representations were compared with the theoretical ones (QualBrowser software, version 2.0.7, Thermo Fischer Scientific). Simultaneous thermogravimetric (TG) and differential thermal (DTA) analyses were performed using an Exstar TG/DTA 6200 thermal analyzer (Seiko Instruments Inc.); ceramic crucible, 100 mL $min^{-1}$ dynamic air atmosphere, 25–700 °C temperature range and temperature gradient of 2.5 °C $min^{-1}$.

$^1H$, $^{13}C$ and $^{195}Pt$ NMR spectra and two dimensional correlation experiments ($^1H$–$^1H$ gs-COSY, $^1H$–$^{13}C$ gs-HMQC, $^1H$–$^{13}C$ gs-HMBC; gs = gradient selected, COSY = correlation spectroscopy, HMQC = heteronuclear multiple quantum coherence, HMBC = heteronuclear multiple bond coherence) of the DMF-$d_7$ solutions were measured at 300 K on a Varian 400 device at 400.00 MHz ($^1H$), 100.58 MHz ($^{13}C$) and 86.00 MHz ($^{195}Pt$). $^1H$ spectra were also, together with $^1H$–$^{15}N$ gs-HMBC experiments, recorded at 340 K ($^{15}N$ at 40.53 MHz). $^1H$ and $^{13}C$ spectra were adjusted against the signals of tetramethylsilane ($Me_4Si$). $^{195}Pt$ spectra were calibrated against potassium hexachloroplatinate ($K_2PtCl_6$) in $D_2O$ found at 0 ppm $^1H$–$^{15}N$ gs-HMBC experiments were obtained at natural abundance and calibrated against the residual signals of the DMF adjusted to 8.03 ppm ($^1H$) and 104.7 ppm ($^{15}N$). The splitting of proton resonances in the reported $^1H$ spectra is defined as s = singlet, d = doublet, t = triplet, sx = sextuplet, sp = septuplet, br = broad band, dd = doublet of doublets, tt = triplet of triplets, m = multiplet.

### 4.4. In vitro cytotoxic activity testing

*In vitro* cytotoxic activities of **1**–**4**, as well as *cisplatin* and *oxaliplatin* employed as positive controls were determined by an MTT assay [MTT = 3-(4,5-dimethylthiazol-2-yl)-2,5-diphenyltetrazolium bromide] in ovarian carcinoma (A2780; ECACC No.

93112517), *cisplatin* resistant ovarian carcinoma (A2780cis; ECACC No. 93112519), malignant melanoma (G-361; ECACC No. 88030401), breast adenocarcinoma (MCF7; ECACC No. 86012803), lung carcinoma (A549; ECACC No. 86012804), osteosarcoma (HOS; ECACC No. 87070202) and cervix epitheloid carcinoma (HeLa; ECACC No. 93021013) human cancer cell lines, as described previously [8,19]. The cells were treated with tested compounds for 24 h. Each experiment was repeated three times and the results were expressed as the $IC_{50}$ (μM) values representing an arithmetic mean.

Human hepatocytes were prepared from the liver resected from an adult multiorgan donor. The donor LH32 (M, 70 years) had normal liver histology, negative virology test (HIV, EBV, CMV and HCV) and normal biochemical parameters. Patient's personal anamnesis considered no alcohol or drug abuse. The tissue acquisition protocol was in accordance with the requirements issued by a local ethical commission in the Czech Republic. Hepatocytes were isolated as previously described [20]. Following the isolation, the cells were plated on collagen-coated culture dishes at density of $1.4 \times 10^5$ cells/cm$^2$. The culture medium was enriched for plating with 2% fetal calf serum (v/v). The medium was exchanged for a serum-free medium the day after and the culture was allowed to stabilize for additional 48 h prior to the treatments. Cultures were maintained at 37 °C and 5% $CO_2$ in a humidified incubator.

## Acknowledgements

This work was financially supported by the Ministry of Education, Youth and Sports of the Czech Republic from a grant no. MSM6198959218, and by PrF_2010_018. We also thank Ms. Pavla Richterová for performing CHN elemental analyses, Ms. Radka Novotná for IR and Raman spectra measurement and Ms. Alena Klanicová for ESI + mass spectra measurement.

## Appendix A. Supplementary data

Supplementary data associated with article can be found in the online version at doi:10.1016/j.ejmech.2010.07.025.

## References

[1] P.J. Davies, Plant Hormones, third ed. Springer, Dordrecht, 1997.
[2] L. Meijer, A. Borgne, O. Mulner, J.P.J. Chong, J.J. Blow, N. Inagaki, M. Inagaki, J.G. Delcros, J.P. Moulinoux, Eur. J. Biochem. 243 (1997) 527–536.
[3] C. Benson, S. Kaye, P. Workman, M. Garret, M. Walton, J. de Bono, Br. J. Cancer 92 (2005) 7–12.
[4] P. Štarha, Z. Trávníček, R. Herchel, I. Popa, P. Suchý, J. Vančo, J. Inorg. Biochem. 103 (2009) 432–440.
[5] Z. Trávníček, J. Marek, J. Mol. Struct. 933 (2010) 148–155.
[6] Z. Trávníček, I. Popa, M. Čajan, R. Zbořil, V. Kryštof, J. Mikulík, J. Inorg. Biochem. 104 (2010) 405–417.
[7] P. Štarha, I. Popa, Z. Trávníček, Inorg. Chim. Acta 363 (2010) 1469–1478.
[8] P. Štarha, Z. Trávníček, I. Popa, J. Inorg. Biochem. 104 (2010) 639–647.
[9] M. Maloň, Z. Trávníček, R. Marek, M. Strnad, J. Inorg. Biochem. 99 (2005) 2127–2138.
[10] M.J. Cleare, Coord. Chem. Rev. 12 (1974) 349–405.
[11] E. Monti, M. Gariboldi, A. Maiocchi, E. Marengo, C. Cassino, E. Gabano, D.J. Osella, J. Med. Chem. 48 (2005) 857–866.
[12] W.J. Geary, Coord. Chem. Rev. 7 (1971) 81–122.
[13] K. Nakamoto, Infrared and Raman Spectra of Inorganic and Coordination Compounds, fifth ed. Willey-Interscience, New York, 1997.
[14] C.J. Pouchert, The Aldrich Library of Infrared Spectra, third ed. Aldrich Chemical Co., Milwaukee, 1981.
[15] T.A. Mohamed, I.A. Shabaan, W.M. Zoghaib, J. Husband, R.S. Farag, A.E.M. A. Alajhaz, J. Mol. Struct. 938 (2009) 263–276.
[16] V. Montoya, J. Pons, J. García-Antón, X. Solans, M. Font-Bardia, J. Ros, Inorg. Chim. Acta 360 (2007) 625–637.
[17] Z. Dhaouadi, M. Ghomi, J.C. Austin, R.B. Girling, R.E. Hester, P. Mojzes, L. Chinsky, P.Y. Turpin, C. Coulombeau, H. Jobic, J. Tomkinson, J. Phys. Chem. 97 (1993) 1074–1084.
[18] L.R. Kelland, N.P. Farrell, Platinum Based Drugs in Cancer Therapy. Humana Press, Totowa, New Jersey, 2000.
[19] J. Ulrichová, Z. Dvořák, J. Vičar, J. Lata, J. Smržová, A. Šedo, V. Šimánek, Toxicol. Lett. 125 (2001) 125–132.
[20] L. Pichard-Garcia, S. Gerbal-Chaloin, J.B. Ferrini, J.M. Fabre, P. Maurel, Meth. Enzymol. 357 (2002) 311–321.

**Supplementary Data**

# *Roscovitine*-based CDK inhibitors acting as N-donor ligands in the platinum(II) oxalato complexes: preparation, characterization and *in vitro* cytotoxicity

Zdeněk Trávníček[a,*], Pavel Štarha[a], Igor Popa[a], Radim Vrzal[b], Zdeněk Dvořák[b]

[a] *Department of Inorganic Chemistry, Faculty of Science, Palacký University, Tř. 17. listopadu 12, CZ-771 46 Olomouc, Czech Republic*

[b] *Department of Cell Biology and Genetics, Faculty of Science, Palacký University, Šlechtitelů 11, CZ-783 71 Olomouc, Czech Republic*

[*] Corresponding author. Tel.: +420 585 634 352; fax: +420585 634 954; e-mail: zdenek.travnicek@upol.cz (Zdeněk Trávníček).



**The results of IR, Raman and NMR spectroscopy, ESI+ mass spectrometry and TG/DTA thermal analysis of [Pt(ox)(Ros)$_2$]·¾H$_2$O (1), [Pt(ox)(*2OMe*Ros)$_2$]·H$_2$O (2), [Pt(ox)(*3OMe*Ros)$_2$]·½H$_2$O (3) and [Pt(ox)(*4OMe*Ros)$_2$]·¾H$_2$O (4)**

**1:** $^1$H NMR (DMF-$d_7$, ppm): $\delta$ 8.62 (s, 1H, C8*H*), 8.51 (bs, 1H, N6*H*), 7.48 (d, 2H, C11*H*, C15*H*, $J$ = 7.6), 7.30 (t, 2H, C12*H*, C14*H*, $J$ = 7.6), 7.23 (tt, 1H, C13*H*, $J$ = 7.6, 2.0), 6.38 (bs, 1H, N2*H*), 4.85 (bs, 1H, O20*H*), 4.80 (bs, 2H, C9*H*), 4.70 (sep, 1H, C16*H*, $J$ = 6.8), 3.95 (sxt, 1H, C19*H*, $J$ = 5.4), 3.65 (m, 1H, C20*H*$^a$), 3.54 (m, 1H, C20*H*$^b$), 1.73 (m, 1H, C21*H*$^a$), 1.56 (m, 1H, C21*H*$^b$), 1.53 (d, 6H, C17*H*, C18*H*, $J$ = 6.8), 0.91 (t, 3H, C22*H*, $J$ = 7.4). $^{13}$C NMR (DMF-$d_7$, ppm): $\delta$ 166.30 (*C*24, *C*25), 160.42 (*C*2), 153.34 (*C*6), 151.02 (*C*4), 140.55 (*C*10), 139.55 (*C*8), 128.83 (*C*12, *C*14), 128.18 (*C*11, *C*15), 127.23 (*C*13), 111.43 (*C*5), 64.09 (*C*20), 55.36 (*C*19), 48.49 (*C*16), 44.49 (*C*9), 24.73 (*C*21), 21.92 (*C*17, *C*18), 10.93 (*C*22). $^{15}$N NMR (DMF-$d_7$, ppm): $\delta$ 204.8 (*N*1), 188.9 (*N*3), 179.9 (*N*9), 125.3 (*N*7), 97.4 (*N*2), 90.4 (*N*6). $^{195}$Pt NMR (DMF-$d_7$, ppm): $\delta$ –1676. TG/DTA: weight loss of 1.2% at 27–175 °C (calc. for ¾H$_2$O: 1.3%); weight loss of 78.8% at 175–474 °C (calc. to PtO residue: 77.7%) with exothermic peaks at 231, 297, 373 and 402 °C. $\Lambda_M$ (DMF solution, S cm$^2$ mol$^{-1}$): 10.9. ESI+ MS (methanol, *m/z*): 1030.3 {[Pt(ox)(Ros)$_2$+K]$^+$; 1030.3 calc. for $C_{40}H_{52}N_{12}O_6PtK$}, 1014.3 {[Pt(ox)(Ros)$_2$+Na]$^+$; 1014.4 calc. for $C_{40}H_{52}N_{12}O_6PtNa$}, 992.3 {[Pt(ox)(Ros)$_2$+H]$^+$; 992.4 calc. for $C_{40}H_{53}N_{12}O_6Pt$}, 902.3 {[Pt(Ros$^-$)$_2$+H]$^+$; 902.4 calc. for $C_{38}H_{51}N_{12}O_2Pt$}, 637.4 {[Pt(ox)(Ros)+H]$^+$; 638.2 calc. for $C_{21}H_{27}N_6O_5Pt$}, 548.2 {[Pt(Ros$^{2-}$)+H]$^+$; 548.2 calc. for $C_{19}H_{25}N_6OPt$}, 355.3 {[Ros+H]$^+$; 355.2 calc. for $C_{19}H_{27}N_6O$}. IR (nujol, cm$^{-1}$): 527vs ν(Pd−N); 566vs ν(Pd−O). IR (KBr, cm$^{-1}$): 1058w ν(C−O)$_{al}$; 1356s ν$_s$(C−O)$_{ox}$; 1545m, 1494s ν(C=C); 1611vs ν(C=N); 1718s, 1671m ν$_a$(C=O)$_{ox}$; 2965w, 2932w, 2875w ν(C−H)$_{al}$; 3121w, 3064w ν(C−H)$_{ar}$. Raman (cm$^{-1}$): 524w ν(Pd−N); 569w ν(Pd−O); 1060w ν(C−O)$_{al}$; 1543w, 1490m ν(C=C); 1609vs ν(C=N); 1710w, 1681w ν$_a$(C=O)$_{ox}$; 2978m, 2937s, 2876m ν(C−H)$_{al}$; 3059m ν(C−H)$_{ar}$.

**2:** $^{1}$H NMR (DMF-$d_7$, ppm): $\delta$ 8.54 (s, 1H, C8*H*), 8.32 (bs, 1H, N6*H*), 7.40 (d, 1H, C15*H*, *J* = 7.0), 7.24 (tt, 1H, C13*H*, *J* = 7.8, 1.7), 7.00 (d, 1H, C12*H*, *J* = 8.3), 6.85 (tt, 1H, C14*H*, *J* = 7.5, 1.0), 6.36 (bs, 1H, N2*H*), 4.81 (bs, 1H, O20*H*), 4.80 (bs, 2H, C9*H*), 4.69 (sep, 1H, C16*H*, *J* = 6.9), 3.93 (m, 1H, C19*H*), 3.89 (s, 3H, C23*H*), 3.65 (m, 1H, C20*H*$^a$), 3.58 (m, 1H, C20*H*$^b$), 1.73 (m, 1H, C21*H*$^a$), 1.57 (m, 1H, C21*H*$^b$), 1.51 (d, 6H, C17*H*, C18*H*, *J* = 6.9), 0.91 (t, 3H, C22*H*, *J* = 7.4). $^{13}$C NMR (DMF-$d_7$, ppm): $\delta$ 166.19 (*C*24, *C*25), 160.48 (*C*2), 157.97 (*C*11), 153.44 (*C*6), 150.88 (*C*4), 139.61 (*C*8), 128.81 (*C*13), 128.73 (*C*15), 127.75 (*C*10), 120.88 (*C*14), 111.52 (*C*5), 110.93 (*C*12), 64.04 (*C*20), 55.84 (*C*23), 55.37 (*C*19), 48.60 (*C*16), 39.80 (*C*9), 24.76 (*C*21), 21.91 (*C*17), 21.87 (*C*18), 10.96 (*C*22). $^{15}$N NMR (DMF-$d_7$, ppm): $\delta$ 199.3 (*N*1), 186.6 (*N*3), 179.4 (*N*9), 125.3 (*N*7), 96.8 (*N*2), 88.1 (*N*6). $^{195}$Pt NMR (DMF-$d_7$, ppm): $\delta$ –1676. TG/DTA: weight loss of 2.1% at 26–145 °C with an endothermic peak at 123 °C (calc. for $H_2O$: 1.7%); weight loss of 77.7% at 186–448 °C (calc. to PtO residue: 78.6%) with exothermic peaks at 283, 295, 337 and 415 °C. $\Lambda_M$ (DMF solution, S cm$^2$ mol$^{-1}$): 10.5. ESI+ MS (methanol, *m/z*): 1090.2 {[Pt(ox)(*2OMe*Ros)$_2$+K]$^+$; 1090.4 calc. for $C_{42}H_{56}N_{12}O_8PtK$}, 1052.4 {[Pt(ox)(*2OMe*Ros)$_2$+H]$^+$; 1052.4 calc. for $C_{42}H_{57}N_{12}O_8Pt$}, 962.3 {[Pt(*2OMe*Ros$^-$)$_2$+H]$^+$; 962.4 calc. for $C_{40}H_{55}N_{12}O_4Pt$}, 667.2 {[Pt(ox)(*2OMe*Ros)+H]$^+$; 668.2 calc. for $C_{22}H_{29}N_6O_6Pt$}, 578.2 {[Pt(*2OMe*Ros$^{2-}$)+H]$^+$; 578.2 calc. for $C_{20}H_{27}N_6O_2Pt$}, 385.3 {[*2OMe*Ros+H]$^+$; 385.2 calc. for $C_{20}H_{29}N_6O_2$}. IR (nujol, cm$^{-1}$): 526vs ν(Pd−N); 569vs ν(Pd−O). IR (KBr, cm$^{-1}$): 1050w $\nu$(C−O)$_{al}$; 1243s $\nu$(C−O)$_{ar}$; 1357s $\nu_s$(C−O)$_{ox}$; 1545s, 1493s ν(C=C); 1611vs ν(C=N); 1714s, 1673m $\nu_a$(C=O)$_{ox}$; 2965m, 2934m, 2875w, 2837w $\nu$(C−H)$_{al}$; 3122w, 3074w $\nu$(C−H)$_{ar}$. Raman (cm$^{-1}$): 524w ν(Pd−N); 570w ν(Pd−O); 1049m $\nu$(C−O)$_{al}$; 1246m $\nu$(C−O)$_{ar}$; 1541w, 1489m ν(C=C); 1607vs ν(C=N); 1713m, 1677w $\nu_a$(C=O)$_{ox}$; 2975s, 2936vs, 2877m, 2840w $\nu$(C−H)$_{al}$; 3069m $\nu$(C−H)$_{ar}$.

**3:** $^{1}$H NMR (DMF-$d_7$, ppm): $\delta$ 8.61 (s, 1H, C8*H*), 8.48 (bs, 1H, N6*H*), 7.20 (t, 1H, C14*H*, *J* = 7.8), 7.07 (d, 1H, C11*H*, *J* = 2.0), 7.04 (d, 1H, C15*H*, *J* = 7.8), 6.80 (dd, 1H, C13*H*, *J* = 8.1, 2.0), 6.38 (bs, 1H, N2*H*), 4.90 (bs, 1H, O20*H*), 4.77 (bs, 2H, C9*H*), 4.71 (sep, 1H, C16*H*, *J* = 6.9), 3.93 (sxt, 1H, C19*H*, *J* = 5.4), 3.79 (s, 3H, C23*H*), 3.64 (m, 1H, C20*H*$^a$), 3.54 (m, 1H, C20*H*$^b$), 1.71 (m, 1H, C21*H*$^a$), 1.53 (d, 6H, C17*H*, C18*H*, *J* = 6.9), 1.43 (m, 1H, C21*H*$^b$), 0.90 (t, 3H, C22*H*, *J* = 7.3). $^{13}$C NMR (DMF-$d_7$, ppm): $\delta$ 166.29 (*C*24, *C*25), 160.47 (*C*12), 160.43 (*C*2), 153.38 (*C*6), 151.02 (*C*4), 142.31 (*C*10), 139.60 (*C*8), 129.88 (*C*14), 120.37 (*C*15), 113.46 (*C*11), 113.11 (*C*13), 111.51 (*C*5), 64.09 (*C*20), 55.48 (*C*23), 55.37 (*C*19), 48.64 (*C*16), 44.49 (*C*9), 24.76 (*C*21), 21.94 (*C*17, *C*18), 10.93 (*C*22). $^{15}$N NMR (DMF-$d_7$, ppm): $\delta$ 204.3 (*N*1), 191.6 (*N*3), 180.5 (*N*9), 124.7 (*N*7), 96.9 (*N*2), 89.7 (*N*6). $^{195}$Pt NMR (DMF-$d_7$, ppm): $\delta$ –1676. TG/DTA: weight loss of 0.8% at 26–112 °C (calc. for ½$H_2O$: 0.8%); weight loss of 80.2% at 160–469 °C (calc. to PtO residue: 79.3%) with exothermic peaks at 291, 308, 372 and 405 °C. $\Lambda_M$ (DMF solution, S cm$^2$ mol$^{-1}$): 13.5. ESI+ MS (methanol, *m/z*): 1090.3 {[Pt(ox)(*3OMe*Ros)$_2$+K]$^+$; 1090.4 calc. for $C_{42}H_{56}N_{12}O_8PtK$}, 1052.3 {[Pt(ox)(*3OMe*Ros)$_2$+H]$^+$; 1052.4 calc. for $C_{42}H_{57}N_{12}O_8Pt$}, 962.4 {[Pt(*3OMe*Ros$^-$)$_2$+H]$^+$; 962.4 calc. for $C_{40}H_{55}N_{12}O_4Pt$}, 667.3 {[Pt(ox)(*3OMe*Ros)+H]$^+$; 668.2 calc. for $C_{22}H_{29}N_6O_6Pt$}, 578.3 {[Pt(*3OMe*Ros$^{2-}$)+H]$^+$; 578.2 calc. for $C_{20}H_{27}N_6O_2Pt$}, 385.3 {[*3OMe*Ros+H]$^+$; 385.2 calc. for $C_{20}H_{29}N_6O_2$}. IR (nujol, cm$^{-1}$): 525vs ν(Pd−N); 571vs ν(Pd−O). IR (KBr, cm$^{-1}$): 1047m $\nu$(C−O)$_{al}$; 1265m $\nu$(C−O)$_{ar}$; 1353m $\nu_s$(C−O)$_{ox}$; 1546m, 1492s ν(C=C); 1610vs ν(C=N); 1720m, 1691m $\nu_a$(C=O)$_{ox}$; 2964m, 2934m, 2875w, 2831w $\nu$(C−H)$_{al}$; 3122w, 3069w $\nu$(C−H)$_{ar}$. Raman (cm$^{-1}$): 529w ν(Pd−N); 569w ν(Pd−O); 1048w $\nu$(C−O)$_{al}$; 1267m $\nu$(C−O)$_{ar}$; 1543m ν(C=C); 1610vs ν(C=N); 1711m, 1677m $\nu_a$(C=O)$_{ox}$; 2975s, 2937vs, 2876m, 2838w $\nu$(C−H)$_{al}$; 3058m $\nu$(C−H)$_{ar}$.

**4:** $^{1}$H NMR (DMF-$d_7$, ppm): $\delta$ 8.57 (s, 1H, C8*H*), 8.39 (bs, 1H, N6*H*), 7.42 (d, 2H, C12*H*, C14*H*, *J* = 8.7), 6.86 (dd, 2H, C11*H*, C15*H*, *J* = 8.7, 2.0), 6.41 (bs, 1H, N2*H*), 4.75 (bs, 1H, O20*H*), 4.71 (bs, 2H, C9*H*), 4.68 (m, 1H, C16*H*), 3.97 (m, 1H, C19*H*), 3.80 (m, 1H, C20*H*$^a$), 3.78 (s, 3H, C23*H*), 3.67 (m, 1H, C20*H*$^b$), 1.75 (sep, 1H, C21*H*$^a$, *J* = 7.8), 1.56 (m, 1H, C21*H*$^b$),

1.51 (d, 6H, C17*H*, C18*H*, *J* = 6.3), 0.93 (t, 3H, C22*H*, *J* = 7.4). $^{13}$C NMR (DMF-$d_7$, ppm): $\delta$ 166.23 (*C*24, *C*25), 160.47 (*C*2), 159.31 (*C*13), 153.31 (*C*6), 150.96 (*C*4), 139.62 (*C*8), 132.37 (*C*10), 129.70 (*C*12, *C*14), 111.44 (*C*5), 114.25 (*C*11, *C*15), 64.16 (*C*20), 55.59 (*C*19), 55.47 (*C*23), 48.48 (*C*16), 44.07 (*C*9), 24.78 (*C*21), 21.92 (*C*17, *C*18), 10.98 (*C*22). $^{15}$N NMR (DMF-$d_7$, ppm): $\delta$ 201.1 (*N*1), 190.0 (*N*3), 180.6 (*N*9), 125.5 (*N*7), 97.1 (*N*2), 91.7 (*N*6). $^{195}$Pt NMR (DMF-$d_7$, ppm): $\delta$ –1676. TG/DTA: weight loss of 1.2% at 28–131 °C with an endothermic peak at 114 °C (calc. for ¾$H_2O$: 1.3%); weight loss of 79.3% at 169–478 °C (calc. to PtO residue: 78.9%) with exothermic peaks at 231, 305, 361 and 421 °C. $\Lambda_M$ (DMF solution, S cm$^2$ mol$^{-1}$): 16.7. ESI+ MS (methanol, *m/z*): 1052.4 {[Pt(ox)(*4OMe*Ros)$_2$+H]$^+$; 1052.4 calc. for $C_{42}H_{57}N_{12}O_8Pt$}, 962.3 {[Pt(*4OMe*Ros$^-$)$_2$+H]$^+$; 962.4 calc. for $C_{40}H_{55}N_{12}O_4Pt$}, 667.2 {[Pt(ox)(*4OMe*Ros)+H]$^+$; 668.2 calc. for $C_{22}H_{29}N_6O_6Pt$}, 578.2 {[Pt(*4OMe*Ros$^{2-}$)+H]$^+$; 578.2 calc. for $C_{20}H_{27}N_6O_2Pt$}, 385.3 {[*4OMe*Ros+H]$^+$; 385.2 calc. for $C_{20}H_{29}N_6O_2$}. IR (nujol, cm$^{-1}$): 520vs ν(Pd−N); 571vs ν(Pd−O). IR (KBr, cm$^{-1}$): 1058w $\nu$(C−O)$_{al}$; 1249s $\nu$(C−O)$_{ar}$; 1353s $\nu_s$(C−O)$_{ox}$; 1546s, 1492s ν(C=C); 1610vs ν(C=N); 1711s, 1670m $\nu_a$(C=O)$_{ox}$; 2965m, 2934m, 2876m, 2837w $\nu$(C−H)$_{al}$; 3126m, 3076w $\nu$(C−H)$_{ar}$. Raman (cm$^{-1}$): 523w ν(Pd−N); 570w ν(Pd−O); 1063w $\nu$(C−O)$_{al}$; 1266m $\nu$(C−O)$_{ar}$; 1542w, 1487w ν(C=C); 1611vs ν(C=N); 1711w, 1678w $\nu_a$(C=O)$_{ox}$; 2978s, 2936vs, 2876m, 2837w $\nu$(C−H)$_{al}$; 3068m $\nu$(C−H)$_{ar}$.



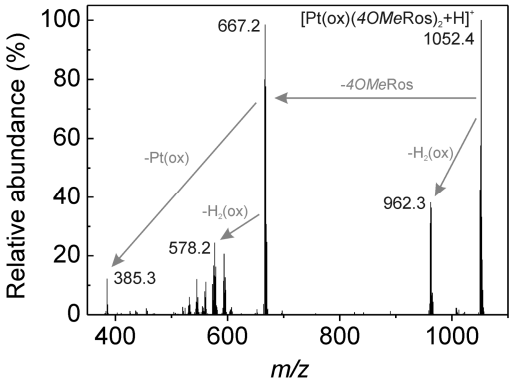


**Fig. S1:** ESI+ mass spectrum of the [Pt(ox)(*4OMe*Ros)$_2$] (**4**) complex dissolved in methanol.

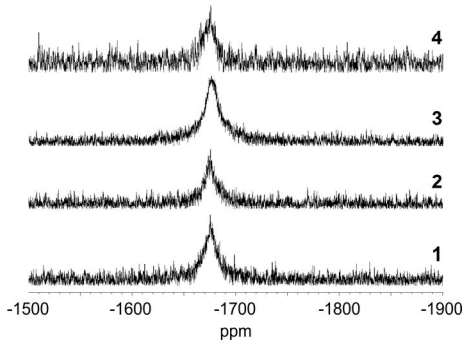


**Fig. S2:** Signals detected in $^{195}$Pt NMR spectra of the complexes **1**–**4** at –1676 ppm.

# APPENDIX V

Journal of Inorganic Biochemistry 104 (2010) 1130–1132

Contents lists available at ScienceDirect

Journal of Inorganic Biochemistry

journal homepage: www.elsevier.com/locate/jinorgbio

Short Communication

# Evaluation of *in vitro* cytotoxicity and hepatotoxicity of platinum(II) and palladium(II) oxalato complexes with adenine derivatives as carrier ligands

Radim Vrzal [a], Pavel Štarha [b], Zdeněk Dvořák [a], Zdeněk Trávníček [b,*]

[a] Department of Cell Biology and Genetics, Faculty of Science, Palacký University, Šlechtitelů 11, CZ-783 71 Olomouc, Czech Republic
[b] Department of Inorganic Chemistry, Faculty of Science, Palacký University, Tř. 17. listopadu 12, CZ-771 46 Olomouc, Czech Republic

ARTICLE INFO

*Article history:*
Received 20 May 2010
Received in revised form 21 June 2010
Accepted 2 July 2010
Available online 31 July 2010

*Keywords:*
Platinum(II)
Palladium(II)
Oxalato complexes
*In vitro* cytotoxicity
Human hepatocytes

ABSTRACT

*In vitro* antitumour activity of the $[Pt(ox)(L_n)_2]$ (**1**–**7**) and $[Pd(ox)(L_n)_2]$ (**8**–**14**) oxalato (ox) complexes involving N6-benzyl-9-isopropyladenine-based N-donor carrier ligands ($L_n$) against ovarian carcinoma (A2780), cisplatin resistant ovarian carcinoma (A2780cis), malignant melanoma (G-361), lung carcinoma (A549), cervix epitheloid carcinoma (HeLa), breast adenocarcinoma (MCF7) and osteosarcoma (HOS) human cancer cell lines was studied. Some of the tested complexes were even several times more cytotoxic as compared with *cisplatin* employed as a positive control. The improved cytotoxic effect was demonstrated for the platinum(II) complexes **3** ($IC_{50} = 3.2 \pm 1.0$ μM and $3.2 \pm 0.6$ μM) and **5** ($IC_{50} = 4.0 \pm 1.0$ μM and $4.1 \pm 1.4$ μM) against A2780 and A2780cis, as compared with $11.5 \pm 1.6$ μM, and $30.3 \pm 6.1$ μM determined for *cisplatin*, respectively. The significant *in vitro* cytotoxicity against MCF7 ($IC_{50} = 8.2 \pm 3.8$ μM for **12**) and A2780 ($IC_{50} = 5.4 \pm 1.2$ μM for **14**) was evaluated for the palladium(II) oxalato complexes, which again exceeded *cisplatin*, whose $IC_{50}$ equalled $19.6 \pm 4.3$ μM against the MCF7 cells. Selected complexes were also screened for their *in vitro* cytotoxic effect in primary cultures of human hepatocytes and they were found to be non-hepatotoxic.



## 1. Introduction

The term “cancer” represents a large group of diseases which are leading causes of death worldwide. Since the discovery of *cisplatin*, *cis*-$[PtCl_2(NH_3)_2]$, a wide variety of solid tumours have been successfully treated by this anticancer drug [1–3]. The success of *cisplatin* was followed by other platinum-based anticancer drugs (e.g. *oxaliplatin* or *carboplatin*). A possible medicinal application of platinum complexes led to the synthesis of lots of next platinum(II/IV) complexes aiming to improve the cytotoxicity of the above-mentioned therapeutics and/or to reduce their negative side effects (nephrotoxicity, neurotoxicity, etc.). The platinum complexes were later followed by the complexes of other transition metals (e.g. palladium) [4], however, no such compound has been approved for clinical use to date.

The main objective of the present study was to test the recently prepared platinum(II) (**1**–**7**) and palladium(II) (**8**–**14**) oxalato (ox) complexes for their *in vitro* cytotoxicity. The synthesis and characterization of tested $[Pt(ox)(L_n)_2]\cdot xH_2O$ (**1**–**7**) and $[Pd(ox)(L_n)_2]\cdot xH_2O$ (**8**–**14**) involving N6-benzyl-9-isopropyladenine derivatives ($L_n$; Scheme 1) were recently reported [5–7]. Although the *in vitro* cytotoxicity was recently screened by an MTT assay against HOS (**1**–**8**, **10**, **12**–**14**) and MCF7 (**1**–**7**) cells and by acetoxymethyl assay against K562 and MCF7 (**9**, **11**), we decided to broaden the number of human cancer cell lines for the following tests [ovarian carcinoma (A2780), ovarian carcinoma cisplatin resistant cells (A2780cis), malignant melanoma (G361), breast adenocarcinoma (MCF7), lung carcinoma (A549), osteosarcoma (HOS) and cervix epitheloid carcinoma (HeLa)], mainly in connection with the previous promising results. Moreover, in an effort to deeply evaluate the impact of these substances on the human organism we performed *in vitro* cytotoxicity testing on primary cultures of human hepatocytes for selected complexes.

The experimental details relating to the culture media and MTT assay are given elsewhere [5]. The tested complexes (**1**–**14**, *cisplatin*, *oxaliplatin* and *carboplatin*) were incubated with cancer cells for 24 h. The discussed results, expressed as $IC_{50}$ values, represent an arithmetic mean of minimally three independent experiments. However, some of the experiments were limited by low solubility of the tested complexes (i.e. **4**, **7**, **9**, **10**, *oxaliplatin* and *carboplatin*) in the medium used. That is why some $IC_{50}$ values are given as e.g. >1.0 or >5.0 μM.

Hepatocytes were prepared from liver resected from an adult multiorgan donor (LH32; M, 70 years; normal liver histology and biochemical parameters, negative HIV, EBV, CMV and HCV virology test; no alcohol or drug abuse), as previously described [8]. The tissue acquisition protocol was in accordance with the requirements issued by a local ethical commission in the Czech Republic. Following the

* Corresponding author. Tel.: +420 585 634 352; fax: +420 585 634 954.
*E-mail address:* zdenek.travnicek@upol.cz (Z. Trávníček).

0162-0134/$ – see front matter © 2010 Elsevier Inc. All rights reserved.
doi:10.1016/j.jinorgbio.2010.07.002

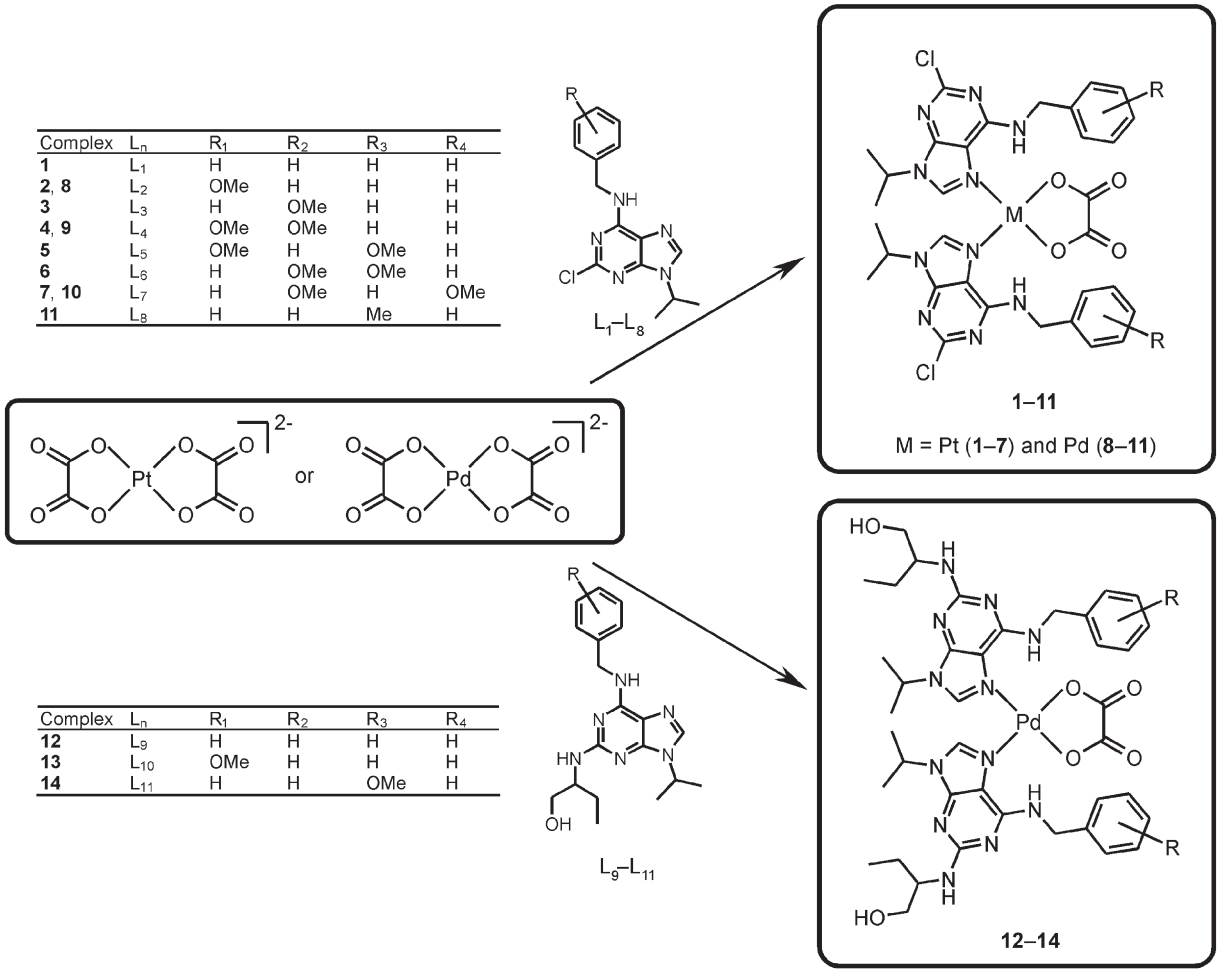


**Scheme. 1.** The synthetic pathways for the preparation of the tested platinum(II) (**1**–**7**) and palladium(II) (**8**–**14**) complexes, together with their schematic structures; $L_1$ = 2-chloro-N6-benzyl-9-isopropyladenine, $L_2$ = 2-chloro-N6-(2-methoxybenzyl)-9-isopropyladenine, $L_3$ = 2-chloro-N6-(3-methoxybenzyl)-9-isopropyladenine, $L_4$ = 2-chloro-N6-(2,3-dimethoxybenzyl)-9-isopropyladenine, $L_5$ = 2-chloro-N6-(2,4-dimethoxybenzyl)-9-isopropyladenine, $L_6$ = 2-chloro-N6-(3,4-dimethoxybenzyl)-9-isopropyladenine, $L_7$ = 2-chloro-N6-(3,5-dimethoxybenzyl)-9-isopropyladenine, $L_8$ = 2-chloro-N6-(4-methylbenzyl)-9-isopropyladenine, $L_9$ = 2-(1-ethyl-2-hydroxyethylamino)-N6-benzyl-9-isopropyladenine, $L_{10}$ = 2-(1-ethyl-2-hydroxyethylamino)-N6-(2-methoxybenzyl)-9-isopropyladenine and $L_{11}$ = 2-(1-ethyl-2-hydroxyethylamino)-N6-(4-methoxybenzyl)-9-isopropyladenine; $x$ = 0 for **1**–**6**, **9**, **11**–**14**, ¾ for **8**, 3 for **10** and 4 for **7**.

**Table 1**
$IC_{50}$ values (μM) evaluated for the platinum(II) (**1**–**7**) and palladium(II) (**8**–**14**) complexes as well as for platinum-based drugs *cisplatin*, *carboplatin* and *oxaliplatin* on different human cancer cell lines and a primary culture of human hepatocytes (LH32).

| Complex | Cell line | | | | | | | |
|---|---|---|---|---|---|---|---|---|
| | A549 | HeLa | A2780 | A2780cis | G-361 | HOS | MCF7 | LH32 |
| **1** | >10.0 | >10.0 | 5.4 ± 0.9 | >10.0 | >10.0 | >10.0[a] | 9.2 ± 1.5[a] | – |
| **2** | >50.0 | >50.0 | 4.6 ± 2.2 | >50.0 | >50.0 | 3.6 ± 1.0[a] | 4.3 ± 2.1[a] | >50.0 |
| **3** | >5.0 | >5.0 | 3.2 ± 1.0 | 3.2 ± 0.6 | 3.8 ± 0.7 | >5.0[a] | >5.0[a] | >5.0 |
| **4** | >1.0 | >1.0 | >1.0 | >1.0 | >1.0 | >1.0[a] | >1.0[a] | – |
| **5** | 34.7 ± 3.8 | 27.5 ± 6.3 | 4.0 ± 1.0 | 4.1 ± 1.4 | 5.5 ± 2.0 | 5.4 ± 3.8[a] | 3.6 ± 2.1[a] | >50.0 |
| **6** | >10.0 | >10.0 | 6.7 ± 2.5 | >10.0 | >10.0 | >10.0[a] | >10.0[a] | – |
| **7** | >1.0 | >1.0 | >1.0 | >1.0 | >1.0 | >1.0[a] | >1.0[a] | – |
| **8** | >50.0 | >50.0 | >50.0 | >50.0 | >50.0 | >50.0[b] | 45.1 ± 4.9 | >50.0 |
| **9** | >1.0 | >1.0 | >1.0 | >1.0 | >1.0 | >1.0 | >1.0 | – |
| **10** | >5.0 | >5.0 | >5.0 | >5.0 | >5.0 | >5.0[b] | >5.0 | – |
| **11** | >50.0 | 14.3 ± 3.7 | 5.9 ± 2.0 | 7.2 ± 2.1 | 26.3 ± 6.1 | 30.6 ± 3.7 | 11.4 ± 1.7 | >50.0 |
| **12** | >25.0 | 16.2 ± 2.4 | 11.1 ± 3.7 | 15.1 ± 1.7 | 17.4 ± 2.3 | >25.0[b] | 8.2 ± 3.8 | >25.0 |
| **13** | 39.9 ± 7.3 | 35.6 ± 8.7 | 27.0 ± 9.4 | 23.9 ± 4.0 | 27.4 ± 2.4 | 34.9 ± 11.0[b] | 23.3 ± 7.6 | >50.0 |
| **14** | 18.7 ± 4.6 | 15.7 ± 3.6 | 5.4 ± 1.2 | 6.2 ± 2.0 | 22.7 ± 4.8 | 39.2 ± 6.0[b] | 11.3 ± 1.6 | >50.0 |
| *cisplatin* | >50.0 | 39.9 ± 4.6 | 11.5 ± 1.6 | 30.3 ± 6.1 | 6.9 ± 1.9 | 34.2 ± 6.4[a,b] | 19.6 ± 4.3[a] | >50.0 |
| *oxaliplatin* | >50.0 | >50.0 | >50.0 | >50.0 | >50.0 | >50.0[a] | >50.0[a] | >50.0 |
| *carboplatin* | >1.0 | >1.0 | >1.0 | >1.0 | >1.0 | >1.0 | >1.0 | – |

[a] Taken from Ref. [5].
[b] Taken from Ref. [7].

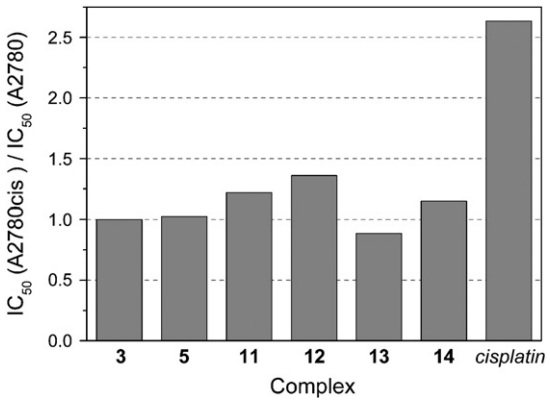


**Fig. 1.** The plot of the $IC_{50}$(A2780cis) to $IC_{50}$(A2780) ratios calculated from the obtained $IC_{50}$ (μM) values of *in vitro* cytotoxicity for the platinum(II) (**3**, **5**) and palladium(II) (**11**–**14**) complexes, and *cisplatin* against ovarian carcinoma (A2780) and ovarian carcinoma *cisplatin* resistant (A2780cis) human cancer cell lines.

isolation, the cells were plated on collagen-coated culture dishes at the density of $1.4\times10^5$ cells/cm$^2$. The culture medium was enriched for plating with 2% fetal calf serum (v/v). The medium was exchanged for a serum-free medium the day after and the culture was allowed to stabilize for additional 48 h prior to the treatments (37 °C, 5% $CO_2$).

The platinum(II) complex **5** displayed higher *in vitro* cytotoxicity against all the tested cancer cell lines than *cisplatin* (Table 1). Its $IC_{50}$ values are in the cases of HOS, MCF7 and A2780cis more than five-times lower as compared with *cisplatin*, which is important especially in the case of *cisplatin* resistant (A2780cis) cells. It can be stated that the calculated $IC_{50}$(A2780cis)/$IC_{50}$(A2780) ratio is more than 2.5-times lower for **5** in comparison with *cisplatin* (Fig. 1). Another highly *in vitro* cytotoxic substance is complex **2**, since it showed quite promising results against HOS, MCF7 and A2780 cancer cell lines (Table 1). On the other hand, although this compound is sufficiently soluble, it was not active up to the concentration of 50.0 μM against A549, HeLa, G-361 and A2780cis cells. In connection with **2** it has to be said that its activity against HOS is almost ten times higher than *cisplatin*, which is the highest ratio for all the obtained values of **1**–**14**. The significant *in vitro* cytotoxicity of **3** against A2780, A2780cis and G-361 cells is worth mentioning (Table 1), especially its ability to inhibit both the ovarian carcinoma cell line and its *cisplatin* resistant analogue.

Complex **14** showed the most promising results of the palladium (II) complexes, its *in vitro* cytotoxicity was higher (MCF7, A549, HeLa, A2780 and A2780cis) or comparable (HOS) to *cisplatin*. However, it has to be mentioned that the activity of **14** was not the highest within the tested palladium(II) complexes against HOS, (exceeded by **11** and **13**), MCF7 (exceeded by **12**), HeLa (exceeded by **11**) and G-361 (exceeded by **12**). Similar to platinum(II) complexes **3** and **5**, complexes **11**–**14** were found to be significantly active against A2780cis cells (Fig. 1).

Talking about particular human cancer cell lines employed in this work, all the complexes, whose *in vitro* cytotoxicity was determined up to the concentration given by their solubility (i.e. **5**, **11**–**14**), were more cytotoxic against HeLa cells than *cisplatin* (Table 1). The same conclusion can be made for complexes **5**, **13** and **14** and A549 cell line, although the *in vitro* cytotoxicity of *cisplatin* was not determined within the tested concentration range ($IC_{50}$>50 μM). Complexes **2**, **5** and **11** are more active, in the sense of *in vitro* cytotoxicity against HOS, than the positive control (*cisplatin*), whose activity is, on the other hand, slightly higher as compared with **13** and **14**.

The results given in Table 1 show that platinum(II) complexes (**2**, **5**) are significantly more *in vitro* cytotoxic against HOS as compared with the palladium(II) ones (**11**, **13**, **14**) and *cisplatin*. Talking about MCF7, again most of the tested complexes (**1**, **2**, **5**, **11**, **12** and **14**) exceeded the *in vitro* cytotoxicity of *cisplatin*. As for the *in vitro* cytotoxic activity against G-361, there is a clear difference between the tested platinum(II) (**3** and **5**) and palladium(II) (**11**–**14**) complexes (Table 1), because only the platinum(II) ones were found to be more active in comparison with *cisplatin*.

The prepared complexes **1**–**14** were also *in vitro* tested against both A2780 and A2780cis to study advantage of these substances over *cisplatin*. Complexes **1**–**3**, **5**, **6**, **11**, **12** and **14** more efficiently inhibit the proliferation of A2780 than *cisplatin*, while complex **13** is more than two times less active (Table 1). On the other hand, only the cytotoxicity of **3**, **5** and **11**–**14** against A2780cis was evaluated by an MTT assay up to the concentration given by the solubility of the appropriate compounds (Table 1), however, their activity was higher in comparison to *cisplatin*. We calculated the $IC_{50}$(A2780cis)/$IC_{50}$ (A2780) ratios of these complexes (Fig. 1), and it was proved that they are significantly more effective than *cisplatin* for the treatment of both A2780 and A2780cis cancer cells. In other words, it can be noted that complexes **3**, **5** and **11**–**14** overcome *cisplatin* resistance.

Further, the *in vitro* cytotoxicity against human hepatocytes culture (LH32) was evaluated for selected representatives of the prepared complexes, *cisplatin* and *oxaliplatin* (Table 1). None of these substances were *in vitro* toxic in the tested concentration range which is again very important for their further study (e.g. *in vivo* cytotoxicity, DNA interactions).

## Acknowledgement

This research was supported by the Ministry of Education, Youth and Sports of the Czech Republic (a grant no. MSM6198959218), and by the Grant Agency of the Palacký University (a grant no. PrF_2010_018).

## References

[1] D.J. Adelstein, J. Moon, E. Hanna, P.G. Giri, G.M. Mills, G.T. Wolf, S.G. Urba, Head Neck 32 (2009) 221–228.
[2] N. Agarwal, M. Hussain, Drugs 69 (2009) 1173–1187.
[3] J.A. Garcia, R. Dreicer, J. Clin. Oncol. 24 (2006) 5545–5551.
[4] M. Gielen, E.R.T. Tiekink, Metallotherapeutic Drugs and Metal-based Diagnostic Agents, Willey, London, 2005.
[5] P. Štarha, Z. Trávníček, I. Popa, J. Inorg. Biochem. 104 (2010) 639–647.
[6] P. Štarha, Z. Trávníček, I. Popa, J. Inorg. Biochem. 103 (2009) 978–988.
[7] P. Štarha, I. Popa, Z. Trávníček, Inorg. Chim. Acta 363 (2010) 1469–1478.
[8] L. Pichard-Garcia, S. Gerbal-Chaloin, J.B. Ferrini, J.M. Fabre, P. Maurel, Methods Enzymol. 357 (2002) 311–321.